THE CITY UNIVERSITY

DEPARTMENT OF SYSTEMS SCIENCE

"A MATHEMATICAL MODEL OF THE HUMAN RESPIRATORY SYSTEM WHICH EXHIBITS BREATHING AND INCLUDES BLOOD FLOW AND VENTILATION CONTROLS"

Hari Har Nath Bali

A thesis submitted for the award of the degree of Doctor of Philosophy in Systems Science.

1976

Dedicated to my wife "SNEH" whose understanding and encouragement has been invaluable in difficult times during the period of this project.

List of Contents

SUMMARY

			Page
Chapter	1.	Introduction	3
	2.	Respiratory Physiology	12
	3.	Control System and Physiology and Problems of Mathematical Representation	25
	4.	Models of Respiratory System:	34
		4.1 A Survey	
		4.2 Model Development	
	5.	Model 1 (Incorporating Dead Space and Circulation Delays)	50
		5.1 Development and Equations	
		5.2 Simulation Results and Discussions	
	6.	Model 2 (Incorporating Oxygen)	77
		6.1 Development of Equations Two Controller Strategies	
		6.2 Results and Discussions	
	7.	Model 3 (Incorporation of Local Blood Flow Controls and Brain Tissue)	121
		7.1 Development of Equations	
		7.2 Results and Discussions	
	8.	Lung Gas Exchange Model: (Actual Ventilation)	181
		8.1 Development of Equations	
		8.2 Results and Discussions	
	9.	Complete Model (Incorporating Breathing)	192
		9.1 Development of Equation	
		9.2 Results and Discussions	
	10.	Model Validation (Problems and Methods)	248
		10.1 Validation of Breathing Model	
	11.	Conclusions	273
Appendix	1.	References	276
Appendix	II.	Nomenclature	280
Appendix	III.	Glossary of Physiological Terms	281
Appendix	IV.	Computer Programs	282

Acknowledgements

The author wishes to express thanks to Professor L. Finkelstein and Dr. E.R. Carson of The City University and [redacted] The Middlesex Hospital, London, for their invaluable assistance and guidance in this project.

Gratitude is also expressed to the [redacted], The City University, and The Middlesex Hospital for provision of funds during this work.

Thanks are also expressed to [redacted] for typing this thesis under difficult conditions.

SUMMARY

A comprehensive mathematical model of the human respiratory system, incorporating events within the respiratory cycle, has been developed. This has been built up in a systematic manner, starting from a simple description and adding in a step-by-step fashion additional features. At each stage of complexity, the model behaviour has been examined and the validity of the assumptions tested.

The initial models involved many gross physiological assumptions with many features lumped into single compartments. Nevertheless, some of the predictions were physiologically plausible. These models highlighted, however, the inability of either central tissue control or arterial chemoreceptor control individually to provide an adequate description of all dynamic phenomena.

Subsequent model development included additional tissue compartmentation and the effects of arterial blood CO_2 and O_2 concentrations on cerebral blood flow and cardiac output.

Further extension involved the separate development of a lung gas exchange model which included the variations of both lung volume and gas concentrations due to inspiration and expiration. This was then combined with the circulatory model to provide a comprehensive description of the respiratory system within which instantaneous values of variables such as arterial blood CO_2 and oxygen concentrations during the respiratory cycle could be studied. Both for breathing and for the excessive production of muscle tissue CO_2 as occurs in exercise, model results were within the range of physiological acceptability.

After obtaining qualitatively acceptable results, two approaches to system identification and parameter estimation were adopted. The first involved functional minimisation using the system trajectory in the hyperspace of the model states. The second used pattern recognition techniques whereby parameters were adjusted in order to match selected features of the simulated response with the corresponding features of physiological test data. This novel approach may provide a powerful technique for the identification of complex systems and in the respiratory context enable alternative hypotheses regarding controller strategy to be evaluated.

Having obtained a satisfactory mathematical model of the human respiratory system, its simulation using a digital computer can provide predictions about the system's behaviour without the use of difficult and time consuming experimentation. Whilst some physiological test data will still be required to validate the model predictions, the understanding of the system dynamics provided by the model enables experiments to be designed much more effectively in order to maximise the information obtained from the minimum number of tests.

1. INTRODUCTION

Traditionally mammalian physiology has been studied by formulating manageable verbal models based partly upon facts, partly upon assumptions. In most cases these verbal models have been a series of statements of observed or presumed causal relationships among system variables. As a number of these causal relationships lengthen with the accumulation of experimental evidence and data, the problem of representing the system behaviour grows more complex. Eventually at some level of complexity, interaction among the system variables make verbal models conceptually difficult and their behaviour is not intuitively obvious. Further the assumed relationships are not explicitly clear and are embodied within the general text. This difficulty can be overcome to a large degree by quantifying the verbal models, that is by restating the causal relationships and assumptions in quantitative symbolic form.

The use of quantitative methods requires a precise statement of the problem and of the assumptions and hypotheses, and also a systematization of the steps required to study the problem which lead to the results and conclusions. The systems science approach provides techniques for this systematization of the method of the study. The physical system may be thought of as a dynamic or static object with well defined boundaries across which flows substance, energy or information. Flows which are adjustable or

are causative agents are system inputs if observed and included in the study. The flows which change due to the changes in the inputs are system outputs. A system may be divided into various smaller systems called the subsystems. A 'mathematical system' is a set of mathematical (algebraic, logical etc.) relations that involve and relate the system inputs and outputs in terms of the characteristics of the subsystems. This mathematical system is termed as a'mathematical model'. A mathematical model can be described by a set of mathematical relationships and symbolically represents a system, which can be manipulated free of most limitations of physical circumstances. Simulation of mathematical models involves numerical methods and often the use of computational hardware, and provides a means for studying the effect of parameter changes or some hypothesis modification in the mathematical model.

In the past decade a considerable effort has been made to study physiological systems in the form of mathematical systems. Progress in this field has been varied across the spectrum, since some physiological systems are more amenable to quantitative representation and study than others. One area most suited to quantification is the 'regulation of respiration'. Because of its dependence upon physical and chemical characteristics of gases, study of respiratory physiology has always made use of mathematical expressions. Indeed as long as 47 years ago (Adolph et al, 1928), fairly complex mathematical problems appear in the context of respiratory physiology. Analytical study for details of a subsystem has been pursued in abundance by physiologists. In the recent past, attempts have been made to formulate

mathematical models of the whole system, emphasising the relevant features within the context of the study.

The objectives which suggest the study of physiological systems from the point of view of system science in the form of mathematical systems may be summed up as follows:

1. Formulation of a neat diagram of all the relevant signal paths within the physiological systems and clearly showing interactions that take place among the subsystems, showing the effect of disturbances at various levels within the system;

2. The prediction of results of experiments or of actions that are yet to be performed and the expression of the experimental results in a neat concise form;

3. The identification of incomplete and therefore ambiguous data, thus highlighting the need for further experimentation in the required field;

5. The identification of some critical experiments which are needed for efficiently confirming or denying a given hypothesis.

6. On the other hand in the field of systems and control engineering the design of engineering control systems involve many interacting variables and the relationships between variables may be linear or non linear. Physiological systems present the system engineer with excellent examples of multivariable, complex and non-linear control systems which are functioning satisfactorily. The study of such systems may well provide a better understanding and insight into the best ways of designing engineering controls. Also the problems involved in identification and parameter estimation

of physiological systems and answers thereof are of great interest to system scientists.

Apart from this there are severe physiological constraints in the real system making experimentation extremely difficult and limited. If a mathematical model is developed, then with the computer's facilities available, various experiments may be simulated on the computer and effects of parameter variations may be studied more easily.

Thus the problem boils down to formulating a realistic mathematical model. To be of value, a model should exhibit some degree of isomorphism (i.e., similarity) with the real system. This isomorphism may occur on any number of levels from integrated whole structure to the single cell or unit process. Of major importance in any modelling and simulation study is the degree of isomorphism which is required to achieve the desired result. This varies with the system under study and 'a priori' knowledge available about the system, interactions between subsystems and parameters thereof. In general physiological systems are complex, multivariable and nonlinear. The study of such systems and formulation of mathematical models with some degree of isomorphism requires a detailed knowledge of various subsystems and their parameters. Thus in the case of respiratory system one may find it both necessary and convenient to group related variables in mathematical models (lumped compartmentation), to allow some broad assumptions, and to try to reproduce the gross effects of interactions in the real system rather than the detailed effects. This will help in the task of

structuring the models and interpreting their results.

In the recent past a number of mathematical models of the respiratory system have appeared in the literature. The scope and complexity of these models depended primarily upon the objectives of the research group and secondly the state of art in the computing and physiological field. In all cases the models have been developed to study one particular feature of the system. As shown in the critical review (chapter 4 of this thesis) there has been a singular lack of a unified approach to the problem.

Among others the main problem facing the researchers in the field is that of model validation. A subsystem model although detailed in certain aspects is of little use if it can be validated only on one set of experiments and falls short of predictions in others. Most of the physiological results are on the whole system, namely on normal healthy man. Thus clearly there is a need for a comprehensive model depicting as many features of the real system as possible though it may be lacking in depth due to lack of physiological details or due to computational problems. One of the main advantages of such a model will be a wider set of experimental results against which it can be tested and validated. Furthermore as such a model includes all the relevant features, a larger set of hypotheses related to subsystems can be tested within the context of the whole providing a wider base for experimentation. Thus in this thesis a mathematical model of the respiratory

system is developed which exhibits breathing. The inclusion of the actual respiratory cycle provides instantaneous time course of the model variables such as fluctuation in arterial blood CO_2 and O_2 with the change in alveolar gas composition. The physiological results show that these oscillations should increase peak to peak with exercise without changing the average (mean) value, whereas the oscillations should become smaller with inhalation of CO_2 gas mixture, with increased mean value. This phenomenon could not be checked in any of the previous models because they all used only time average values of these variables.

Another important feature of mathematical modelling is developing the model itself. It is extremely difficult if not impossible to structure directly a complete, complex model of the respiratory system and still have a degree of confidence in the time course of variables and values of parameters. It is much simpler to start from a very model model and to successively add more and more complex features. At each stage of complexification, the hypotheses associated with that feature may be studied in conjunction with some parameter sensitivity of the whole model in relation to real system which may point towards further complexification. Thus the final model, which will develop through this process of step by step complexification, will be more complete and one may be able to put more confidence upon the model predictions.
Thus in this thesis, starting from a simplified version, the model is made more complex in various stages by the addition of one or more physiological phenomenon and at each stage of complexification the effect of one or more parameter changes is studied and results presented.

First of all in chapter 2 a brief description of the real system is presented. This includes the way the gases are carried by the blood from one site of the body to others and various interactions that take place at each site. This then serves as a physiological guide to subsequent models. In chapter 3, the physiological system is looked at from a control system point of view and it is shown that the respiratory system exhibits a feed back control loop formation. Some aspects of other local controls within the real system are also put forward. In chapter 4 some of the mathematical models published in the literature are reviewed and a comparative study is presented.

In chapter 4, some of the problems of developing a mathematical model of the respiratory system are highlighted and a step by step complexification approach is presented. From chapter 5 to 9 this approach is used to develop a comprehensive breathing model of the respiratory system. In chapter 5 a two compartment model (lung and tissues) is used to study the effect of dead space and circulation delays. Inclusion of dead space required a slightly higher controller gain. By further variation of controller gain and/or circulation delays, the phenomenon of Cheyne-Stokes breathing is developed, but it is shown that changes required in parameters to develop the above phenomenon are far beyond physiological limits. This led to inclusion of oxygen in the model (chapter 6) which provided the facility to use an alternative controller, which provided higher gain than the previous controller. But this

model although suitable for exhibiting Cheyne-Stokes breathing, did not provide satisfactory results for CO_2 breathing. In the next chapter (chapter 7)a brain tissue compartment is included in to the controlled system. Also local blood flow controls are included. In chapter 8 a lung gas exchange model is developed which when attached to the brain tissue model, results in an overall model which exhibits breathing (chapter 9). This is probably the first model to show breath by breath variations with the system variables providing a facility for testing instantaneous variations in variables due to some disturbances.

The problems of identification and parameter estimation are highlighted in chapter 10. It is shown that where a certain feature of the results is an important factor e.g. presence or absence of oscillations, the techniques of pattern recognition may be gainfully applied for the purposes of identification and parameter estimation on the complex, multivariable, non linear system . An attempt is also made to develop a new control structure for the model with a functional minimisation technique. In the following chapters the results obtained are discussed in comparison to relevant physiology and some conclusions are put forward. In conclusion the areas of uncertainty are highlighted and some recommendations for future work are made.

As far as the study of the respiratory system is concerned, it is right to underline the fact that modelling is but a part of the overall research program to gain deeper understanding of the respiratory control system. The other part, the clinical and

experimental program is extremely important. Modelling cannot provide any new knowledge about the respiratory system; only measurements and tests on the real system can do that. Modelling, however as shown in this thesis, can be of great service in integrating the large amount of knowledge available, it can test hypotheses to a certain extent, and can suggest the areas where further experimental knowledge and data are required. Apart from that, mathematical modelling can suggest some questions and hypotheses. The answering of these questions and testing of these hypotheses will lead to new knowledge. This process, moving from laboratory to computer centre to laboratory and back again, requires the closest cooperation between medical researcher and systems scientist. Where such a close relationship exists, this approach is sure to provide increased understanding of the respiratory control system, and as a result, make a substantial contribution to the knowledge available.

CHAPTER 2

PHYSIOLOGY OF RESPIRATION

The function of a respiratory system is to supply the required amount of oxygen (O_2) to the body and to remove excess carbon dioxide (CO_2). This is achieved by the process of inspiration and expiration in a cyclic fashion. Oxygen is provided to the body during respiration and the excess carbon dioxide is removed during expiration. A functional diagram of the system is shown in figure 2.1. Blood acts as the carrier of gases to and from the lungs and tissues. This exchange of gas depends upon the partial pressure gradient between the blood and the site through which it is passing.

Due to ventilation, the partial pressure of O_2 in the alveoli increases well above that in the venous blood flowing through the alveolar capillaries. This loads the blood destined for the tissue cells with O_2. On the other hand ventilation lowers the partial pressure of CO_2 in the alveoli, below that of the venous blood thus allowing excess CO_2 to pass into the lungs. Thus the arterial blood has a higher partial pressure of O_2 and a lower partial pressure of CO_2 than the venous blood. In the tissues O_2 is being consumed and metabolic CO_2 is being produced, resulting in the lower O_2 partial pressure and higher CO_2 partial pressure. The excess O_2 of the arterial blood is unloaded into the tissues and CO_2 passes from tissues to the blood. Thus the venous blood has a lower partial pressure of CO_2 and a higher partial pressure of CO_2 than in the alveoli and the circuit starts again.

The gas exchange between lungs and atmosphere takes place due to the variation of pressure and volume within the lungs. During inspiration the diaphragm descends and the chest wall is pushed outwards, decreasing the total pressure within the lungs. This results in the fresh air being sucked into the lungs. During expiration the elastic recoil force brings the chest wall the pre-inspiration position, increasing the total pressure within the lung, which results in the alveolar gas being pushed out to atmosphere. Thus the total volume of the lung and the partial pressure of CO_2 and O_2 are continuously changing within the lung in an oscillatory fashion, which in turn produces oscillations of P_{CO_2} and P_{O_2} in the arterial blood. However the table below gives the approximate average normal values for the partial pressures of gases in the various parts of the system, assuming total pressure to be 760mm Hg.

Conversion of Physiological Units to S.I. Units

	Physiological	S.I.
Pressure	1 mm Hg	133.0 kg $m^{-1}s^{-2}$
Volume	1 ml	1.0 X $10^{-6}m^{+3}$

TABLE 2.1

TOTAL AND PARTIAL PRESSURES OF GASES IN mm Hg

	DRY AIR	MOIST (37°C) TRACHEAL AIR	ALVEOLAR GAS	ARTERIAL BLOOD	MIXED VENOUS BLOOD
P_{O_2}	159.0	149.0	102.0	100.0	40.0
P_{CO_2}	0.3	0.3	42.0	42.0	47.0
P_{H_2O}	0.0	47.0	47.0	47.0	47.0
P_{N_2}	600.7	563.7	569.0	571.0	572.0
TOTAL	760.0	760.0	760.0	760.0	706.0

2.1 LUNG VOLUMES AND CAPACITIES

Fig 2.2 shows the lung volumes and capacities.

i. VOLUMES

TV - 'Tidal Volume' is the volume of air breathed in or out during quiet respiration (about 500 ml).

IRV - 'Inspiratory Reserve Volume' is the maximal volume of air which can be inspired after completing a normal total inspiration; i.e., inspired from the end inspiratory position (2-3.2).

ERV - 'Expiratory Reserve Volume' is the maximal volume of air which can be expired after a normal tidal expiration; i.e., expired from the end expiratory position (750 - 1000 ml).

RV - 'Residual Volume' is the volume of gas which remains in the lungs after a maximal expiration (about 1200 ml).

ii. CAPACITIES

VC - 'Vital Capacity' is the maximal volume of air which can be expelled from the lungs by forceful effort following a maximal inspiration (3.2 - 4.8 ℓ).

TLC - 'Total Lung Capacity' is the volume of gas contained in the lungs after a maximal inspiration (about 6 ℓ).

FRC - 'Functional Residual Capacity' is the volume of gas remaining in the lungs at the resting expiratory level.

In quiet respiration, an adult breathes 5-7 ℓ/min, his breathing rate is 12-14 breaths/min., and the amount of air inspired or expired per breath (tidal air) is approximately 500 ml. At rest an adult uses about 250 ml O_2/min and expires about 200 ml/min.

In heavy exercise the ventilation rate may exceed 80 ℓ/min. and the oxygen usage may rise above 3.5 ℓ/min.

2.2 ALVEOLAR VENTILATION AND PHYSIOLOGICAL DEAD SPACE

In quiet breathing a normal man inspires and expires about 500 ml of air. Some of this inspired air (about 150 ml) merely fills the conducting air passages between the mouth and nose and the respiratory bronchioles. The remainder effectively ventilates the alveoli thereby lowering the P_{CO_2} and raising the P_{O_2} of the alveolar air. As the alveoli still contain some of the 2-2.5 litres of gas after a quiet expiration (functional residual capacity), the overall reduction of P_{CO_2} and rise of P_{O_2} by one subsequent quiet inspiration of 350 ml is small; nevertheless the expulsion of about 350 ml of this 'diluted' alveolar air containing 6 per cent CO_2 and 14 per cent O_2 by the following expiration ensures that the alveolar gas pressures of oxygen and carbon dioxide are kept relatively constant, despite the continuous delivery of CO_2 and removal of O_2 by the pulmonary capillary blood. Clearly the volume of alveolar ventilation is of paramount importance in this respect. The total ventilation per minute (5-7 litres/min) at rest is usually achieved by a tidal volume of 500 ml and a respiratory frequency of 12-14/min. If the ventilatory volume be kept steady then the breathing can be modified by altering the frequency. Thus at a rate of 36 breaths/min a pulmonary ventilation of 6 litres/min would require a tidal air of only 167 ml; conversely at a rate of 6 breaths/min. the same pulmonary ventilation would require a tidal volume of 1000 ml. Although the total ventilation would be the same, the respective alveolar ventilations would be vividly different, for 150 ml of air in each breath merely fills the dead space.

The alveolar ventilation can only be deduced by measuring the total ventilation and subtracting the volume required for ventilation of the dead space.

Thus it can be seen that

Total Ventilation/min = Tidal volume X frequency of respiration/min.

i.e. $\dot{V}_T = V_{TV} \times f$

but also $\dot{V}_T = (V_D + V_A)f$ (dead space + alveolar volume)

therefore alveolar ventilation per min is given by

$$\dot{V}_A = (V_{TV} - V_D).\ f$$

2.3 RESPIRATORY QUOTIENT 'R.Q.'

The respiratory quotient is defined as the ratio of total body CO_2 production to the total O_2 consumption by the body per unit time. That is to say

$$R.Q. = \frac{\dot{M}_{CO_2}}{\dot{U}_{O_2}}$$

2.4 THE CARRIAGE OF GASES

As shown in figure 2.3 the blood circulating between the lungs and tissues acts as a carrier of gases, carbon dioxide and oxygen. These gases are carried in chemical combination, in solution or in both.

2.4.1 CARRIAGE OF OXYGEN

Oxygen is carried in two ways by the blood.

i. DISSOLVED IN THE PLASMA

The amount of oxygen dissolved in the plasma is proportional to the partial pressure (tension). At a tension of 100 mm Hg, about

0.13 ml volume per cent of oxygen is dissolved in the blood. These small volumes may be neglected as far as the oxygen supply to the tissues is concerned.

ii. IN CHEMICAL COMBINATION

The amount of oxygen combined with haemoglobin in the red cell (the oxygen content) depends upon the partial pressure of oxygen, but the relationship is non-linear as shown in figure 2.4. This is known as the oxygen dissociation curve. At partial pressures of 100 mm Hg the haemoglobin in the red cell is fully saturated and the volume per cent oxygen is about 20. Thus the oxygen concentration in the arterial blood is about 0.2. The oxygen tension in the resting tissues is about 35 mm Hg. Owing to this great difference in the partial pressures, oxygen quickly passes to the tissues and oxygen tension in the blood falls to about 40 mm Hg. As a result the venous blood leaves with an oxygen content of about 14 ml/100 ml blood and the arterio - venous difference in oxygen content is 5 ml/100 ml blood. The reduced haemoglobin gets saturated again when the blood passes through the lungs. Thus the oxygen loop is completed.

2.4.2 CARRIAGE OF CARBON DIOXIDE

Carbon dioxide is carried in the blood in three ways:

i. IN SOLUTION

Carbon dioxide is more soluble than oxygen. The amount in solution is proportional to the partial pressures within physiological limits. At a partial pressure of 40 mm Hg, 3 ml carbon dioxide is dissolved in every 100 ml. of blood.

ii. COMBINED WITH PROTEIN

Carbon dioxide forms a neutral carbamino compound with haemoglobin and to a lesser extent with the plasma proteins.

It combines with the haemoglobin in the red cell at a different part of the molecules from that at which the oxygen combines. At tensions in excess of 10 mm Hg saturation occurs. The amount combined then depends not so much on the partial pressures as on the state of oxygenation of the haemoglobin molecule. With full reduced haemoglobin 8 ml carbon dioxide is carried as carbamino by 100 ml blood whereas with saturated haemoglobin only 3ml carbon dioxide is carried.

iii. AS BICARBONATE

The greatest portion of carbon dioxide in the blood is in the form of bicarbonate-sodium bicarbonate in the plasma and potassium bicarbonate in the red cells.

The relationship between total carbon dioxide content and its partial pressure is given in figure 2.5 which is known as the carbon dioxide dissociation curve. As shown in the figure, the shape of the curve varies with oxygen partial pressure. The linear relationship may be assumed between 40 to 60 mm Hg P_{CO_2}.

This arterial blood reaches the tissues with a P_{CO_2} of about 40 - 42 mm Hg and CO_2 content of about 48 ml/100 ml blood. The P_{CO_2} of the resting tissues is about 46 mm Hg; thus CO_2 in solution rapidly diffuses into the blood to reach an equilibrium tension of about 46 mm Hg, The CO_2 content eventually rises to 52 ml/100 ml blood.

2.5 THE CHEMICAL REGULATION

In the regulation of respiration several processes are involved.

i. Venous blood, low in O_2 and high in CO_2, returns from all of the tissues of the body (mixed venous blood) to the right atrium and ventricle and is pumped through the pulmonary circulation.

ii. The mixed venous blood flowing through the pulmonary capillaries is arterialised - i.e., receives O_2 from the alveolar gas and gives off excess CO_2.

iii. The arterial blood is distributed to all the tissues of the body.

ix. O_2 and CO_2 are exchanged between the blood in the tissue capillaries and the tissue cells themselves.

Obviously, multiple and complex mechanisms regulate the cardiovascular and respiratory systems to enable them to maintain a proper chemical and physical environment for function of all cells. There are centres to receive information from parts of the body about their needs for gas exchange. In the case of chemical regulation, there are receptors (chemoreceptors) which respond to changes in either CO_2 or O_2 or both, and then send signals to the respiratory centre from where the central signals emerge for the required ventilation, which is controlled by either changing depth or frequency of respiration or both.

2.6 CHEYNE-STOKES BREATHING

Cheyne-Stokes breathing is characterised by regular, recurring periods of more than normal breathing and very little or no breathing at all. The time course of ventilation and breathing pattern is shown in figure 2.6. It can be seen that the tidal volume gradually increases to a peak and then gradually decreases to either zero or a very low value, resulting in sustained (or damped) oscillations in average ventilation flow rate. In normal subjects this pattern may occur after hypoventilation (Douglas and Haldane 1909), or after arrival at high altitudes (Douglas and Haldane 1913). It has also been observed in patients with congestive heart failure in whom the circulation time is prolonged.

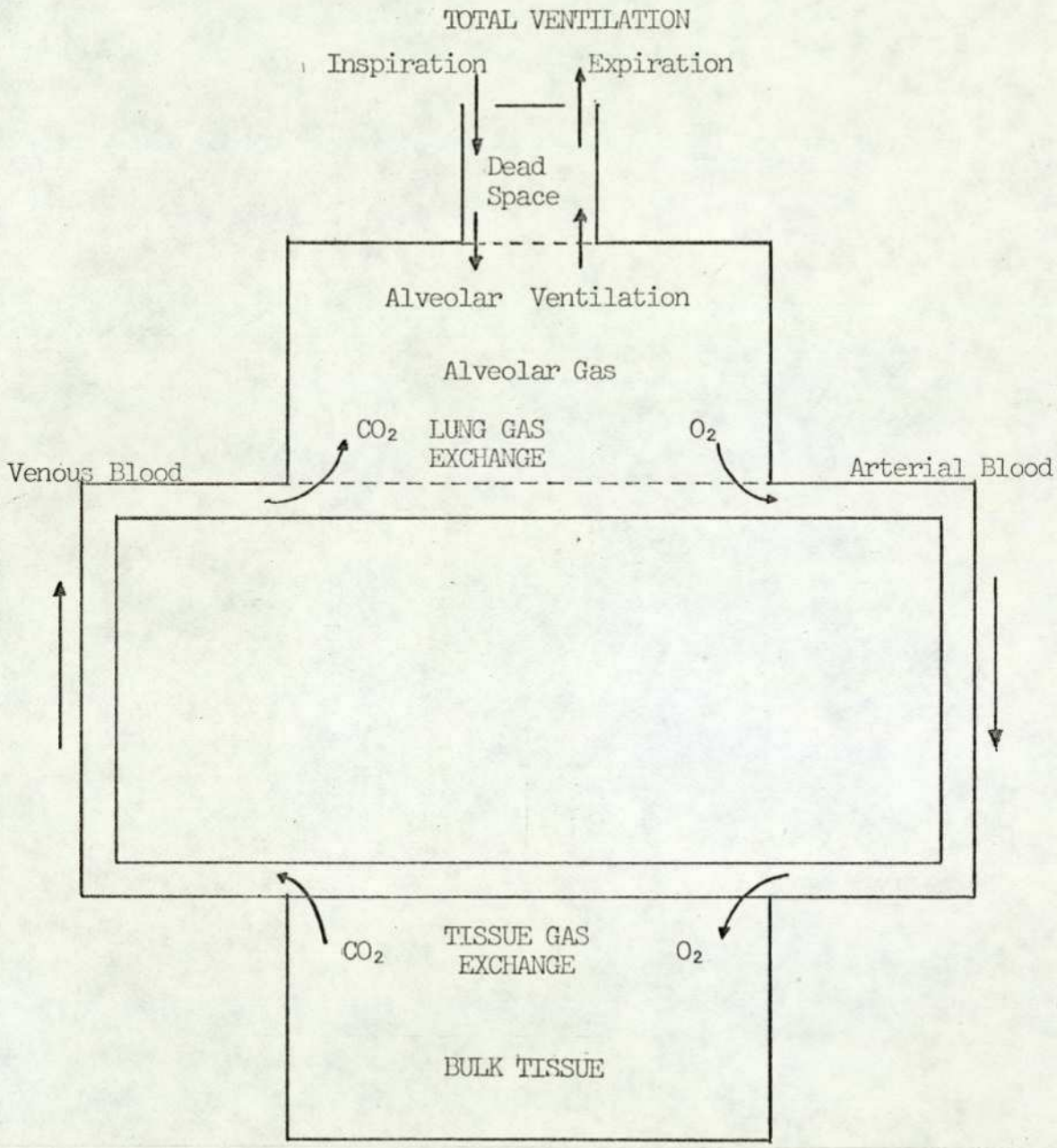
TOTAL VENTILATION
Inspiration
Expiration
Dead
Space
Alveolar Ventilation
Alveolar Gas
CO_2 LUNG GAS EXCHANGE O_2
Venous Blood
Arterial Blood
CO_2 TISSUE GAS EXCHANGE O_2
BULK TISSUE

Figure 2.1

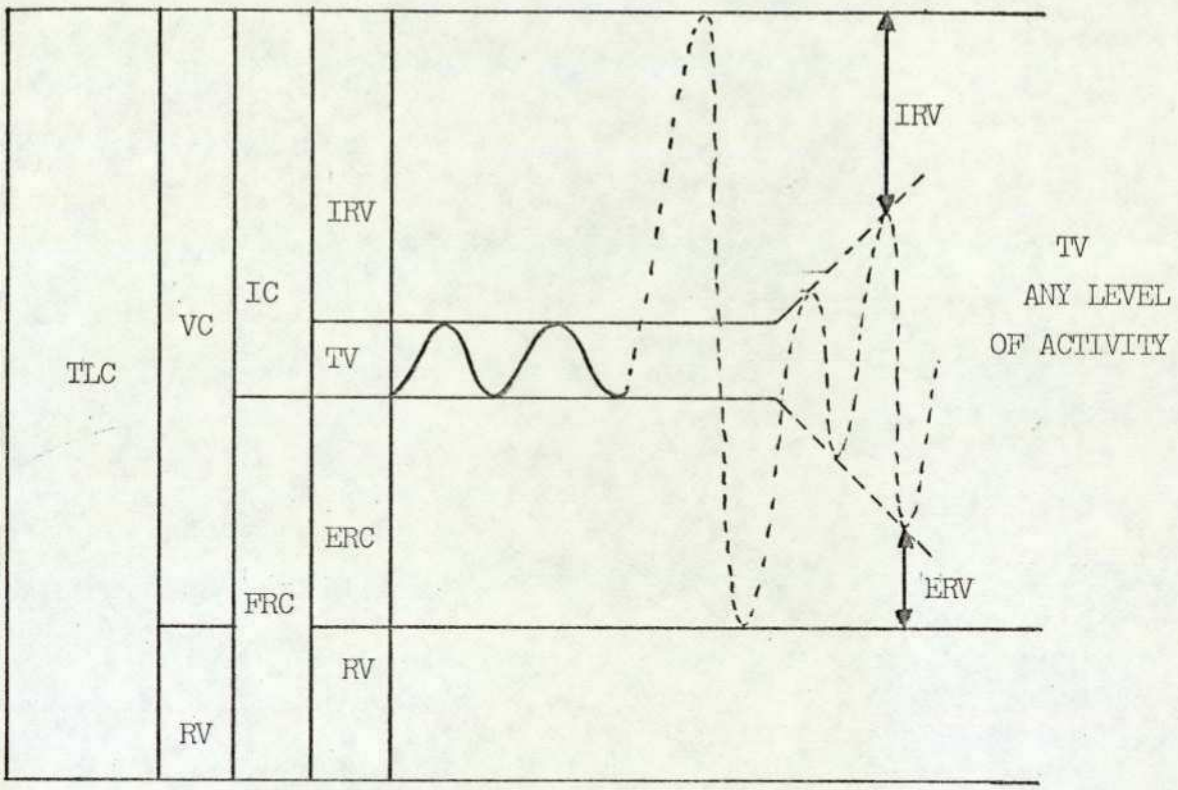

Figure 2.2

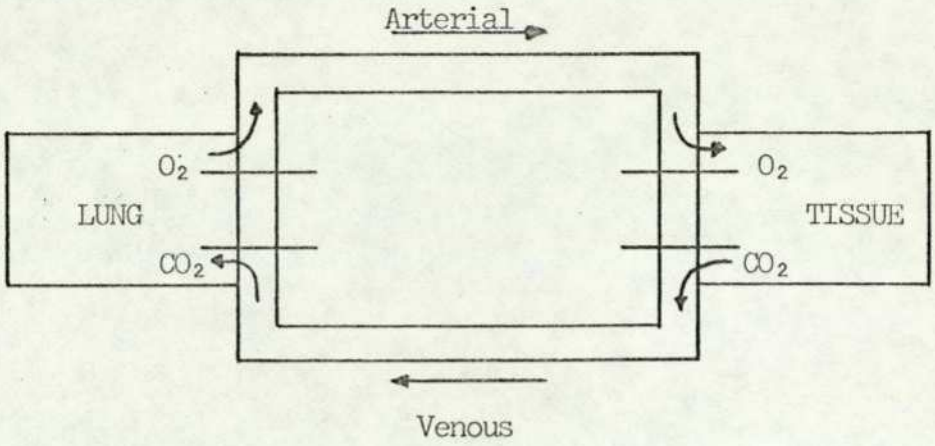

Figure 2.3

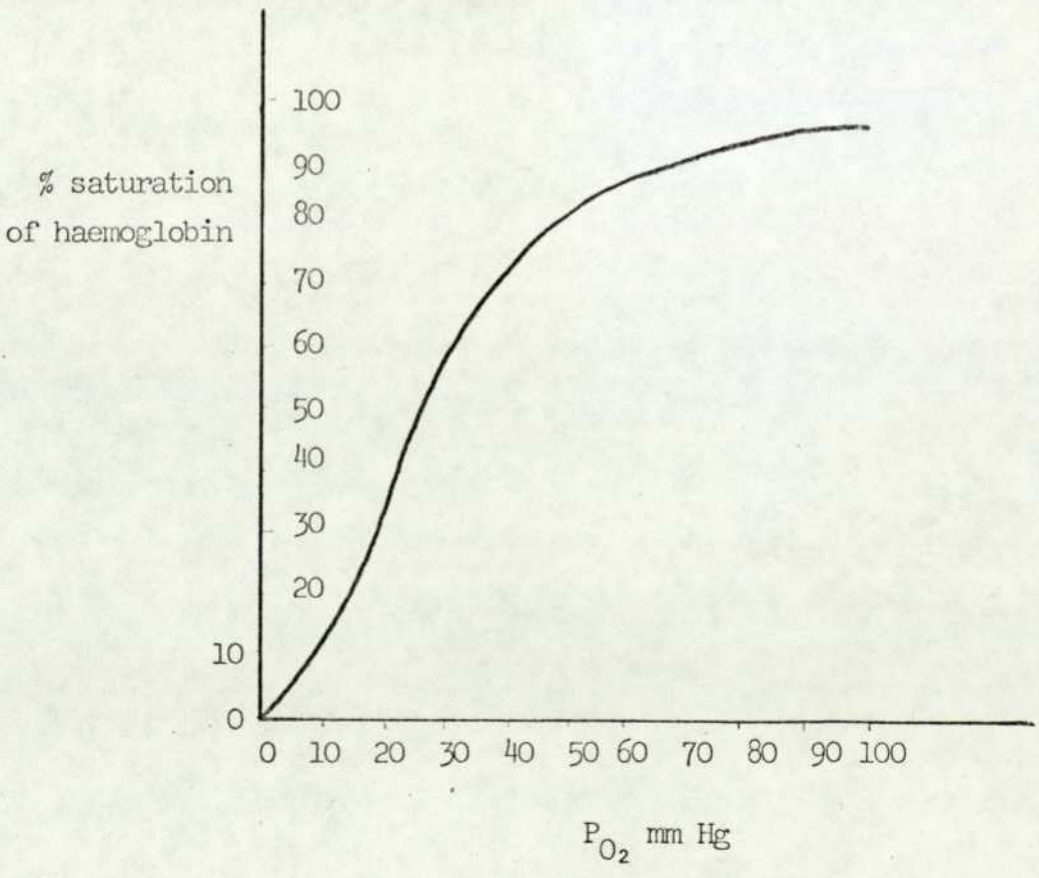

Figure 2.4

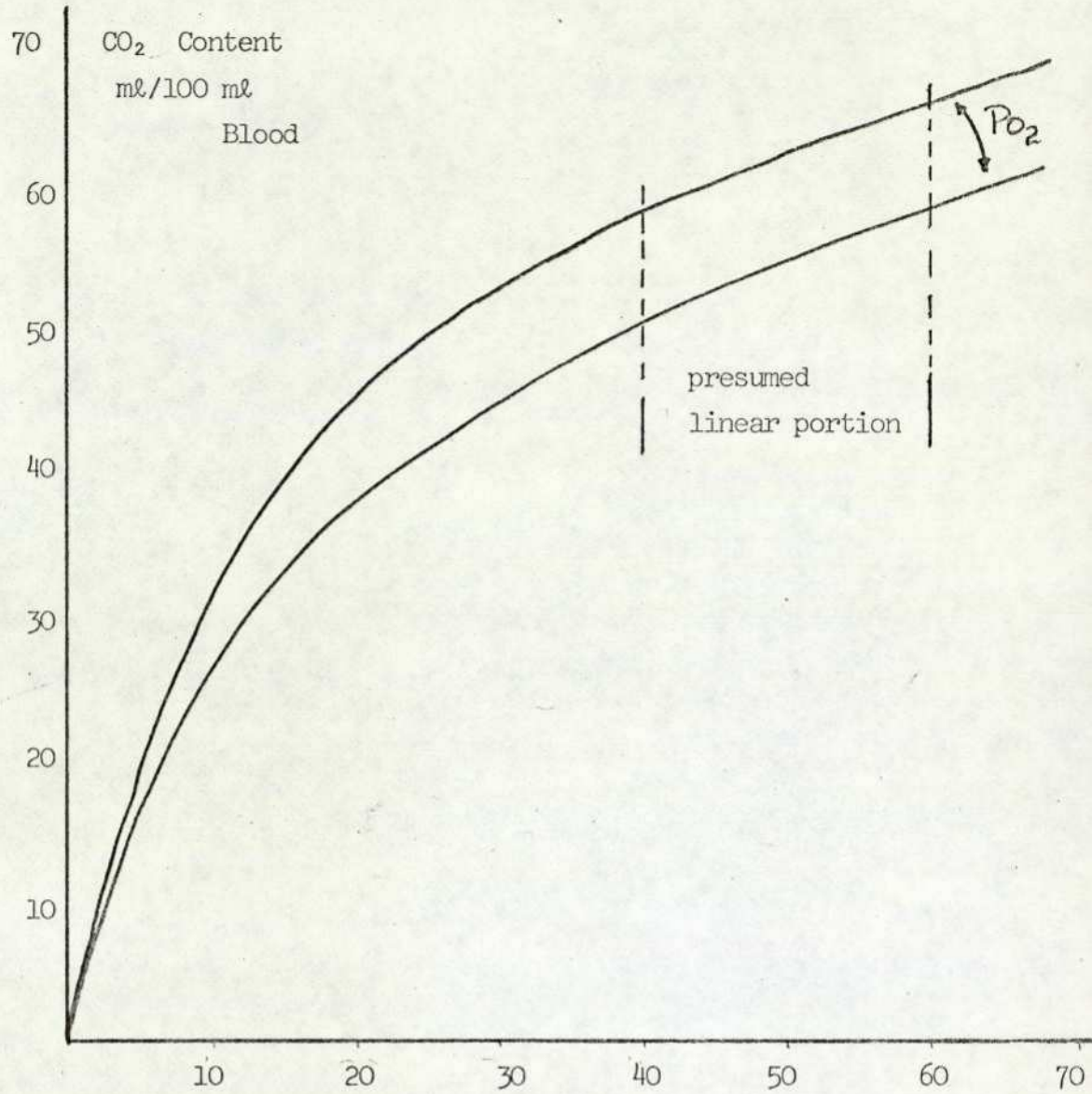

Figure 2.5

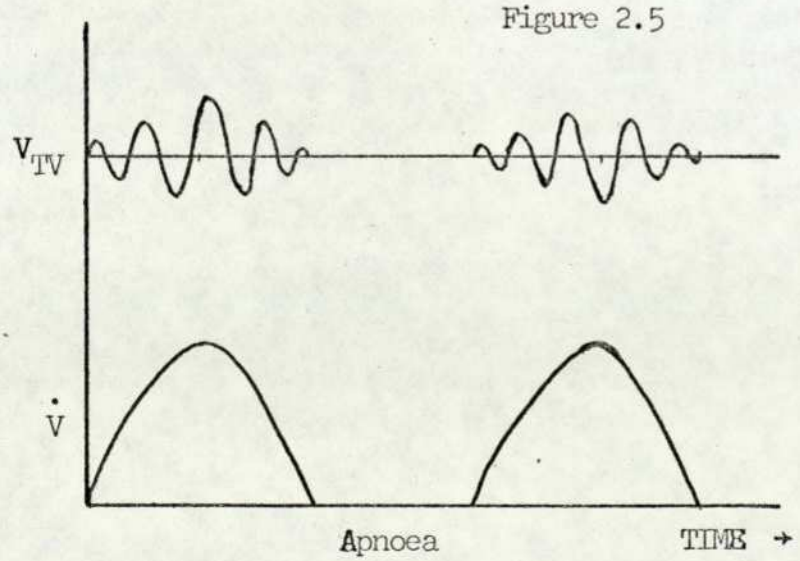

Figure 2.6

CHAPTER 3

CONTROL IN RESPIRATORY SYSTEM AND PROBLEMS OF MATHEMATICAL REPRESENTATION

All bodily functions exhibit the phenomena of regulation and control in some form or another. In many cases overall control is achieved by multiple feed-back loops, which may be simultaneous or hierarchical. The control of breathing, cardiac output, body water balance and temperature are examples of regulation, whereas the position control of limbs, muscle systems and chest cavity are examples of servo-control.

Breathing is regulated by a complex system of multiple feed-back loops in which operating levels satisfy input-output relationships in a cyclic fashion. The time varying course of all respiratory variables is affected by metabolic functions within the body cells, external stimuli mediated through climatic or chemical elements, and inherent oscillations due to the processes of inspiration and expiration.

Respiration is dependent upon neural impulses which originate in the lower brain (medulla) and are transmitted to the chest wall and diaphragm to govern both the rate and depth of breathing. In the lungs, exchanges of both oxygen (O_2) and carbon dioxide (CO_2) take place by diffusion across the alveolar membrane separating gas and blood. O_2 and CO_2 are then carried in solution and chemical combination to the cell system, where gas exchange across membranes again takes place.

Control of both rate and depth of breathing is governed primarily by neural signals initiated at central and peripheral sites in the body and transmitted to the respiratory centre. Because of the importance

of the chemoreceptors in the control of respiration, it is customary to distinguish between chemical control and non-chemical control and to refer to the latter as neural control. The neural control can be reflex in nature, as are the signals arising from stretch receptors in the lung, or it can be at the conscious level, associated with vocalisation, emotion, or exercise anticipation.

Chemoreceptors involved in respiration are located centrally at or near the respiratory centre and peripherally in the carotid and the aortic body. The central chemoreceptors are responsive primarily to carbon dioxide and hydrogen ion concentration. Their location in the medulla, perfused with blood and bathed in cerebrospinal fluid, suggests that they might respond to chemical changes either in cerebral blood or in cerebrospinal fluid or both. The carotid chemoreceptor is located in the neck near the bifurcation of the common carotid artery. The aortic chemoreceptors are situated in the arch of the aorta, the main blood vessel leaving the heart. Information about the oxygen concentration of the blood comes primarily from these peripheral chemoreceptors, although they are also sensitive to carbon dioxide changes. A detailed discussion of the physiology involved is given in Chapter 2.

Thus the controlling system for respiration can be classified as:

i) Mechanical Control: occuring through the lung mechanisms where frequency of breathing and tidal volume are directly controlled to provide ventilation by the pressure-volume characteristics of the lung and chest wall.

ii). Chemical Control: incorporating the control of breathing through neural signals indicating the chemical states of various sites in the body.

Three chemical factors, involved in the control of ventilation, are: Carbon dioxide tension (CO_2): Hydrogen ion concentration, H^+ (pH level): Oxygen tension (O_2)

That is to say:

VENTILATION = f (CO_2, H^+, O_2)

When a subject inhales a CO_2 mixture, ventilation increases, as does the CO_2 concentration in the blood stream and tissue. It can therefore be assumed that ventilation is in some way controlled by the CO_2 concentration. If now by breath holding this rise in ventilation is prevented, the concentration of CO_2 rises to an even higher level than when the normal ventilatory response is permitted; indicating that the CO_2 concentration in the blood and tissue is in turn controlled by ventilation. The loop is thus closed with CO_2 controlling ventilation which in turn controls the body CO_2 concentration. On the other hand, supply of oxygen seems to be linked with the body tissue CO_2 concentration. Oxygen requirements of the body rise dramatically in muscular effort. In a trained athlete making an all out effort, a steep rise occurs in the metabolic output of carbon dioxide of the muscle tissue, requiring as much as twenty fold increase in ventilation. This may partly be due to large oxygen requirement of the body and partly due to removal of the excess carbon dioxide so formed in the body.

The effects of blood and body tissue carbon dioxide concentration changes and ventilation are thus opposite in direction. A rise in CO_2 concentration increases ventilation which in turn tends to reduce the CO_2 concentration. Teleologically this implicates the ventilatory response to carbon dioxide inhalation or CO_2 production within the body, in the minimisation of the increase in CO_2 concentration in the blood and tissue.

The respiratory system appears therefore to conform, both in pattern and purpose, to a feed-back control system. A simplistic representation in the terms of three main chemical variables, CO_2, H^+, and O_2 is given in figure 3.1. Disturbances may be attributed to a variety of phenomena such as changes in the physical state or changes in inspired gas composition.

In brief the function of the respiratory system is to supply oxygen to the blood, remove metabolic carbon dioxide and to maintain a stable pH level within the body so that the tissue cells may function efficiently. Gas exchange takes place within the lung and tissue compartments. These two are connected through the flow of blood which provides a vehicle for gas transport from lungs to tissues and back to lungs.

It is apparent that the control of the three principal chemical variables already listed may be achieved in two ways, either by changing ventilation or by changing the blood flow rate or both. Changes in ventilation may be achieved either by changing the frequency or the depth (tidal volume) of breathing, or a combination of the two. There is some evidence to suggest that both the frequency and the tidal volume are some function of the total ventilation. Due to mechanical factors

there is a limit on the extent to which frequency may be changed and tidal volume is, in the limit, restricted to vital capacity. Furthermore, due to the presence of dead space there is also a lower limit to tidal volume, below which no ventilation takes place no matter what the frequency is.

In the case of changing the blood flow rate, there is evidence of local feed-back effects. Cerebral blood flow is a function of arterial carbon dioxide and oxygen concentrations. If the total cardiac output remains unchanged while a change in arterial CO_2 and O_2 concentrations alters the flow rate of the blood to the brain tissues, the blood flow rate to other parts of the body will also change. However, the total cardiac output is known to be a function of arterial CO_2 and O_2 concentrations, providing another local control. During exercise the metabolic carbon dioxide production of muscle tissue greatly increases. This is accompanied by an increased blood flow to the muscle tissue which can be achieved by increasing the cardiac output, by reducing the flow of blood to other tissues or by a combination of the two effects.

Physiological observations for these local or central control actions are far from complete, particularly during transient events. Some empirical relationships exist for local blood flow control and some equations for chemical control of respiration have been derived from steady-state data assuming that the controller equations hold for the transient situation as well as the steady state. (Grodins et al, 1967). Much respiratory physiology remains uncertain and there is a clear need for improved experimental data particularly in regard to the dynamic state.

3.1 SOME PROBLEMS INVOLVED IN DEVELOPING A MODEL

For the purpose of developing a mathematical model, the respiratory system can be divided into convenient and relevant sub-systems such as lungs, tissues (brain, muscle and others), heart, arterial blood and venous blood. The more detailed the compartmentation, the closer the approach to isomorphism although in practice the state of knowledge of sub-system behaviour and parameter values impose the limiting constraints.

The mathematical relationships for each sub-system may be written in terms of continuity equations either in the steady state (excluding the effect of variable time lags in diffusion and transport) or in dynamic terms. In general very small time constants may be regarded as instantaneous (for example, from the respiratory centre to phrenic nerve activity at the abdomen). Equally very large time constants may be regarded as tending to infinity (for example body adaptation to a new climate). Thus in many cases, the model may be systematically reduced by excluding these two extremes, depending of course, upon the time course within the field of interest and the accuracy required.

Many questions remain unanswered regarding the physiology of respiratory phenomena such as location and action of chemoreceptors, variable time lags involved in diffusion and transport, and controller system parameters. Initially therefore, more importance will be attached to the general shape of model responses than to exact replication of magnitudes. The model shown in figure 3.1 is in its simplest form. In fact the equations governing the controlled

and controlling system are exceedingly complex. In general, steady state relationships are well defined but there is a singular lack of dynamic information.

Some of the main problems in producing a comprehensive mathematical model of the respiratory system may be summarised as follows:

LUNG

i) Ventilation is a cyclic process with lung volume undergoing periodic changes. It's amplitude and periodicity can vary independently, so for a given ventilation there could be a number of frequencies and tidal volumes.

ii) A variable portion of the total ventilation is not effective due to the existence of dead-space, the space from the thorax down to the alveoli. The volume of this dead-space is a function of tidal volume.

iii) Both oxygen and carbon dioxide are exchanged across the alveolar membrane, but rates of diffusion differ widely between the two gases involved. Also the respiratory quotient (R.Q.) is not unity, i.e., dry expired and inspired volumes differ.

iv) A blood element requires a finite time to traverse the lung and during its passage gas diffusion occurs at a rate proportional to the partial pressure gradient.

v) Ventilation perfusion ratios differ in different parts of the lung so that the alveolar gas tensions are functions of both space and time.

TISSUES

The tissues actually consist of a group of individual elements connected either in parallel or in a parallel-series combination. Each element has its own metabolic rate and blood flow and probably also a characteristic buffer capacity for the gases involved. Thus one might expect as many tissue concentrations as there are individual circuits. Each tissue is at a different 'time-distance' from the lung and this 'time distance' may differ between the arterial and venous side of the same tissue. Again a blood element requires a finite time to traverse a tissue element, and gas diffusion occurs at a finite rate proportional to the partial pressure (tension) gradients.

These apart there are many other problems including:

i) Lack of knowledge concerning the controller mechanisms particularly in the case of neural information flow.

ii) The pulsatile nature of blood flow.

iii) Limitations of the sites at which measurements can be made in the intact functioning organism.

iv) Lack of physiological data regarding dynamic relationships between system variables and of parameter estimates.

All of this means that a number of simplifying assumptions have to be made before building up the model. There is clearly a trade off between such assumptions and the accuracy obtained, but it is possible to improve upon previous simplifications as the size and complexity of the model are increased. Even so new approximations have to be made at each step of complexification.

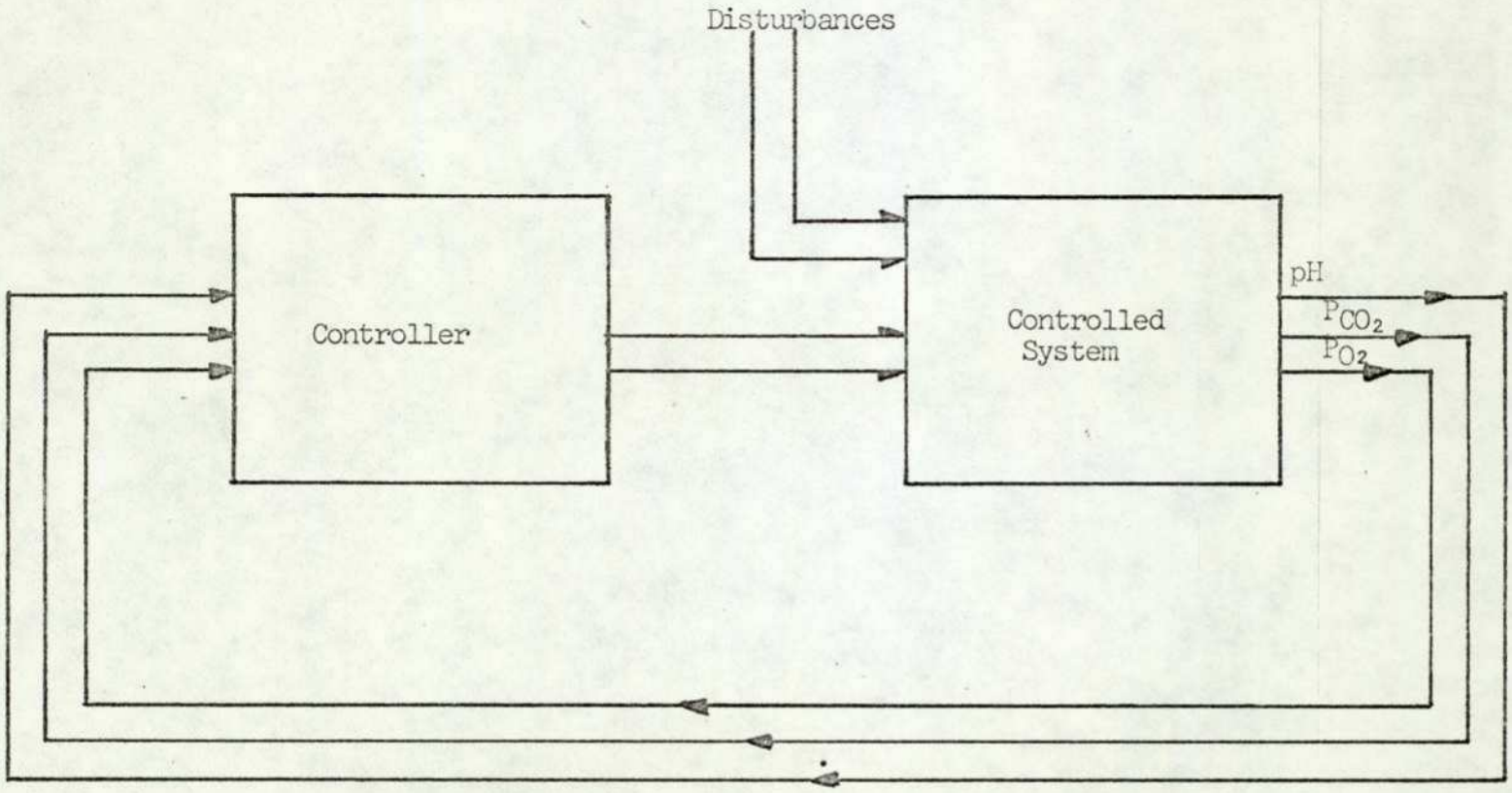

Figure 3.1

CHAPTER 4

MODELS OF RESPIRATORY SYSTEM

4.1 A SURVEY

In the last two decades several mathematical models of the human respiratory system have been published. These models, although different in nature and purpose, seem to share certain characteristics. As a set of mathematical equations, they are all non-linear and sufficiently complex to defy any analytical calculations, but require the use of computing devices. Some have been relatively less complex and allowed solutions through the use of analog computers. Others being more complex required the use of larger digital computers. The solutions of these mathematical models represent one or more time varying functions which correspond to experimental results. In each case some assumptions and simplifications have been applied to varying degree depending upon the complexity of the model. Here a comparative study is put forward of some of the mathematical models and their achievements are discussed.

Grodins and his associates were the first to apply the techniques of mathematical modelling to the respiratory control system (Grodins et al, 1954). This model was concerned with the response to inhalation of carbon dioxide gas mixture. As subsequent models followed the same basic pattern, it seems appropriate that this model be discussed in more detail. Grodins and his associates recognised that when the CO_2 content of the inspired mixture was altered, pulmonary ventilation changed in such a manner as to suggest that the mechanisms of the body

were trying to maintain the body CO_2 concentration at a fixed level. In developing the mathematical model, concepts and terminology of control system engineering were applied. The following illustrates the analysis and compartmentation of the system:

i. Controlled System - the network of physiological elements such as lung, tissues, blood circulation, through which ventilation and inspired carbon dioxide fraction affect the total CO_2 content of the body.

ii. Controlling System - the relationship through which body CO_2 content affects pulmonary ventilation.

iii. Controlled Quantity - body tissue carbon dioxide concentration.

iv. Controlling Quantity - pulmonary ventilation.

v. Disturbing Quantity - carbon dioxide concentration of the inspired gas.

Within the above frame work of the system the following simplifying assumptions were made:

1. The body consists of two rigid compartments (lung and tissue) which are connected by the circulating blood.

2. The time required for the blood to travel round the circuit i.e. transportation delays, and the delays associated with the diffusion of gases across the membrane are negligibly small.

3. Alveolar gas partial pressure of carbon dioxide (P_{CO_2}) is equal to arterial blood P_{CO_2} and tissue fluid P_{CO_2} is equal to venous blood P_{CO_2} at all times, i.e. during the dynamic period as well as in the steady state.

4. The CO_2 dissociation curves for arterial blood, venous blood and tissue fluid are identical and linear.

5. The entire cardiac output passes through the tissue compartment and is constant. The cardiac output is independent of arterial blood P_{CO_2}.

6. The CO_2 production of the tissue is the total CO_2 production of the body and is constant.

7. Respiratory Quotient is unity i.e. the production of body CO_2 is equal to body consumption of O_2 at all times.

8. The lung compartment has a constant volume and ventilation is a unidirectional flow through this compartment.

Thus two differential equations were formed describing the controlled system, one for the gas exchange in the lung compartment and the other for the gas exchange in the tissue compartment.

The mathematical description of the controlling system (Controller) was based upon the assumption that the ventilation is linearly dependent on the P_{CO_2} of the venous blood (equal to the P_{CO_2} of tissue). The linear, steady state relationship between alveolar ventilation and the P_{CO_2} of the arterial blood had been established earlier by Gray et al [1950]. It was supposed that a similar expression relates ventilation and tissue fluid P_{CO_2}. It was further assumed that the controller equation holds for the dynamic as well as the steady state.

This model when simulated on an analog computer produced 'disturbingly good results' as Grodins himself put it. The model

was reasonably successful in predicting the relatively slow response associated with sudden inhalation of air containing a small percentage of CO_2. The results obtained can be classified as follows:

1. During the CO_2 on-transient ventilation rose slowly to a new steady state level without any overshoot, while arterial blood P_{CO_2} rose much more sharply, overshot to a certain extent and then gradually fell back to a new steady state level.
2. The time to achieve a new steady state was a function of the percentage of CO_2 in inhaled gas mixture and was larger for higher percentage of CO_2 inspired.
3. Overshoot of arterial P_{CO_2} diminished with the increased percentage of CO_2 inhaled but undershoot during the off-transient increased with the percentage of inhaled CO_2.

Although the agreement between the theoretical and experimental curves of ventilation versus time was good, there were serious discrepancies in the off-transient curves of CO_2 partial pressure versus time. The model predicted much more undershoot than had been observed experimentally. Furthermore Grodins noted certain high-frequency oscillatory components in his experimental work which could not be simulated with this model. However if the simplicity of the model and the obvious gross assumptions are considered, the results were tolerably good. The high frequency phenomena absent from the model may be attributed to the absence of oxygen from the controller equation and the controlled system. It is known that any decrease in arterial oxygen content tends to increase the gain of the controller, and higher controller gain tends to make systems more

oscillatory. The inclusion of transportation delays may also have made the model more oscillatory.

Defares [Defares et al, 1962] produced an improved model, pointing out several weaknesses in the assumptions of the previous model and modifying two important features of the controlled system:

1. The body tissue compartment was subdivided into two compartments i.e. a brain tissue compartment and an 'other tissue' (not brain)compartment.

2. While the total cardiac output was maintained constant and independent of the inspired CO_2 fraction, the blood flow rate to the brain tissue compartment was made a function of the arterial blood P_{CO_2}. This feature was based upon the findings of Kety and Schmidt [1948].

They also made their controller equation a function of brain tissue CO_2 content as opposed to the bulk tissue CO_2 concentration used by Grodins et al, but by so doing, to maintain the steady state conditions of the model, the controller gain had to be doubled and the intercept of the controller equation had to be changed accordingly, maintaining the normal operating point. The brain blood flow controller equation expressed brain blood flow as a non-linear function of arterial blood P_{CO_2}. Consequently the model became a two level controller problem, i.e. a local blood flow control to the brain tissue compartment, and an overall ventilation control.

The results of this model were not substantially different from the previous one. In the text, some experimental data are presented,

tending to support the suggestion that the effect of cardiac output variations upon the respiratory off-transient is simulated better by this model. Clearly the added feature of a separate brain tissue compartment whose blood flow rate is dependent upon the arterial P_{CO_2}, is a realistic improvement in the model. A detailed study and simulation of these two models was presented in a report by the author in his M.Sc. dissertation [Bali, 1971].

Grodins and James [1964] provided an extended model which was used to simulate the effect of increased metabolic rate and cardiac output during exercise. This required several modifications on the previous models. The most important of these was the choice of controlling equation during exercise simulation. As a step towards this end, the authors test the hypothesis put forward by Yamamoto and Edwards [1960]- that the dynamic characteristics of controller may differ from the static and, therefore among others, a potential signal source may be the oscillatory changes in arterial P_{CO_2} which reflect the cyclic pattern of breathing. Inclusion of such a feature demanded the explicit mathematical description of the events of the respiratory cycle, making this the first respiratory system model to include a variable lung volume. This was achieved by using a sinusoidal curve to show changes in tidal volume which enabled the arterial P_{CO_2} to oscillate with the respiratory cycle, and the predictions made by Yamamoto [1960] to be tested. These were that 'the magnitude of the P_{CO_2} oscillations should change with the respiratory cycle and that in exercise states such fluctuations should increase in size without increasing the time average value,

whereas in CO_2 inhalation the size of oscillations (peak to peak) should decrease with increased average value'. This phenomenon is shown in figure 4.1.

To employ the dynamic signal from arterial P_{CO_2}, the ventilatory controller equation was modified to include integral as well as proportional control. The inclusion of integral control was based upon the assumption that in the real system, an integral control was responsible for the zero steady-state error of mean arterial blood P_{CO_2} during exercise. Other alterations in the model were as follows:

1. Blood flow rate to the brain is a function of brain tissue CO_2 concentration.

2. Cardiac output is a linear function of the total body CO_2 production.

The simulation results of this model are much better. Despite the modifications, the results are unchanged for CO_2 inhalation, but in addition, as in the organism, there is no steady state error in the mean arterial blood P_{CO_2} with increased metabolic output. The transients during onset and recession of exercise agree closely with the experimental results of Dejours [1959]. Thus one major improvement of this model is that it can be tested against a larger set of physiological experimental results. Still the model includes a large number of gross assumptions which include; zero transportation delays around the body circuit, omission of oxygen in the model and no separate compartment for the muscle tissue.

Admittedly separation of muscle tissue compartment would require another local feed-back loop i.e. muscle tissue blood flow control.

A further improvement on the model was made by Milhorn [Milhorn et al, 1965] . They were the first to include oxygen flow into the model and improved upon some of the previous assumptions, the most important being the inclusion of transport delays. But due to inclusion of oxygen some new simplifying assumptions had to be made. Some of the important features of their model are as follows:

1. Blood flow rate to the brain tissue compartment is a function of arterial blood P_{O_2} and P_{CO_2}.

2. Pulmonary ventilation is controlled by the arterial blood P_{O_2} at the peripheral chemoreceptors (Carotid - Aortic bodies) as well as the P_{CO_2} in the brain tissue.

3. Circulation times between the lung and the two tissue compartments are finite and constant.

4. The arterial blood P_{O_2} is a linear proportional function of alveolar gas P_{O_2}, i.e. a gradient exists between the two; such that the arterial blood P_{O_2} is equal to alveolar gas P_{O_2} times a constant less than unity.

5. Venous blood P_{O_2} is equal to the tissue fluid P_{O_2} at all times for each tissue compartment.

6. The O_2 dissociation curves are identical for arterial and venous blood.

When this model was simulated, the results for the steady state CO_2 inhalation and hypoxia were found to be in close agreement with the experimental evidence. The dynamic response i.e. transient results were also presented but due to lack of experimental results, the comparison was rather scant, and CO_2 inhalation transients were more rapid than experimental evidence suggested.

In 1967 Grodins [Grodins et al, 1967] presented a model of the respiratory system which is one of the most detailed to date. One of the main extensions from the previous models was the inclusion of local control loops for blood flow. The blood flow to the brain and also the total cardiac output were formulated to be a function of arterial blood P_{O_2} as well as P_{CO_2}. In addition the model included the chemical details of transport and acid-base behaviour, and the dependence of transport delays on cardiac output. These variable tissue delays were computed by considering the volume of arteries and veins to be fixed and dividing these volumes by the time integral of blood flow rate. Thus more realistic time delays were achieved within the model.

The inclusion of chemical details of acid base behaviour allowed metabolic disturbances in acid base balance to be simulated, in addition to CO_2 inhalation, hypoxia and hyperventilation. As the model included a separate cerebro-spinal fluid compartment, two control strategies were tested. In the first, the central component of control was assumed to be dependent upon chemical states of the brain tissue compartment, in the second the controller equation

included the effect of cerebro-spinal fluid hydrogen ion concentration and arterial blood P_{CO_2} and P_{O_2}.

In spite of some obvious gross assumptions, e.g. ventilation is a unidirectional flow, this model perhaps is more complete and general. In the author's own words, 'the treatment of tissue buffering and material exchange across the blood brain barrier is, at best, only a very crude first approximation'. Nevertheless this model includes all the features of the previous models with the exception of sinusoidal variations of lung volume and arterial P_{CO_2} with respiratory cycle as in Grodins and James [1964]

The models discussed above all attempt, with varying degrees of complexity, to simulate the changes in ventilation and arterial blood gas composition which follow changes in the composition of inspired gas or metabolism.

Another series of respiratory models, those of Horgan and Lange, are concerned with other features of the respiratory system behaviour namely Cheyne-Stokes respiration and the role of cerebro-spinal fluid P_{CO_2} in ventilatory regulation.

The first model [Horgan and Lange, 1962-1], like the Grodins [1954] model, consisted of two rigid compartments, lung and bulk tissue, and dealt only with CO_2. Its novel feature was the inclusion of transportation delays, possibly the first model to include circulation lags. The controller strategy implied that the controlling system had a linear Gray type response over the normal and high range of arterial P_{CO_2} but zero sensitivity on the lower ranges. A modified version of this model appeared soon after [Horgan and Lange, 1962-2].

The new model included a controller function dependent upon arterial P_{CO_2} and P_{O_2}. A non-linear expression was employed for the O_2 dissociation curve.

This new model when used to simulate the phenomenon of Cheyne-Stokes breathing following simulated hyper-ventilation, produced results which closely represented the experimental results obtained by Douglas and Haldane [1909]. The most interesting feature was the relationship it showed between periodic breathing pattern and lung to chemoreceptor circulation delays. It was predicted by the model that the longer the circulation delay, the more oscillatory became the breathing pattern. This behaviour is consistent with some experimental results available [Guyton et al, 1956]. However, quantitatively the results differed from experimental evidence in two respects. First it was necessary to employ circulation lags of between 40 seconds to 5 minutes in dogs to obtain the oscillatory pattern of respiration predicted by the model with 6 seconds lag. Second, there is no evidence that Cheyne-Stokes breathing pattern results from a sustained, voluntary hyper ventilation for 5 seconds. In addition the authors themselves agree that the model is deficient in simulating CO_2 inhalation.

In an attempt to improve the model, Horgan and Lange [1963], modified the controlling system by including three additional compartments, namely, brain tissue, ventralateral surface of the medulla and cerebrospinal fluid. It was assumed that the chemoreceptors for CO_2

are located both within the brain tissue and at the ventra-lateral surface of the medulla. The latter was treated as having neither blood flow nor metabolism and as being dependent upon cerebrospinal fluid for its chemical composition. The ventilatory equation was assumed to have two components, 40% of the response being due to the chemoreceptors at the ventrolateral surface and the remainder due to the brain tissue in contact with the arterial blood.

When the new model was simulated to study the effects of altering the cerebrospinal fluid P_{CO_2}, the results obtained for ventilation and arterial blood P_{CO_2}, were found to be similar to experimental data of Mitchel et al [1963]. Since the presumed dual nature of the ventilatory controller and several parameters for the simulation were based directly upon the results of Mitchel et al, the performance of the model in these results is hardly surprising. The model also successfully simulated CO_2 inhalation and Cheyne-Stokes breathing.

Longobardo et al [1966] published a model of human respiratory system with the view to study the causes of Cheyne-Stokes breathing. This model is very similar to the one published by Milhorn et al [1965] with two important alterations. In the controlled system the brain tissue is embodied in the bulk 'other tissue' compartment and a separate muscle tissue compartment is formulated. In the controlling system the chemoreceptors are assumed to be responsive to arterial blood P_{CO_2} and P_{O_2} rather than cerebral venous blood and response to arterial P_{CO_2} and P_{O_2} is taken to be multiplicative rather than additive as in all previous published models. Evidence for this

multiplicative relationship has been presented by Nielsen and Smith [1951]. In this study Cheyne-Stokes respiration induced in a number of situations is simulated on the model. No attempt was made to simulate relatively slow responses, such as those associated with CO_2 inhalation. The use of non-linear controller is a novel feature of the model. Here again the relationship between the circulation delays and the time period of Cheyne-Stokes respiration was emphasised.

Considering the above models it is apparent that they can be divided into two groups; Grodins, Milhorn and their associates, and Horgan, Longobardo and associates. The first group primarily concerned itself with the CO_2 inhalation and metabolic disturbances, whereas the second group concerned itself with the effects of cerebrospinal fluid in regulation of breathing and the phenomenon of Cheyne-Stokes breathing. The difference between the two groups lies mainly in the control strategy employed, i.e. the mathematical form in which controller equation for ventilation is employed. In each case a new controller function is developed to produce one or the other feature of experimental respiratory response. The models which simulated successfully the response to CO_2 inhalation, could not produce the phenomenon of Cheyne-Stokes breathing and vice-versa. With the exception of Grodins 1967 model all the models were simulated with only one control strategy. The reason for that may well be that the models have not been sufficiently general. One important feature which has been completely ignored, with the

exception of Grodins 1964 model, is that breathing consists of breaths. Oscillatory events in time with the respiratory cycle are not formulated. Another interesting aspect of the review is the process of development of the models. The models have developed step by step from a very modest [Grodins et al, 1954] to a comparatively very complex [Grodins 1967], but the development has not been altogether systematic in the sense that the effect of introducing a new feature has not always been tested for a wider range of stimuli. If at each stage of complexification the importance of one or more added parameters is more completely studied then eventually it should be possible to construct a more detailed model which predicts most of the features of the real system with greater certainty.

4.2 Several levels of mathematical representation are evident in current studies of respiratory system (as reviewed above). Some are simplistic, others more complex and yet others tend towards isomorphic description of the process of respiration. The level adopted will clearly depend upon the particular aims and objectives of the study. For example a simple representation may be adequate as a diagnostic tool for clinicians, whereas for the system scientist, seeking insight into the behaviour of the respiratory system, a model must, as far as possible, mirror the true structure and dynamics of the process.

Due to the system being very complex the approach to complete respiratory system modelling requires the adoption of lumped compartmentation, starting from a relatively simple model and adding further complex phenomena. The aim is to try to reproduce the gross effects of interactions in the real system rather than necessarily being concerned with detailed effects.

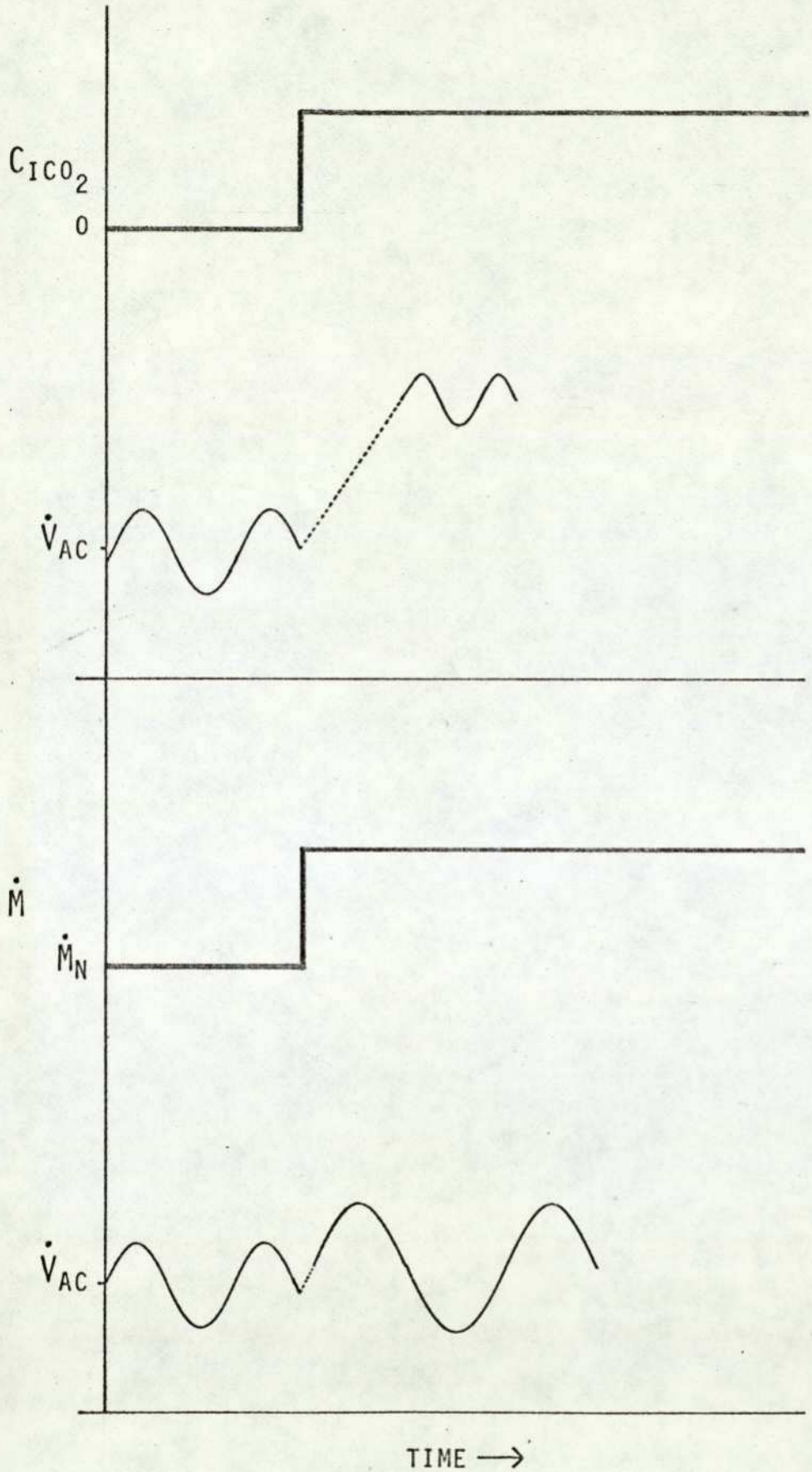

Figure 4.1

CHAPTER 5

MODEL 1. (Incorporating dead-space and time delays).

This model, as shown in figure 5.1, is a three compartment model, dead-space, lungs and tissues. Delay times due to the circulation of blood from lungs to tissues and back are also included. Apart from CO_2 breathing, the phenomenon of Cheyne-Stokes breathing is also developed in the simulation of this model. Any factor which decreases the damping of the respiratory control system would be an adequate cause of Cheyne-Stokes breathing.

The two factors are postulated to be:

1. Increased circulation delay times, which increases the delay time from lungs to the tissues.

2. Increased controller gain.

The following assumptions are introduced in the development of the model.

1. Respiration (Ventilation) is controlled by the tissue CO_2 concentration and there is a linear relationship between ventilation and tissue CO_2 concentration which holds for steady-state as well as the dynamic state.

2. Tissue elements are lumped into a single compartment.

3. The rapid changes in alveolar and blood gas concentrations with each respiratory cycle are ignored and alveolar volume is considered constant.

4. Cardiac output is considered to be constant and the pulsatile nature of the cardiac output is ignored.

5. CO_2 dissociation curves are equal and linear for arterial blood, venous blood, and tissues.

6. Venous P_{CO_2} is equal to tissue P_{CO_2}.

7. Arterial P_{CO_2} is equal to alveolar P_{CO_2}

8. Circulation times are finite and are constant during each simulation.

9. The respiratory quotient is constant and equal to unity.

5.1 DERIVATION OF EQUATIONS:

The body is divided into three compartments representing dead space, lung, and tissue (figure 5.1). The continuity equations are developed for each compartment as follows:

i. DEAD SPACE

The air pathways from the mouth down to the alveoli are known as the dead space since during inspiration they are filled with fresh air and during expiration with the alveolar gas. Thus the portion of inspired air filling these pathways does not reach the alveoli. Instead the alveolar ventilation is a mixture of inspired fresh air minus the dead space volume plus the alveolar gas in the dead space trapped at the end of the previous expiration. Thus:

Alveolar Ventilation = Total Ventilation - dead space X frequency

$$\therefore \quad \dot{V}_A = \dot{V} - V_D \cdot f \qquad (5.1)$$

where f is the respiratory frequency.

Now if V_{TV} is the tidal volume:

$$\dot{V} = V_{TV} \cdot f \qquad (5.2)$$

Assuming a linear relationship between tidal volume and respiratory frequency we can write:

$$V_{TV} = K_3 . f \qquad (5.3)$$

where K_3 is a constant.

From equations 5.2 and 5.3

$$\dot{V} = K_3 . f^2$$

$$\text{or } f = (\dot{V}/K_3)^{1/2} \qquad (5.4)$$

From equation 5.1 therefore:

$$\dot{V}_A = \dot{V} - V_D (\dot{V}/K_3)^{1/2} \qquad (5.5)$$

ii. LUNGS:

In the lungs, inputs of CO_2 are from air by ventilation and from venous blood, and outputs are to air and arterial blood, thus

$$V_L . \frac{d}{dt} . C_{ACO_2} = \dot{V}_A (C_{TCO_2} - C_{ACO_2}) + \dot{q} (C_{vCO_2} (\tau_{TL}) - C_{aCO_2}). \qquad (5.6)$$

iii. TISSUES

In the tissues inputs of CO_2 are from arterial blood and metabolic production of CO_2 and the output is to the venous blood. Thus:

$$V_T . \frac{d}{dt} C_{TCO_2} = \dot{M} + \dot{q} (C_{aCO_2} (\tau) - C_{vCO_2}) \qquad (5.7)$$

Equations (5.5) and (5.7) thus define the controlled system behaviour.

iv. CONTROLLER:

The form developed by Grodins (1954) of the controller equation is retained viz. a proportional relationship between

ventilation and the tissue CO_2 concentration as shown in figure 5.2. Thus the equation of the controlling system may be written as:

$$\dot{V} = a.\ C_{TCO_2} - b \qquad (5.8)$$

where 'a' and 'b' are constants; 'a' relating to the controller gain and 'b' evaluated from steady state results for a given 'a'. Assuming the normal steady state value of ventilation to be (Reynolds and Milhorn, 1973) 6 litre/min. for an initial value of C_{TCO_2} as $(C_{TCO_2})_o$, equation 5.8 becomes:

$$6.0 = a.\ (C_{TCO_2})_o - b$$

$$\text{and } b = a.(C_{TCO_2})_o - 6 \qquad (5.9)$$

Substituting this value of b (5.9) to equation (5.8), the controller equation becomes

$$\dot{V} = 6.0 + a\ (C_{TCO_2} - (C_{TCO_2})_o) \qquad (5.10)$$

v. CO_2 DISSOCIATION CURVE

Assuming the CO_2 dissociation curves to be the same for arterial blood, venous blood and for the tissues, we can write:

$$C_{vCO_2}(\tau) = C_{TCO_2}(\tau) \qquad (5.11)$$

Further assuming the CO_2 dissociation curve to be linear:

$$C_{aCO_2}(\tau) = (K_1\ P_B.C_{ACO_2} + K_2)\ (\tau) \qquad (5.12)$$

Figure 5.3 shows the comparison between the linearised CO_2 dissociation curve and the experimental curve, for K_1 equal to 0.00425 mm Hg (0.566 N/m^2) and K_2 equal to 0.32. The τ implies transportation delays.

The following normal values are adopted for the purpose of simulation: (Grodins et al,1954; Defaris et al,1962; Green 1970).

V_L = 3.0 ℓ V_D = 0.15 ℓ

V_T = 40.0 ℓ P_B = 760.0 mm Hg (10^5 N/m^2)

$\dot{q}$ = 6.0 ℓ/min. a = 500.0

$\dot{M}$ = 0.263 ℓ/min. K_3 = 0.035

Using these values in the system equations

$$\frac{d}{dt} C_{ACO_2} = (6.0 (C_{TCO_2}(\tau) - C_{AX}) + \dot{V}_A (C_{ICO_2} - C_{ACO_2})) / 3.0 \quad (5.13)$$

$$\frac{d}{dt} C_{TCO_2} = (0.263 + 6.0 (C_{AX}(\tau) - C_{TCO_2}))/40.0 \quad (5.14)$$

where

$$C_{AX} = 3.2 C_{ACO_2} + 0.32 \quad (5.15)$$

$$\dot{V}_A = \dot{V} - 0.15 (\dot{V}/0.035)^{1/2} \quad (5.16)$$

$$\dot{V} = 6.0 + 500.0 (C_{TCO_2} - (C_{TCO_2})_o) \quad (5.17)$$

Equations (5.13) - (5.17) were solved for various conditions as follows

1. 1, 3, 5, 7% CO_2 breathing
2. Variation of controller gain 'a'
3. Variation of time delays 'τ'

5.2 RESULTS AND DISCUSSIONS:

i. CO_2 Breathing:

In the model simulation, a step of 3%, 5% or 7% CO_2 is introduced in the ventilation at time equal to two minutes and then the step is removed at time equal to twenty two minutes and normal conditions are restored.

Graphs 5.1.1 to 5.1.3 show the time variation of ventilation due to 3%, 5% and 7% CO_2 inhalation respectively with the value of 'a' (controller gain) equal to 500. (Grodins 1954). Thin lines with crosses show the experimental curves produced by Reynolds et al (1972). Three features are evident in these results:

(a) The time course of ventilation in the model responses and the experimental results, seems to follow an exponential pattern suggesting that the system can be approximated by a first order lag. Thus structurally the model seems to represent the real system.

(b) There is a marked difference in transient responses between onset and offset of the stimuli, the latter being much faster in time. Thus it is possible to make a comparison in terms of time constants (or half times ≡ ·693 x Time Constant - as is customary in physiological studies) during dynamic states.

(c) Time to reach the steady state at the onset of step increases with increased percentage of CO_2 inhaled, but there is no marked difference in the time to reach back to prestimulus value after the removal of the step. Thus non-linearity of the system is more evident at the higher percentages of CO_2 inhaled.

Although qualitatively the model responses conform to the above features, in quantitative terms there are substantial differences between the model responses and the experimental results. The time constants of the model response are much smaller than that of the experimental results in both on transients as well as off transients. This is particularly evident for the smaller values of the step applied. In the steady state, as can be seen, the model values are

far below the experimental results and percentage error increases with the size of the step. A summary of these values and differences is given in Table 5.1.

Although there is no nonlinear element in the system equations, nonlinearity is introduced due to multiplication of $\dot{V}_A$ (function of C_{TCO_2}) and C_{ACO_2} (equation 5.6). In general it is recognised that increasing the controller gain results in a faster time response. Furthermore the analysis of controller equation suggests that the steady state value of $\dot{V}$ is directly dependent upon the value of 'a' (equation 5.9) for a given final steady state value of C_{TCO_2} after the step input of CO_2.

In an attempt to improve the model performance the controller gain was increased to the value of 1000 (a = 1000, equation 5.9). Graphs 5.1.4 to 5.1.6 show the ventilation time response to CO_2 inhalation on the experimental curves obtained by Reynold et al (1972) for comparison (Thin lines with crosses). Clearly as expected the model response is faster and the difference in steady state values between model and experimental results is very small in comparison to the previous case (a = 500). The following main features of the curves are evident:

(a) In the case of 3% CO_2 step input (graph 5.1.4) the model response is faster than the experimental results, i.e. the time constant of the predicted curve is smaller than the experimental results. On the other hand the steady state value predicted is still smaller than the experimental results. If now the controller gain is increased

for this case the steady state results may improve but the transient response will become still faster; even some oscillations may occur.

(b) In graph 5.1.5 (5% CO_2 input) the predicted results closely follow the experimental results in the dynamic as well as the steady state within the variations of experimental results.

(c) The graph 5.1.6 shows a comparison between predicted and experimental results for 7% CO_2 inhalation. It is evident that the model response is slower in the dynamic state but the steady state results are higher than the experimental results. If now the controller gain is increased to improve the dynamic response, the steady state value will become still larger.

Comparison of time constants and steady state values between the two model predictions and the experimental results is given in table 5.1.

% CO_2	25 MINUTE VALUE IN LITRES/MINUTE			TIME CONSTANT IN SECONDS					
				ON TRANSIENT			OFF TRANSIENT		
INPUT	EXPERIMENTAL	a=500	a=1000	Exp.	a=500	a=1000	Exp.	a=500	a=1000
3	11.25	9.5	9.7	94	180	84	52	60	30
5	17.4	15.4	17.4	134	168	138	48	72	42
7	41.0	28.2	42.5	194	240	216	24	110	28

Table 5.1
COMPARISON OF RESULTS FOR VENTILATION

Graphs 5.2.1 to 5.2.3 show the time response of alveolar CO_2 with CO_2 inhalation for each controller gain setting. With higher controller gain the rise in C_{ACO_2} is less than in the case of lower controller gain, which is expected because the ventilation rise is steeper and higher with a higher controller gain which reduces the CO_2 increase. The common feature of each response is that the over-shoot of the C_{ACO_2} at the onset of the step, decreases with increased CO_2. This phenomenon is found experimentally by Reynolds et al (1972).

ii. Cheyne-Stokes Breathing:

The phenomenon of Cheyne-Stokes breathing is the oscillations in ventilation with time, with or without periods of 'apnoea' i.e. zero breathing. The two parameters tested are the variation in controller gain and/or increased transportation delays. Once the required time delay and controller gain are set, the model is allowed to run for 2 min at which point a step input of 3% CO_2 is applied. This step is removed at time equal to 5 min.

Graphs 5.3.1 to 5.3.3 show the effect of increasing controller gain on the time response of ventilation. With the gain equal to 4, oscillations appear but are damped and no periods of apnoea occur, but with the gain increased to 6 and 8, sustained oscillations appear with periods of apnoea. Thus it can be concluded that for a given time delay (48 seconds in these graphs), the presence and absence of Cheyne-Stokes breathing depends upon controller gain. Three separate features are evident from the study of these graphs (Graphs 5.3.1 to 5.3.3):

1. The maximum ventilation during sustained oscillations increases with increased controller gain; i.e. maximum ventilation is a function of controller gain.

2. The period of apnoea increases with increased gain.

3. Time period of the sustained oscillation increases with increased controller gain.

Graphs 5.4.1 and 5.4.2 show the effect of varying time delay on the Cheyne-Stokes breathing for a given controller gain. It can be seen that the periods of apnoea, i.e. the time for which there is zero breathing, remains unchanged and so does the peak ventilation during each oscillation with the change in circulation delay. However the time period decreases with increased circulation delay.

iii GENERAL DISCUSSION:

From the above analysis it can be concluded that the structural features of the model responses are similar in pattern to the experimental results, although the model contains some gross simplifications. The characteristics of the controller functions were developed from empirical relationships between the system variables. No 'a priori' knowledge exists for the controlling system and therefore the controller gain was changed - to improve model performance. Even with doubling the gain, although the dynamic and steady state predictions of the model improve, as shown in Graph 5.1.6, the dynamic response is still much slower in the model prediction than the experimental results and the steady state result is higher. Thus two conclusions can be drawn from the CO_2 breathing results:

1. The characteristics of the proportional controller should be changed with the percentage inhalation of CO_2.

2. There is a possibility of a dynamic term in the controller, i.e. the controller not only responds to the changes in the tissue CO_2 concentration but also to the rate of change of tissue CO_2 concentration. In other words a differential plus preoportional controller should be postulated.

The study of the stability of the system utilising CO_2 control only has indicated two factors which by themselves can produce the phenomenon of Cheyne-Stokes breathing. These are (1) increased circulation delays and (2) increased controller gain.

Although the parameter changes required to produce Cheyne-Stokes breathing are well outside the physiological limits, this exercise shows the importance of time delays and controller gain in the Cheyne-Stokes breathing. It is probable that cardiac patients who have enlarged left hearts, and therefore, increased lung to brain tissue circulation times, and are exhibiting Cheyne-Stokes breathing are those patients who normally have higher than normal controller gain, since the two factors, controller gain and circulation time, are additive.

The failure to produce Cheyne-Stokes breathing with physiologically feasible model parameters may well stem from the omission of oxygen from the model equations. It is a physiological fact that any decrease in oxygen level in arterial blood tends to increase the controller gain. This will occur, particularly in apnoea with the rise in CO_2 concentration in arterial blood. Thus the inclusion of oxygen control in the model may well enable Cheyne-Stokes breathing to be produced with transport delay values which are within reasonable limits.

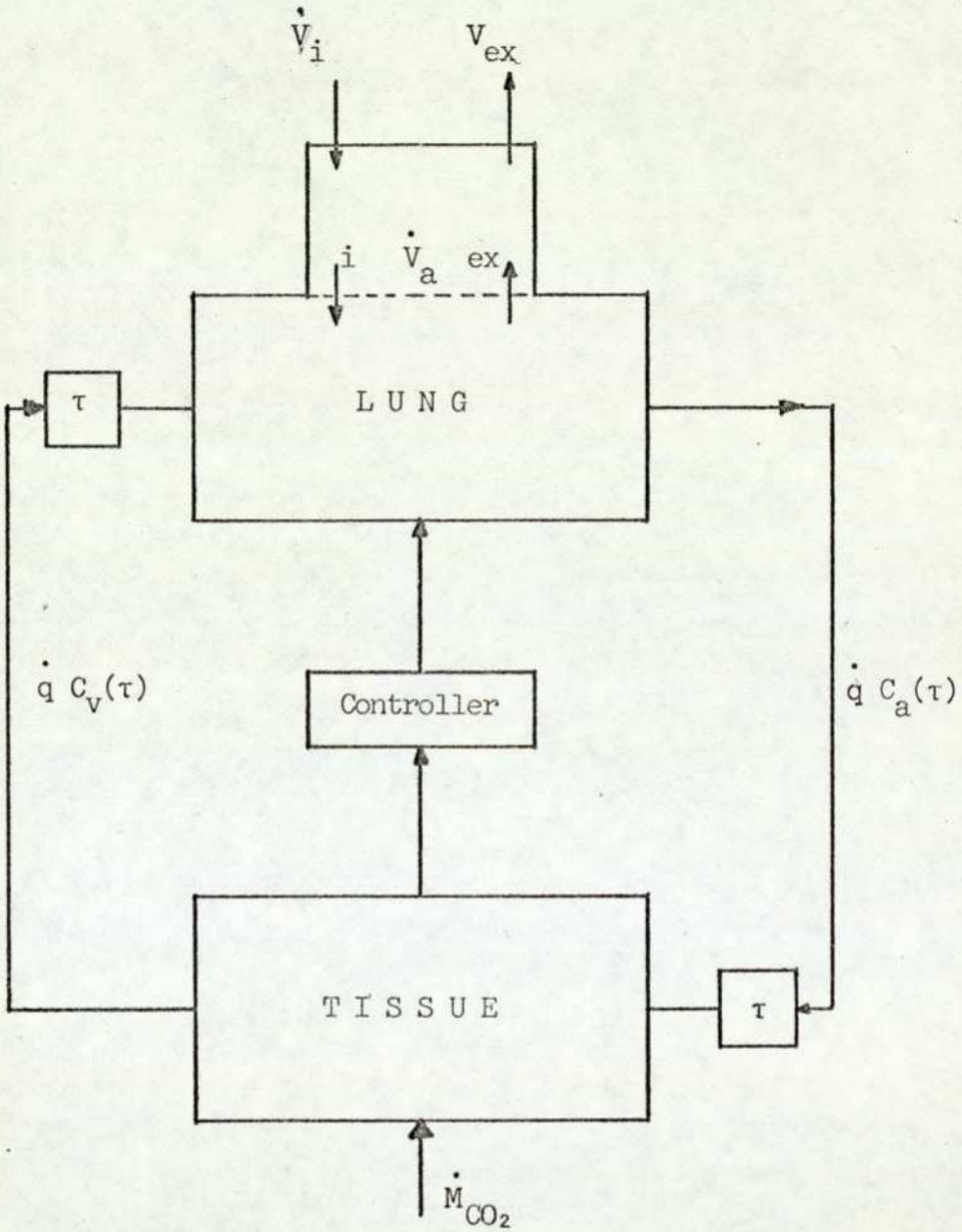
$\dot{V}_i$
V_{ex}
i
$\dot{V}_a$
ex
τ
LUNG
$\dot{q}\ C_v(\tau)$
Controller
$\dot{q}\ C_a(\tau)$
TISSUE
τ
$\dot{M}_{CO_2}$

Figure 5.1

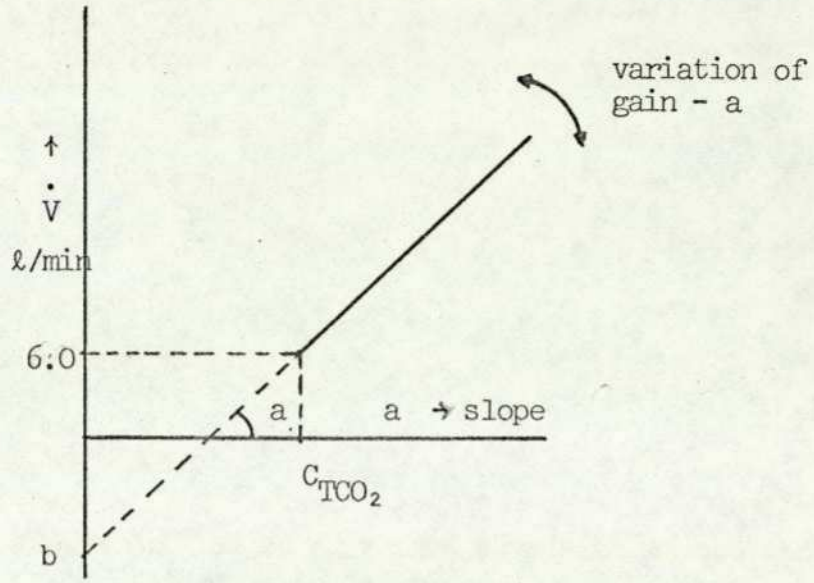

figure 5.2

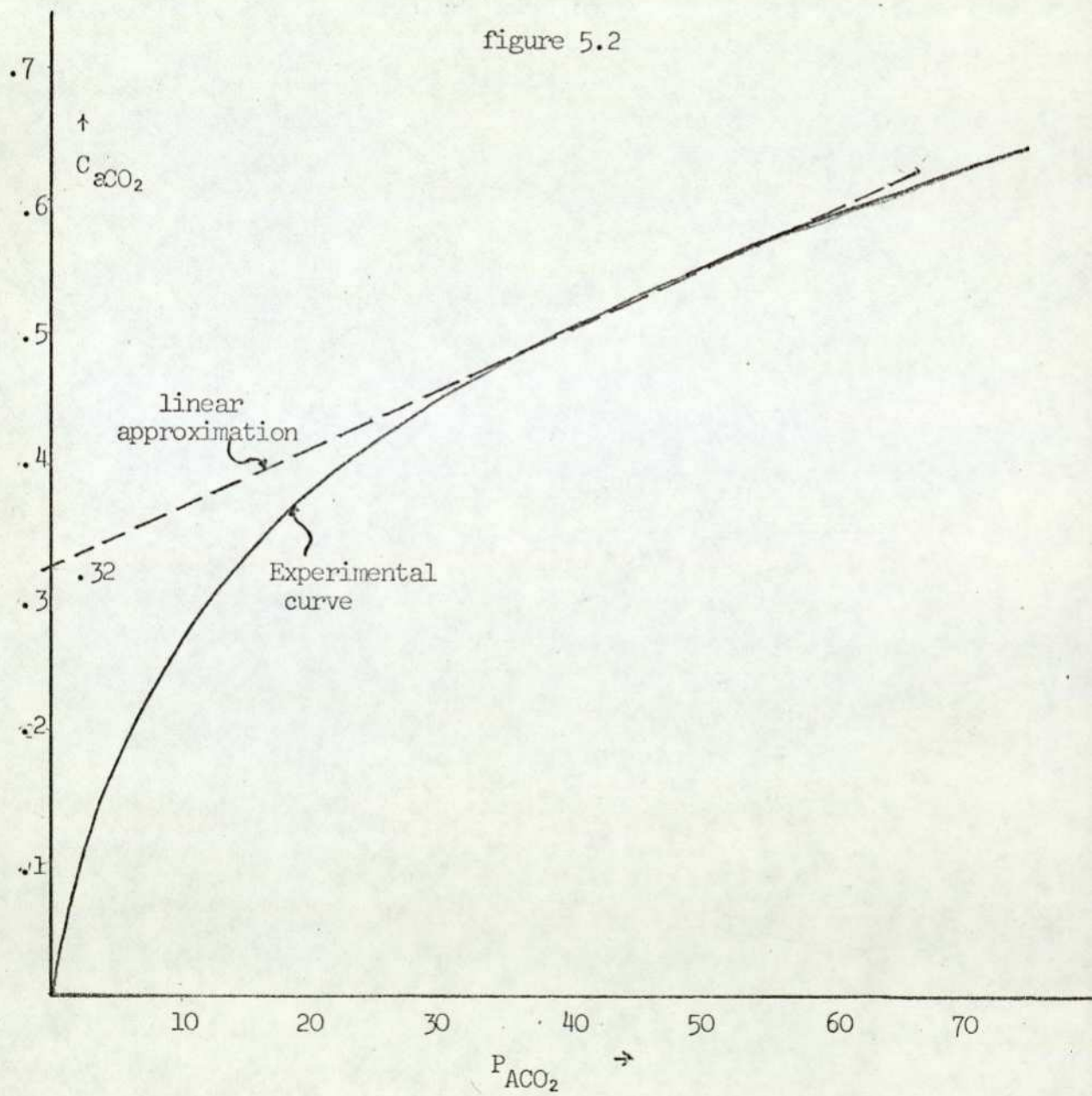

Figure 5.3

Graph 5.1.1

C_{ICO_2} = 3% a = 500

* Experimental points

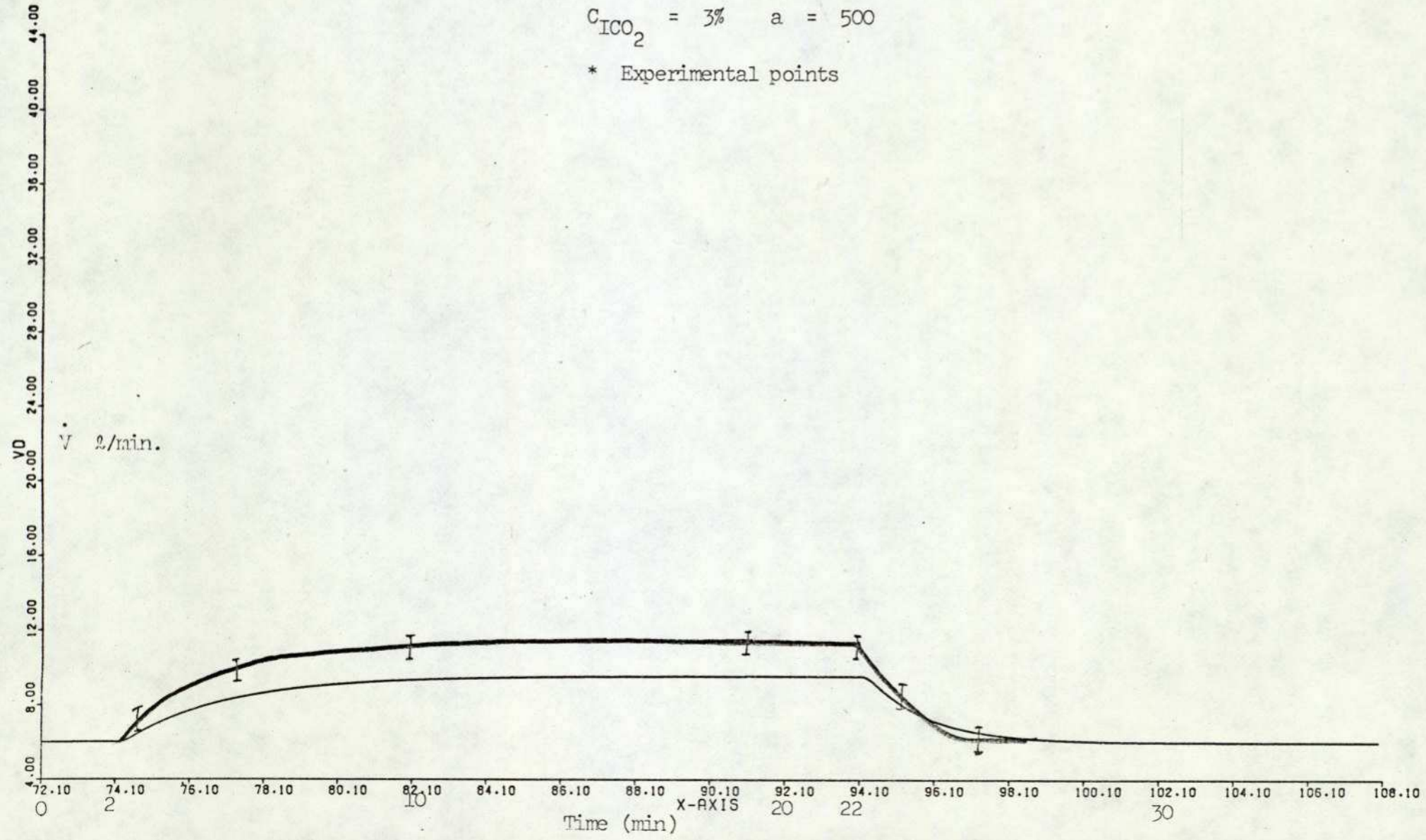

Graph 5.1.2

C_{ICO_2} = 5% a = 500

* Experimental results

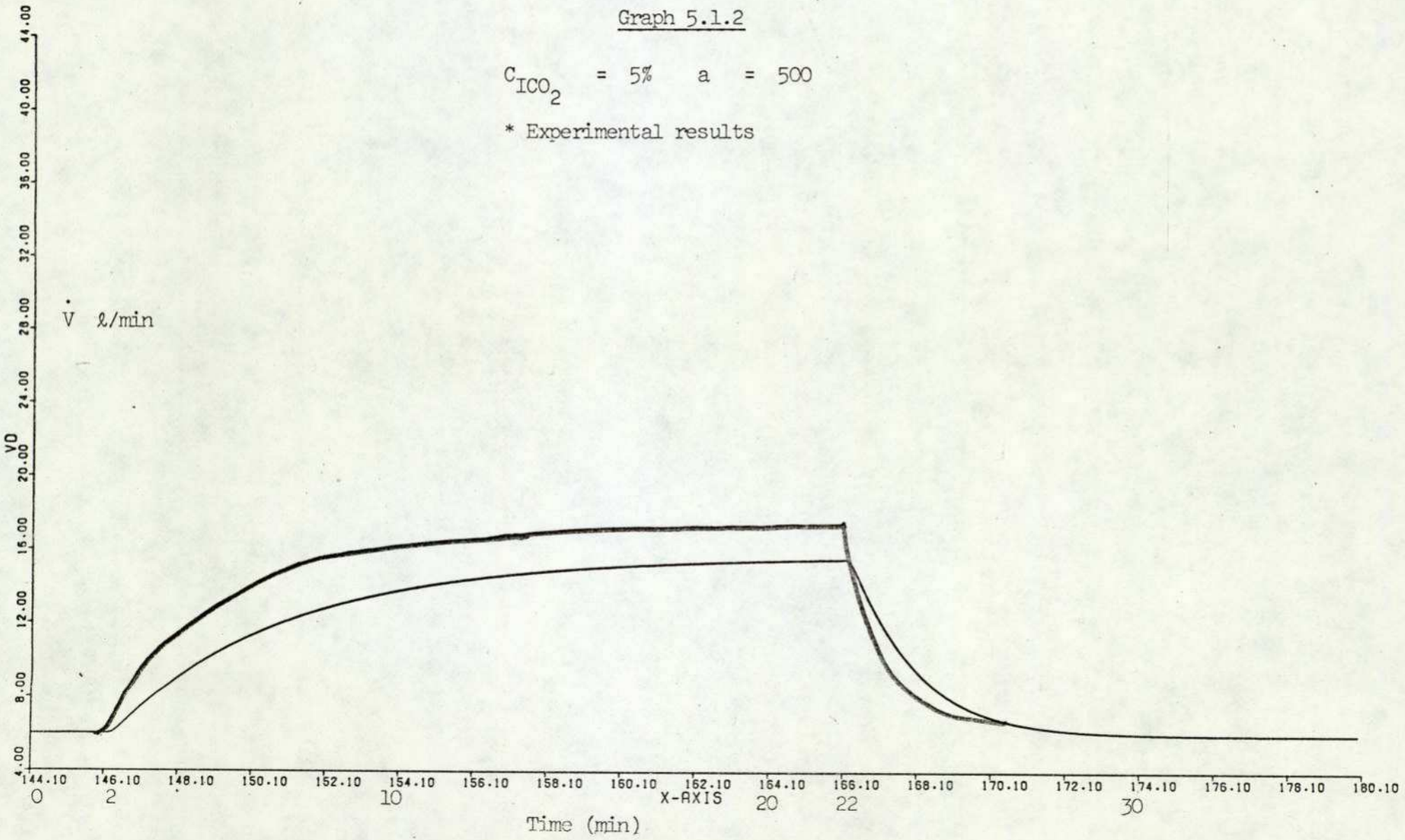

Graph 5.1.3

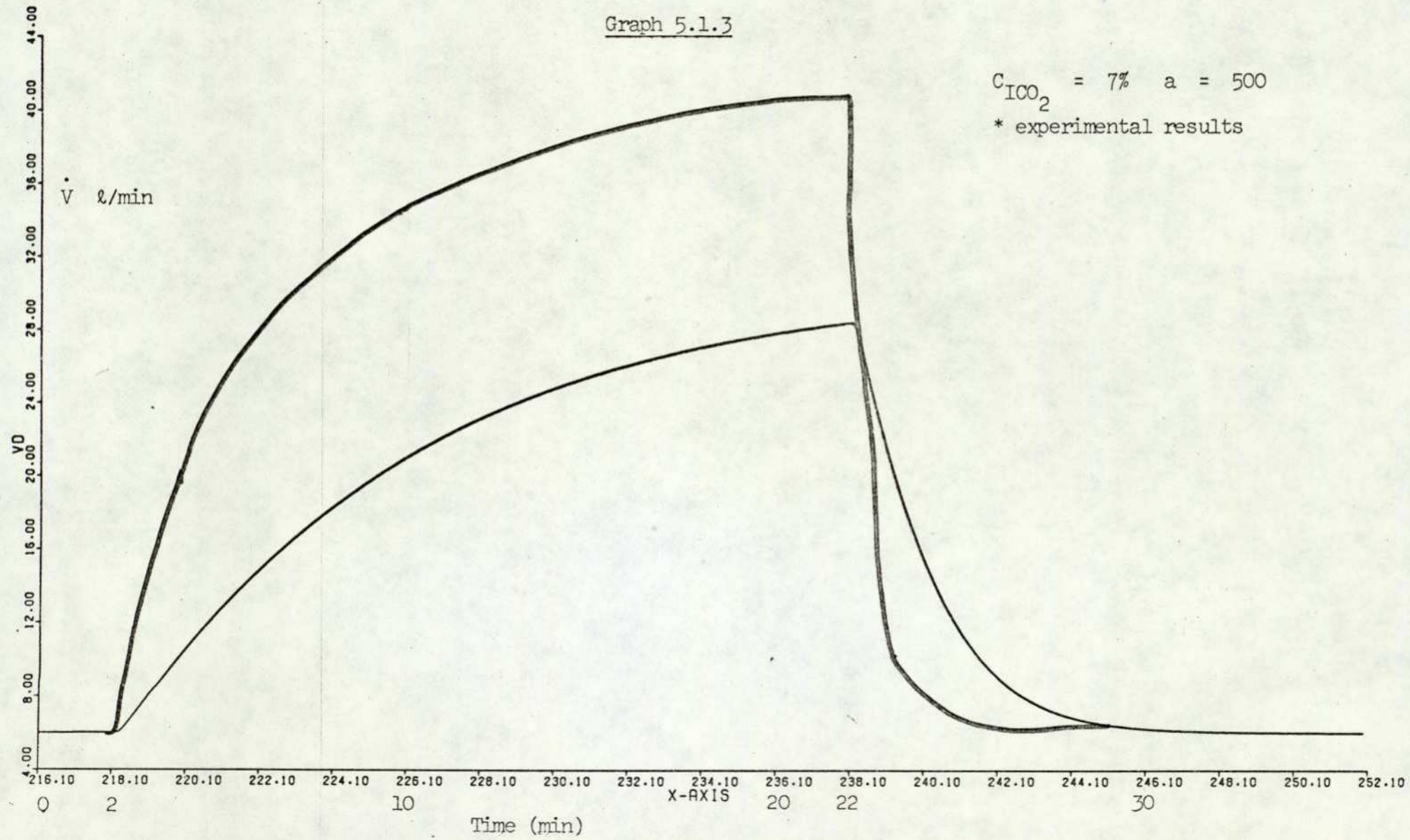
C_{ICO_2} = 7% a = 500
* experimental results
$\dot{V}$ ℓ/min
VD
4.00
8.00
12.00
16.00
20.00
24.00
28.00
32.00
36.00
40.00
44.00
216.10
218.10
220.10
222.10
224.10
226.10
228.10
230.10
232.10
234.10
236.10
238.10
240.10
242.10
244.10
246.10
248.10
250.10
252.10
0
2
10
X-AXIS
20
22
30
Time (min)

Graph 5.1.4

C_{ICO_2} = 3% a = 1000

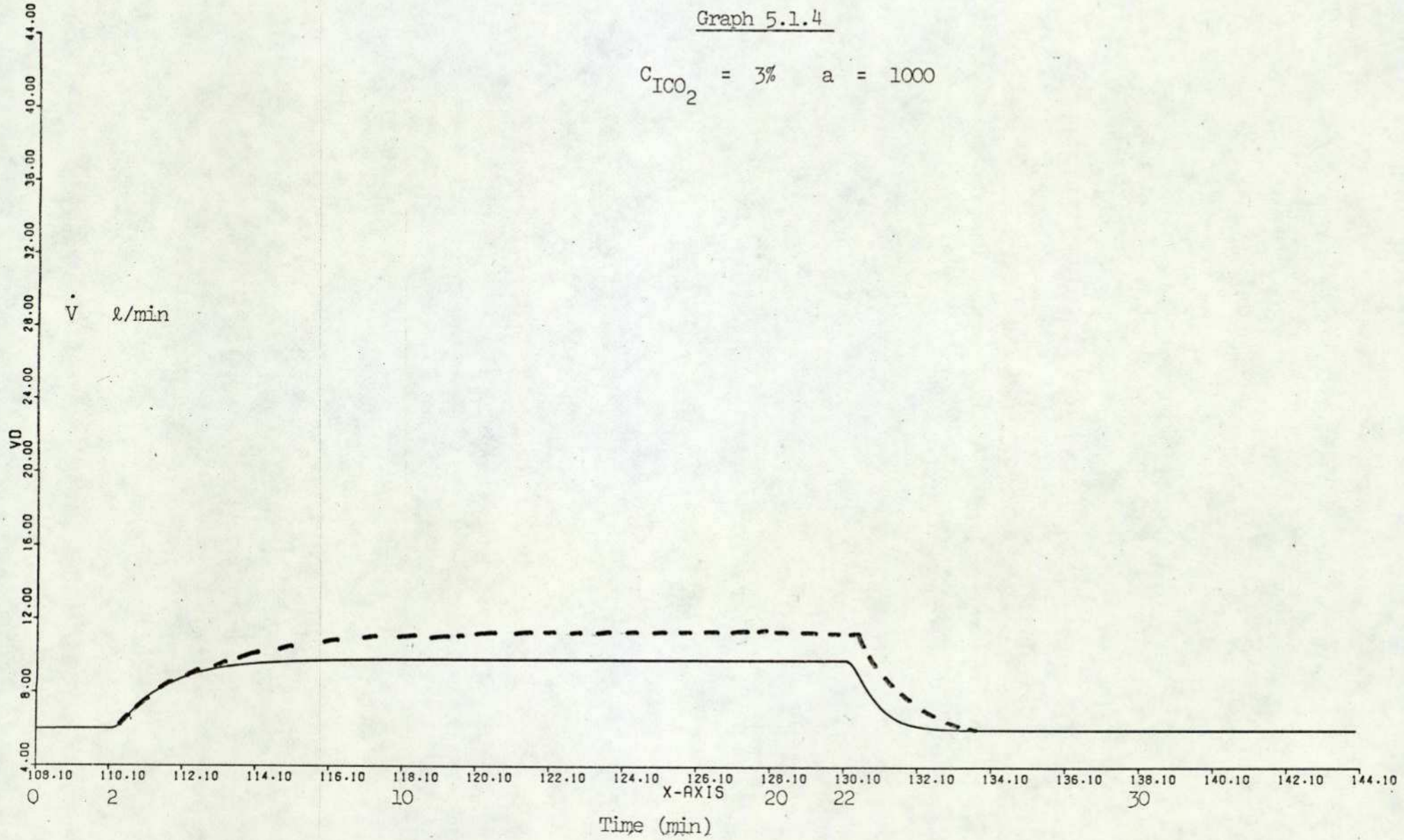

Graph 5.1.5.

C_{ICO_2} = 5% a = 1000

* Experimental results

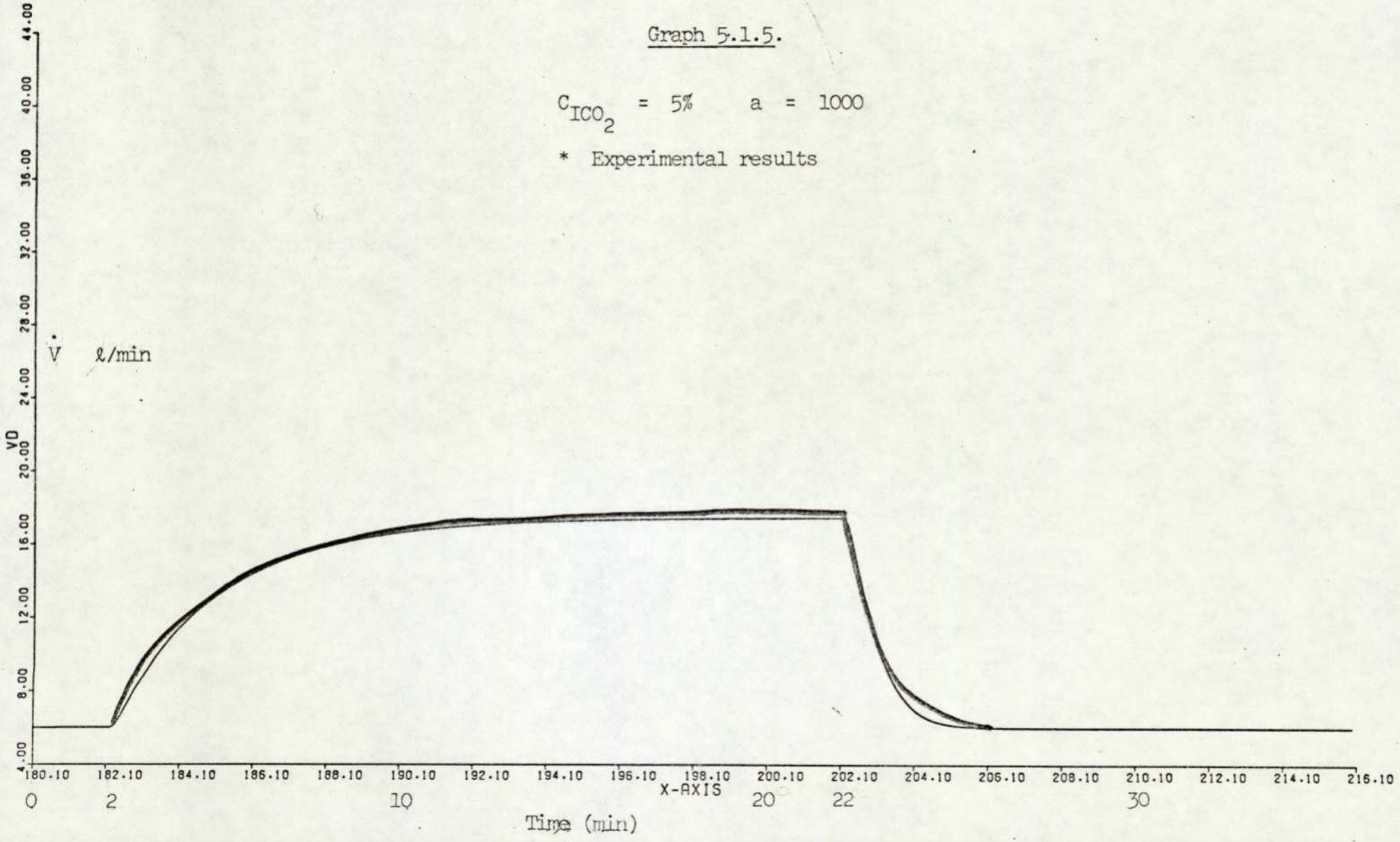

Graph 5.1.6

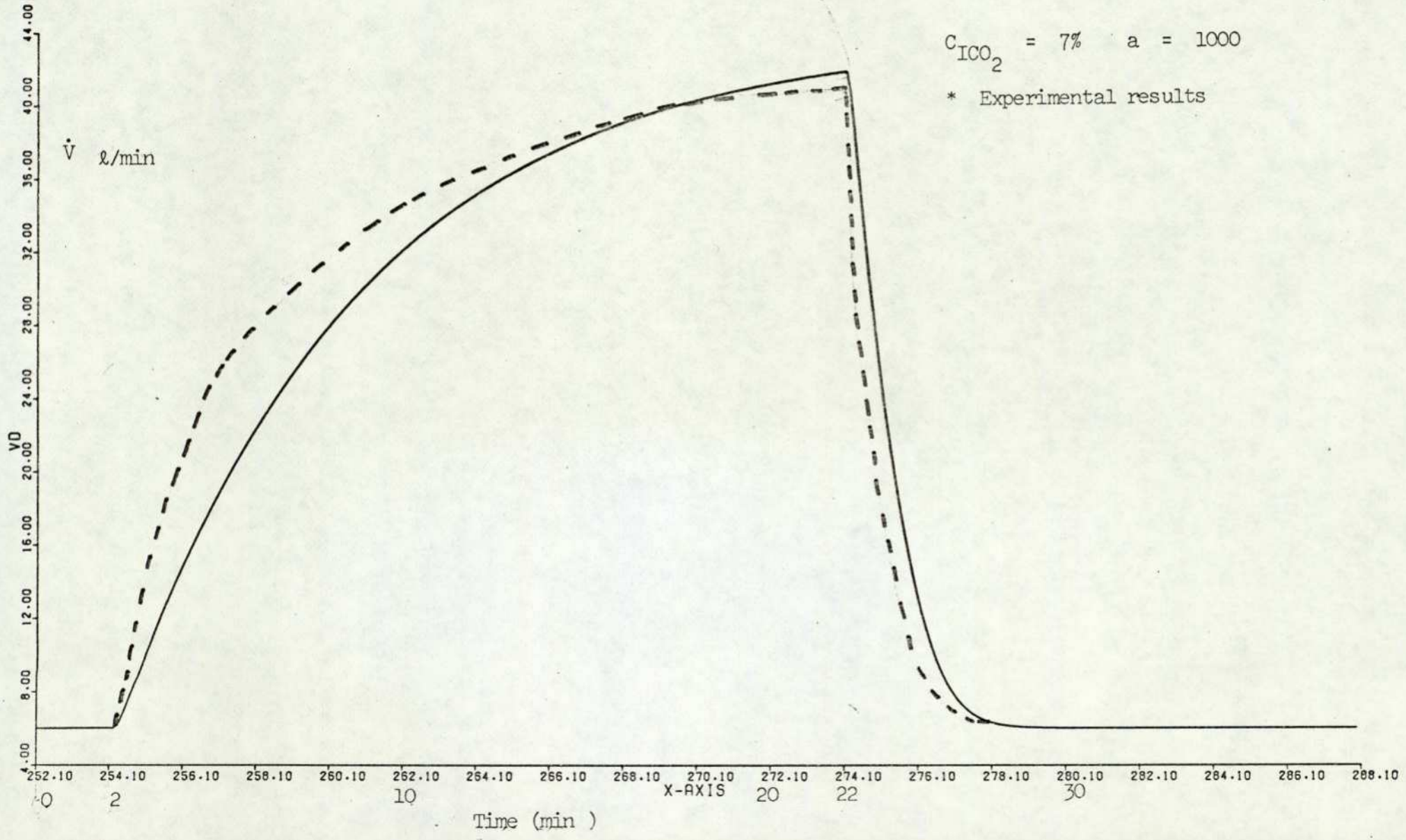
C_{ICO_2} = 7% a = 1000
* Experimental results
$\dot{V}$ ℓ/min
VD
44.00
40.00
36.00
32.00
28.00
24.00
20.00
16.00
12.00
8.00
4.00
252.10
254.10
256.10
258.10
260.10
262.10
264.10
266.10
268.10
270.10
272.10
274.10
276.10
278.10
280.10
282.10
284.10
286.10
288.10
0
2
10
20
22
30
X-AXIS
Time (min)

Graph 5.2.1.

C_{ICO_2} = 5%

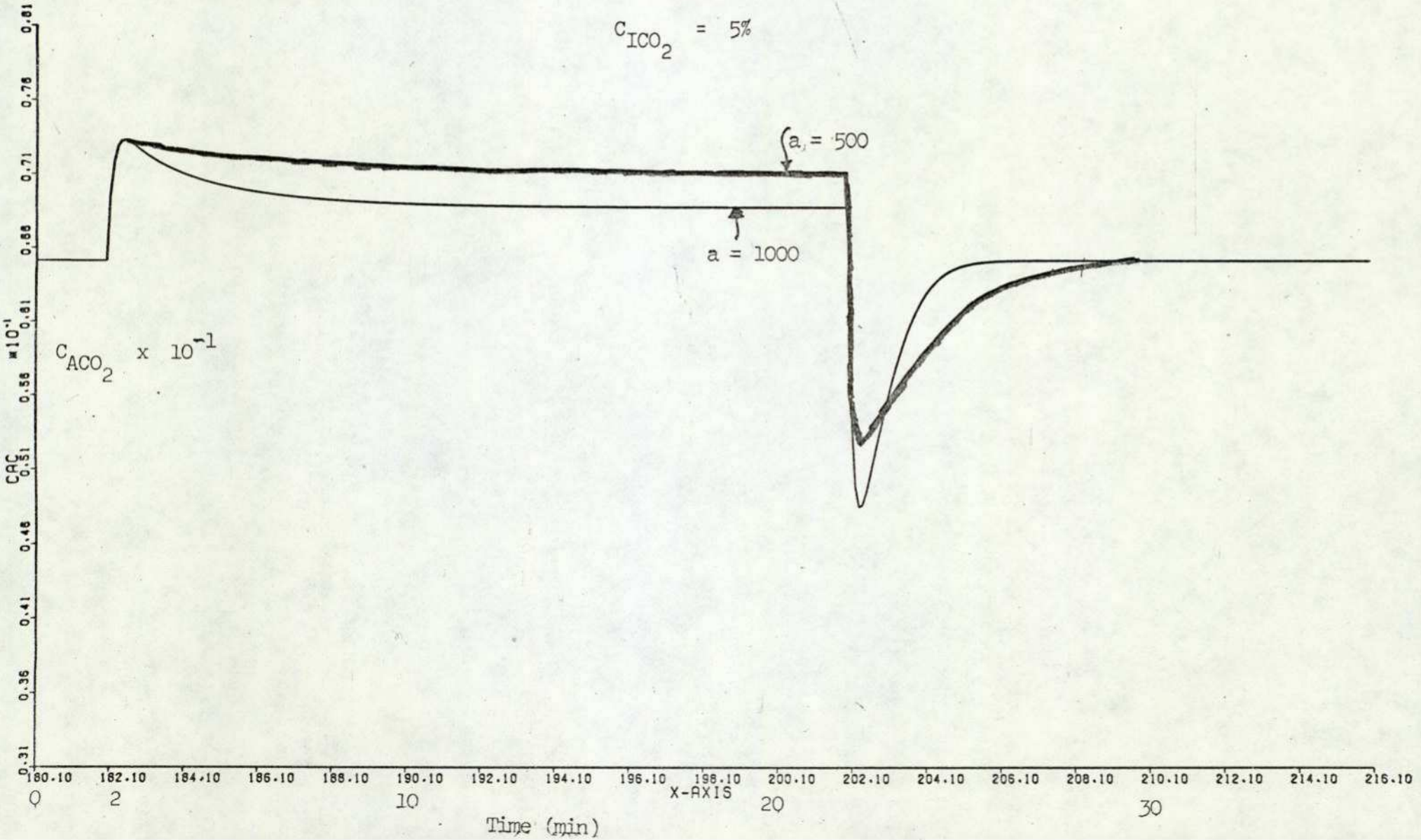

Graph 5.2.2.

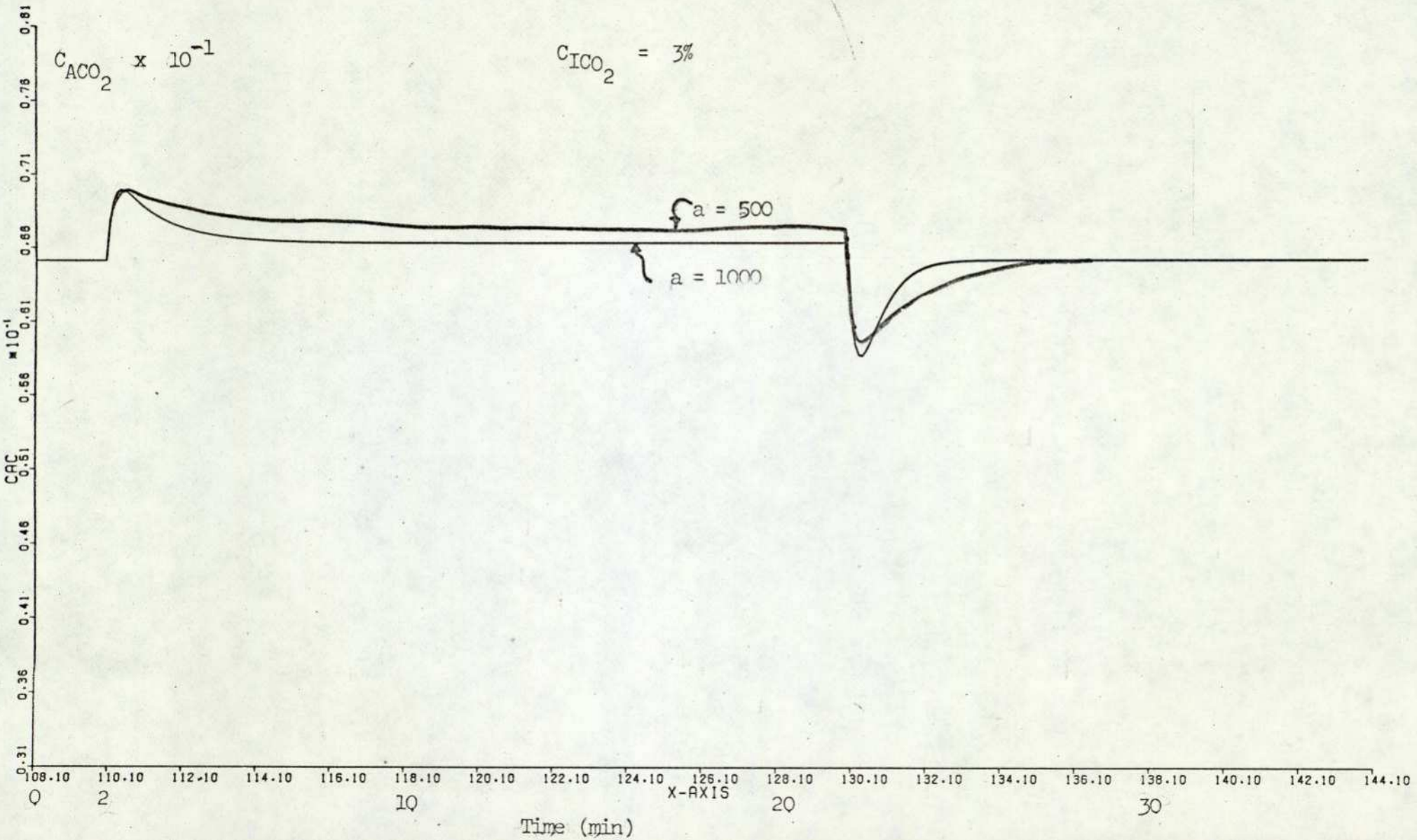
C_{ACO_2} x 10^{-1}
C_{ICO_2} = 3%
a = 500
a = 1000
CAC
0.81
0.76
0.71
0.66
0.61
0.56
0.51
0.46
0.41
0.36
0.31
108.10
110.10
112.10
114.10
116.10
118.10
120.10
122.10
124.10
126.10
128.10
130.10
132.10
134.10
136.10
138.10
140.10
142.10
144.10
0
2
10
20
30
X-AXIS
Time (min)

Graph 5.2.3.

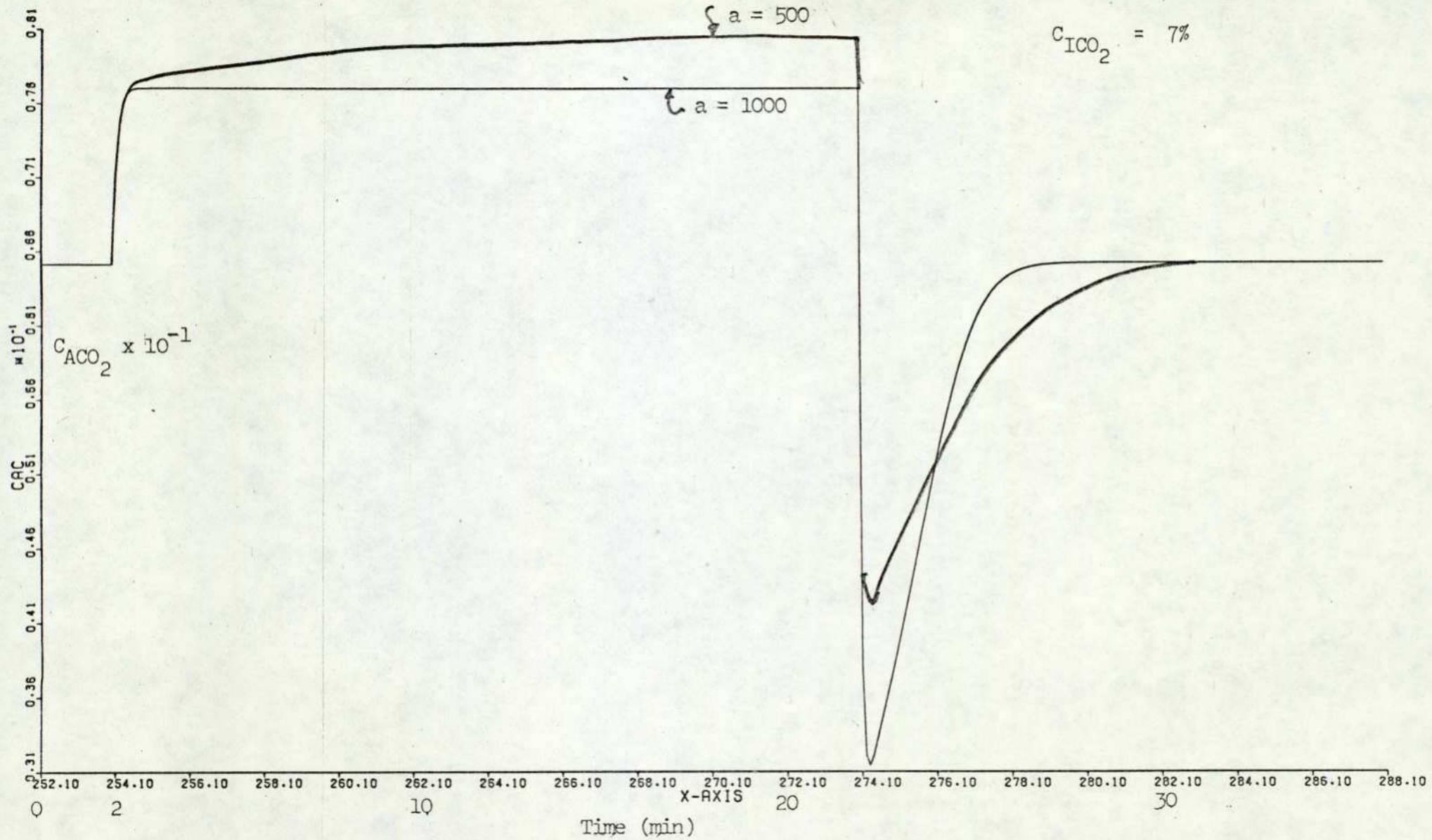
a = 500
a = 1000
C_{ICO_2} = 7%
C_{ACO_2} x 10^{-1}
CAC
0.81
0.76
0.71
0.66
0.61
0.56
0.51
0.46
0.41
0.36
0.31
252.10
254.10
256.10
258.10
260.10
262.10
264.10
266.10
268.10
270.10
272.10
274.10
276.10
278.10
280.10
282.10
284.10
286.10
288.10
X-AXIS
0
2
10
20
30
Time (min)

Graph 5.3.1.

TDL → 48 sec.

Gain → 4 x normal

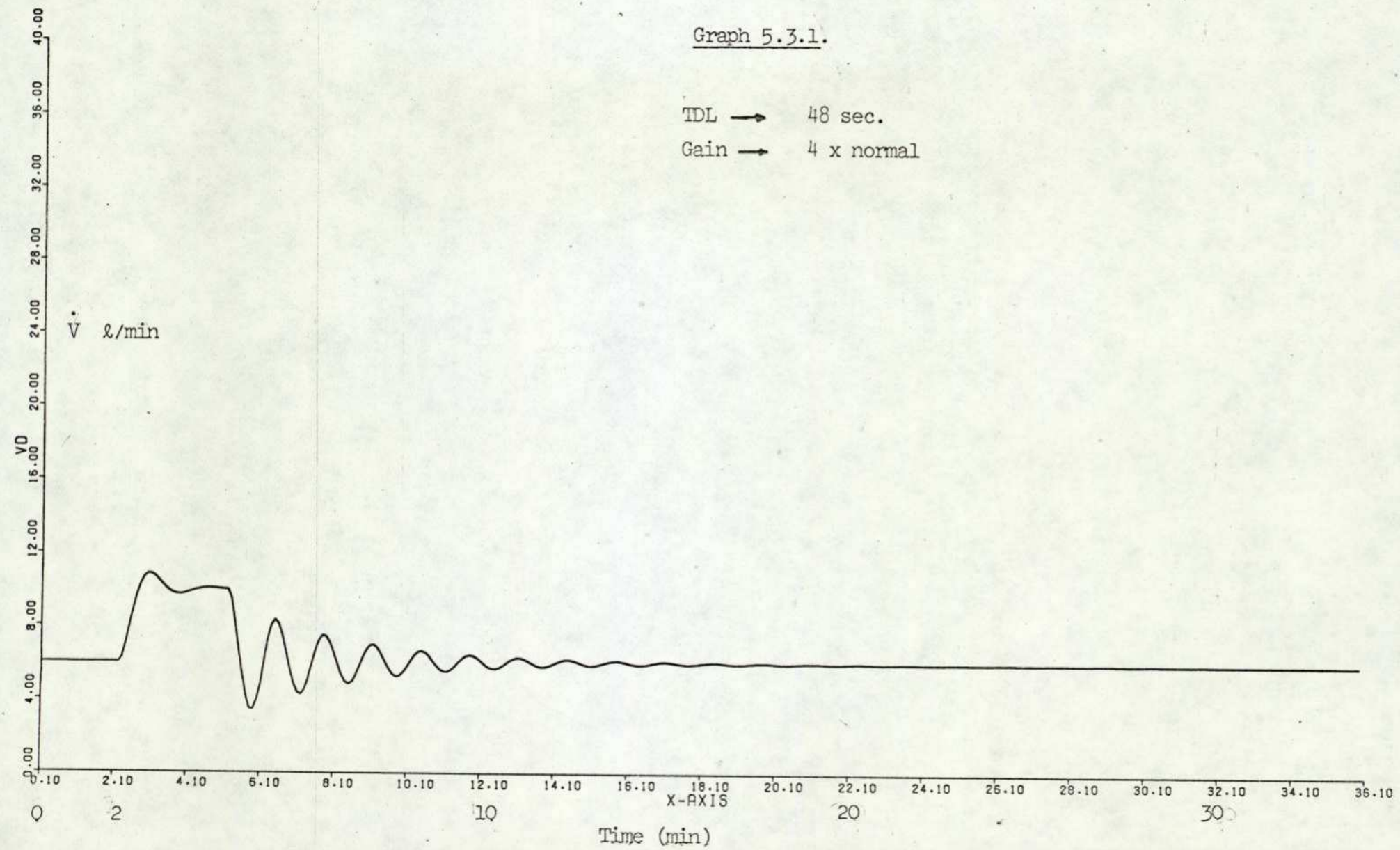

Graph 5.3.2.

TDL 48 sec.

Gain 6 x normal

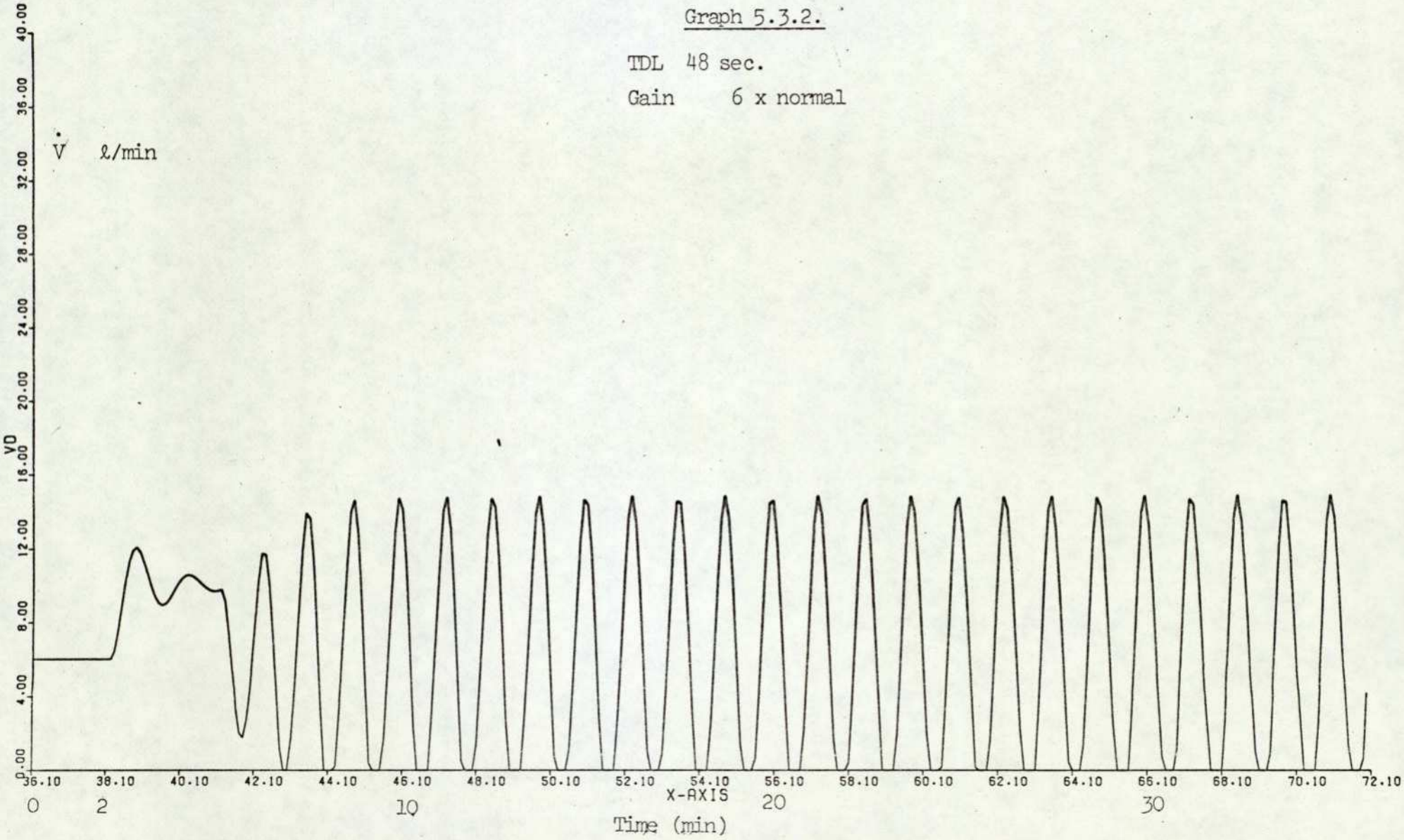

Graph 5.3.3.

TDL 48 sec.

Gain 8 x normal

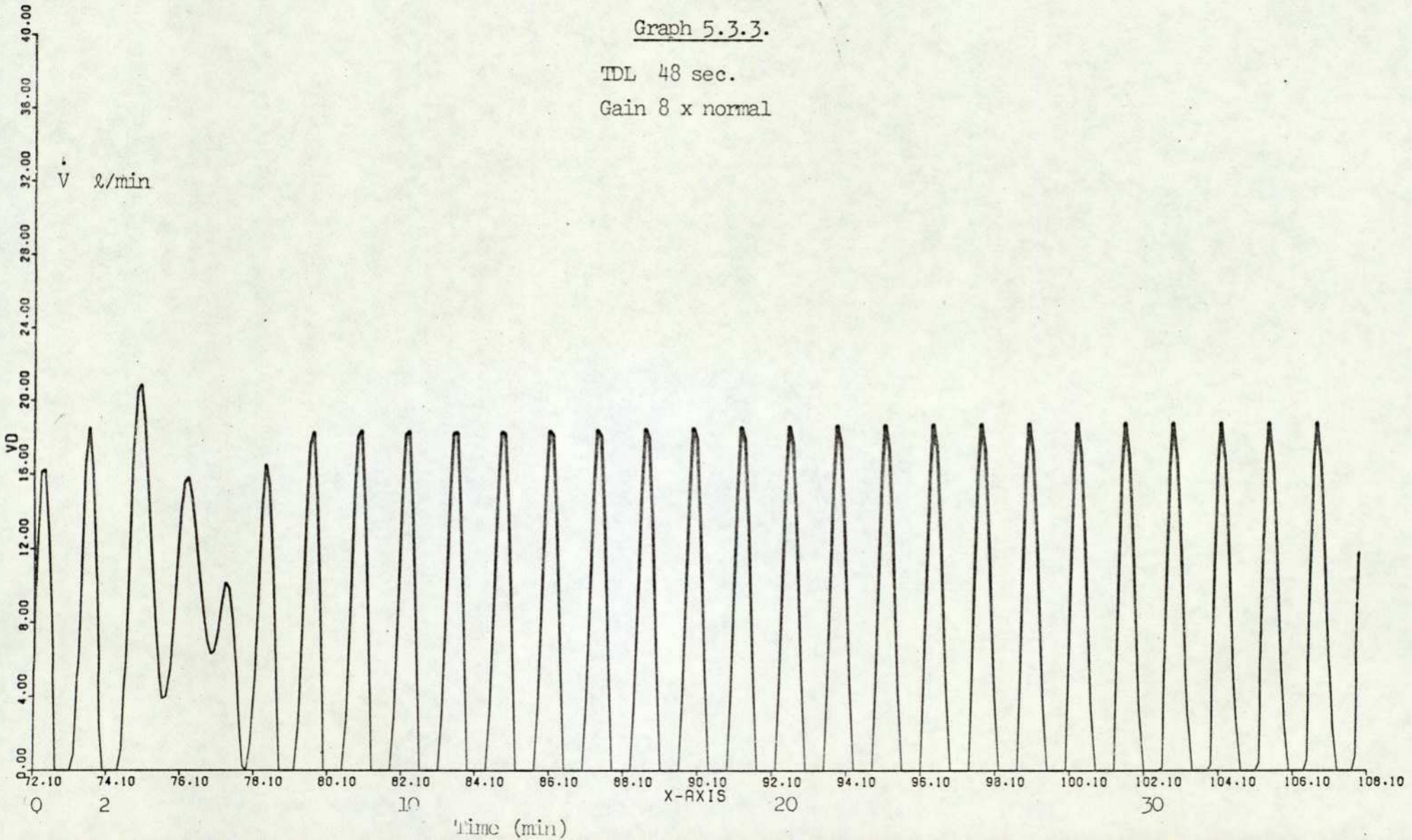

Graph 5.4.1.

Gain 14

Delay 1 min.

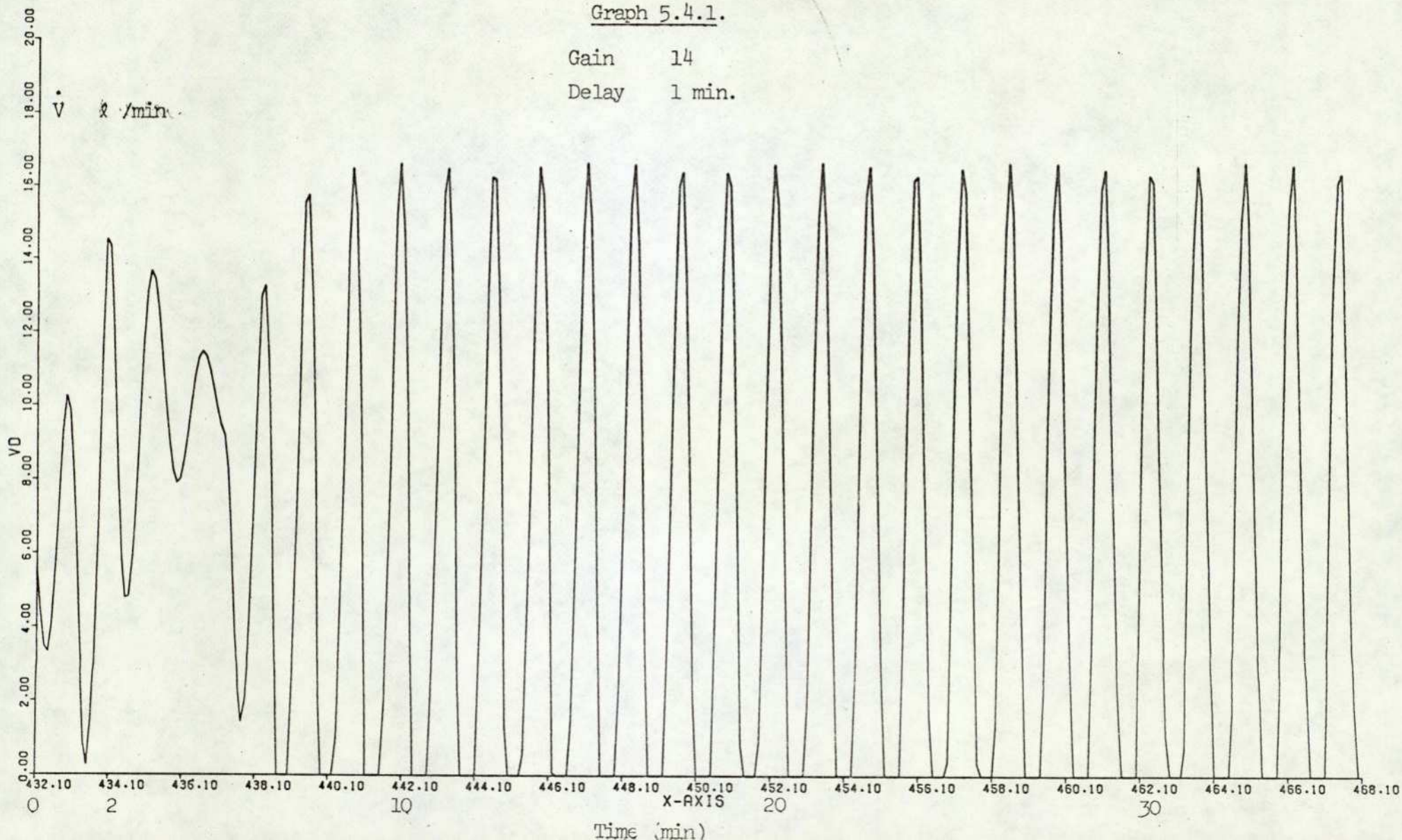

Graph 5.4.2.

Gains 14

Delay 4 min.

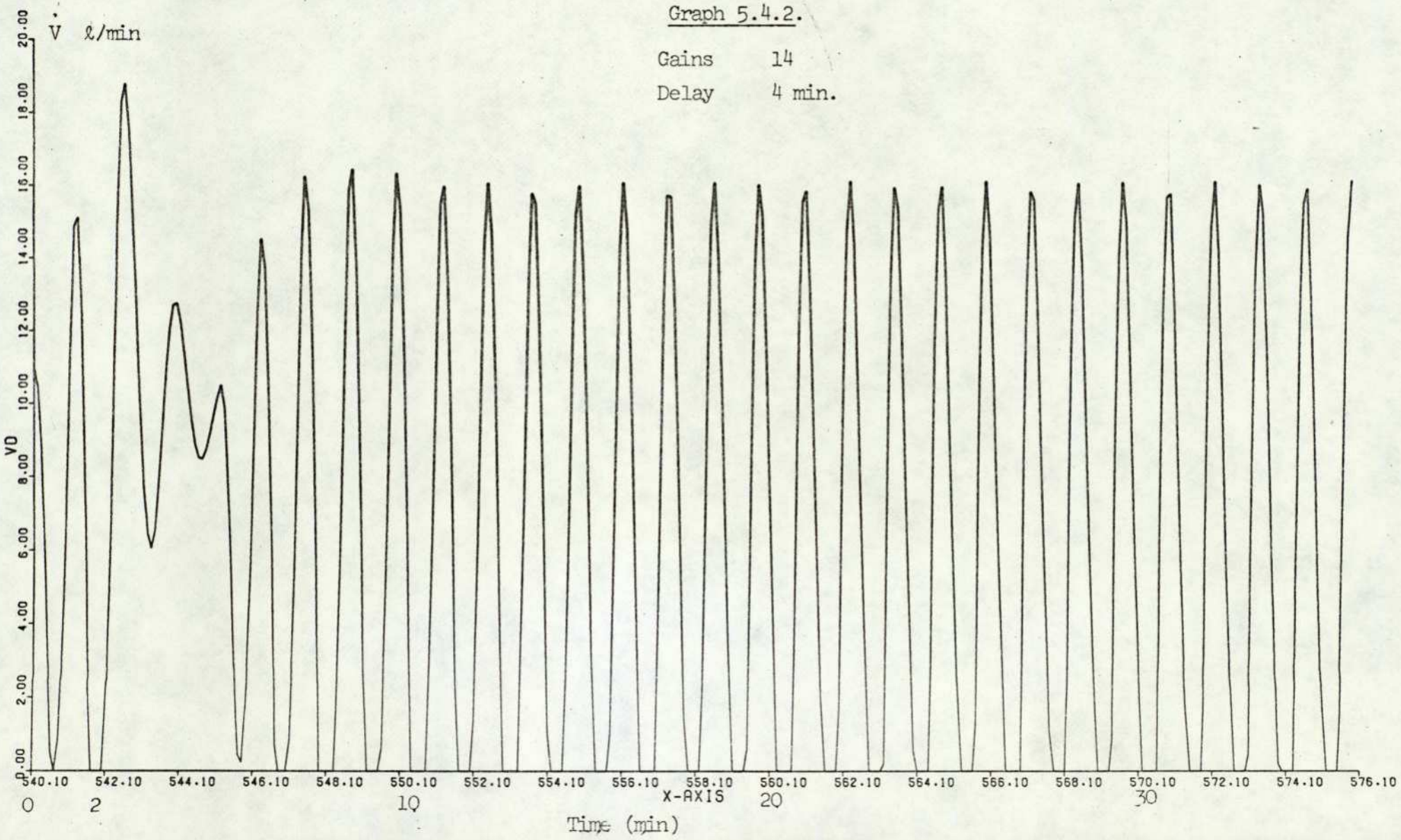

CHAPTER 6

MODEL II (INCORPORATING OXYGEN)

In the previous chapter (5) the inadequacy of the proportional controller (Grodins, 1954) in producing Cheyne-Stokes breathing was discussed. However, it is established that the two factors responsible for the Cheyne-Stokes breathing are the controller gain and the circulation delays and it is proposed that inclusion of oxygen in the controller equation may well produce Cheyne-Stokes breathing within physiologically feasible parameters of the model. Thus the following improvements are made on the previous model.

1. Oxygen as well as carbon dioxide is included in the model formulation.

2. Along with the previous controller equation, a new controlling system is postulated, that ventilation is a function of arterial CO_2 and O_2 concentrations.

3. The body respiratory quotient is less than unity, i.e. the total CO_2 production of the body tissues is less than the total O_2 consumption of the body tissues.

Apart from the above, all the assumptions made in the previous model are retained and further following simplifications are postulated:

1. Oxygen dissociation curves are equal for arterial and venous blood and the two tissue compartments. Due to gross non-linearity of the oxygen dissociation curve, a three part linear representation is assumed. (Figure 6.2).

2. Muscle and other tissue compartments are at equal time distance from the lung on the arterial as well as the venous side.

3. Arterial chemoreceptors are situated at half the distance between the lung and the tissues and are responsive to the arterial carbon dioxide as well as oxygen concentrations.

4. The partial pressure of alveolar oxygen is equal to that of arterial blood, and the venous blood P_{O_2} is equal to tissue P_{O_2} at all times.

6.1 STRUCTURE AND FORMULATION OF THE MODEL

The present model of the respiratory control system is divided into a regulated system and controller. The regulated system consists of the stored quantities of oxygen and carbon dioxide in body tissues and in the lung, as described by Fahri and Rahn (1955 and 1960). The magnitudes of these stores are reflected in the arterial and venous carbon dioxide and oxygen gas concentrations in the blood. There are two types of controllers used in the body. In the first controller, ventilation is considered to be linearly dependent upon the mixed venous CO_2 concentration. The second controller consists of chemoreceptors that are sensitive to arterial CO_2 and O_2 concentration changes and directly effect ventilation. Although these effects are not the only ones, for the present other stimuli are considered to affect ventilation by modifying the relationship between the P_{CO_2} and P_{O_2} and ventilation.

The functional diagram of the model is given in figure 6.1.

6.1.1 Arterial Stores

The arterial carbon dioxide and oxygen stores contain these two

gases at a partial pressure which is identical with the corresponding gas tensions of the arterial blood. This compartment is made up of the arterial blood and the functional residual capacity of the lung. (chapter 2).

The dynamic equations, using the principal of continuity, for the gases in arterial stores can be written as follows:

(i) CO_2 :

$$\frac{d}{dt}\left(\frac{V_r}{P_B-47} \cdot P_{ACO_2} + V_a \cdot C_{aCO_2}\right)$$

$$= \dot{q}\,(C_{vCO_2}(\tau) - C_{aCO_2}) + \frac{\dot{V}}{P_B-47}\,(P_{ICO_2} - P_{aCO_2}) \qquad \ldots. \quad 6.1$$

where $\dot{q}\,(C_{vCO_2}(\tau) - C_{aCO_2})$ is the net rate at which CO_2 is brought into the arterial store by blood, $\frac{\dot{V}}{P_B-47}\,(P_{ICO_2} - P_{aCO_2})$ is the net rate at which the CO_2 is brought to the arterial stores from the atmosphere by ventilation (P_{ICO_2} is normally zero except in the case of CO_2 breathing). The arterial stores have been divided into two terms: $\frac{V_r}{P_B-47} P_{ACO_2}$, which equals the CO_2 storage as gas in the functional residual capacity and $V_a.C_{aCO_2}$, which equals the CO_2 storage in the arterial blood.

(ii) O_2 :

similarly for oxygen we can write

$$\frac{d}{dt}\left(\frac{V_r.P_{AO_2}}{P_B-47} + V_a.C_{aO_2}\right)$$

$$= \dot{q}\,(C_{vO_2}(\tau) - C_{aO_2}) + \frac{\dot{V}}{P_B-47}\,(P_{IO_2} - P_{aO_2}) \qquad \ldots. \quad 6.2$$

6.1.2. Venous Stores:

There are two venous stores. The first compartment (venous CO_2 stores in the muscle) consists of the gas stored in the muscle and is in equilibrium with the gas partial pressure of venous blood leaving the muscle. The second (venous gas stores in the other tissues) consists of the gas stored in all other tissues in the body except muscle. The gas partial pressure of these tissues is the same as that of the venous blood leaving these tissues.

(i) CO_2 :

Equations similar to those of arterial stores can be written for the venous stores:

a) Muscle Tissue:

$$\frac{d}{dt}\left(V_m \cdot C_{m\,CO_2}\right) = \dot{M}_m + \dot{q}_m \left(C_{a\,CO_2}(\tau) - C_{vmCO_2}\right) \quad \ldots\ldots 6.3$$

where $V_m \cdot C_{m\,CO_2}$ is the CO_2 in the muscle tissue, $\dot{q}_m \left(C_{a\,CO_2}(\tau) - C_{vm\,CO_2}\right)$ is the net rate at which CO_2 is being added to the tissue compartment (in fact $C_{vm\,CO_2}$ is normally higher than $C_{a\,CO_2}$, thus the quantity is - ve; representing removal of CO_2 from the tissue store) and $\dot{M}_m$ is the metabolic rate of muscle tissue CO_2 production.

b) Other Tissues:

Similarly for the compartment to which all the remaining tissues of the body are assigned:

$$\frac{d}{dt}\left(V_{OT} \cdot C_{OTCO_2}\right) = \dot{M}_{OT} + \dot{q}_{OT} \left(C_{aCO_2}(\tau) - C_{vOTCO_2}\right) \quad \ldots\ldots 6.4$$

(ii) O_2 :

For oxygen, as no appreciable O_2 is stored in the tissues, only one equation in the form of venous O_2 store has been formulated, i.e.

$$\frac{d}{dt}(V_v . C_{vO_2}) = -\dot{U} + \dot{q}\,(C_{aO_2}(\tau) - C_{vO_2}) \quad \ldots. 6.5$$

where $\dot{U}$ represents the rate of oxygen consumption by the whole body and $\dot{q}\,(C_{aO_2}(\tau) - C_{vO_2})$ represents the net transfer rate of oxygen to the tissues.

6.1.3 Other equations of the controlled system:

(a) The total cardiac output is equal to the blood flow rate to muscle tissue compartment plus the other tissue compartments, that is:

$$\dot{q} = \dot{q}_m + \dot{q}_{OT} \quad \ldots. 6.6$$

(b) On the assumption that the carbon dioxide partial pressure in muscle and in all other tissues is equal to that of the venous blood with which each is perfused and the partial pressure of the alveolar gas is equal to the partial pressure of arterial blood at all times (that is during the transient as well as in the steady state), we can write

$$P_{mCO_2} = P_{vmCO_2} \quad 6.7$$

$$P_{OTCO_2} = P_{vOTCO_2} \quad 6.8$$

$$P_{ACO_2} = P_{aCO_2} \quad 6.9$$

$$P_{AO_2} = P_{aO_2} \quad 6.10$$

Once the equality in partial pressure is assumed (equations 6.7 and 6.8) and as the CO_2 dissociation curves are assumed to be equal and linear for tissues and venous blood, it follows that

$$C_{vmCO_2} = C_{mCO_2} \quad 6.11$$

and $$C_{vOTCO_2} = C_{OTCO_2} \quad 6.12$$

6.1.4. Dissociation curves:

(a) Carbon dioxide

The CO_2 dissociation curve is assumed to be linear, for arterial and venous blood and for tissues, and is of the form

$$C_{aCO_2} = K_1 \cdot P_{aCO_2} + K_2 \qquad 6.13$$

where K_1 and K_2 are constants. Considering K_1 (slope of the curve) equal to 0.0065 and K_2 equal to .244 (Grodins 1954), equation 6.13 may be written as

$$C_{aCO_2} = .0065. P_{aCO_2} + 0.244 \qquad 6.14$$

(b) Oxygen:

Due to gross non-linearity of the curve a three piece linearised representation is assumed for the arterial blood, of the form

$$C_{aO_2} = K_3 . P_{aO_2} + K_4 \qquad 6.15$$

where K_3 and K_4 are constants for a given range of values of volumetric concentrations as follows (Dittmer and Grebe, 1958).

i) Concentration > 0.187

$K_3 = 0.0001625$

$K_4 = 0.1756$

ii) $0.155 <$ concentration ≤ 0.187

$K_3 = 0.00107$

$K_4 = 0.1123$

iii) Concentration ≤ 0.155

$K_3 = 0.00388$

$K_4 = 0.0$

Figure 6.2 shows the comparison between the experimental oxygen dissociation curve and the piecewise linearised version given by equation 6.15 .

6.1.5 Controller Equations:

1). Tissue CO_2 control:

The equation relating tissue CO_2 concentration to ventilation is used as in the previous case:

$$\dot{V} = \dot{V}_o + K\,(C_{TCO_2} - (C_{TCO_2})_o) \qquad 6.16$$

where $\dot{V}_o$ is equal to the steady state ventilation at rest and $(C_{TCO_2})_o$ is the corresponding value of the tissue CO_2 concentration. K is the gain of the controller.

2). Arterial CO_2 and O_2 control:

By allowing subjects to breath gas mixtures containing various percentages of CO_2 (thus varying alvolar P_{CO_2}) for different alvolar partial pressures of oxygen, a set of curves is obtained as shown in figure 6.3A. (Lloyd and Cunningham, 1963 .) Each curve is iso P_{AO_2}. The dotted lines represent extrapolation. Thus it is clear that the slope of the curve is changing with the oxygen partial pressure in the alvoli, and these curves can be represented by a linear equation with variable slope, of the form

$$\dot{V} = K_5\,(P_{ACO_2} - K_6);\ P_{ACO_2} \geqslant K_6 \qquad 6.17$$

where K_5 is the variable slope and K_6 is the point on the figure for zero ventilation.

Lloyd and Cunningham (1963) found that K_5 can be represented as a hyperbolic function of P_{AO_2} as shown in figure 6.3B. This curve can be represented by an equation of the form:

$$(K_5 - K_7)\,(P_{AO_2} - K_8) = \text{constant K say}$$

$$\text{or} \quad K_5 = K_7 + \frac{K}{P_{AO_2} - K_8}$$

$$\text{or} \quad K_5 = K_7\,(1 + \frac{K_9}{P_{AO_2} - K_8}) \qquad 6.18$$

where K_9 is such that $K_9 \cdot K_7 = K$.

Substituting this value K_5 (equation 6.18) into equation 6.17 we get

$$\dot{V} = K_7 (P_{aCO_2} - K_6) \left(1 + \frac{K_9}{P_{aO_2} - K_8}\right) > 0 \quad \ldots\ldots 6.19$$

replacing P_{ACO_2} by P_{aCO_2} and P_{AO_2} by P_{aO_2} as assumed. Thus equation 6.19 represents the form of arterial chemoreceptor control action.

Using the data of Nielson and Smith (1951) as shown in fig.6.4, Longobardo et al (1966) developed a controller equation as follows:

$$\dot{V} = 1.81 (P_{aCO_2} - 31.0) + \frac{23.53 (P_{aCO_2} - 31)}{P_{aO_2} - 32.44} - 15.0 \quad \ldots\ldots 6.20$$

The following normal values were used in the above equations:

Symbol	Value Used	Reference
V_r	2.5 ℓ	Grodins et al (1954)
V_a	2.4 ℓ	Farhi & Rahn (1960)
V_v	3.6 ℓ	"
$\dot{q}$	5.6 ℓ/min	Grodins et al (1954)
$\dot{q}_m$	0.895 ℓ/min	Farhi & Rahn (1960)
$\dot{q}_{OT}$	4.705 ℓ/min	"
M_{CO_2}	0.228 ℓ/min	Grodins et al (1954)
$\dot{M}_m$	0.038 ℓ/min	Farhi & Rahn (1960)
$\dot{M}_{OT}$	0.19 ℓ/min	"
$\dot{U}_{O_2}$	0.28 ℓ/min	Grodins et al (1954)
V_m	29.14 ℓ	Farhi & Rahn (1960)
V_{OT}	12.0 ℓ	"

Table 6.1

Using equations 6.14, 6.15 and 6.20 the following intermediate variables are generated to ease the presentation of the model equations:

$$KK_2 = V_r + (P_B - 47)\ V_a\ K_3 \qquad \ldots\ldots 6.21$$

$$KK_3 = C_{aCO_2} - K_2 - 31.0\ K_1 \qquad \ldots\ldots 6.22$$

$$KK_4 = C_{aO_2} - K_4 - 32.44\ K_3 \qquad \ldots\ldots 6.23$$

Using the above normal values the following system equations are formulated for simulation:

$$C_{vCO_2} = (0.895\ C_{mCO_2} + 4.705\ C_{OICO_2}) / 5.6 \qquad \ldots\ldots 6.24$$

$$KK_2 = 2.5 + 1711.2\ K_3 \qquad \ldots\ldots 6.25$$

$$KK_3 = C_{aCO_2} - 0.4455 \qquad \ldots\ldots 6.26$$

$$KK_4 = C_{aO_2} - K_4 - 32.44\ K_3 \qquad \ldots\ldots 6.27$$

$$\frac{d}{dt}(C_{aCO_2}) = (25.953\ (C_{vCO_2}(\tau) - C_{aCO_2}) - \dot{V}\ (\tau/2)\ (C_{aCO_2} - 0.244 - K_1\ (P_B - 47)\ P_{ICO_2})\ /13.623 \qquad \ldots\ldots 6.28$$

$$\frac{d}{dt}(C_{mCO_2}) = (0.038 + 0.895\ (C_{aCO_2}(\tau) - C_{mCO_2}))/29.14 \qquad \ldots 6.29$$

$$\frac{d}{dt}(C_{OICO_2}) = (0.19 + 4.705\ (C_{aCO_2}(\tau) - C_{mCO_2}))/12.0 \qquad \ldots 6.30$$

$$\frac{d}{dt}(C_{aO_2}) = (5.6\ (C_{vO_2}(\tau) - C_{aO_2})\ 713.0\ K_4 + 150.0\ K_3\ \dot{V}\ (\tau/2) - \dot{V}\ (\tau/2)\ (C_{aO_2} - K_3))/KK_2 \qquad \ldots\ldots 6.31$$

$$\frac{d}{dt}(C_{vO_2}) = (5.6\ (C_{aO_2}(\tau) - C_{vO_2}) - 0.28)\ /3.6 \qquad \ldots\ldots 6.32$$

$$\dot{V} = (1.81KK_3 + 23.53KK_3 \cdot K_3/KK_4)\ /0.0065 - 15.0 \qquad \ldots 6.33$$

or

$$\dot{V} = 470.6\ C_{vCO_2} - 268.0 \qquad \ldots\ldots 6.33A$$

These equations were solved using MIMIC digital simulation language. As the arterial controller is assumed to be sited half-way between the lung and muscle or other tissues, $\dot{V}$ is delayed by half the time taken for the blood to travel from lung to tissues. A normal circulatory time delay of 12 seconds is assumed (Milhorn et al, 1965). For studying the behaviour of the model, however, the time delays are varied for each input or disturbance (e.g. CO_2 breathing, hyperventilation, asphyxia). Simulations were carried out for each controller in turn.

The model was simulated for following conditions.

1. CO_2 Breathing : 3%, 5% CO_2 input
2. Asphyxia : $\dot{V} = 0.0$ for $t < 1.5$ min.
3. Hyperventilation : $\dot{V} = 60$ for $t < 1.5$ min.
   $\dot{V} = 30$ for $t < 1.6$ min.

Under each input or disturbance various time delays were simulated for each of the controller strategies.

6.2 RESULTS AND DISCUSSION :

i. CO_2 BREATHING

Step inputsof 3% and 5% were applied to the model. The model was run for approximately 5 minutes to achieve a steady state and then the required CO_2 step was applied for 15 minutes. The CO_2 level was then switched back to zero and the pre-stimulus conditions were restored. In each case both control strategies (i.e. arterial P_{CO_2} and P_{O_2}, and tissue CO_2) were applied in turn for circulation delays between 12 seconds and 48 seconds.

Graph numbers 6.1.1 to 6.1.3 show the results of 3% CO_2 inhalation with 12, 24, 48 seconds circulation delays respectively using the tissue CO_2 controller. It is apparent that the model now behaves like a second order system in which the damping decreases with increasing circulation delays. Assuming the off-transient response to be an exponential delay of oscillations, the damping factor calculated using the logarithmic decrement, reduces from .8 for 12 seconds delay to .6 for a 48 seconds delay. But Cheyne-Stokes breathing for which the damping factor is effectively zero is not present. The responses for 5% CO_2 inhalation with 12 and 24 seconds time delays are shown in fig. 6.1.4 and 6.1.5 respectively. There is no appreciable difference between the two responses again confirming that the damping factor of this system is dependent upon circulation delays. Thus it is possible that for an increased circulation delay the damping factor will become zero exhibiting Cehyne-Stokes breathing, but this time delay will certainly be outside physiological limits as the delay of about 48 seconds in circulation is present only in patients with acute heart congestion and any further delay will normally result in death.

Graph numbers 6.1.6 to 6.1.8 show the time response of ventilation for 3% CO_2 inhalation with 12, 24, 48 seconds circulation delay respectively, using arterial chemoreceptor control. It is evident that although the system still behaves like a second order system, the damping factor is certainly smaller than in the case of tissue CO_2 control. This certainly is due to the higher gain of the controller equation (equation 6.20), which is not only dependent upon increase in carbon dioxide concentration but also upon the decrement in oxygen concentration in arterial blood due to inhalation of CO_2 gas

mixtures. Furthermore these two effects are additive as well as multiplicative resulting in a non-linear control. The period of oscillation in this case for 24 second delay (graph number 6.1.7) is 0.9 minutes in comparison to 5 minutes in the case of tissue CO_2 control for a similar delay (graph number 6.1.2). Thus the response produced by the arterial chemoreceptor is much faster with a frequency of oscillation about 5 times the frequency of oscillation produced by the tissue CO_2 control. With 48 seconds time delay (graph 6.1.8), the damping factor is zero producing Cheyne-Stokes breathing with sustained oscillations of ventilation with periods of apnoea, i.e. zero breathing. The period of oscillations is 1.1 minute which is slightly larger than in the case of 24 seconds time delay response. Graph 6.1.9 shows the results for 5% CO_2 inhalation with 24 seconds time delays. Although oscillations are larger, the time period of these oscillations is very similar to the time period in the case of 3% CO_2. Thus the time period of oscillations seems to be a function of circulation delays.

An important feature of these responses for both controller strategies is the fact that although at higher time delays, oscillations appear even before the stimulus is applied in the model. These oscillations die off very quickly with the input of CO_2. In graph 6.1.8, the damping factor is zero for the off-transients, but for the on-transients it is approximately 0.5. Also comparing the on-transients for 24 seconds delay of 3% and 5% CO_2 input (graph numbers 6.1.7 and 6.1.9 respectively) there is a marked overshoot for 3% CO_2 which is not present in the case of 5% CO_2 input. Thus it can be concluded that input of carbon dioxide increases the damping factor. In other words the gain is smaller and the

damping factor is larger during on-transients than during off-transients.

From the above it is evident that there is a marked difference between the two control strategies. In the case of tissue CO_2 control the results are similar in structure to the experimental results for CO_2 input, but in the case of arterial CO_2 control certain high frequency phenomena are present which are not comparable to experimental results. Another feature of interest is that for similar conditions the steady state results for tissue CO_2 control are higher than for the arterial chemoreceptor control. In the case of 5% CO_2, the steady state value of 5% CO_2 input is about 17 ℓ/min (graph number 6.1.4) whereas in the case of arterial controller ventilation is about 15 ℓ/min (graph number 6.1.9). This is true for 3% CO_2 input as well. Thus CO_2 inhalation responses of the arterial controller are not even structurally similar to experimental evidence, but Cheyne-Stokes breathing is produced within physiological limits of parameters.

ii. ASPHYXIA

In this case ventilation was held at zero for 1.5 minutes after which normal control was allowed to function. Both controller equations and the variation of time delays were tested.

For tissue CO_2 control, again the time response of ventilation became more oscillatory with the increase in circulation delay but the initial overshoot of ventilation after removal of the breath holding remained unchanged. (Graphs 6.2.1 to 6.2.3). Again Cheyne-Stokes breathing did not occur even with 48 seconds circulation delay.

When the arterial controller was used, the initial overshoot after removal of the restriction on ventilation was much larger than in the previous case and furthermore this overshoot increased with the increased circulation delay. After this overshoot of ventilation a period of apnoea occurred and the duration of this period of zero breathing increased with high circulation delays. The results were of high frequency and Cheyne-Stokes breathing occurred at 48 seconds circulation delay.

iii. HYPERVENTILATION

The model was hyperventilated (forced higher than normal ventilation) at two levels : 30 litres/min and 60 litres/min for 1.6 minutes and 1.5 minutes respectively, after which normal conditions were restored. For tissue CO_2 control the period of apnoea following hyperventilation is practically constant and so is the magnitude of the first overshoot following the onset of normal control.(Graphs 6.3.1. to 6.3.2). For arterial control this period of apnoea becomes smaller with increasing circulation delays but the first overshoot following apnoea becomes larger. The periods of apnoea for higher level of hyperventilation are larger for both controllers. (Fig. 6.3.8. to 6.3.11.)

From the above results it is clear that the tissue CO_2 controller is slow acting and produces low frequency effects. Under normal conditions the simulated results are similar in structure to experimental observations. Cheyne-Stokes breathing cannot be produced, however, even for the case of acute heart congestion. On the other hand the arterial CO_2 and O_2 controller is fast acting and produces high frequency results. Those obtained for CO_2 input under normal circulation conditions are not even structurally similar to experimental evidence. (Reynolds et al, 1972). As is apparent in graph 6.1.6 the model response is at least

that of a second order system due to the overshoot and undershoot present. On the other hand Cheyne-Stokes breathing can be reproduced realistically within physiological limits of the parameter values, irrespective of the input. This confirms the results discussed in chapter 5, which suggested that circulation delays and controller gains were the two most important factors in the production of Cheyne-Stokes breathing. The arterial controller equation has oxygen in its denominator, so with an increase in arterial CO_2, oxygen concentration normally falls thereby causing an increase in the controller gain.

Neither of these controller equations produced satisfactory results for all inputs. Particularly the tissue CO_2 control is based upon the physiological hypothesis that the central chemoreceptors are sensitive to CO_2 concentration changes and are situated near the brain. Thus it is not possible to test such a controller in a quantitative analysis unless a separate brain tissue compartment is formulated with its own blood flow and metabolic production rate. Another aspect of this controller is its inherent time lag, i.e. any change in lung gas composition is not reflected in the ventilation until this new composition of gas traverses to the chemoreceptor site. Having tissue CO_2 controller in the brain tissues will reduce this time by approximately 50 per cent as brain is that much nearer to lungs than tissue. Thus if ventilation is made to be a function of brain tissue CO_2 concentration, then even the tissue CO_2 controller will act slightly faster than at present. Another factor affecting the response is the circulation time delay. More realistic formulation of blood flow and time delays may improve the model response and certainly will make the model more isomorphic.

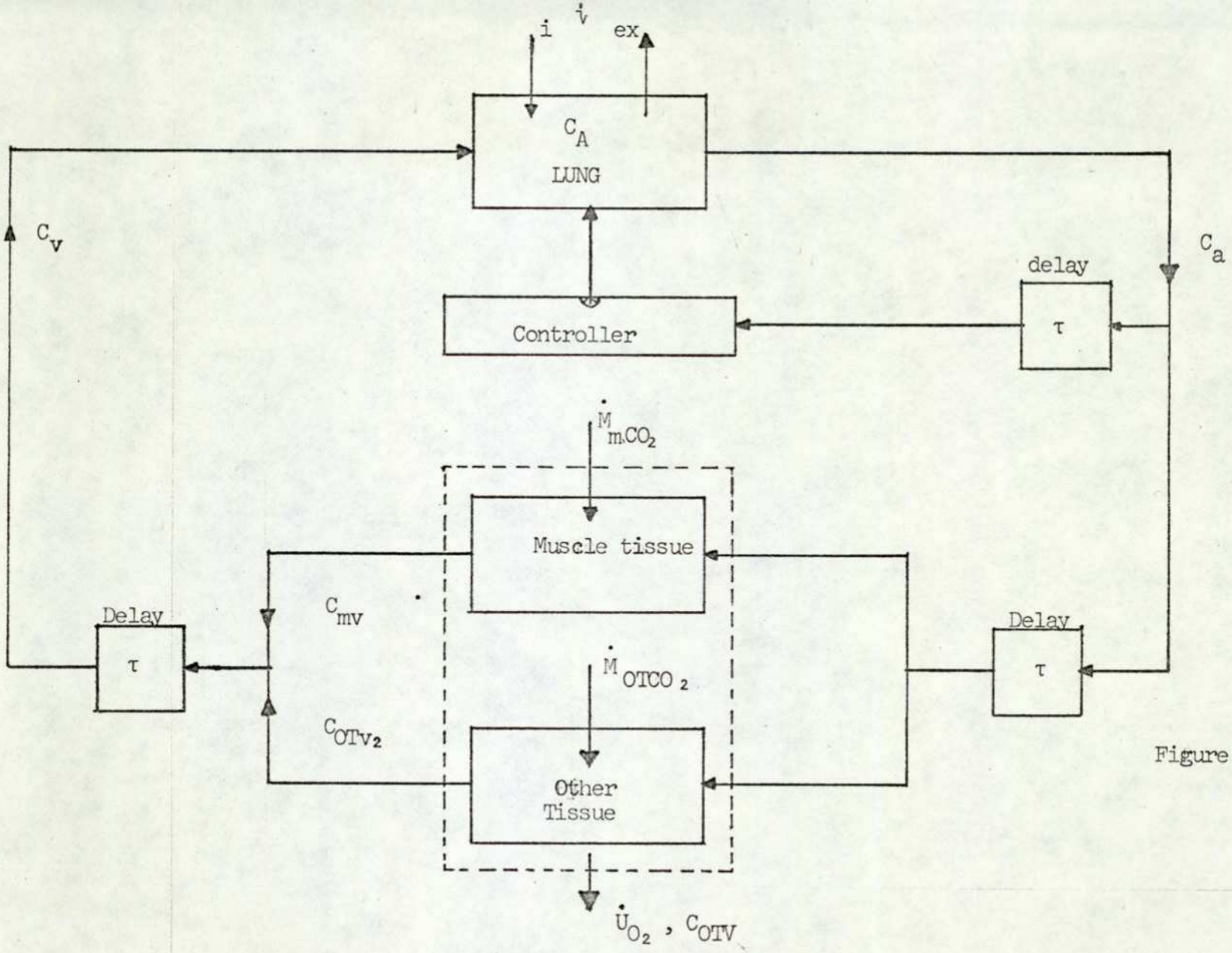
$\dot{V}_i$
$\dot{V}_{ex}$
C_A
LUNG
C_v
C_a
delay
τ
Controller
$\dot{M}_{mCO_2}$
Muscle tissue
Delay
τ
C_{mv}
$\dot{M}_{OTCO_2}$
C_{OTv_2}
Delay
τ
Other Tissue
$\dot{U}_{O_2}$, C_{OTV}

Figure 6.1.

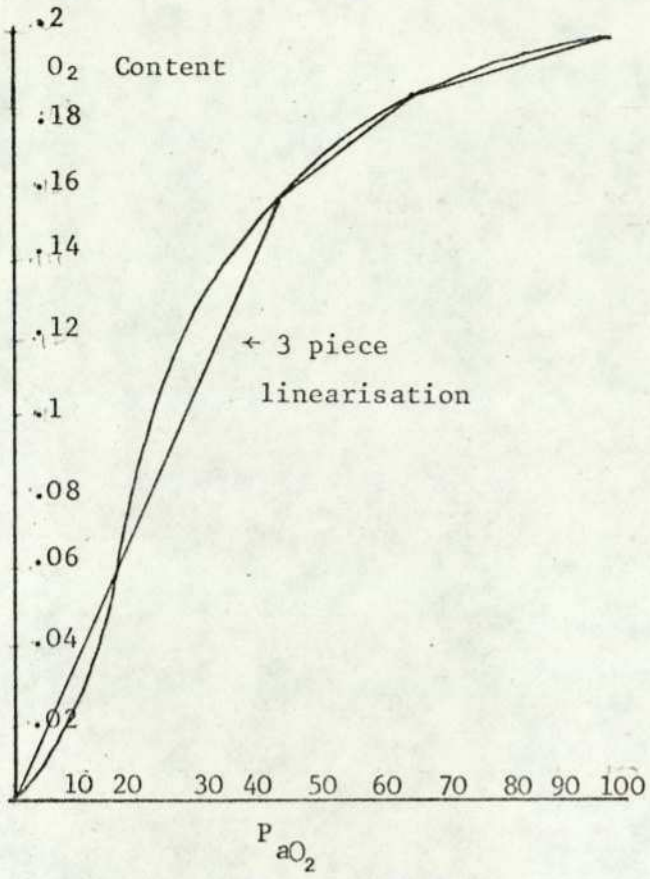

Figure 6.2

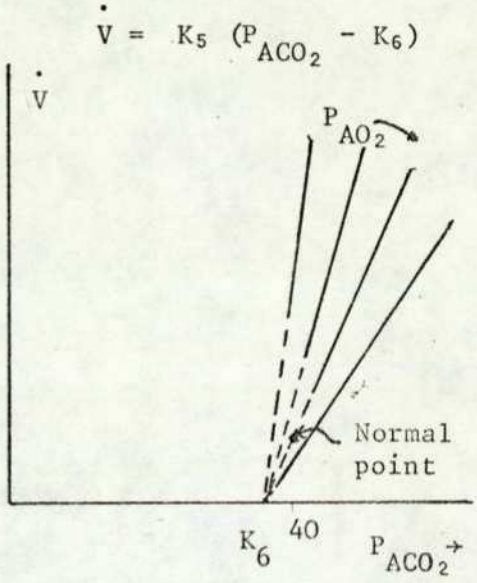

Figure 6.3A

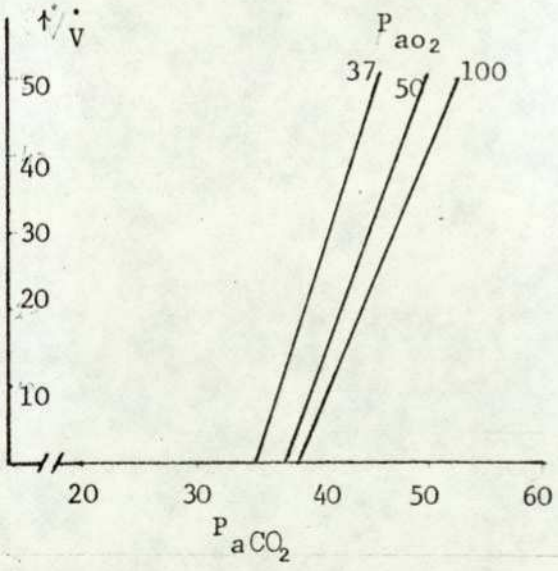

Figure 6.4

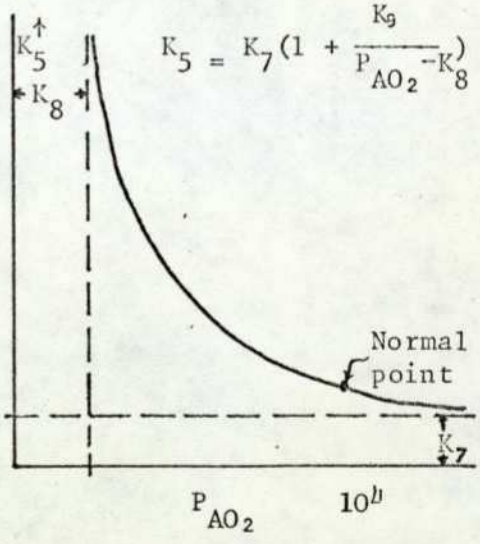

Figure 6.3B

Graph 6.1.1

τ_{a-v} = 12 sec.

C_{aco_2} = 3%

$\dot{V} = f(C_{TCO_2})$

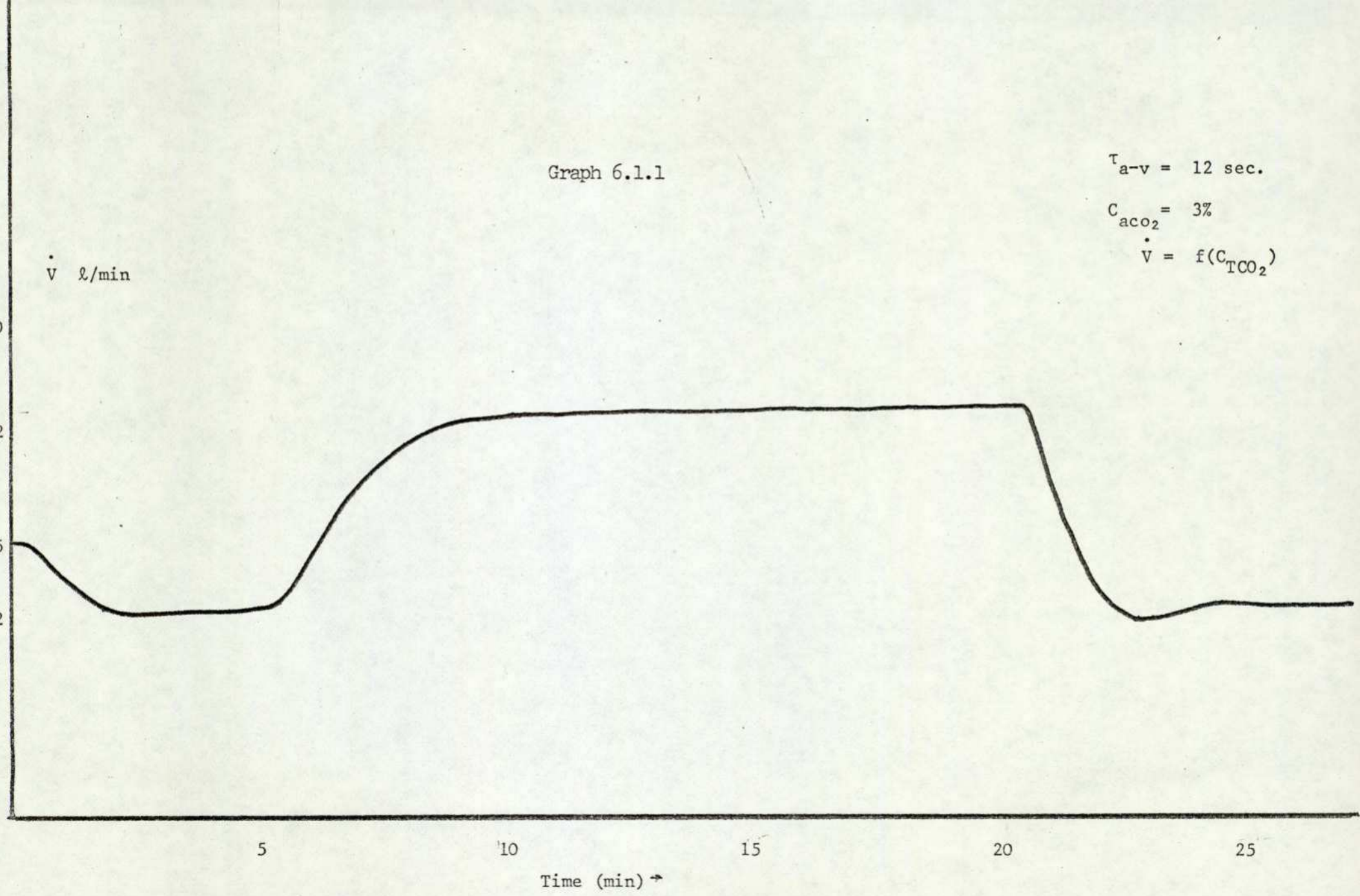

Graph 6.1.2

C_{ICO_2} = 3%

$\tau_{a-\dot{V}}$ = 24 sec

$\dot{V} = f(C_{TCO_2})$

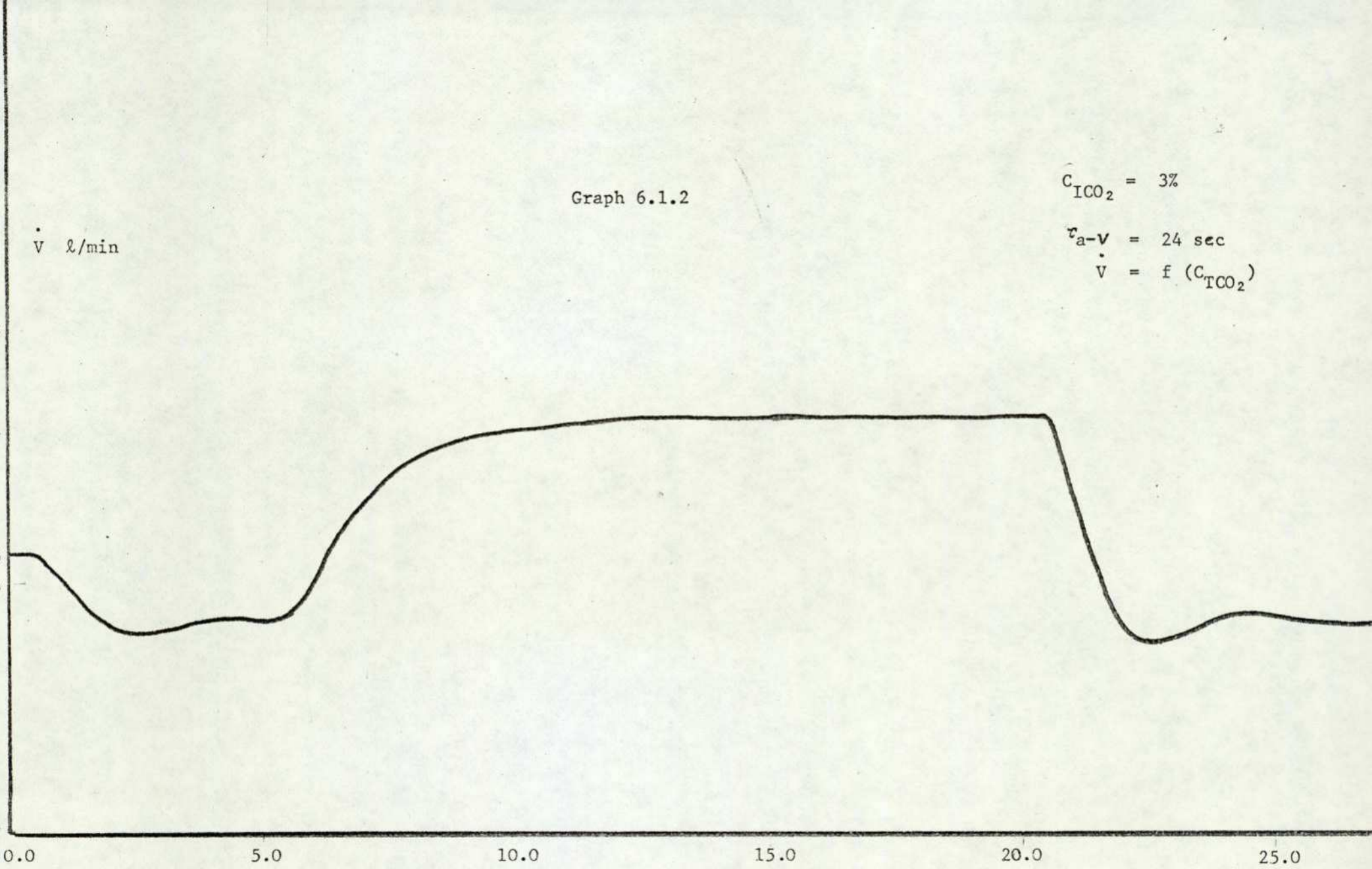

Graph 6.1.3

$\dot{V} = f(C_{TCO_2})$

$\tau_{a-v} = 48$ sec

$C_{ICO_2} = 3\%$

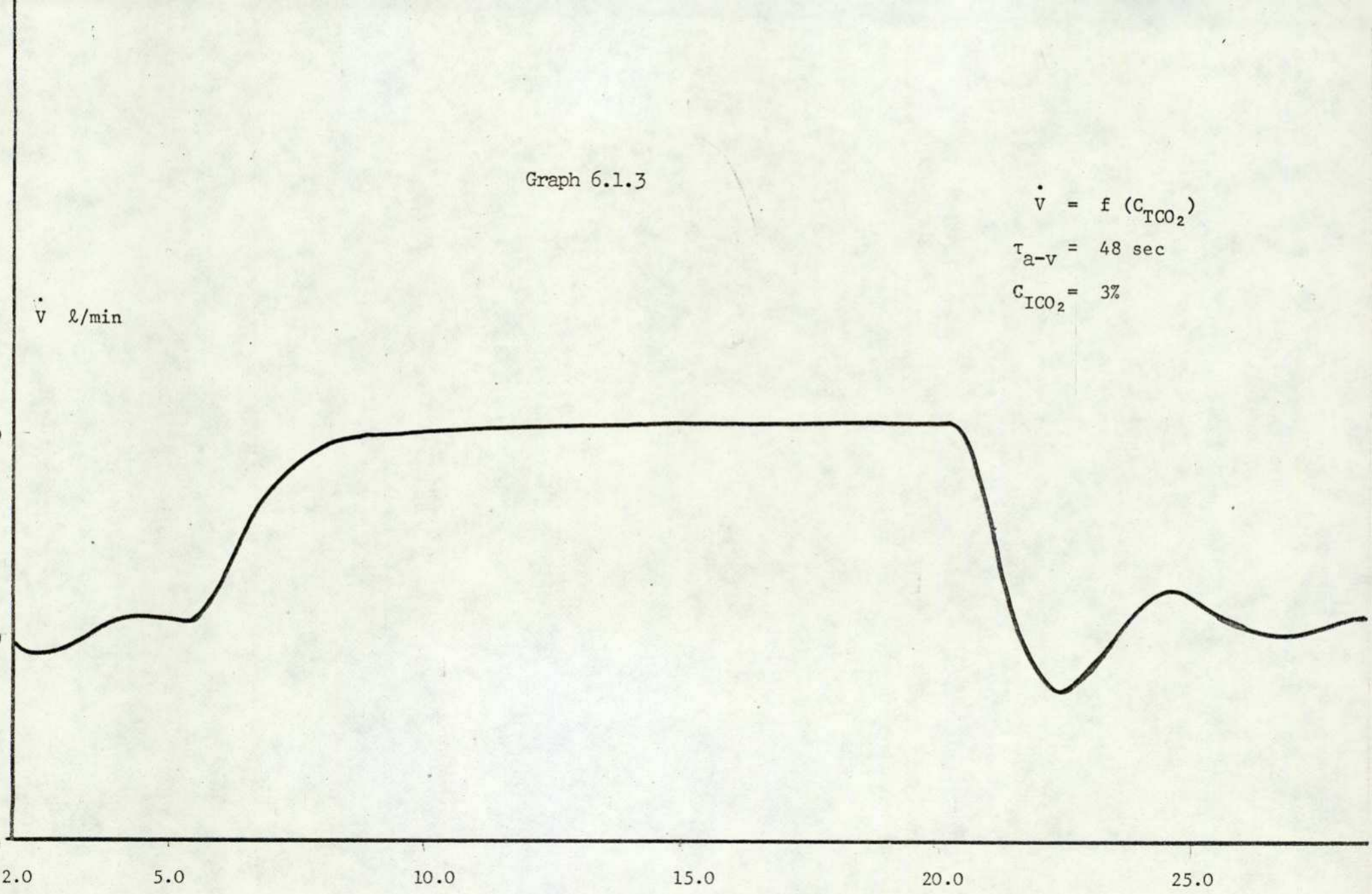

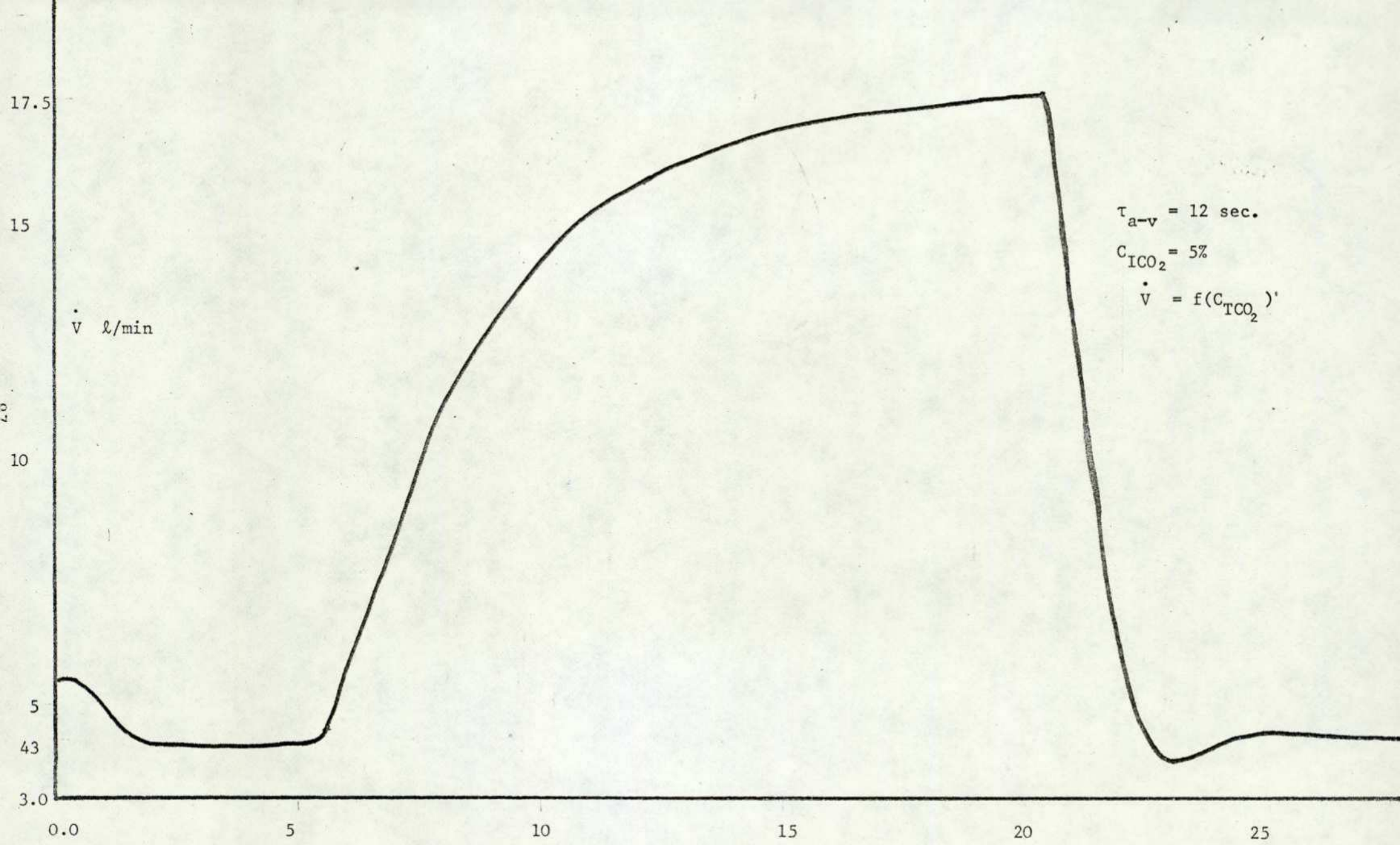

Time (min) →
Graph 6.1.4

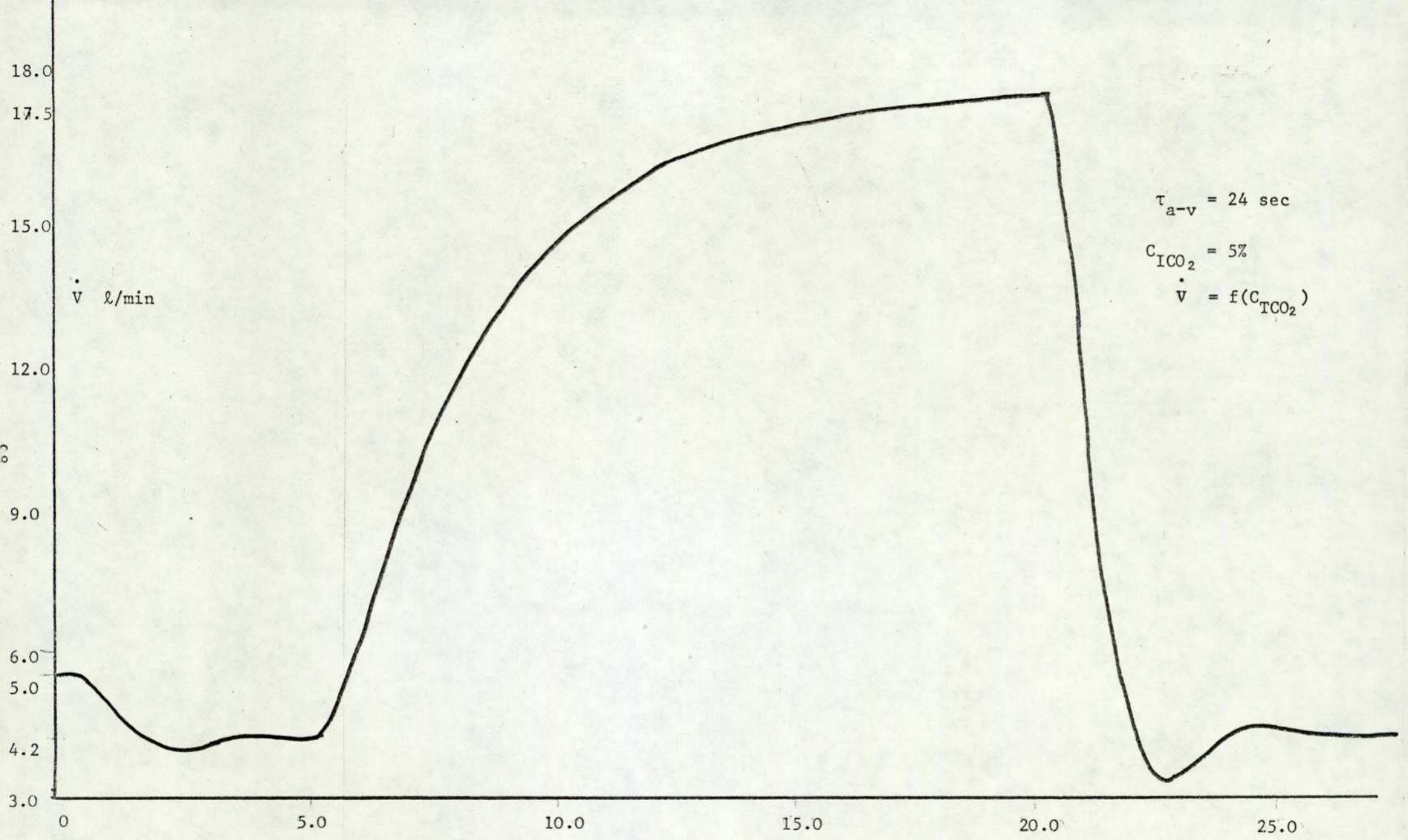
18.0
17.5
15.0
12.0
9.0
6.0
5.0
4.2
3.0
$\dot{V}$ ℓ/min
τ_{a-v} = 24 sec
C_{ICO_2} = 5%
$\dot{V}$ = f(C_{TCO_2})
0
5.0
10.0
15.0
20.0
25.0
Time (min)

Graph 6.1.5

Graph 6.1.6

τ_{a-v_2} = 12s

C_{ICO_2} = 3%

$\dot{V}$ = f (C_{aCO_2} and C_{aO_2})

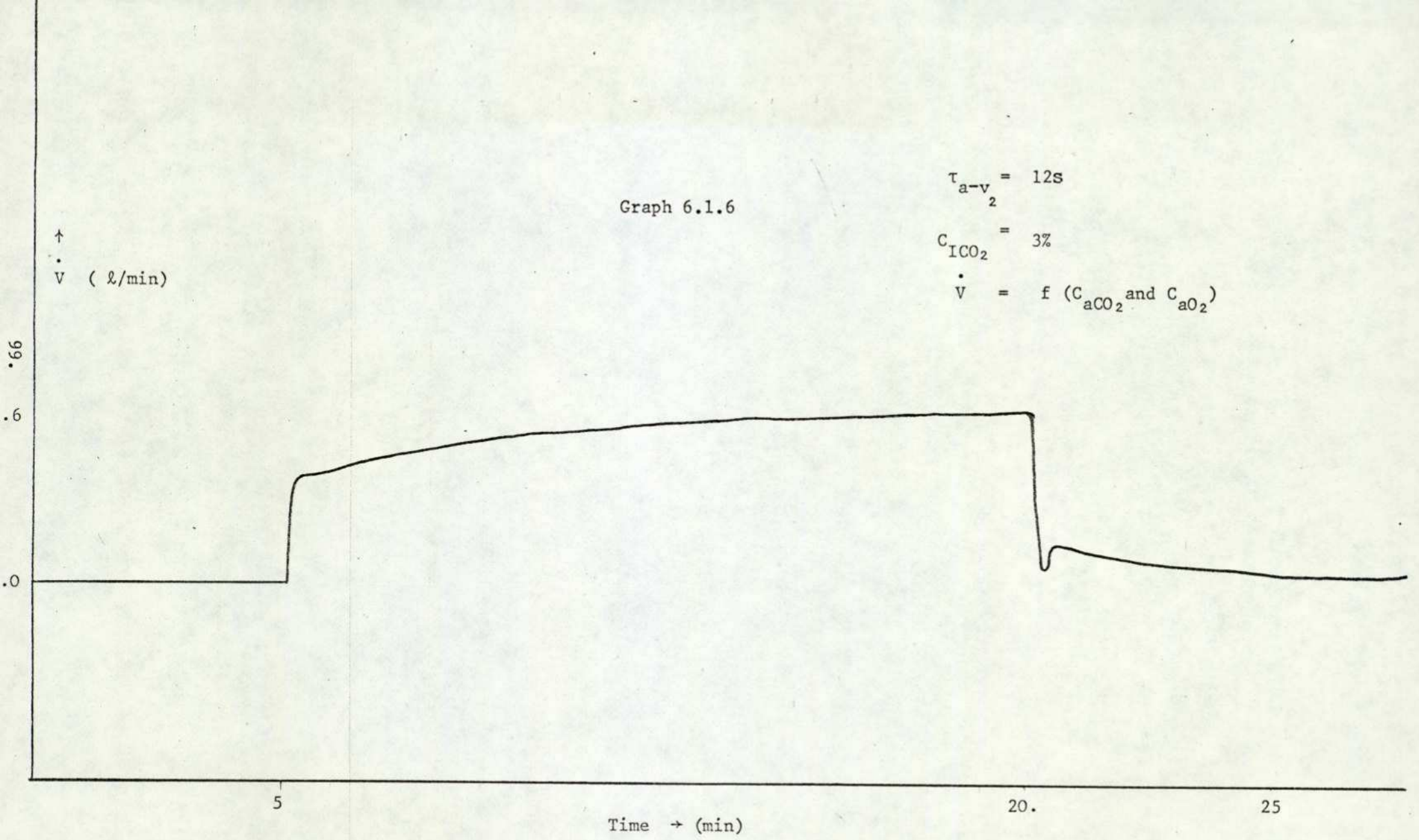

Graph 6.1.7

τ_{a-v} = 24s

C_{ICO} = 3%

$\dot{V}$ = f (C_{aCO_2} and C_{aO_2})

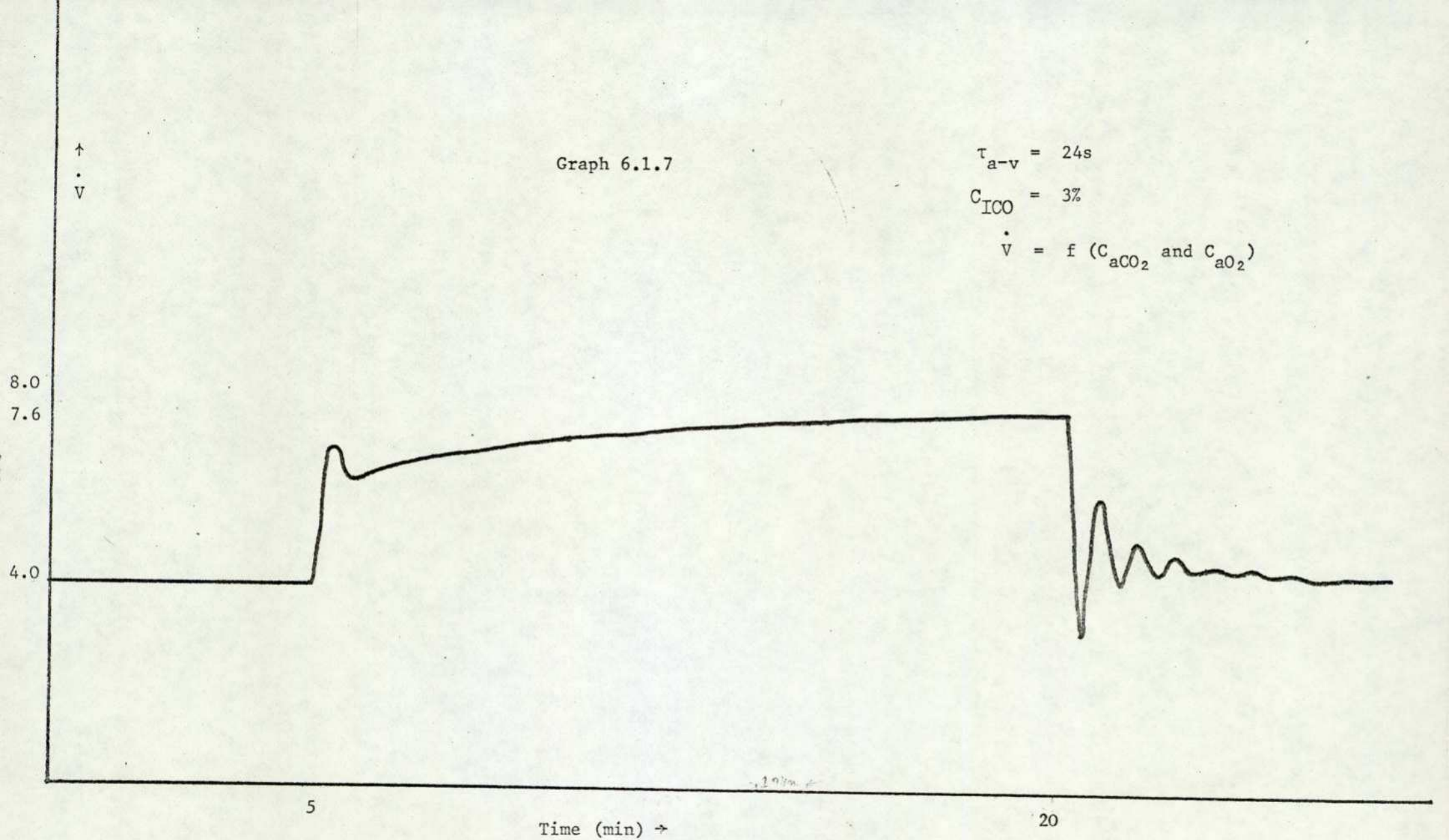

Graph 6.1.8

τ_{a-v} = 48 sec

C_{ICO_2} = 3%

$\dot{V}$ = $f(P_{aCO_2}$ and $P_{aO_2})$

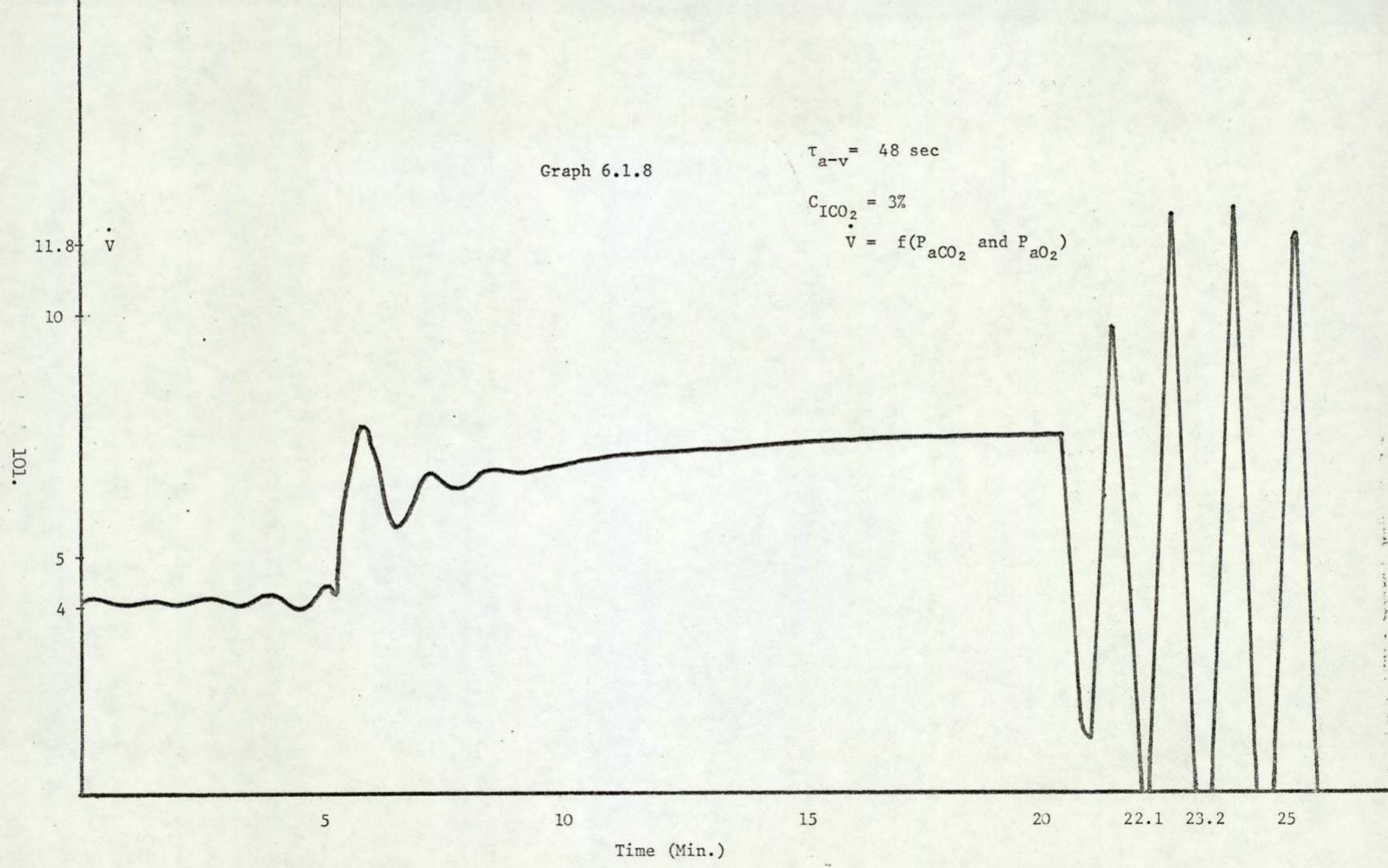

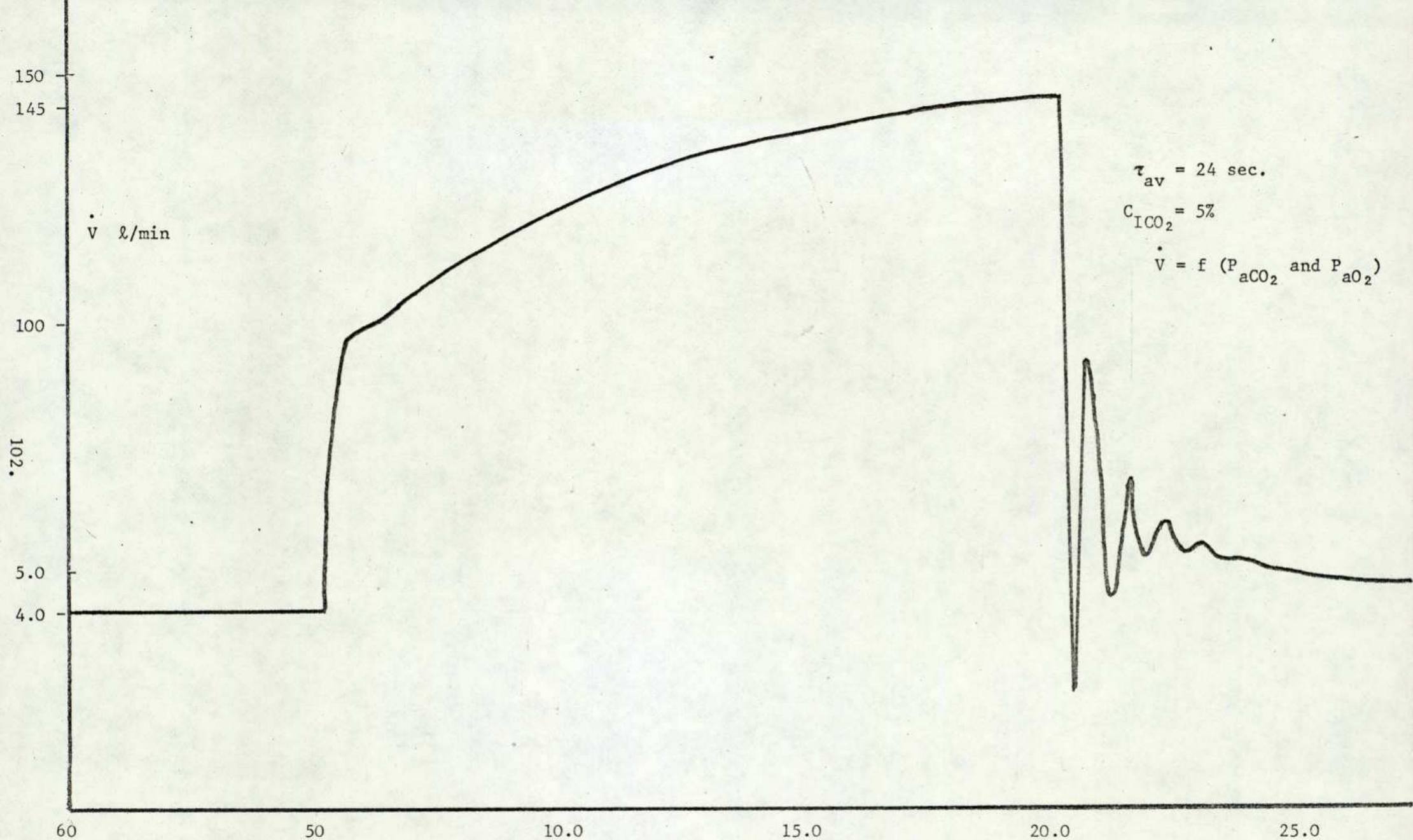
150
145
$\dot{V}$ ℓ/min
100
102.
5.0
4.0
τ_{av} = 24 sec.
C_{ICO_2} = 5%
$\dot{V}$ = f (P_{aCO_2} and P_{aO_2})
60
50
10.0
15.0
20.0
25.0
Time (min) →

Graph 6.1.9

Graph 6.2.1

τ_{av} = 24 Sec.

$\dot{V}$ = f (C_{TCO_2})

$\dot{V}$ = 0 $t \leq$ 1.5 min.

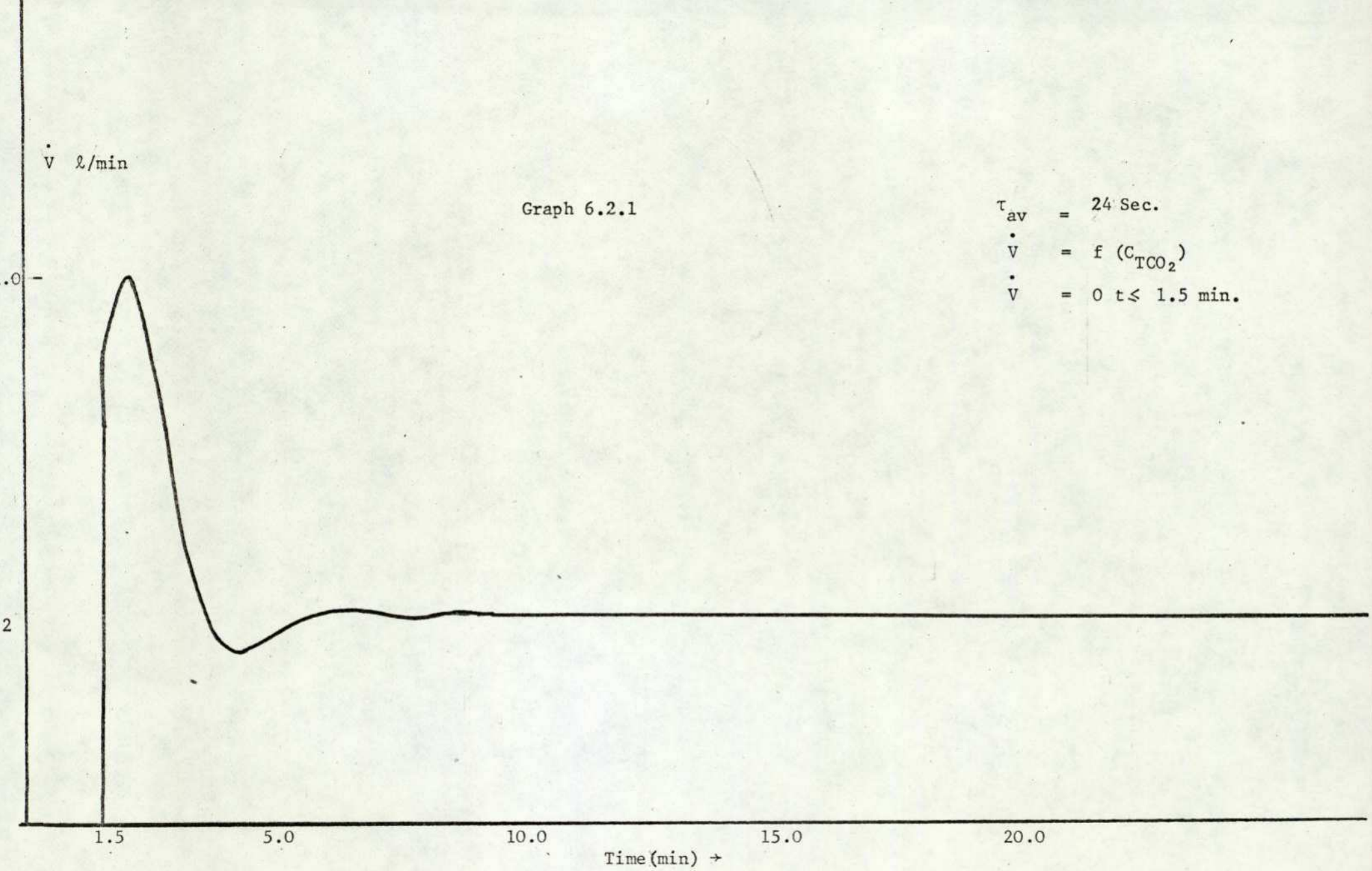

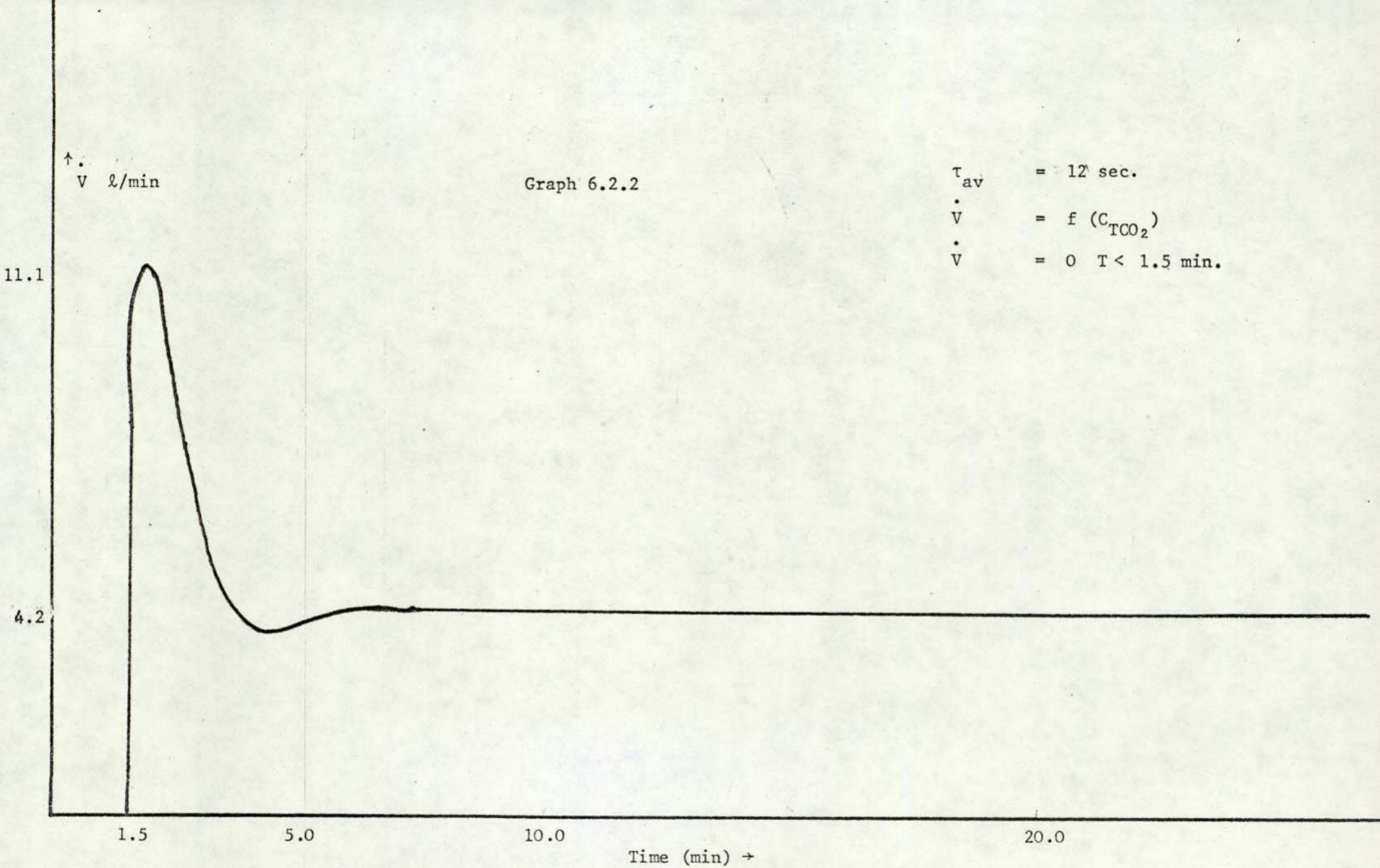

Graph 6.2.2

τ_{av} = 12 sec.

$\dot{V}$ = f (C_{TCO_2})

$\dot{V}$ = 0 T < 1.5 min.

Graph 6.2.3

$\dot{V}$ = 0 (for t < 1.5 min)

$\dot{V}$ = f (C_{TCO_2})

τ_{av} = 48s

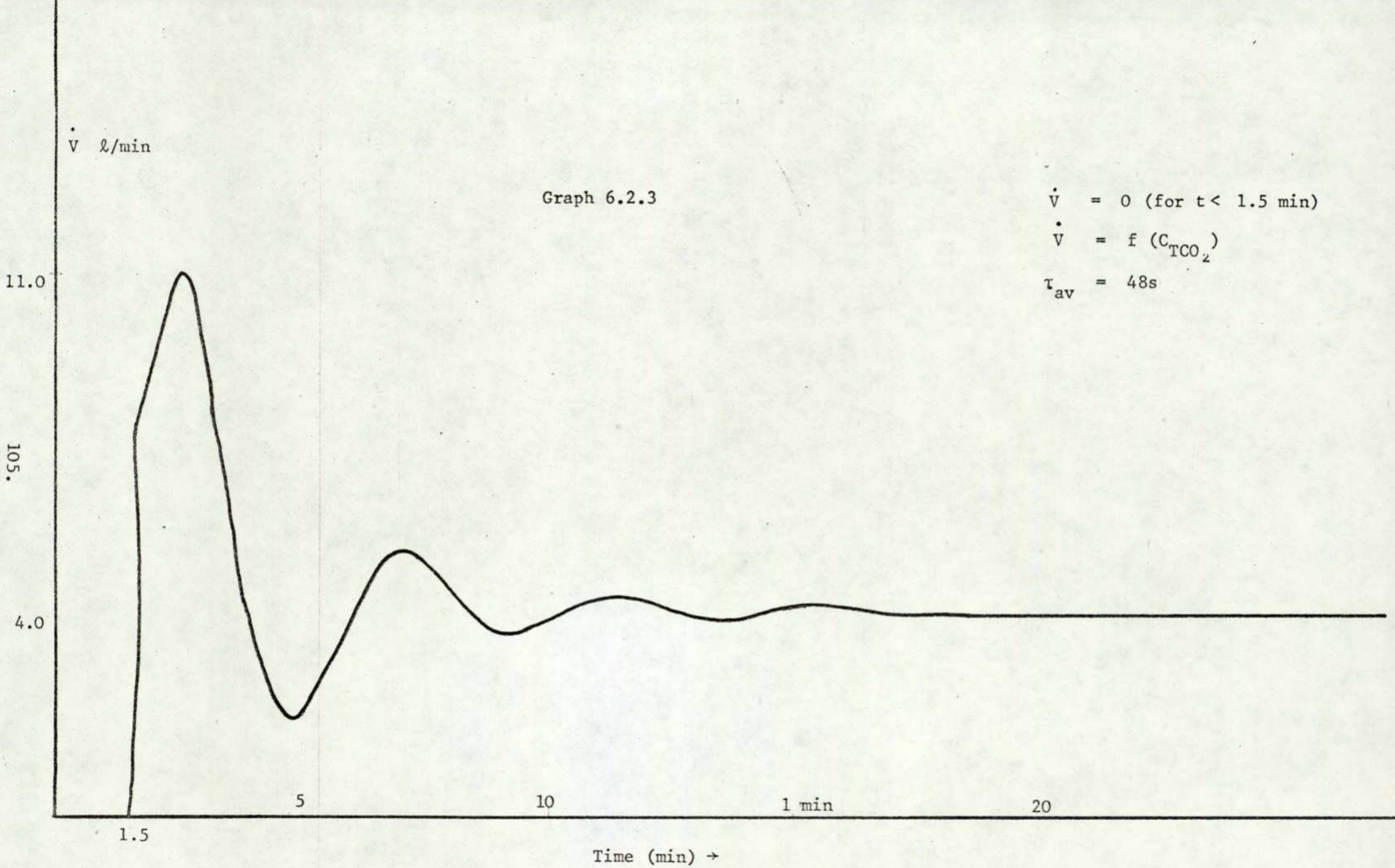

Graph 6.2.4

$\dot{V} = f(P_{aO_2} \& P_{aCO_2})$

$\dot{V} = 0 \quad t < 1.5$ min

$\tau_{a-v} = 12$ sec

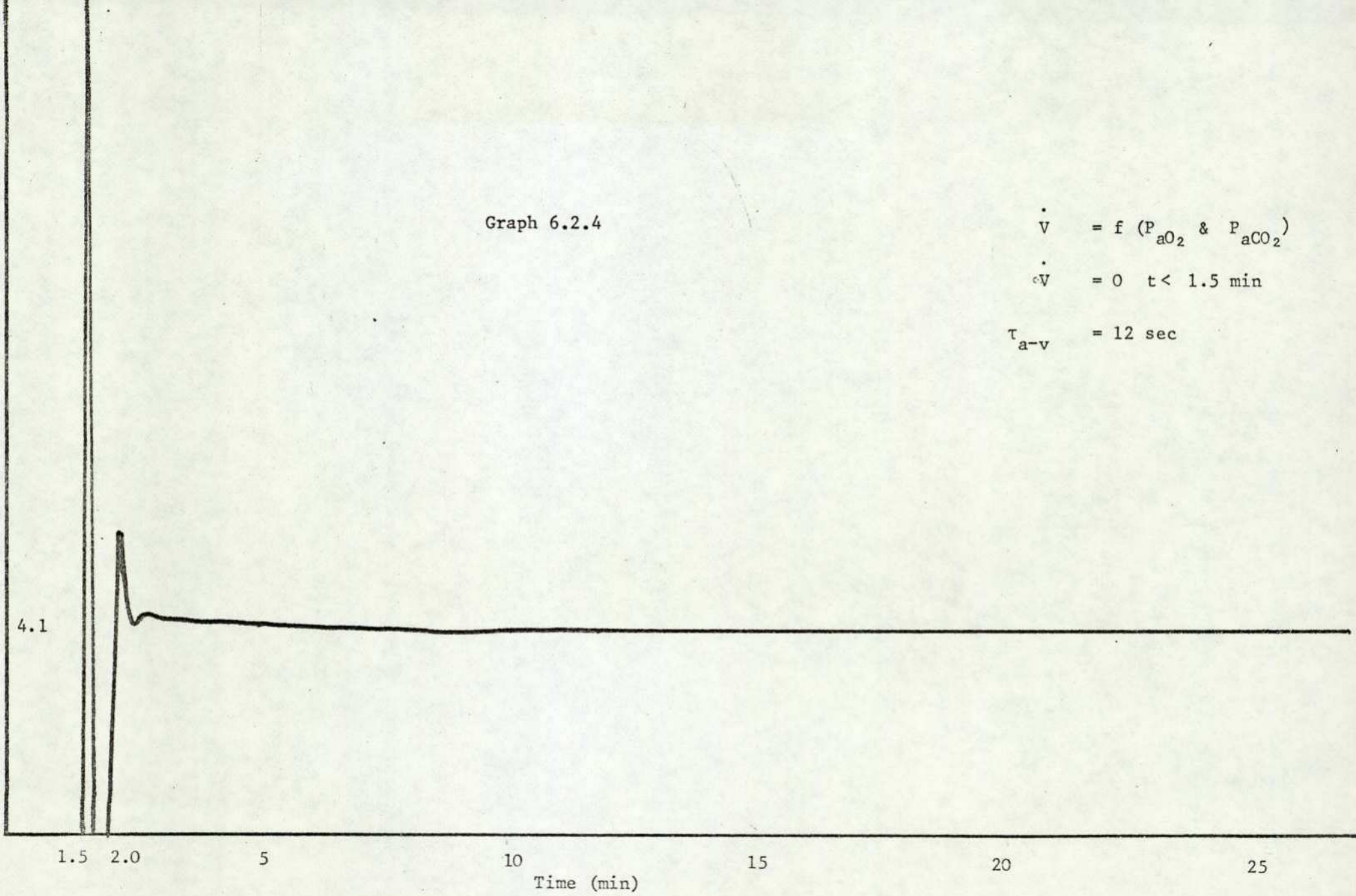

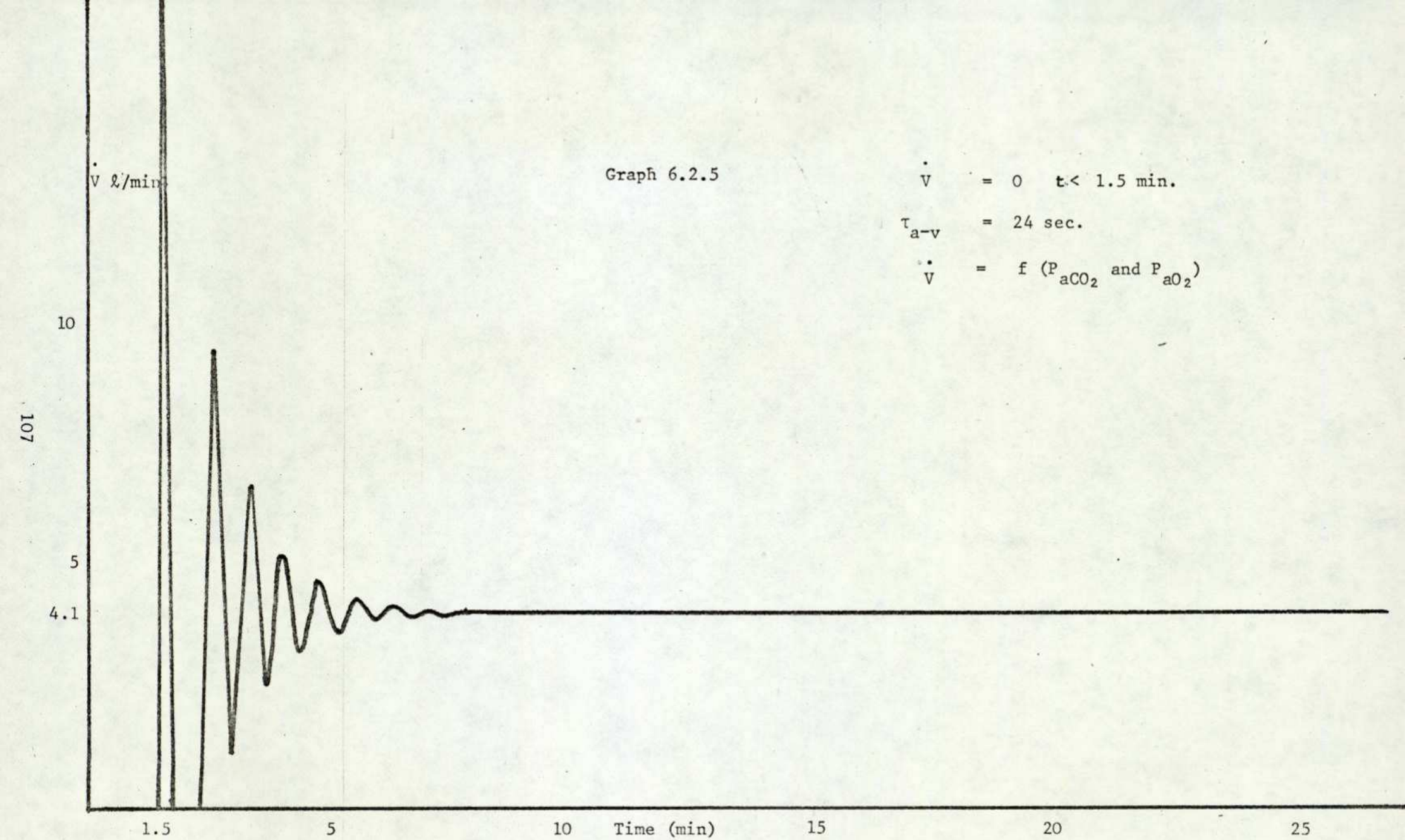

Graph 6.2.5

$\dot{V} = 0 \quad t < 1.5$ min.

$\tau_{a-v} = 24$ sec.

$\dot{V} = f\ (P_{aCO_2}$ and $P_{aO_2})$

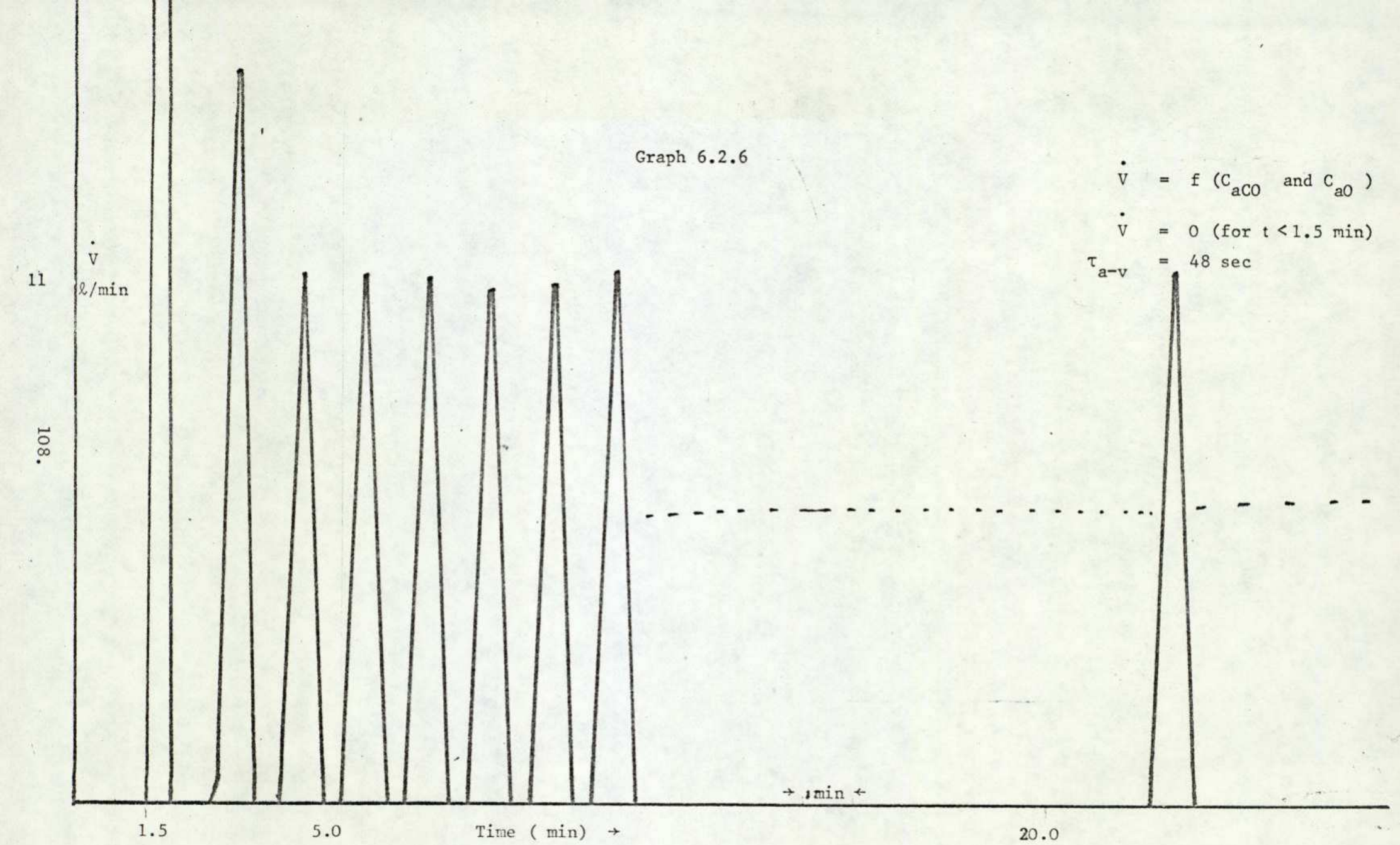
Graph 6.2.6
$\dot{V}$ = f (C_{aCO} and C_{aO})
$\dot{V}$ = 0 (for t < 1.5 min)
τ_{a-v} = 48 sec
$\dot{V}$
ℓ/min
11
108.
→ 1 min ←
1.5
5.0
Time (min) →
20.0

Graph 6.3.1

$\dot{V}$ = 30 ℓ/min. $t < 1.6$ min.

τ_{a-v} = 12 sec.

$\dot{V} = f(C_{TCO_2})$

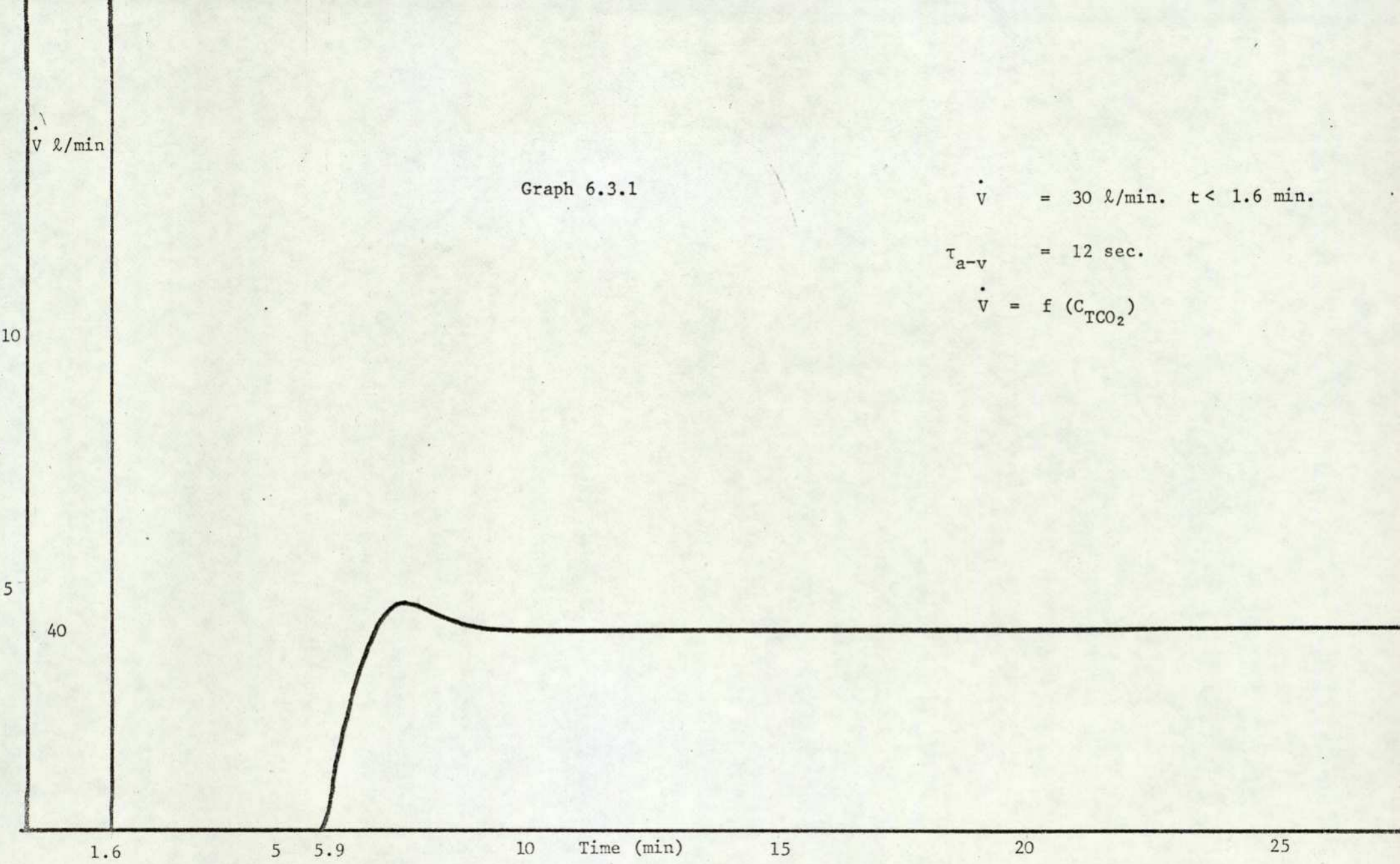

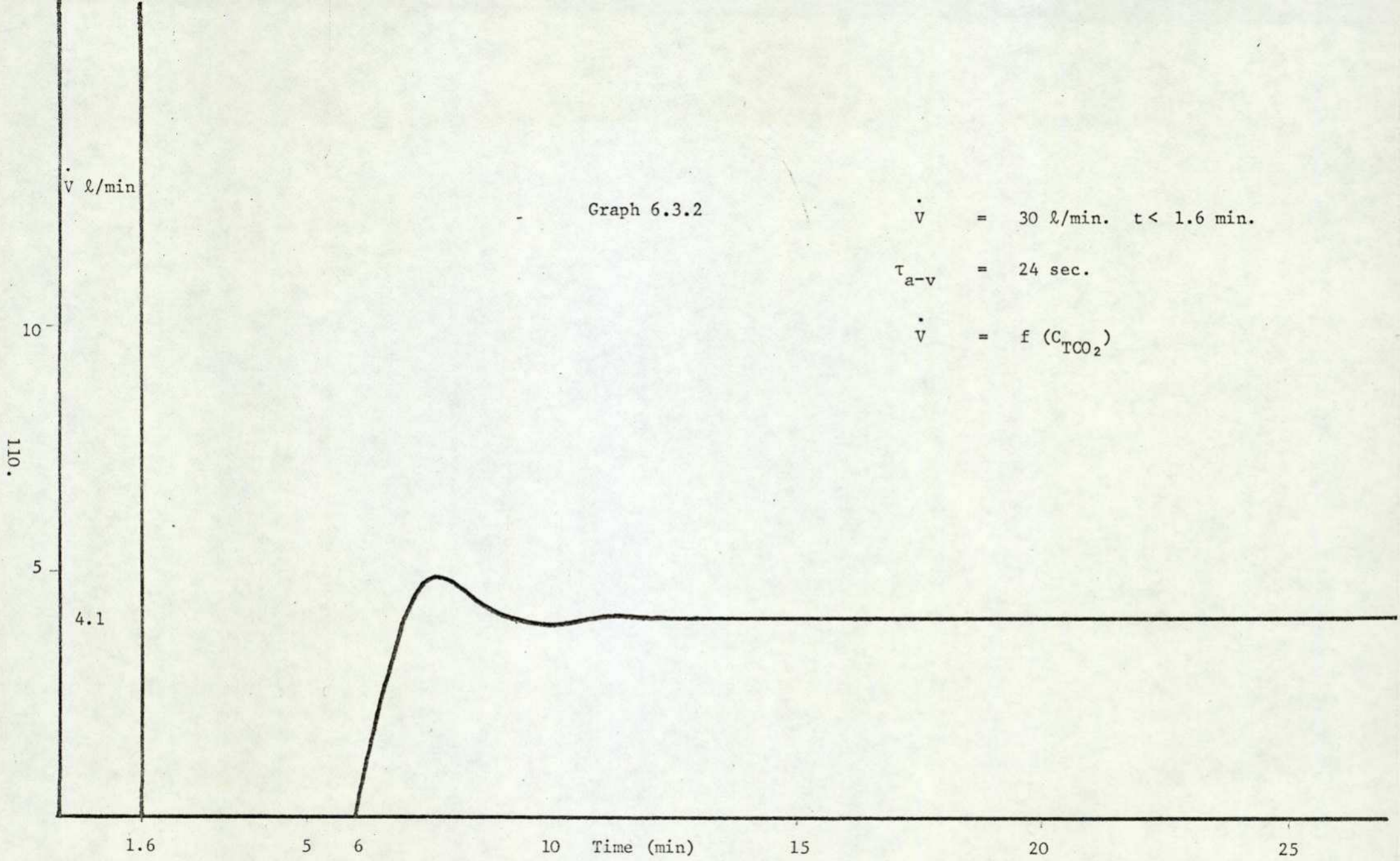

Graph 6.3.2

$\dot{V}$ = 30 ℓ/min. t < 1.6 min.

τ_{a-v} = 24 sec.

$\dot{V}$ = f (C_{TCO_2})

Graph 6.3.3

τ_{a-v} = 48 sec.

$\dot{V}$ = 30 ℓ/min.
for t < 1.6 min.

$\dot{V}$ = f (C_{TCO_2})

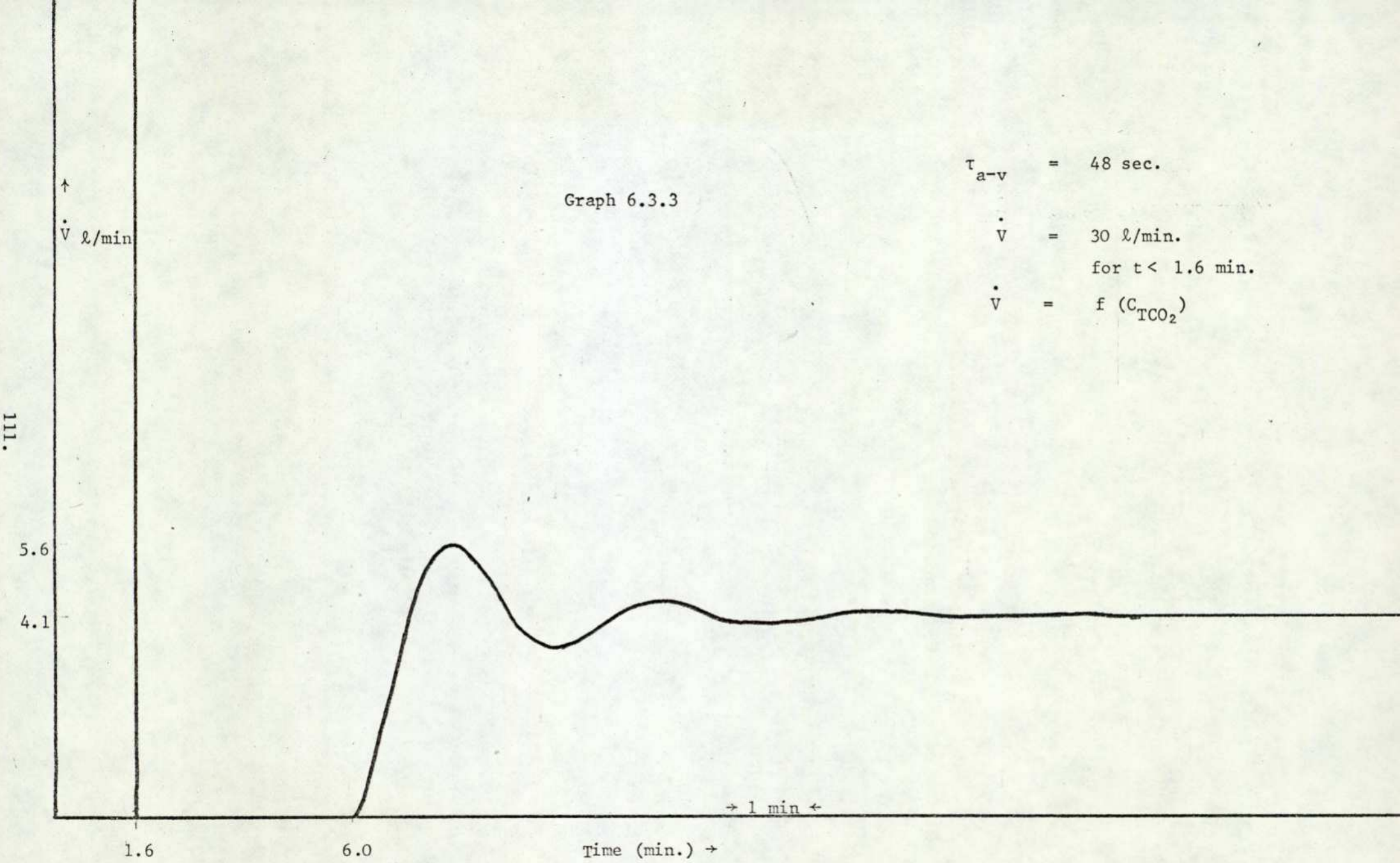

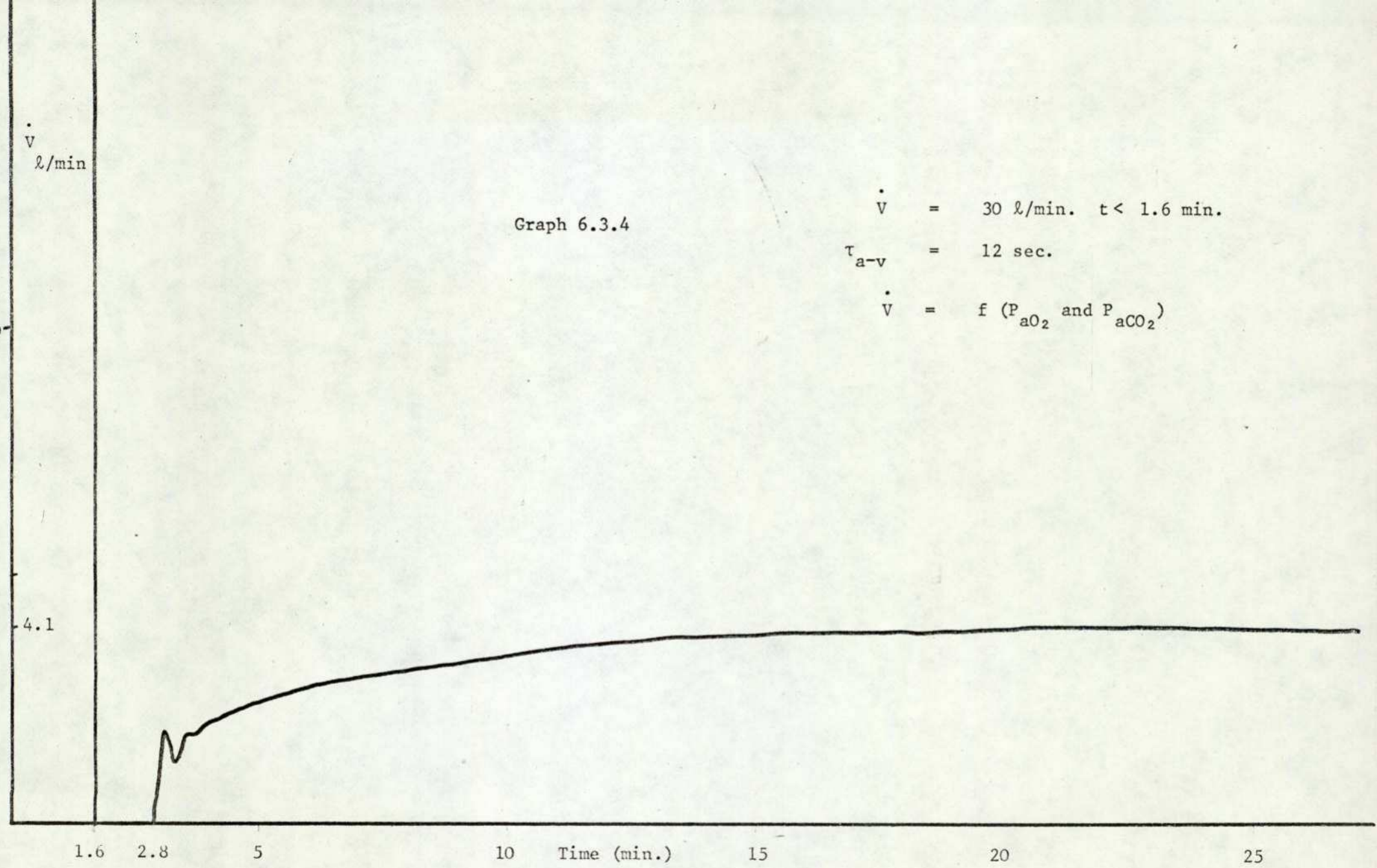

Graph 6.3.4

$\dot{V}$ = 30 ℓ/min. t < 1.6 min.

τ_{a-v} = 12 sec.

$\dot{V}$ = f (P_{aO_2} and P_{aCO_2})

Graph 6.3.5

$\dot{V}$ = 30 t < 1.6 min.

τ_{a-v} = 24 sec.

$\dot{V}$ = f (P_{aCO_2} and P_{aO_2})

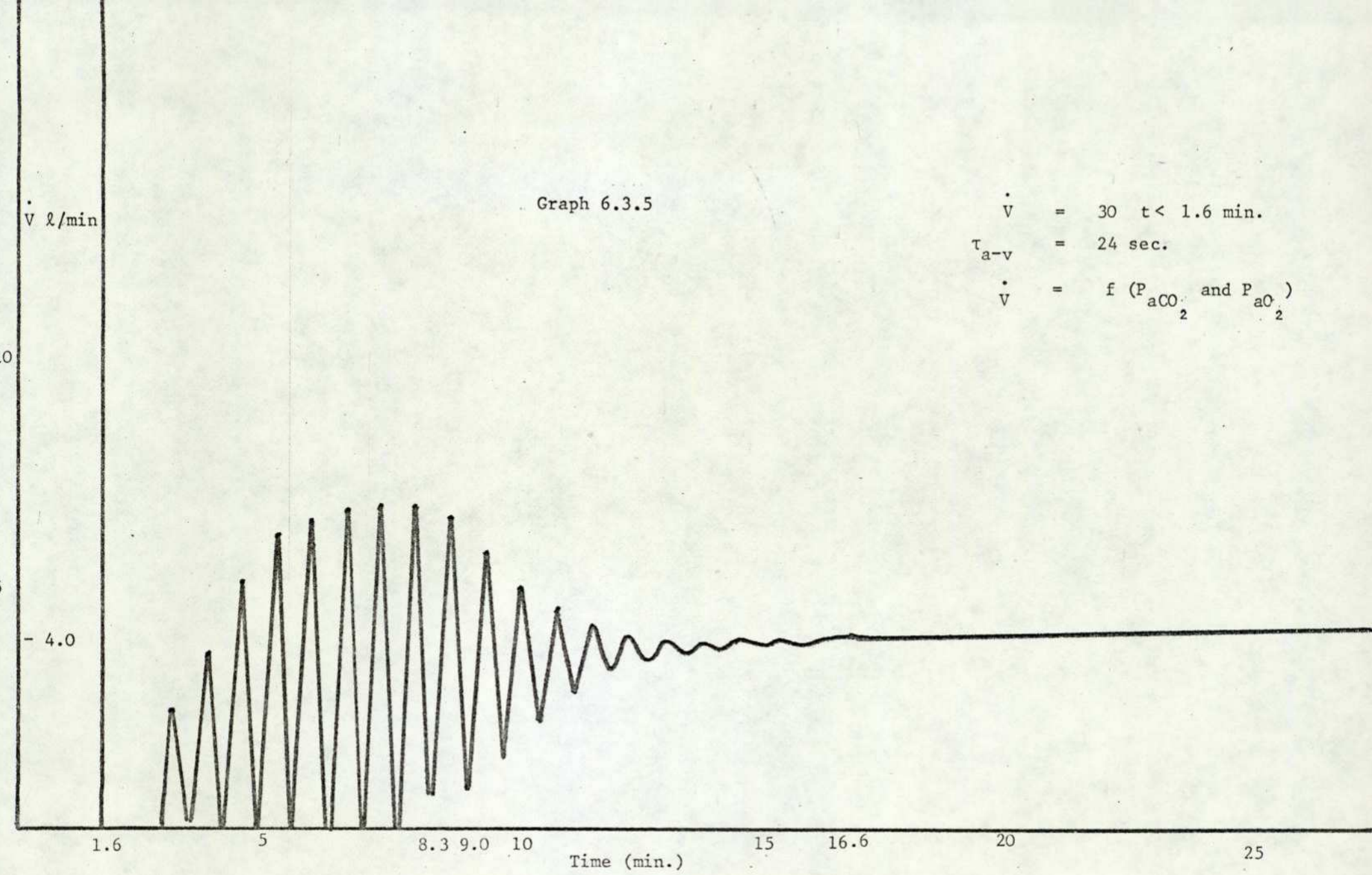

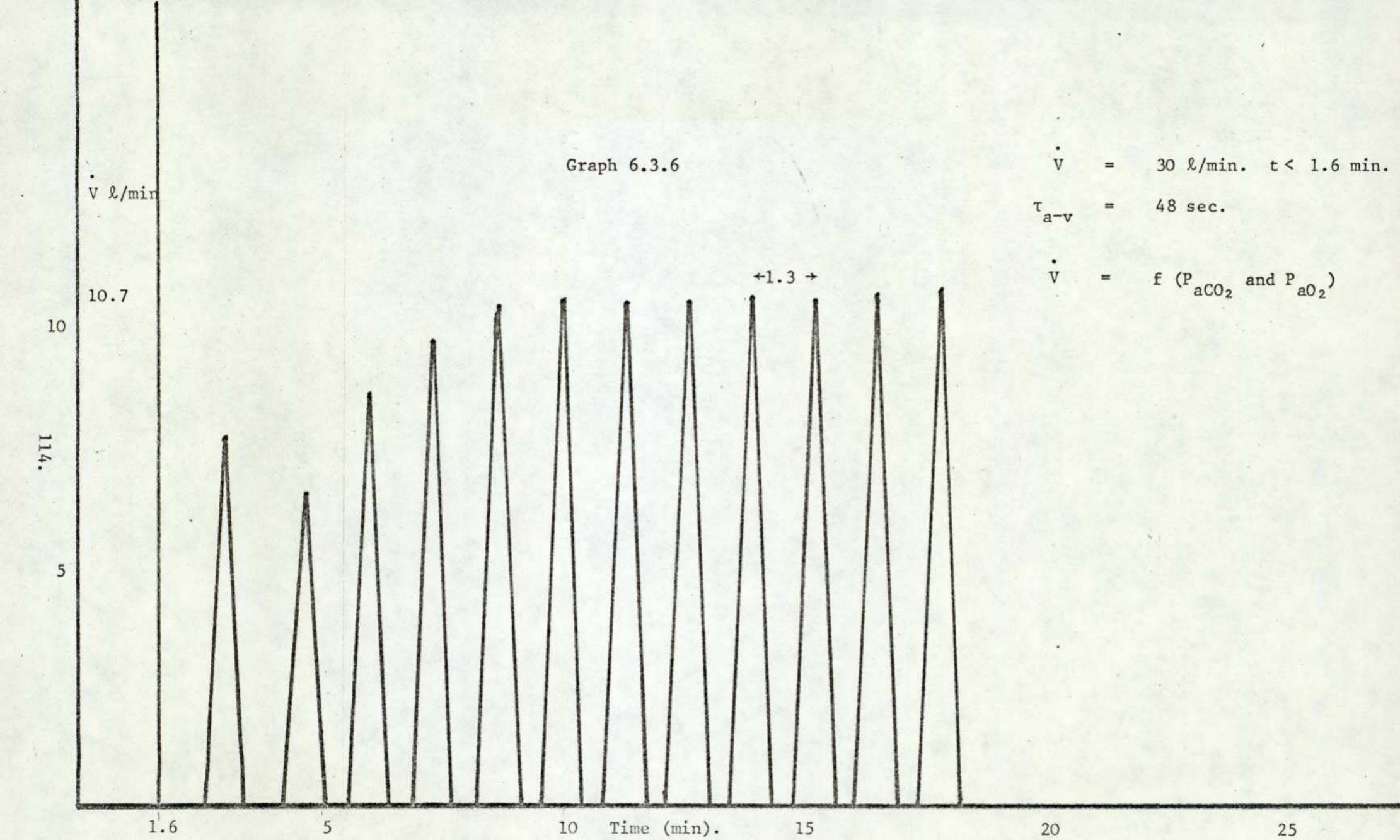
Graph 6.3.6
$\dot{V}$ = 30 ℓ/min. t < 1.6 min.
τ_{a-v} = 48 sec.
$\dot{V}$ = f (P_{aCO_2} and P_{aO_2})
$\dot{V}$ ℓ/min
10.7
10
5
114.
←1.3→
1.6
5
10
Time (min).
15
20
25

Graph 6.3.7

$\dot{V}$ = 60 ℓ/min. $t < 1.5$ min.

τ_{a-v} = 12 sec.

$\dot{V}$ = $f(C_{TCO_2})$

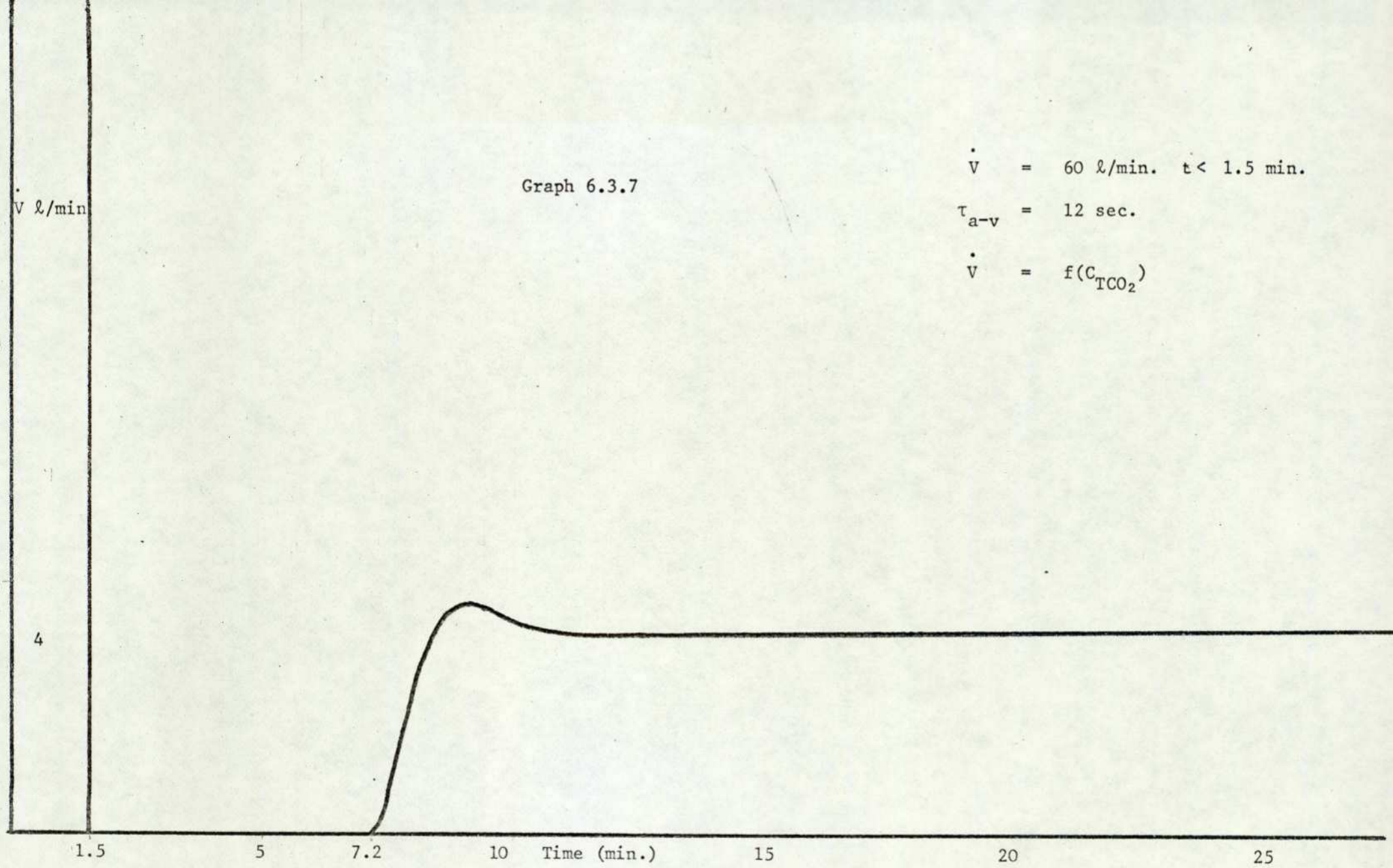

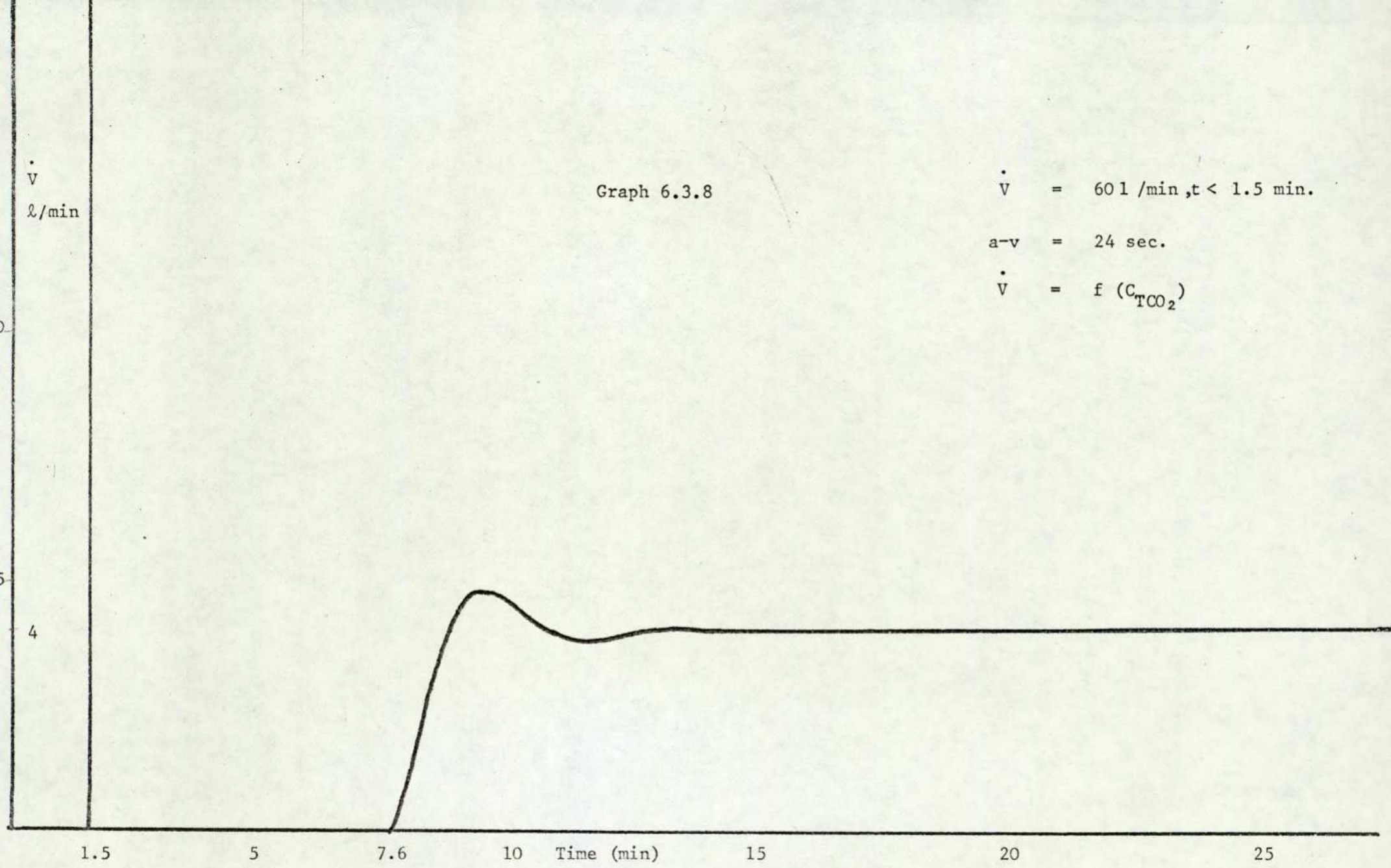

Graph 6.3.8

$\dot{V}$ = 60 l /min , t < 1.5 min.

a-v = 24 sec.

$\dot{V}$ = f (C_{TCO_2})

Graph 6.3.9

τ_{a-v} = 48 sec.

$\dot{V}$ = 60 ℓ/min.
for t < 1.5 min.

$\dot{V}$ = $f(C_{TCO_2})$

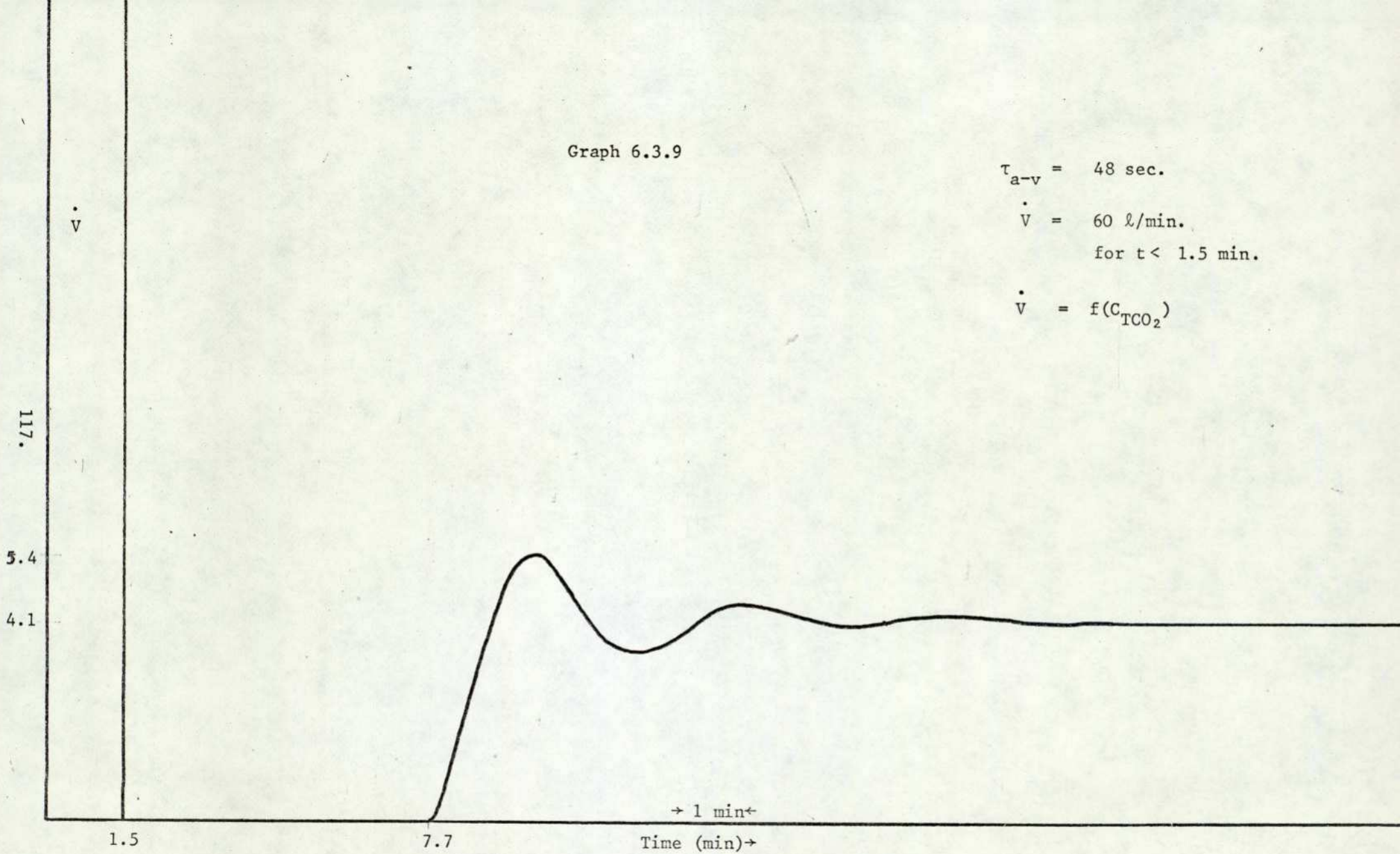

Graph 6.3.10

$\dot{V} = f(P_{aO_2} \& P_{aCO_2})$

$\dot{V} = 60\ T < 1.5$ min.

$\tau_{a-v} = 12$ sec.

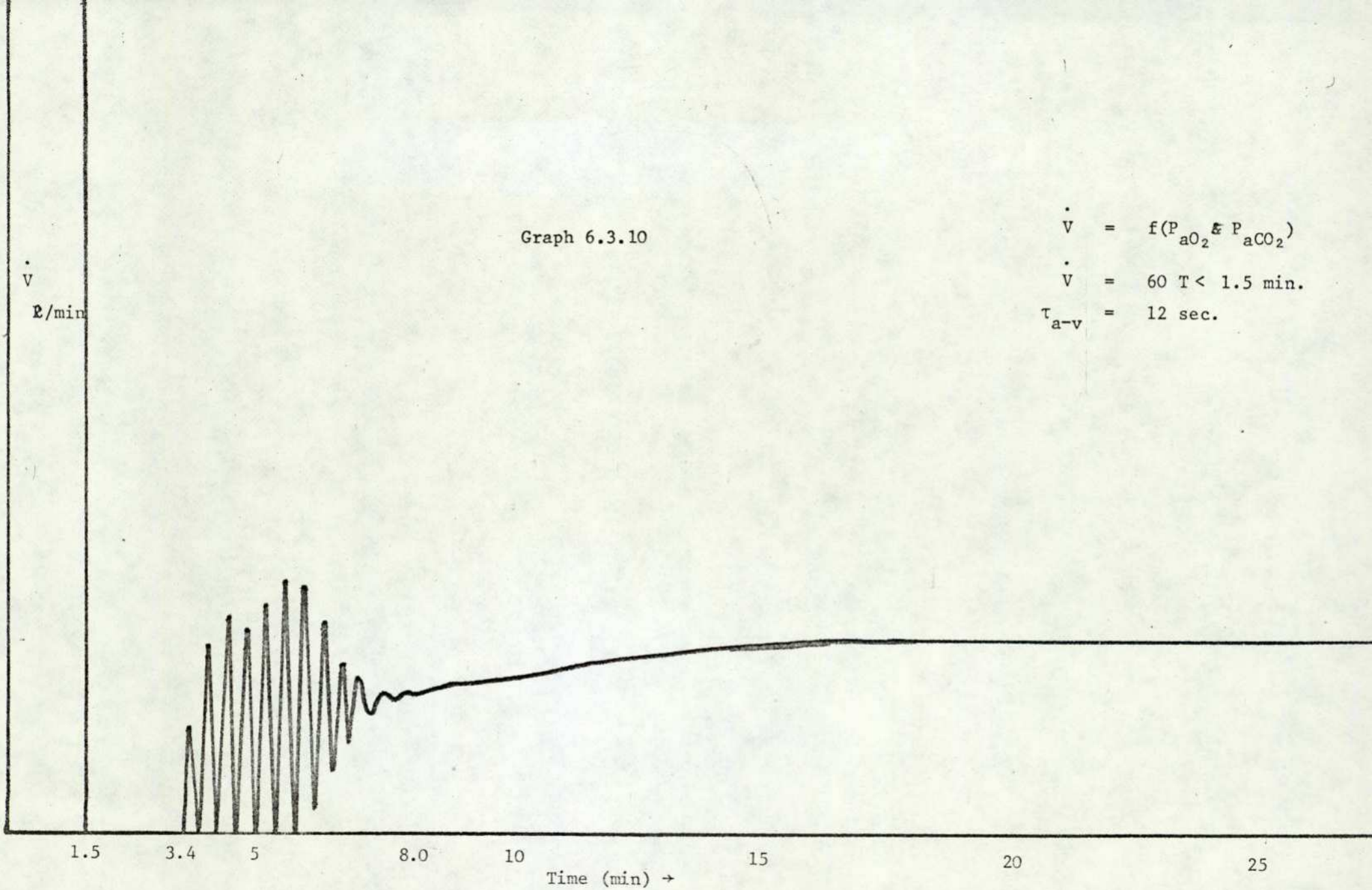

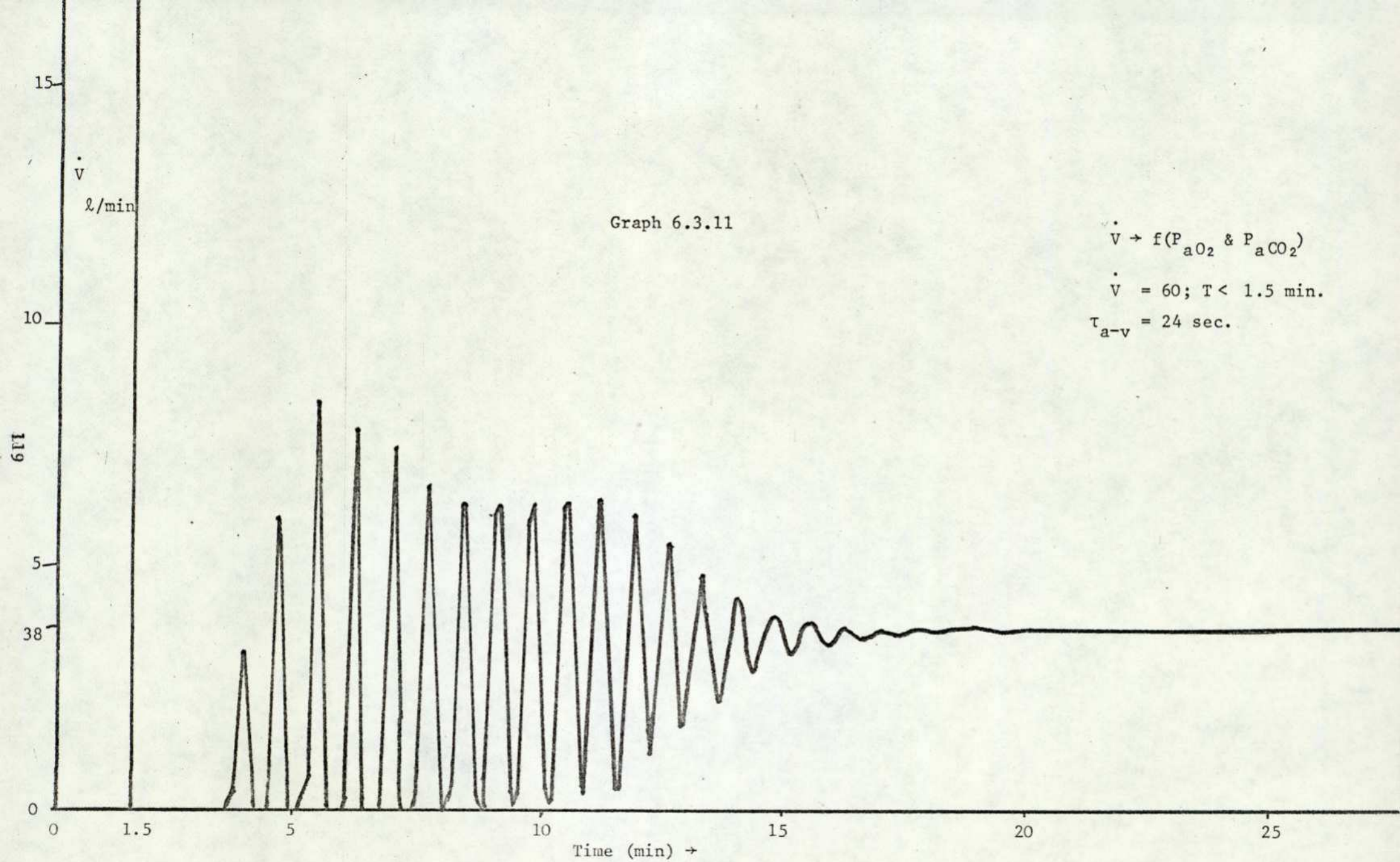

Graph 6.3.11

$\dot{V} \rightarrow f(P_{aO_2}$ & $P_{aCO_2})$

$\dot{V}$ = 60; T < 1.5 min.

τ_{a-v} = 24 sec.

Graph 6.3.12

$\dot{V} \rightarrow f(P_{aCO_2} \& P_{aO_2})$

$\dot{V}$ = 60, T< 1.5 min.

τ_{a-v} = 24 sec.

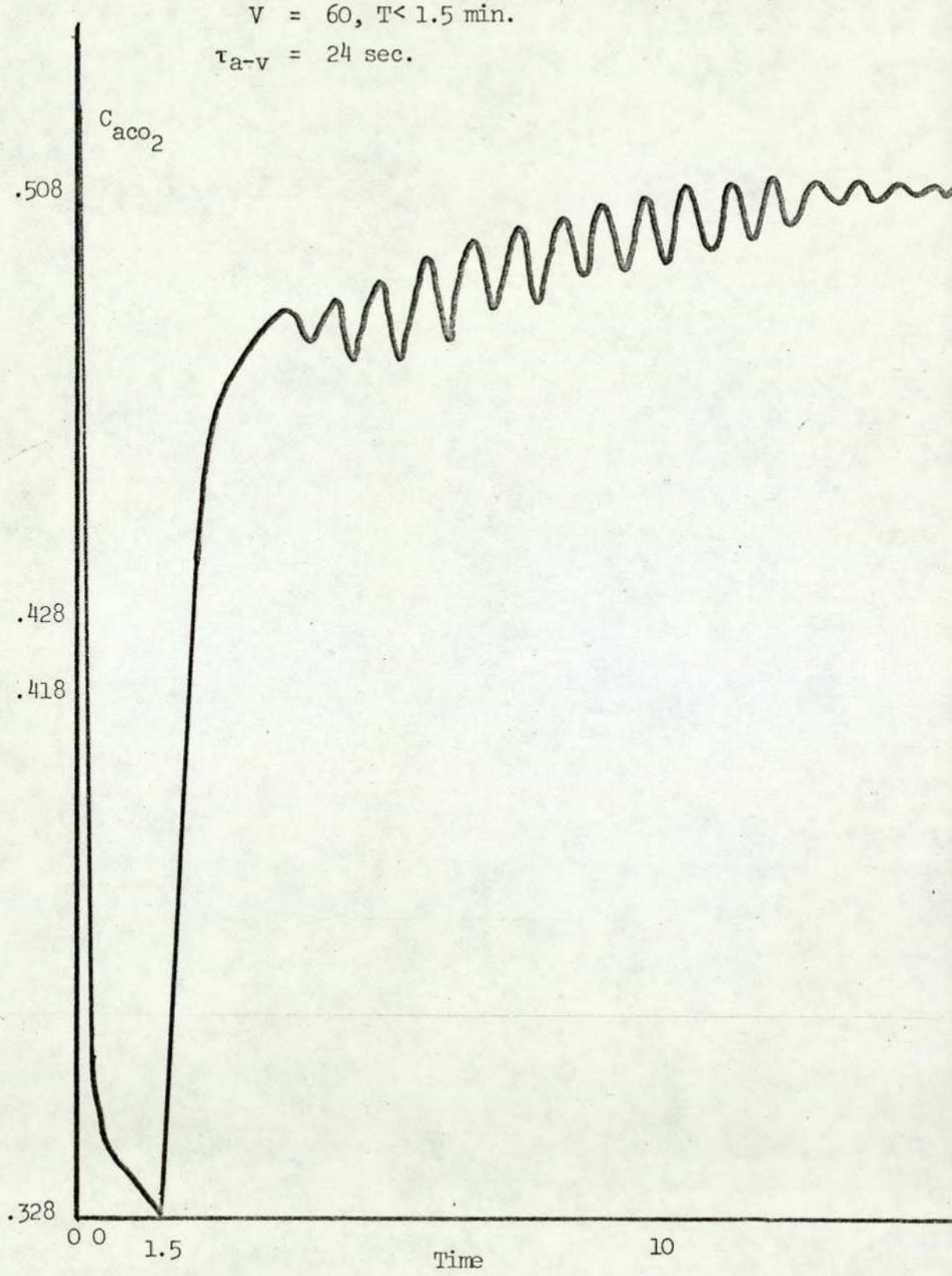

CHAPTER 7

MODEL III. (Incorporating brain tissue compartment and variable time delays).

From the discussion of the models so far (Model I and II) it can be seen that the major area of uncertainty in the respiratory physiology is the action and location of the controller. The controller equations used have been tested for various disturbances to the model and the model response is compared with corresponding experimental evidence. Clearly there is need to look further into the development of controller equations and testing of the model against a wider set of experimental evidence. Also there is a need to develop the model further to include brain tissues and muscle tissues so that the model represents various physiological sections more closely. As shown before (chapter 5 and 6),time delays play an important part in determining the modelling response, thus there is a need to include more realistic circulation delay equations into the model.

The central chemoreceptor controller equation used in Model II (chapter 6) had as its basis mixed venous CO_2 concentration. Clearly this is not true as the central chemoreceptors are sited near the brain. There is therefore a need to extend the model by incorporating a brain tissue compartment. Furthermore there is physiological evidence to show that cardiac output and cerebral blood flow are both functions of arterial P_{CO_2} and P_{O_2} (Grodins et al,1967). With the inclusion of brain tissue compartment and local controls for cardiac output and cerebral blood flow, it is difficult to use fixed time delays (transport delays) with any accuracy. These time delays are

functions of blood flow rates and as the blood flow rate changes with changes in arterial P_{CO_2} and P_{O_2}, the time delays will also change.

Thus a new set of equations is derived to produce the desired time delays which are functions of cardiac output and cerebral blood flow which themselves vary with arterial P_{CO_2} and P_{O_2}. Also oxygen flow equations are developed for each compartment as opposed to total oxygen consumption of body tissues (Model II). This will facilitate the simulation of various metabolic CO_2 production and oxygen consumption rates for each individual tissue compartment in which the carbon dioxide chemoreceptors are postulated to be; and will be of prime importance to the model response for CO_2 inhalation. Furthermore there is physiological evidence to show that the blood flow rate to the brain (cerebral blood flow) and the total cardiac output are both functions of arterial partial pressures of oxygen and carbon dioxide (Grodins et al,1967). Thus blood flow rates to each compartment and particularly to the brain compartment will change with any changes in the arterial blood gas composition.

On the other hand the circulation delay to various tissue compartments to and from the lung have so far been assumed constant. Clearly any changes in blood flow rates are going to change these circulation delays, further affecting the model response. Thus there is also a need to develop a new set of equations to provide the desired time delays which are direct functions of the blood flow rate and the volume through which this blood has to flow to reach any compartment. Assuming the passage volume to be constant, the time delays may be postulated as a direct function of blood flow rate flowing through that path.

Thus the circulation delay from lung to each tissue compartment will in the first instant depend upon the cardiac output and cerebral blood flow rate, but as the latter are themselves variable functions of arterial P_{CO_2} and P_{O_2}, the arterial gas composition will also affect the circulation delays.

As the metabolic rate of CO_2 production and O_2 consumption is different for each tissue compartment, and also the ratio of total CO_2 production rate to total oxygen consumption rate is different for each tissue compartment (brain, muscle and other tissues), there is a need to develop oxygen flow equations for each compartment as opposed to one equation of total oxygen flow through the tissues to the venous side of lung (chapter 6). For example the ratio of CO_2 production to oxygen consumption of brain tissues is unity whereas for muscle and other tissues it is less than unity.

Considering the above, the following new features and assumptions are incorporated in the present model.

1. A separate brain tissue compartment is added whose blood flow rate is formulated to be a function of arterial P_{CO_2} and P_{O_2} after Grodins et al (1967).
2. Total cardiac output is postulated to be a function of arterial P_{CO_2} and P_{O_2} after Grodins et al (1967).
3. The volume of the passage through which blood flows to each compartment is assumed to be constant and the passage volume differs on the arterial and venous sides of the same tissue compartment (Grodins et al 1967).
4. Oxygen as well as carbon dioxide flow equations are formulated for each tissue compartment and the ratio of CO_2 production to oxygen

consumption is different for each compartment and is constant (Lloyd and Cunningham, 1963, Longobardo et al, 1965).

5. The central chemoreceptors, sensitive to changes in carbon-dioxide concentration, are assumed to be situated in the brain tissue compartment.

6. The time delays on the arterial as well as the venous side are variable and are functions of cardiac output and cerebral blood flow rates. Also a simple first order lag is assumed in changes of cardiac output amd cerebral flow rate following a sudden change in arterial gas composition. The time constant of these simple lags is assumed to be 6 seconds (Grodins et al 1967).

7. The arterial chemoreceptors are assumed to be situated at the same time distance from the lungs as the blood transportation time from the lungs to the brain.

As mentioned above further considerations are given to formulation of new controller equations so that a wider set of experimental data can be compared with the model responses. One section which has not been dealt with so far is the response of the model to Hypoxic breathing, i.e., breathing less than normal oxygen concentration in the air. To be able to incorporate that into the model, development and action of the controller equations will have to be looked at in greater detail. Clearly the new equation will have to be developed on the basis of published experimental results which are based on steady state data.

7.1 Controller Actions: Development of controller equations:

(a) Arterial Controller:

Cunningham et al (1963) performed some experiments on humans for CO_2 breathing. These data were used to show that the slope of graphs

between P_{ACO_2} and ventilation rate is a function of oxygen. Lloyd and Cunningham (1963) suggested that there is a straight line relationship between ventilation and alveolar P_{CO_2}, but the slope of this line varied with P_{AO_2} in a hyperbolic fashion. The form of equation suggested by Lloyd and Cunningham has been discussed in chapter 6.

This structure was based upon the assumption that the ventilation in the P_{ACO_2} line at any alveolar P_{O_2} may be extrapolated to a zero ventilation which corresponds to an alveolar P_{CO_2} value. This theoretical value of P_{ACO_2} may be regarded as that at which CO_2 causes no respiratory stimulation of itself. Nielson and Smith (1951) who first noted this called the point of intersection the 'Apnoea-point'. All the $\dot{V} \sim P_{ACO_2}$ lines though differing in slope according to P_{AO_2}, when extrapolated meet at this one point and the $\dot{V} \sim P_{ACO_2}$ relationship at any given P_{AO_2} may be expressed by the equation

$$\dot{V} = S\ (P_{ACO_2} - B) \qquad \ldots\ldots\ 7.1$$

where S is the slope of the line and B the 'apnoea point'.

The hyperbolic relationship between S and P_{AO_2} has been described by Lloyd and Cunningham (1963) in the following equation

$$S = D\ (1 + \frac{A}{P_{AO_2} - C}) \qquad \ldots\ldots\ 7.2$$

which when substituted in equation 7.1 for S gives:

$$\dot{V} = D\ (1 + \frac{A}{P_{AO_2} - C})\ (P_{ACO_2} - B) \qquad \ldots\ldots\ 7.3$$

This equation has four parameters A, B, C, D; of these B has already been defined as the alveolar value of P_{CO_2} at which CO_2 by itself exerts no effect on breathing. It can be seen that D is the minimum slope of the $\dot{V} \sim P_{ACO_2}$ line, i.e. the value of S when P_{AO_2} is infinity

and there is no hypoxic drive. C on the other hand is the critical alveolar PO_2 value at which the slope becomes infinite. A is a parameter which describes the sensitivity to Hypoxia.

Using the data of Nielson and Smith (1951), Longobardo et al (1966) derived the following values of the parameters of the above equation:

$$D = 1.81 \ , \quad B = 31.0 \ , \quad C = 32.44 \ , \quad A = 13.0$$

but due to discrepancies in steady state results they included a factor of -15.0 into the equation so that the equation now became

$$\dot{V} = 1.81 \ (P_{ACO_2} - 31.0) \ (1 + \frac{13.0}{P_{AO_2} - 32.44}) - 15.0 > o. \quad \ldots\ldots \quad 7.4$$

This equation was used in chapter 6 to represent the response of arterial chemoreceptors.

On the other hand using the experimental data of Lloyd and Cunningham (1963), Milhorn and Brown (1971) found the following values of the parameters:

$$D = 2.0 \ , \quad B = 37.24 \ , \quad C = 25.0 \ , \quad \text{and } A = 13.6$$

To produce the above values Milhorn and Brown only considered one experiment (No.26) out of a large number of experiments. Thus their equation became

$$\dot{V} = 2.0(P_{ACO_2} - 37.24)(1 + \frac{13.6}{P_{AO_2} - 25.0}) \geq o \qquad \ldots\ldots \quad 7.5$$

Graph (7.1) shows the plot of $\dot{V}$ versus P_{ACO_2} for various P_{AO_2} values for the equations number 7.4 and 7.5.

From these figures it can be seen that the values of slopes for very low P_{AO_2} (41.5 and 54.0) given by the Longobardo equation (4)

are higher whereas for higher P_{AO_2} (64, 100, 153) the slopes of the Milhorn et al equation (5) are higher. Thus in the case of hypoxia i.e. less than normal oxygen breathing, the Longobordo equation will show higher sensitivity.

Cunningham et al (1963) produced results for a large number of experiments and the data showed considerable variance with the subjects. Thus it will be more accurate to average the data, rather than to develop an equation based upon only one set of data. Furthermore these experiments were done only for CO_2 breathing, i.e. at the higher end of P_{ACO_2} scale. It is known in physiology that when a subject inhales less than normal oxygen gas mixtures, the ventilation goes up. This increase in ventilation tends to reduce the carbon dioxide in the system and consequently P_{ACO_2} falls. Considering the above equations it can be seen that neither of them on its own is suitable for testing the model for hypoxic conditions as ventilation goes to zero at a P_{ACO_2} value of approximately 37.0 mm Hg, which is not true.

Weil et al (1970) performed experiments on human subjects for hypoxia for a constant P_{ACO_2}. They assumed that hypoxic drive for ventilation is of the form

$$\dot{V} = \dot{V}_o + \frac{A}{P_{AO_2} - K} \qquad \ldots\ldots 7.6$$

where K had the value of 32. Equation 7.16 is similar to equation 7.3, where P_{ACO_2} is constant, and the sensitivity of oxygen to ventilation is studied. The hyperbolic relationship between $\dot{V}$ and P_{AO_2} is maintained as discussed above.

Thus $\dot{V}$ was calculated for the mean values of $\dot{V}_o$ and A for varying P_{AO_2}.

Thus a new controller equation may be developed by combining the data of Cunningham et al (1963) and Weil et al (1970). For the sake of clarification some tables of data are reproduced here from the two papers.

1. Data of Cunningham et al: (1963) CO_2 breathing:

Assume the same structure for the controller function,

i.e. $$\dot{V} = D\,(P_{ACO_2} - B)\,(1 + \frac{A}{P_{AO_2} - C}) \qquad \ldots\ldots 7.7$$

The following table (Table 7.I) shows the entire data from Table II of the publication grouped together for various P_{AO_2} and the values of B and S for each. The averages are calculated by the arithmetic mean

Range	P_{AO_2} Mean	B Mean	S Mean
143-156	153	36.0	2.6
96-102	100	39.7	3.7
60-67	64.1	36.4	4.0
52-57	54.1	37.4	5.7
48.2-49.8	49.1	39.8	7.3
43-45.6	44.8	38.5	7.26
40.2-42.9	41.5	39.9	9.3

Mean B = 38.0

TABLE 7.1

Thus equation 7.7 becomes

$$\dot{V} = S\,(P_{ACO_2} - 38.0) \qquad \ldots\ldots 7.8$$

Graph 7.2 shows the plot of

$$\dot{V} \sim (P_{ACO_2} - 38.0) \text{ for various } P_{AO_2}$$

Now assuming the relationship of S to P_{AO_2} to be hyperbolic after Lloyd and Cunningham (1963)

$$S = D\left(1 + \frac{A}{P_{AO_2} - C}\right) \qquad \ldots\ldots 7.9$$

Assuming the value of C to be 30 for which S becomes infinite, from Graph No. 7.3 ($S \sim P_{AO_2}$).

$$S = X + \frac{Y}{P_{AO_2} - 30}$$

where X = D and Y = A D.

Now plotting S versus $\frac{1}{P_{AO_2} - 30}$ from table 7.1 the straight line obtained is shown in graph (7.4) from which the values are X = 2.2 and Y = 85.83.

Therefore

$$S = 2.2\left(1 + \frac{39.0}{P_{AO_2} - 30}\right)$$

The overall equation now becomes

$$\dot{V} = 2.2\,(P_{ACO_2} - 38.0)\left(1 + \frac{39.0}{P_{AO_2} - 30}\right) \qquad \ldots\ldots 7.10$$

Equation 7.10 describes the relationships for CO_2 breathing. Graph 7.2 shows the plot of $\dot{V} \sim P_{ACO_2}$ for equation 7.10

2. Data from Weil et al (1970): Hypoxic Drive:

Weil et al assumed the following relationship between ventilation and arterial PO_2

$$\dot{V} = \dot{V}_o + \frac{A}{P_{AO_2} - 32.0} \qquad \ldots\ldots 7.11$$

for constant values of P_{ACO_2}. The values of A and $\dot{V}_o$ are the average values for various subjects.

for P_{CO_2} = 37.5

$\dot{V}_o$ = 4.6 and A = 181

for P_{CO_2} = 42.3

$\dot{V}_o$ = 5.2 and A = 453.4

The plots of $\dot{V}$ versus P_{ACO_2} for various values of P_{AO_2} from equation 7.10 and from equation 7.11 are shown in graph number 7.5. From this graph it can be seen that it is possible to construct a controller equation which will account for hypoxia as well as CO_2 breathing by changing the slope equation. Assuming the value of minimum ventilation to be 4 litres per minute at P_{ACO_2} less than or equal to 30mm Hg, the form of the equation becomes

$$\dot{V} = S_2 (P_{ACO_2} - 30.0) + 4.0 \quad \ldots\ldots 7.12$$

for $30 \leq P_{ACO_2} \leq 40$

In other words at P_{ACO_2} = 40 mm Hg there is a sharp change in slope.

But from equation 7.10

$$\dot{V} = S_1 (P_{ACO_2} - 38.0) \quad \ldots\ldots 7.13$$

for $P_{ACO_2} > 40.0$

where $S_1 = 2.2 \left(1 + \frac{39.0}{P_{AO_2} - 30.0}\right)$

from equation 7.12 and 7.13

$$S_1 (P_{ACO_2} - 38.0) = S_2 (P_{ACO_2} - 30.0) + 4.0 \quad \ldots\ldots 7.14$$

$$\therefore S_2 = \frac{S_1 (P_{ACO_2} - 38.0) - 4.0}{(P_{ACO_2} - 30.0)} \quad \ldots\ldots 7.15$$

but as the cut-off point is at P_{ACO_2} = 40.0;

$$S_2 = \frac{2 S_1 - 4.0}{10}$$

or

$$S_2 = 0.2 (S_1 - 2.0) \quad \ldots\ldots 7.16$$

Thus the new controller equation becomes

$$\dot{V} = S\,(P_{ACO_2} - 38.0)$$

$$\text{for } P_{ACO_2} \geq 40.0$$

$$= 0.2\,(S - 2.0)(P_{ACO_2} - 30.0) + 4.0$$

$$\text{for } 30 \leq P_{ACO_2} < 40 \qquad \ldots\ldots 7.17$$

$$= 4.0$$

$$\text{for } P_{ACO_2} < 30$$

Graph 7.6 shows the relationship between $\dot{V}$ and P_{ACO_2} for various P_{AO_2}.

Thus the three equations for arterial controllers are as follows:

Longobardo et al (1966)

$$\dot{V} = 1.81\,(P_{ACO_2} - 31.0)\left(1 + \frac{13.0}{P_{AO_2} - 32.44}\right) - 15.0 \geq 0 \qquad \ldots\ldots 7.18$$

Milhorn and Brown (1971)

$$\dot{V} = 2.0\,(P_{ACO_2} - 37.24)\left(1 + \frac{13.6}{P_{AO_2} - 25.0}\right) \geq 0 \qquad \ldots\ldots 7.19$$

New controller equation

$$\dot{V} = 2.2\left(1 + \frac{39.0}{P_{AO_2} - 30.0}\right)(P_{ACO_2} - 38.0)$$

$$P_{ACO_2} \geq 40.0$$

$$= 0.04\left(1 + \frac{428}{P_{AO_2} - 30.0}\right)(P_{ACO_2} - 30.0) \qquad \ldots\ldots 7.20$$

$$30.0 \leq P_{ACO_2} < 40.0$$

$$= 4.0$$

$$P_{ACO_2} < 30$$

However equation 7.20 has been derived assuming that the hyperbola between S and P_{AO_2} has its asymptotes at P_{AO_2} equal to 30.0 and S equal to 2.2. The most recent experimental evidence (Reynolds and Milhorn, 1973) shows that these values are equal to 37.5 and 2.4 respectively. Thus equation 7.20 can be modified to:

$$\dot{V} = S\,(P_{ACO_2} - 38.0)$$

for $P_{ACO_2} \geq 40.0$

$$= \cdot 2\,(S - 2.0)(P_{ACO_2} - 30.0) + 4.0$$

for $30 \leq P_{ACO_2} \leq 40$ 7.21

$$= 4.0$$

for $P_{ACO_2} < 30$

where

$$S = 2.4\,(1 + \frac{20}{P_{AO_2} - 37.5})$$

(b) Brain Tissue CO_2 control:

The original form of equation, produced by Grodins et al is retained, i.e.

$$\dot{V} = \dot{V}_N + K\,(C_{BTCO_2} - (C_{BTCO_2})_N) \quad \ldots\ldots 7.22$$

where $\dot{V}_N$ is the normal ventilation rate and $(C_{BTCO_2})_N$ is the corresponding brain tissue CO_2 concentration and K represents the gain of the controller equation. It can clearly be seen that equation 7.32 is not suitable for hypoxic conditions as it does not contain any sensitivity to oxygen, except indirectly through the fact that any decrease in oxygen concentration in the lung compartment will increase the concentration of CO_2 for a while, which in turn will increase ventilation, reducing the CO_2 content of the body, reducing ventilation and finally the ventilation level may well be even lower than normal, which is contrary to physiological evidence. However brain tissue CO_2 control is retained for CO_2 breathing as the discussions in previous chapter show that the CO_2 content of the body can be described

more accurately using brain tissue CO_2 control. Further, this confirms the physiological hypothesis that the main controller action for the CO_2 content of the body is sited near the brain whereas primarily arterial chemoreceptors control the oxygen content of the body. There is further evidence which suggests that central chemoreceptors are sensitive to CO_2 concentration whereas the arterial chemoreceptors are sensitive to oxygen concentration as well as the rate of change of arterial P_{CO_2} from breath to breath.

7.2 FORMULATION OF SYSTEM EQUATIONS

The four compartment model (Lung, Brain Tissues, Muscle Tissues, Other Tissues) is as shown in figure 7.1. There are two equations for each compartment, oxygen flow and carbon dioxide flow. The equations are formulated on a similar basis to that adopted for Model II.

i. CARBON DIOXIDE

$$\frac{d}{dt}\left(\frac{V_r}{P_B-47} \cdot P_a + V_a C_a\right) = \dot{q}\,(C_v(\tau_{T-L}) - C_a) - \frac{\dot{V}}{P_B-47}(P_a - P_I) \quad \ldots\ldots 7.23$$

$$\frac{d}{dt}(V_{OT} \cdot C_{OT}) = \dot{M}_{OT} + \dot{q}_{OT}\,(C_a(\tau_{L-OT}) - C_{vOT}) \quad \ldots\ldots 7.24$$

$$\frac{d}{dt}(V_m \cdot C_m) = \dot{M}_m + \dot{q}_m\,(C_a(\tau_{L-m}) - C_{vm}) \quad \ldots\ldots 7.25$$

$$\frac{d}{dt}(V_B \cdot C_B) = \dot{M}_B + \dot{q}_B\,(C_a(\tau_{L-B}) - C_{vB}) \quad \ldots\ldots 7.26$$

$$C_v(\tau_{T-L}) = \frac{\dot{q}_m C_m(\tau_{m-L}) + \dot{q}_{OT} C_{OT}(\tau_{OT-L}) + \dot{q}_B(\tau_{B-L})}{\dot{q}} \quad \ldots\ldots 7.27$$

where C_v is the mixed venous CO_2 concentration at the venous side of the lung.

ii. OXYGEN

$$\frac{d}{dt}\left(\frac{V_r}{P_B-47} \cdot P_a + V_a\ C_a\right) = \dot{q}\,(C_v(\tau) - C_a) - \frac{\dot{V}}{P_B-47}\,(P_a-P_I) \qquad \ldots\ldots 7.28$$

$$\frac{d}{dt}\left(V_{OT} \cdot C_{OT}\right) = -\dot{U}_{OT} + \dot{q}_{OT}\left(C_a(\tau_{L-OT}) - C_{vOT}\right) \qquad \ldots\ldots 7.29$$

$$\frac{d}{dt}\left(V_m \cdot C_m\right) = -\dot{U}_m + \dot{q}_m\left(C_a(\tau_{L-m}) - C_{vm}\right) \qquad \ldots\ldots 7.30$$

$$\frac{d}{dt}\left(V_B \cdot C_B\right) = -\dot{U}_B + \dot{q}_B\left(C_a(\tau_{L-B}) - C_{vB}\right) \qquad \ldots\ldots 7.31$$

$$C_v(\tau_{T-L}) = \frac{\dot{q}_m C_m(\tau_{M-L}) + \dot{q}_{OT} C_{OT}(\tau_{OT-L}) + \dot{q}_B C_B(\tau_{B-L})}{\dot{q}} \qquad \ldots\ldots 7.32$$

where $C_v(\tau_{T-L})$ is the mixed venous O_2 concentration at the venous side of lungs.

iii. CARDIAC FLOW CONTROL

If we consider that the total cardiac output at any given time is equal to the normal cardiac output plus any changes due to changes in arterial P_{CO_2} and P_{O_2}, we can write

$$\dot{Q} = \dot{q}_N + \Delta\,\dot{q}_{CO_2} + \Delta\,\dot{q}_{O_2} \qquad \ldots\ldots 7.33$$

where $\dot{q}_N$ is the normal cardiac output and $\Delta\,\dot{q}_{O_2}$ and $\Delta\,\dot{q}_{CO_2}$ represent any changes that may occur due to changes in arterial P_{O_2} and P_{CO_2} respectively .

The following equations were developed by Grodins et al, (1967) by curve fitting to experimental data.

$$\dot{\Delta q}_{CO_2} = 0.3\ (P_{aCO_2} - 40.0)$$

$$\text{for } 40.0 < P_{aCO_2} < 60.0 \qquad \ldots\ldots 7.34$$

$$= 0.0 \text{ for all other } P_{aCO_2}.$$

$$\dot{\Delta q}_{O_2} = 9.6551 - 0.2885\ P_{aO_2} + 2.9241 * 10^{-3}\ (P_{aO_2})^2$$

$$- 1.0033 * 10^{-5}\ (P_{aO_2})^3 \qquad \ldots\ldots 7.35$$

$$\text{for } P_{aO_2} < 104.0$$

$$= 0 \text{ for } P_{aO_2} > 104.0$$

$$\text{and } \dot{q} = \frac{1}{1 + \tau s} \cdot \dot{Q} \qquad \ldots\ldots 7.36$$

where $\frac{1}{1 + \tau s}$ represents a first order lag with a time constant $\tau = 6$ seconds assumed.

iv. CEREBRAL BLOOD FLOW CONTROL

Similar to equation 7.13 we can write

$$\dot{Q}_B = \dot{q}_{BN} + \Delta\ \dot{q}_{BCO_2} + \Delta\ \dot{q}_{BO_2} \qquad \ldots\ldots 7.37$$

where $\dot{\Delta q}_{BCO_2}$ and $\dot{\Delta q}_{BO_2}$ represent changes in cerebral blood flow due to changes of P_{CO_2} and P_{O_2} in arterial blood respectively.

Again the following equations were developed by Grodins et al (1967) by curve fitting to experimental data.

$$\dot{\Delta q}_{BO_2} = 2.785 - 0.1323\ P_{aO_2} + 2.6033\ \ 10^{-3}\ (P_{aO_2})^2$$

$$- 2.324\ \ 10^{-5}\ (P_{aO_2})^3 + 7.6559\ \ 10^{-8}\ (P_{aO_2})^4 \qquad \ldots\ldots 7.38$$

$$\text{for } P_{aO_2} < 104.0$$

$$= 0.0 \text{ for } P_{aO_2} > 104.0$$

$$\dot{\Delta q}_{BCO_2} = 2.323 * 10^{-2} - 3.1073 * 10^{-2} P_{aCO_2} + 8.0163 * 10^{-4} (P_{aCO_2})^2 \quad \text{for } P_{aCO_2} < 38.0$$

$$= 0 \text{ for } 38.0 < P_{aCO_2} < 44.0 \qquad \ldots\ldots 7.39$$

$$= -15.58 + 0.7607 P_{aCO_2} - 1.2947 * 10^{-2} (P_{aCO_2})^2 + 9.3918 * 10^{-5} (P_{aCO_2})^3 - 2.1748 + 10^{-7} (P_{aCO_2})^4 \quad \text{for } P_{aCO_2} < 44.0$$

and

$$\dot{q}_B = \frac{1}{1 + \tau_B s} \dot{Q}_B \qquad \ldots\ldots 7.40$$

where $\frac{1}{1 + \tau_B s}$ represents a 1st order lag of time constant τ_B equal to 6 seconds assumed

v. CALCULATION OF CIRCULATION DELAYS: (Figure 7.2)

The governing equation for the calculation of time delay is:

$\tau = \frac{\text{Volume}}{\text{Flow Rate}}$ at any instant, assuming the volume to be fixed.

In figure 7.2 the values for the fixed volumes of passages through which blood flows are taken from Grodins et al (1967) and thus the following equations are developed:

Arterial Delays:

$$\tau_{L-B} = \frac{1.062}{\dot{q}} + \frac{0.015}{\dot{q}_B} \qquad \ldots\ldots 7.41$$

$$\tau_{L-OT} = \frac{1.062}{\dot{q}} + \frac{0.3675}{\dot{q}_{OT}} \qquad \ldots\ldots 7.42$$

$$\tau_{L-m} = \tau_{L-OT} \qquad \ldots\ldots 7.43$$

Venous Delays:

$$\tau_{B-L} = \frac{0.06}{\dot{q}_B} + \frac{0.188}{\dot{q}} \quad \ldots\ldots 7.44$$

$$\tau_{OT-L} = \frac{1.457}{\dot{q}_{OT}} + \frac{0.188}{\dot{q}}$$

$$\tau_{m-L} = \tau_{OT-L} \quad \ldots\ldots 7.45$$

In addition to the normal values given in table 6.1 (chapter 6) the following values were used in simulation of the above equations:

Symbol	Value	Reference
$\dot{q}_{BN}$	0.75 ℓ/min	Grodins et al, 1967
$\dot{q}_{mN}$	0.776 ℓ/min	Longobardo et al, 1966
$\dot{q}_{OTN}$	4.074 ℓ/min	Longobardo et al, 1966
$\dot{M}_{BCO_2}$	0.068 ℓ/min	Milhorn et al, 1965
$\dot{M}_{mCO_2}$	0.038 ℓ/min	Milhorn et al, 1965
$\dot{M}_{OTCO_2}$	0.14 ℓ/min	Longobardo et al, 1966
$\dot{U}_{BO_2}$	0.068 ℓ/min	Milhorn et al, 1965
$\dot{U}_{mO_2}$	0.049 ℓ/min	Longobardo et al, 1966
$\dot{U}_{OTO_2}$	0.18 ℓ/min	Longobardo et al, 1966

Using the above normal values, the model was simulated on a CDC 7600 computer using FORTRAN with each controller action, i.e. using each of equations 7.18 to 7.21 in turn for various disturbances.

7.2 RESULTS AND DISCUSSIONS

The above model was tested for following disturbances using each controller in turn.

i. CO_2 breathing

ii. Increased circulation delays

iii. Effect of CO_2 breathing on oscillatory ventilation

iv. Hypoxic breathing :

7, 8, 9% oxygen mixture in nitrogen for isocapnic and hypocapnic conditions.

The results are discussed for each controller in turn.

7.2.1 Brain Tissue CO_2 Control :

$$\dot{V} = \dot{V}_N + K\,(C_{BCO_2} - (C_{BCO_2})_N)$$

(A) CO_2 Breathing

Graphs number 7.1.1 to 7.1.3 show the time responses of ventilation with 3%, 5% and 7% CO_2 inhalation with the value of K(gain)equal to 900. It can be seen that the steady state values of $\dot{V}$ from simulation are higher than in experimental results (Reynold and Milhorn, 1971); 25 ℓ/min compared to 17.4 in the case of 5% CO_2 inhalation and 49 ℓ/min as compared to 42 in the case of 7% CO_2 inhalation. But in the case of 3% CO_2 inhalation the simulation value of $\dot{V}$ at steady state is lower than the experimental result; 10.3 compared to 11.4 ℓ/min. Apart from that the following features are evident in these results:

1. For 3% CO_2 inhalation (graph 7.1.1) the on-transient response is of 2nd order with a damping factor of 0.7 whereas for 5% and 7% CO_2 inhalation, the response is of 1st order with time constants of 2.4 minutes in the case of 7% CO_2 inhalation and 2 minutes in the case of 5% CO_2 inhalation.

2.During the off-transient again the response is of at least a 2nd order under damped system, with a damping factor of 0.6. Further there is no difference in the frequency of the damped oscillations during off-transients.

3. An important feature is the slight overshoot in the off-transient response after the removal of the step in the case of 5% and 7% CO_2 inhalation, the overshoot being about 4% of the final steady state value in the case of 5% CO_2 inhalation and approximately 7% in the case of 7% CO_2 inhalation.

Graphs number 7.1.5 to 7.1.6 show the results for time variation of P_{ACO_2} for 3%, 5% and 7% CO_2 inhalation respectively. There is approximately 100% overshoot and undershoot in the case of 3% CO_2 inhalation, graph 7.1.4. The overshoot during the on transients reduced with increased CO_2 inhalation but undershoot during the off transient increases with higher percentages of CO_2 inhalation, but the frequency of these damped oscillations does not differ with the percentage CO_2 inhalation.

From the above it can be concluded that the controller gain of 900 is very high, producing higher steady state values for 5% and 7% CO_2 inhalation. Also high gain may well be the reason for the oscillations during off transients in the time course of ventilation. To compensate for that, the value of gain was reduced to 550 from 900.

Graphs number 7.2.1 to 7.2.3 show the time course of ventilation after a step input of 3, 5 and 7% CO_2 respectively, as compared with the dynamic results obtained by Milhorn et al,1972. It can be seen that the dynamic as well as the steady state results for the ventilation are very similar to those produced by experiments on the human body. This is

certainly true for the case of 5% CO_2 inhalation where the two results follow very closely except for the extra oscillation produced by the simulation during the off-transient. In the case of 3% CO_2 inhalation slight overshoot is also observed during the on-transient and also the dynamics of the model response are much faster. The time constant for on-transient of the model response is of the order of 24 seconds compared with the time constant of about 2 minutes for the experimental curve. For 7% CO_2 inhalation, clearly the controller gain is too low as the steady state value of the model response after the step input is about 30% less than that of the experimental evidence. Again the dynamics of the model response are clearly faster than that of the experimental evidence.

The curious feature of the overshoot after the removal of the step input of CO_2 is still observable. At this stage there is no physiological evidence to show that this happens in real life. On the other hand experimental results do not have the required resolution in time to monitor these changes. Therefore it is difficult to comment upon these at this stage.

From the above discussion it can be seen that by increasing the model complexity, the controller gain had to be reduced to 550 from 900 the latter producing more satisfactory results for CO_2 breathing than a less complicated model (Model 1). Another fact that emerges from this discussion is that no single controller gain can simulate the results to match the experimental evidence for all the levels of CO_2 inhalation. As the dynamic as well as the steady state response depends upon the value of controller gain, this again cannot be increased for the inhalation of 7% CO_2 to produce higher steady state

results because it will make the time constant of the model response even smaller. Thus, at this stage of complexity, the CO_2 controller does not produce satisfactory results even for CO_2 breathing except for the case of 5% CO_2 breathing.

(B) Increased Circulation delays and effect of CO_2 input on oscillatory ventilation :

Results for these tests are shown in graphs 7.4.1 to 7.4.3 for circulation delays of 24 seconds, 36 seconds and 48 seconds respectively. The CO_2 is inhaled as a step function for 20 minutes from time equal to 2 minutes to time equal to 22 minutes. For a circulation delay of 24 seconds, although ventilation becomes oscillatory with the step input of 1% CO_2, these oscillations die out quicker during on transients than during off transients. In the case of a 36 seconds circulation delay Cheyne Stokes breathing is produced, but again the amplitude of the oscillations is very much smaller (nearly half) during the period in which CO_2 is being inhaled, although there is no change in the frequency of oscillations. No periods of apnoea appear , however, that is at no time is ventilation zero. In the case of a 48 seconds circulation delay, Cheyne Stokes breathing appears with periods of apnoea. Here again there is a marked effect of CO_2 inhalation. It can be seen that during the CO_2 inhalation, periods of zero breathing are very much smaller (nearly 20 seconds) as compared to about 30 seconds after the CO_2 input is removed.

These results show that Cheyne-Stokes breathing may be produced by the tissue CO_2 controller even within physiological limits of circulation delays, but the time period of oscillations is about 75 seconds. Also it can be concluded that CO_2 inhalation has the effect of damping these oscillations and reducing the amplitude of these oscillations which seems to confirm the general physiological belief.

(C) Hypoxic Breathing :

Graph 7.5.1 shows the time course of ventilation when oxygen in the breathing mixture is reduced to 9% from 21.3%. Clearly as expected the results are in no way comparable to experimental evidence produced by Milhorn et al (1973). The reason for this may be that as oxygen does not appear in the controller equation, it is not consistent to use such a controller for simulating breathing patterns produced by changes in oxygen percentage in the breathing mixture.

Considering the above discussion it can be concluded that although brain tissue CO_2 control produces similar results to those produced by experimentation, except in the case of 5% CO_2 inhalation the comparison is qualitative rather than quantitative, that is to say that although the responses are similar in appearance they have a wide difference in magnitude and time scale, i.e. in dynamic as well as steady state results. Although with this model Cheyne-Stokes breathing patterns are produced, the time period of oscillations is too large, about 70 seconds compared with the physiological evidence which is of the order of 15 seconds (Longobardo et al, 1967).

7.2.2. ARTERIAL CONTROL :

During the development of this model (section 7.1) along with the arterial controller equation developed by Longobardo et al, 1966 (equation number 7.28) a new controller equation was developed using experimental data available, (equation 7.30).

Graphs 7.6.1 to 7.6.3 show the results of 3, 5 and 7 per cent CO_2 inhalation compared with the experimental evidence. It is apparent that the dynamic results produced by the simulation are much faster, and there is a discrepancy in the steady state

results as well, except for 5% CO_2 inhalation. When the same equation is used to simulate the effect of hypoxia (9% O_2 inhalation), the results obtained are as shown in graph number 7.7.1. It can be seen that the simulation results are completely irrelevant. Thus it can be concluded that although this equation produces satisfactory results for Cheyne-Stokes breathing produced by increased circulation delays, the results produced for CO_2 breathing and hypoxia breathing are in no way comparable with physiological evidence. The reason for this may well be that, as shown in the development of arterial controller equations, this particular equation does not cater for the low oxygen concentration in the arterial blood produced by hypoxia. The high controller gain on the other hand may be responsible for unrealistic results produced by CO_2 breathing particularly during off-transients. It may further be added that this high controller gain is responsible for very much faster (nearly 5 times) response for CO_2 on-transient as compared to experimental evidence.

Very similar results are obtained for 3, 5 and 7% CO_2 inhalation using equation number 7.29, produced by Milhorn et al (1971) as shown by graphs number 7.8.1 to 7.8.3 respectively. Comparison with the results produced by the Longobardo controller equation (equation 7.2.8) shows that the steady state results in this case are higher in the case of 5% and 7% CO_2 inhalation. This is due to even higher gain of this equation (that is, the overall gain is 2.0 instead of 1.81 as in the case of equation 7.28). The results of 9% oxygen breathing are shown in graph number 7.9.1. It is apparent that although the model response does not break down as quickly as in the case of the

Longobardo equation (equation 7.28), the results are still far from comparable with the experimental evidence. The reason for the comparatively better performance with this controller equation is that the denominator of equation 7.29 has a lower oxygen threshold of P_{aO_2} = 2.50 as compared with equation 7.28 in which the oxygen threshold is given by P_{aO_2} = 32.44 below which, due to-ve sign, the controller equation breaks down.

Another aspect which is not included in the above two controller strategies is that the slope of the controller equation due to oxygen changes is constant throughout the whole range of P_{aO_2} and P_{aCO_2} values which result from hypoxic breathing. This feature of these equations was discussed previously in section 7.1.

Considering the above a new equation was developed which, although similar in behaviour for CO_2 breathing, will take into account the change in slopes due to low P_{aO_2} values attained due to hypoxic breathing. This equation is equation number 7.31.

As there is no marked difference in the controller characteristics for higher P_{aCO_2} and P_{aO_2} values, the results expected for CO_2 breathing are very similar to the two previous equations, that is qualitatively all the features of CO_2 inhalation response produced by experimental evidence are present, but quantitatively the results are far from comparable. This is evident from graph number 7.10.1 for 7% CO_2 inhalation and graph number 7.11.1 for Cheyne-Stokes breathing produced by a circulation delay of 48 seconds. Again it can be seen that periods of zero breathing are smaller during the CO_2 inhalation but after the normal gas mixture is restored the

period of apnoea becomes slightly larger although there is no marked difference in frequency of this oscillation which is of the order of 12 - 15 seconds which corresponds closely with the results produced by Longobardo et al (1967).

Milhorn et al (1973) produced two sets of dynamic experimental results for hypoxic breathing. The first set was hypocapnic, that is the partial pressure of carbon dioxide in the alveoli and hence in the arterial blood was allowed to vary. In the second, isocapnic set, the alveolar partial pressure of carbon dioxide was maintained at pre-stimulus level through artificial means. This is the first ever set of dynamic results produced by hypoxic breathing. The human subjects were given 9% oxygen to breathe for 12 minute periods and experimental results were obtained for on-and-off transients.

The new controller equation developed in section 7.1 using experimental data was used to test the model response for 9% oxygen inhalation for both cases, that is for hypocapnic and isocapnic conditions. The results obtained are shown in graphs number 7.12.1 and 7.12.2 and are compared with the experimental results obtained by Milhorn et al (1973).

In the case of the isocapnic set, the results obtained by the model seem to be well in agreement with the experimental evidence. The slight difference in the steady state values after 14 minutes may well be due to the difference in pre-stimulus level of ventilation which is about 0.5 higher than the experimental results. Otherwise the simulated results match very well with experimental results in the dynamic as well as the steady state case.

Graph number 7.12.2 shows the simulated results for the hypocapnic case for 9% oxygen inhalation in comparison with the experimental evidence. Although qualitatively there seems to be good agreement between the two responses, there are two features which are different. The steady state value of the model response is about 15% lower than the experimental result and there is a slight undershoot during the off transient. Although difficult to judge from the graphs produced by experimentation, in the text of the publication Milhorn et al (1973) state that some of the subjects did exhibit some overshoot and undershoot in the ventilatory response. Thus this undershoot and very slight overshoot apparent in the simulated response may well be consistent with the experimental evidence.

In general from the above discussion taken overall it can be concluded that there are two distinct features of ventilatory response. First is that there are two chemoreceptor sites in the body, namely the central chemoreceptors near the brain and the arterial chemoreceptors in the aortic and carotid bodies. From the above results it seems that for the CO_2 balance of the body, the central chemoreceptor controls are predominant. Arterial chemoreceptors seem to be more dominant for the development of Cheyne Stokes breathing which again appears to be consistent with the above statement as Cheyne Stokes breathing is related to apnoea and/or hyperventilation disturbing the oxygen balance of the body primarily as generally CO_2 is not present in normal breathing air mixtures. In fact the input of CO_2 through the mouth is an unnatural phenomenon and may be described as a disturbance to the system in the terms of system and control engineering. The only way in which

the body CO_2 balance is normally disturbed is due to the changes in metabolic output of the body tissues as a result of exercise, taking just one example. It will be interesting to study the role of the brain tissue CO_2 controller equation in exercise conditions when excessive CO_2 is being liberated by the muscle tissues. One physiological aspect is that the oscillations in arterial blood P_{CO_2} due to breath by breath oscillations as a result of inspiration and expiration, are strangely affected by the means by which CO_2 increases in the body. If the CO_2 is induced through the mouth, breathing CO_2 gas mixtures, the oscillations in arterial P_{CO_2} decrease in size although the mean rises to a higher level, but if CO_2 is increased by increased muscle tissue CO_2 production rate due to exercise, these oscillations become larger with little or no change in the mean level. For this purpose the model must be extended to include a variable lung volume to facilitate breath by breath analysis.

GRAPH 7.1

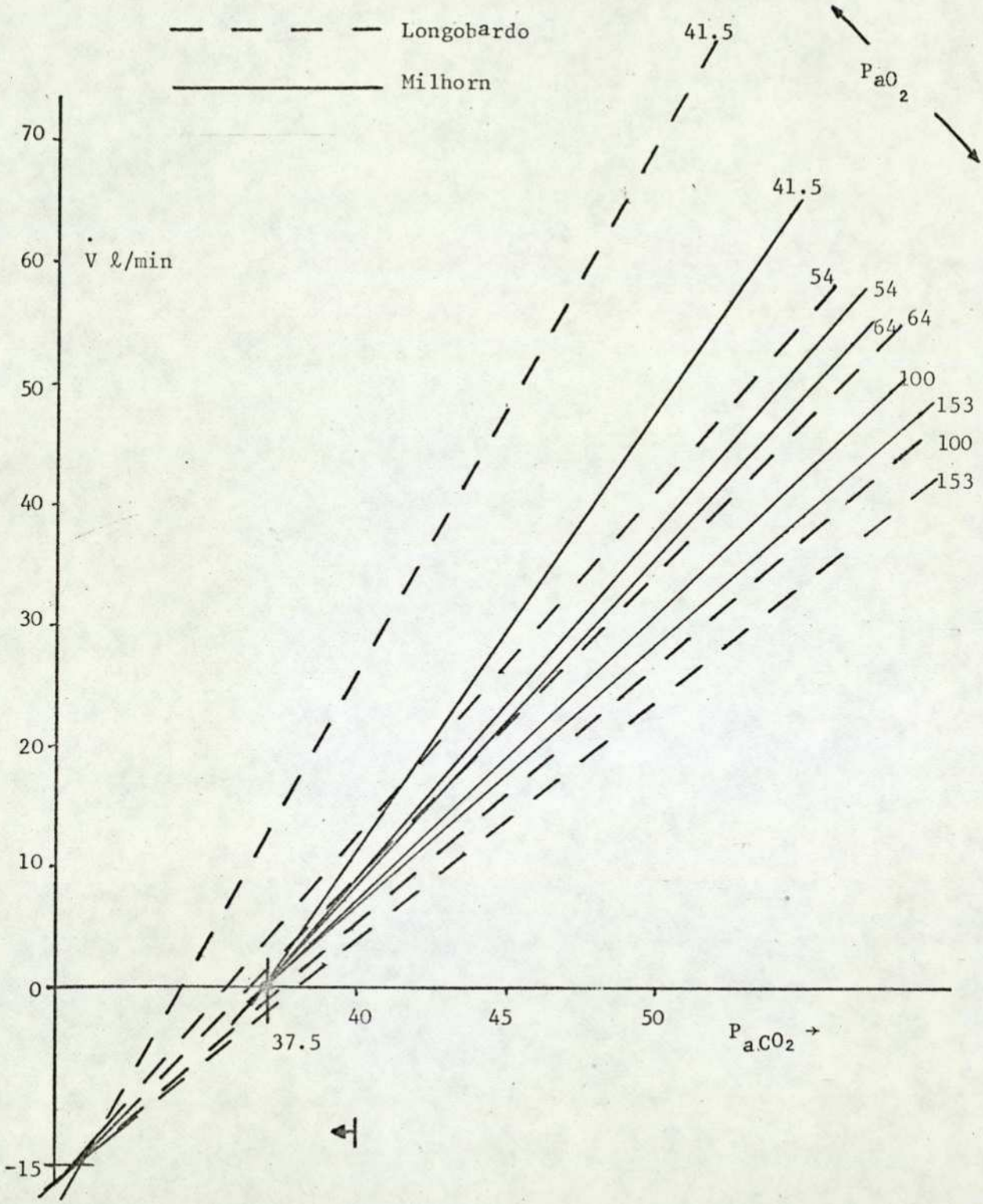
Longobardo
Milhorn
41.5
P_{aO_2}
41.5
54
54
64
64
100
153
100
153
$\dot{V}$ ℓ/min
70
60
50
40
30
20
10
0
-15
37.5
40
45
50
P_{aCO_2}

GRAPH 7.2

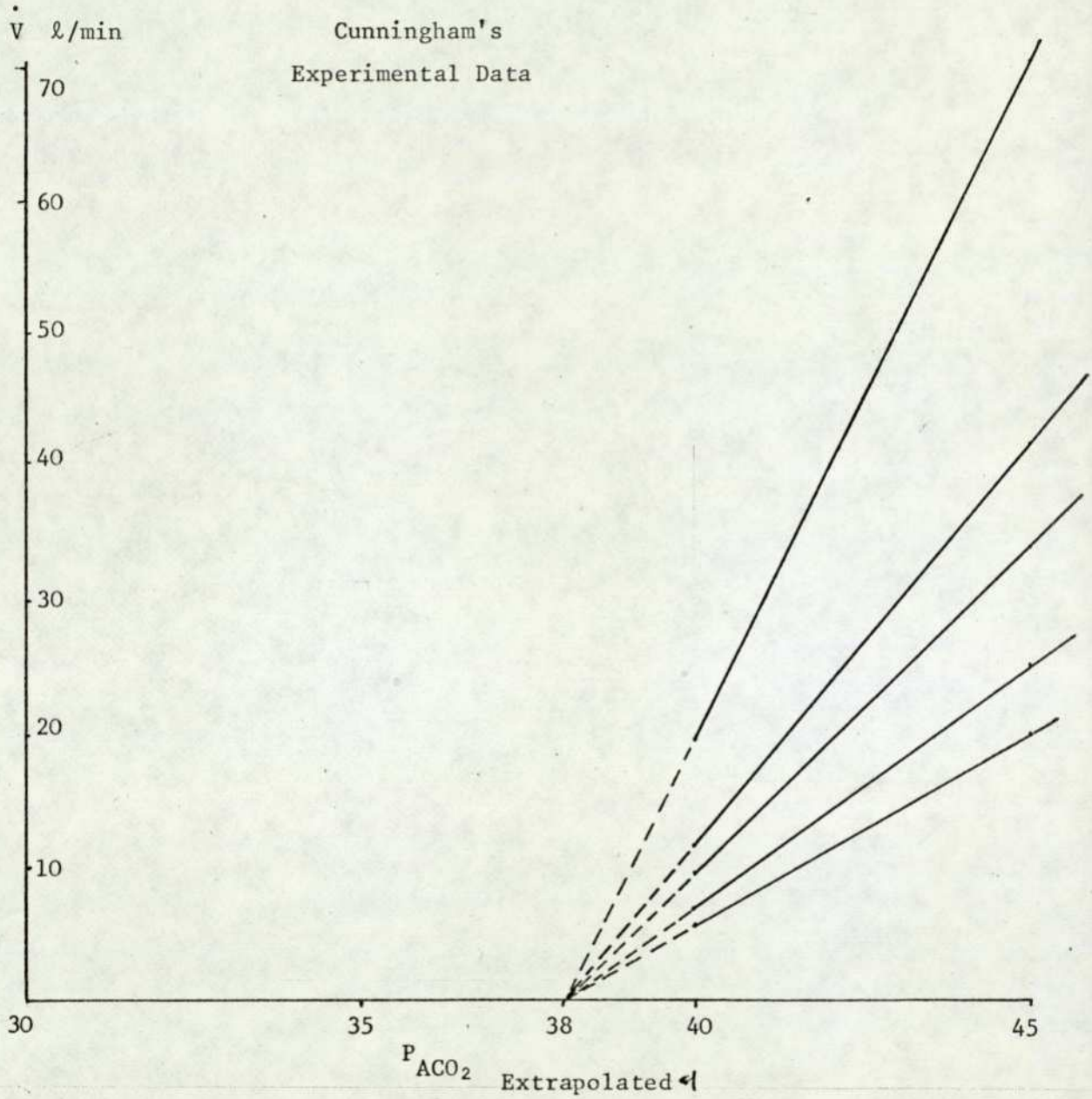
$\dot{V}$ ℓ/min
Cunningham's
Experimental Data
70
60
50
40
30
20
10
30
35
38
40
45
P_{ACO_2}
Extrapolated

GRAPH 7.3

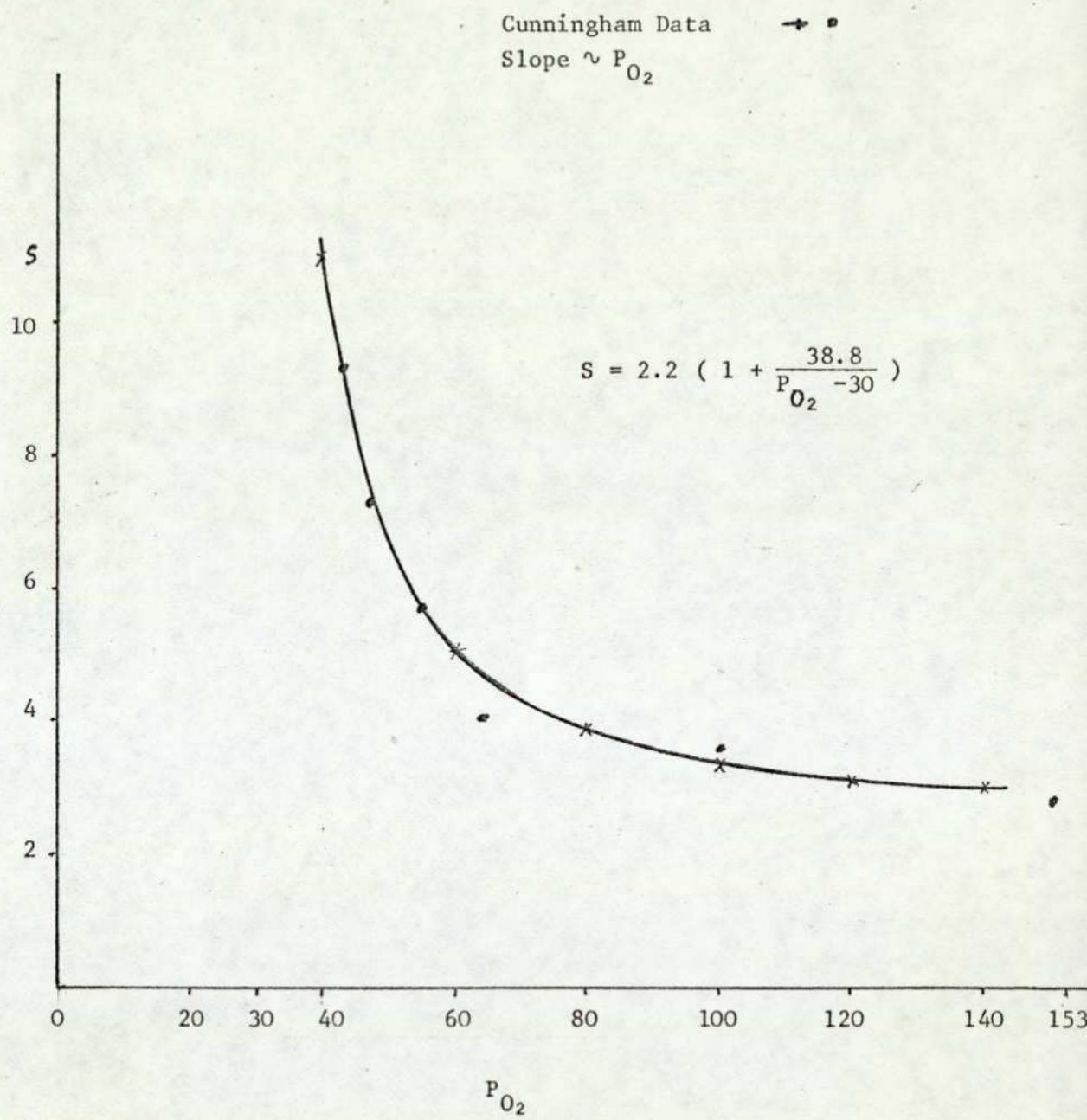
Cunningham Data
Slope ∿ P_{O_2}
$S = 2.2 \left(1 + \frac{38.8}{P_{O_2} - 30} \right)$
S
10
8
6
4
2
0
20
30
40
60
80
100
120
140
153
P_{O_2}

GRAPH 7.4

Cunningham's Data

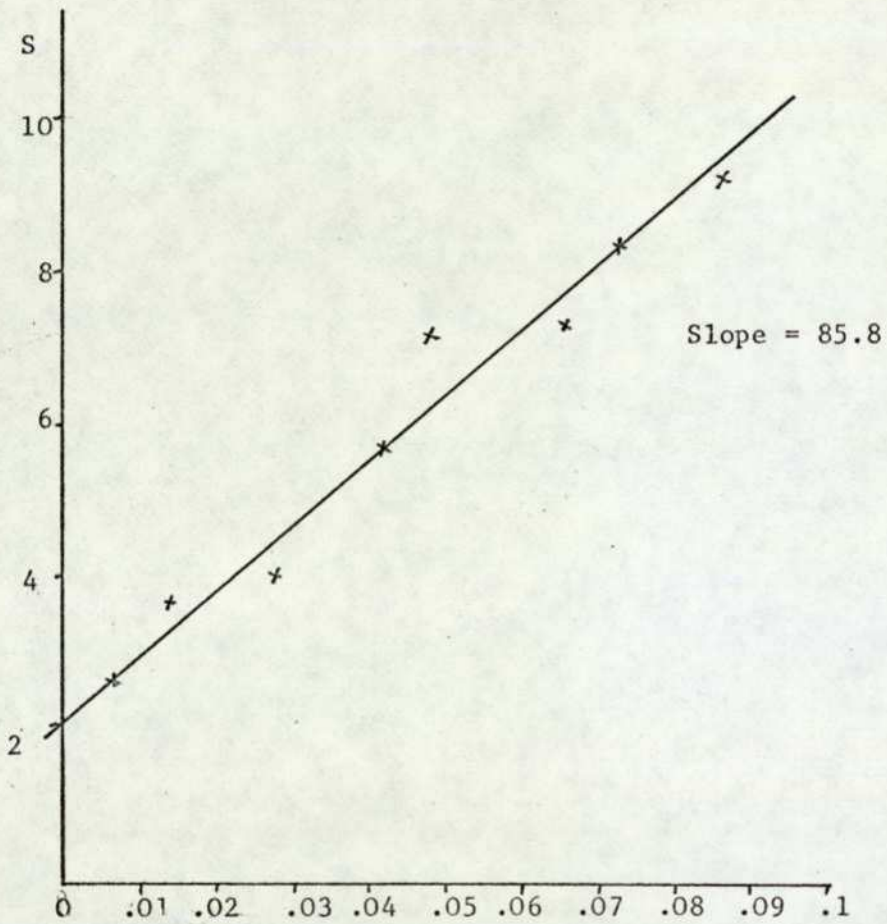

$$\frac{1.0}{P_{O_2} - 30}$$

GRAPH 7.5

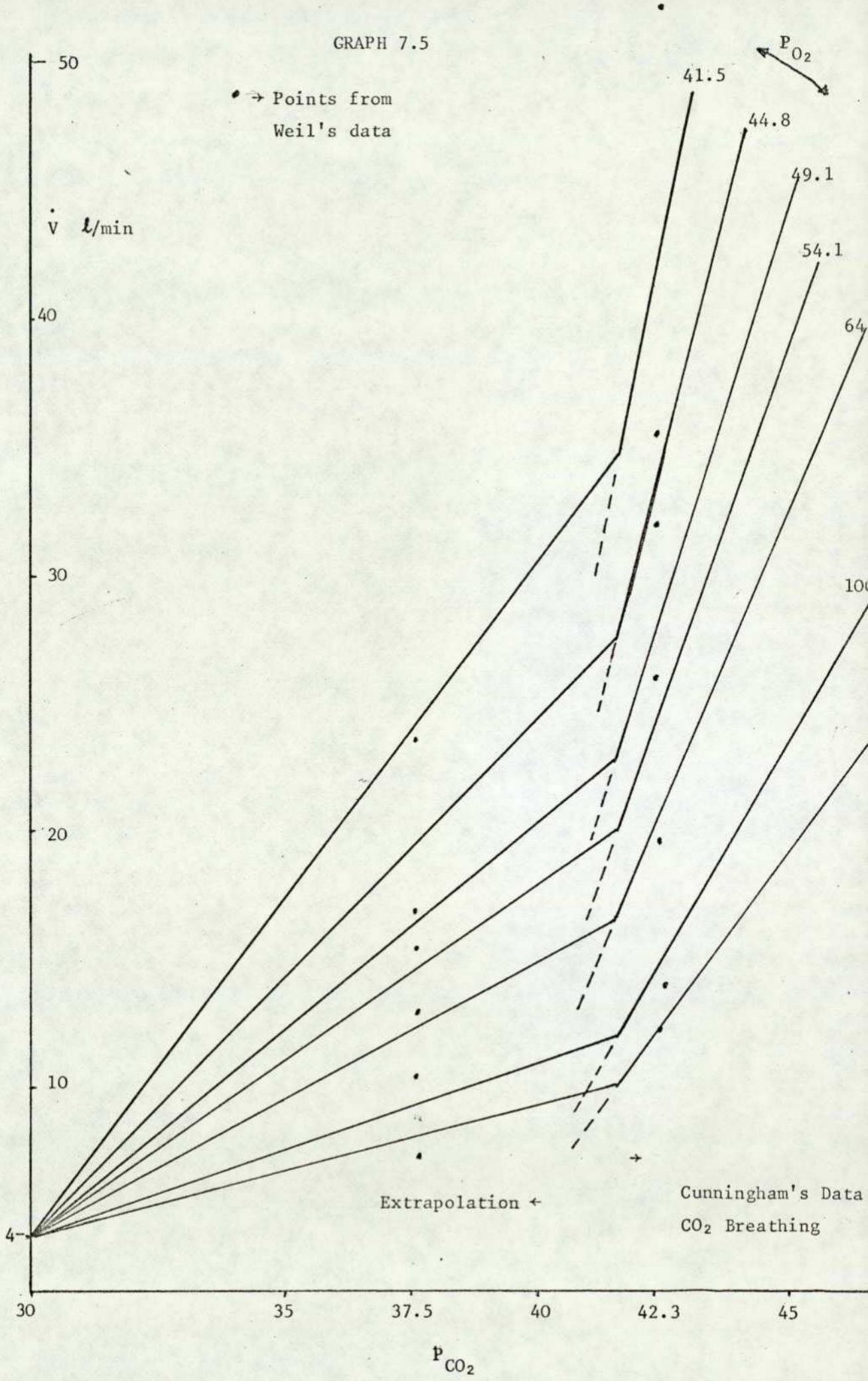
P_{O_2}
41.5
44.8
49.1
54.1
64
100
• → Points from Weil's data
$\dot{V}$ ℓ/min
50
40
30
20
10
4
30
35
37.5
40
42.3
45
P_{CO_2}
Extrapolation ←
Cunningham's Data
CO_2 Breathing

Graph 7.1.1.

C_{ICO_2} = 0.03

$\dot{V}$ = f (C_{BCO_2})

GAIN = 900

* = Experimental Data

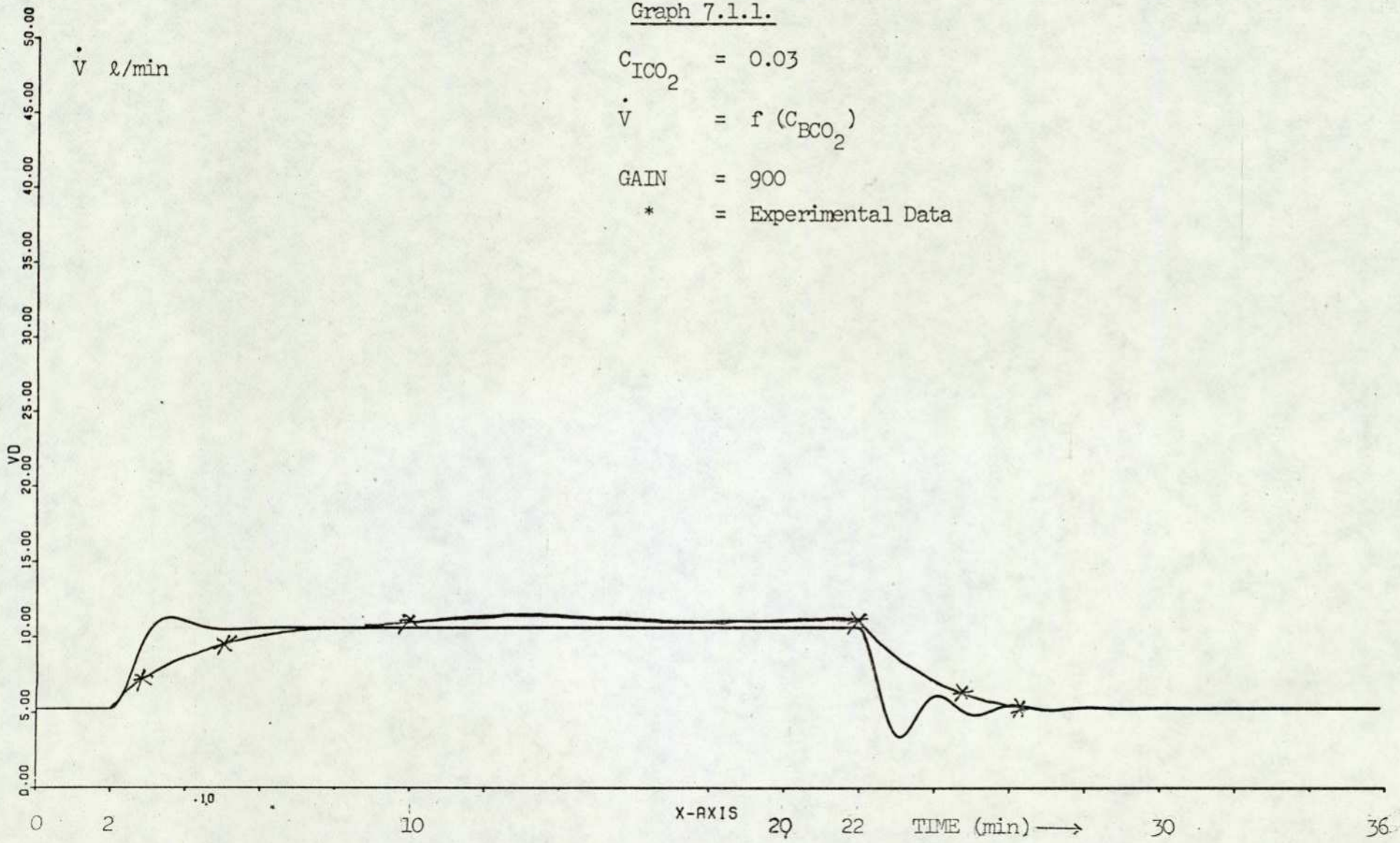

Graph 7.1.2.

C_{ICO_2} = 0.05

$\dot{V}$ = f (C_{BCO_2})

GAIN = 900

* = Experimental Data

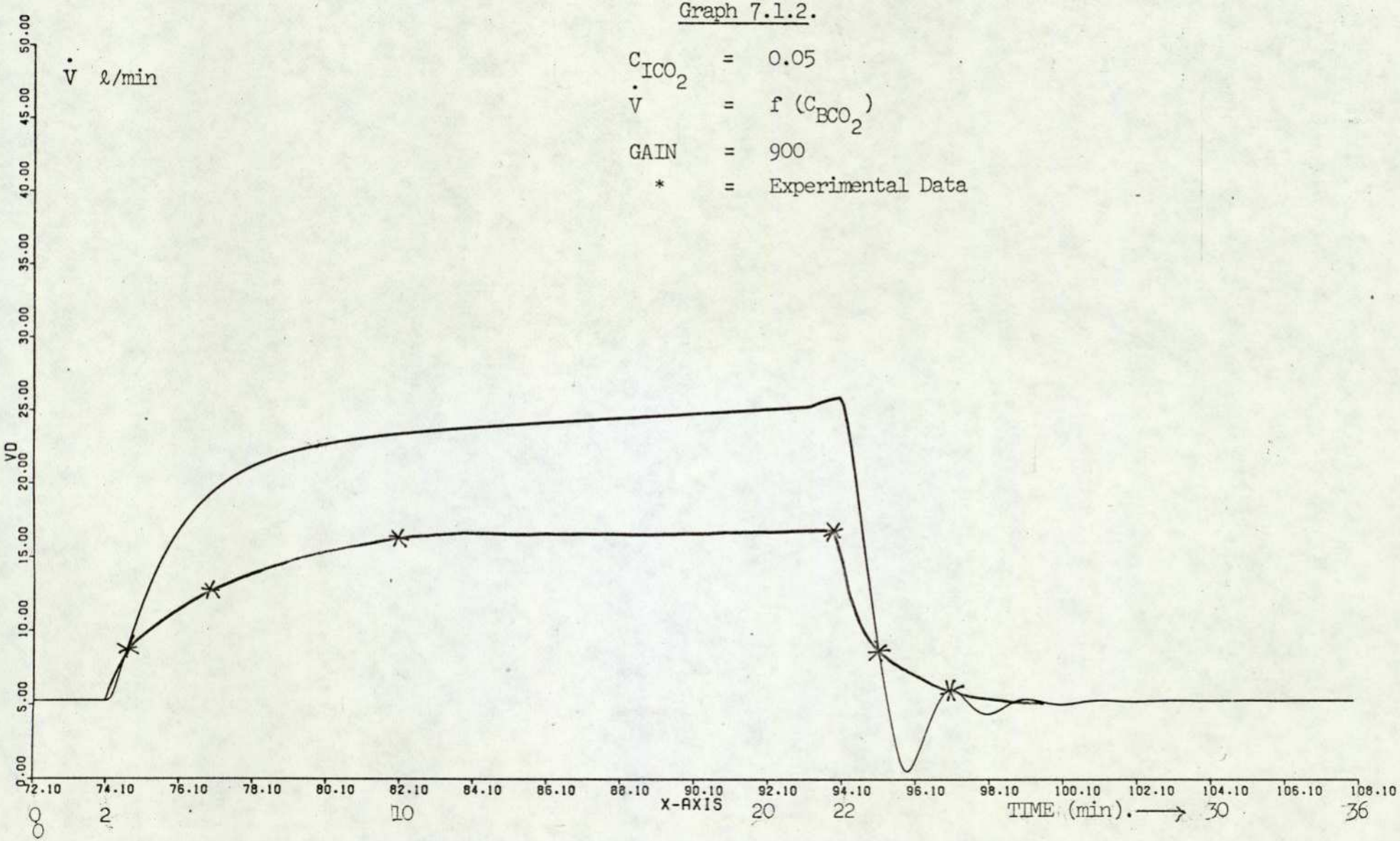

Graph 7.1.3.

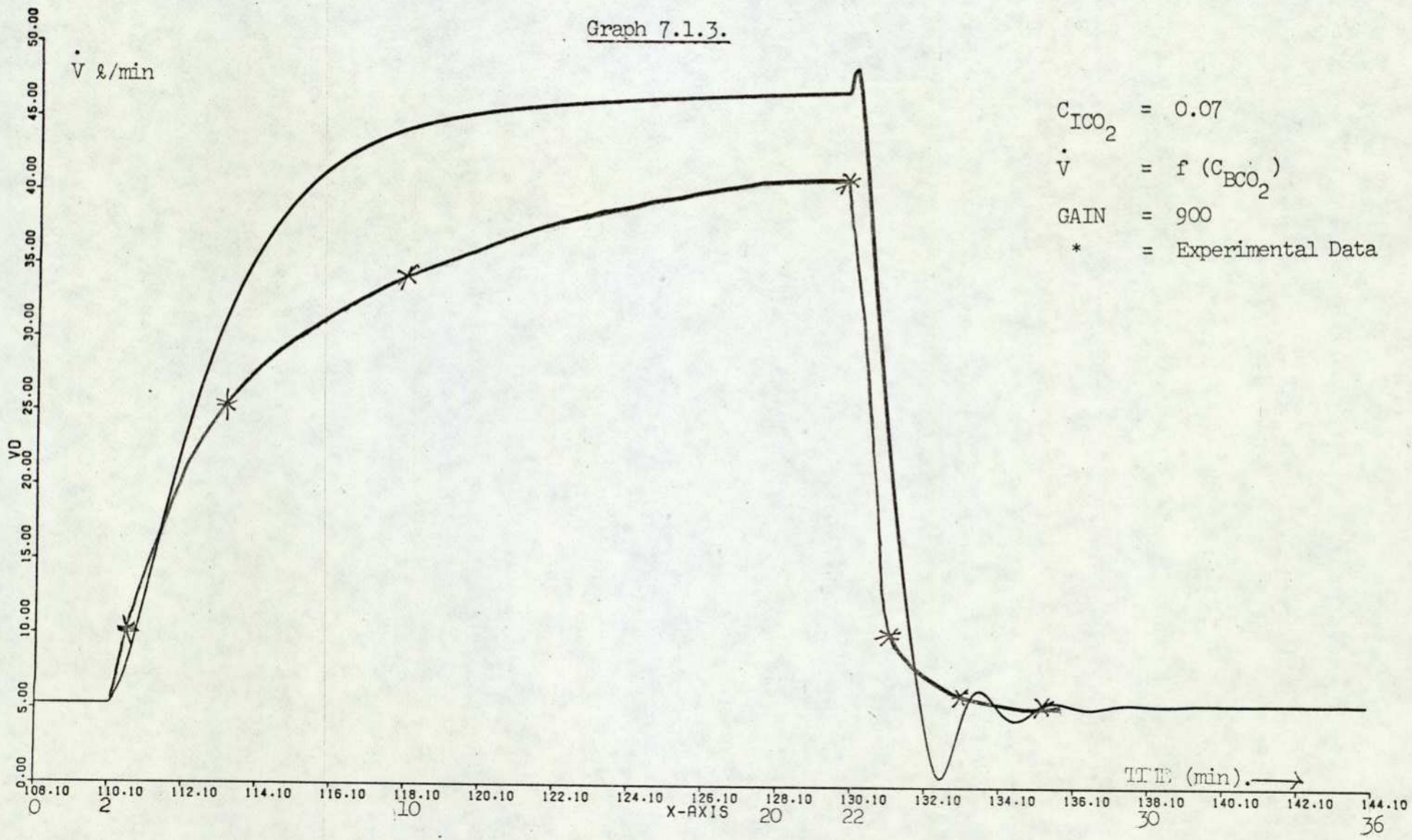

C_{ICO_2} = 0.07

$\dot{V}$ = f (C_{BCO_2})

GAIN = 900

* = Experimental Data

Graph 7.1.4.

C_{ICO_2} = 3%

$\dot{V}$ = f (C_{BCO_2})

Gain = 900

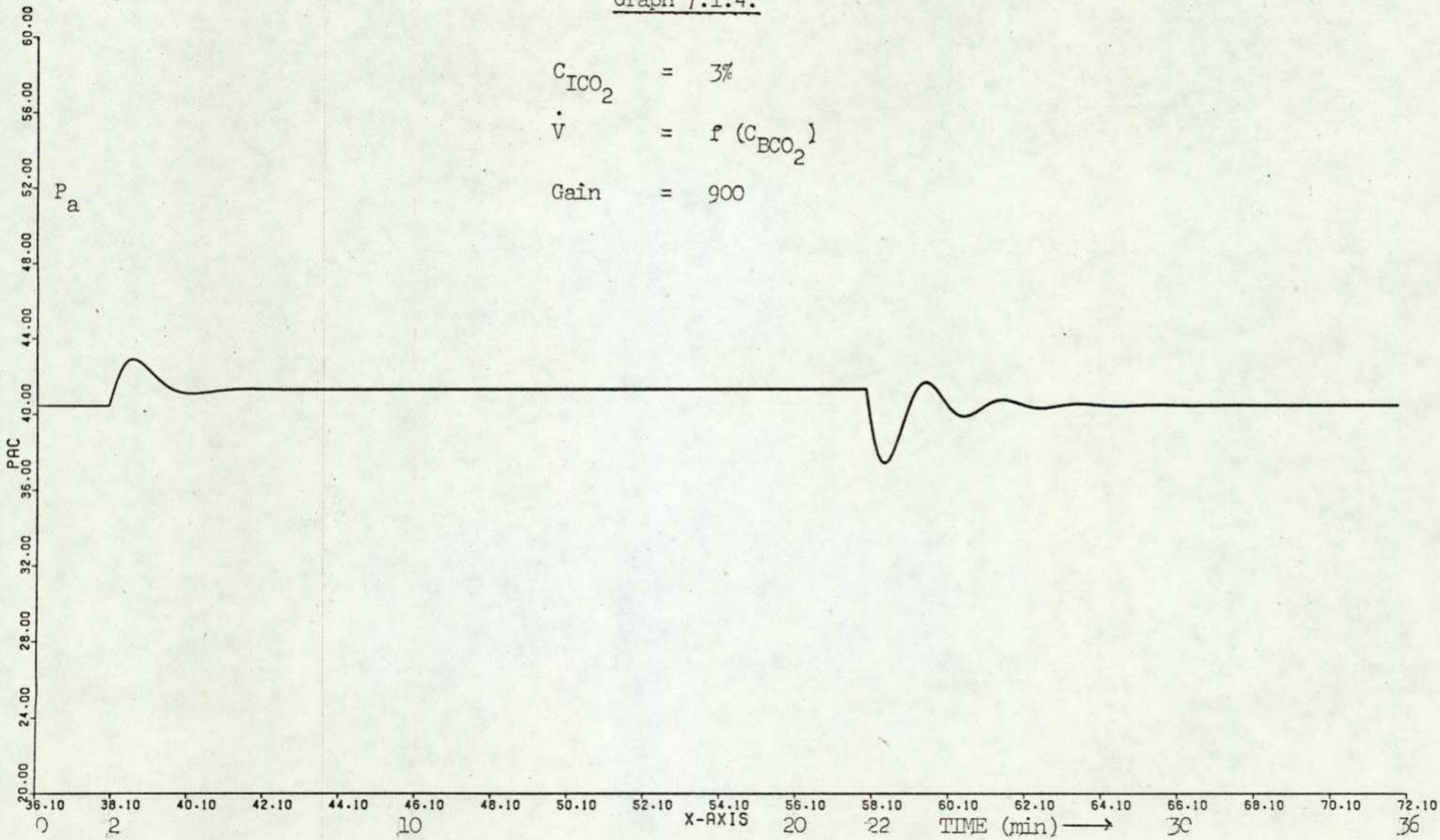

Graph 7.1.5.

C_{ICO_2} = 5%

$\dot{V}$ = (C_{BCO_2})

GAIN = 900

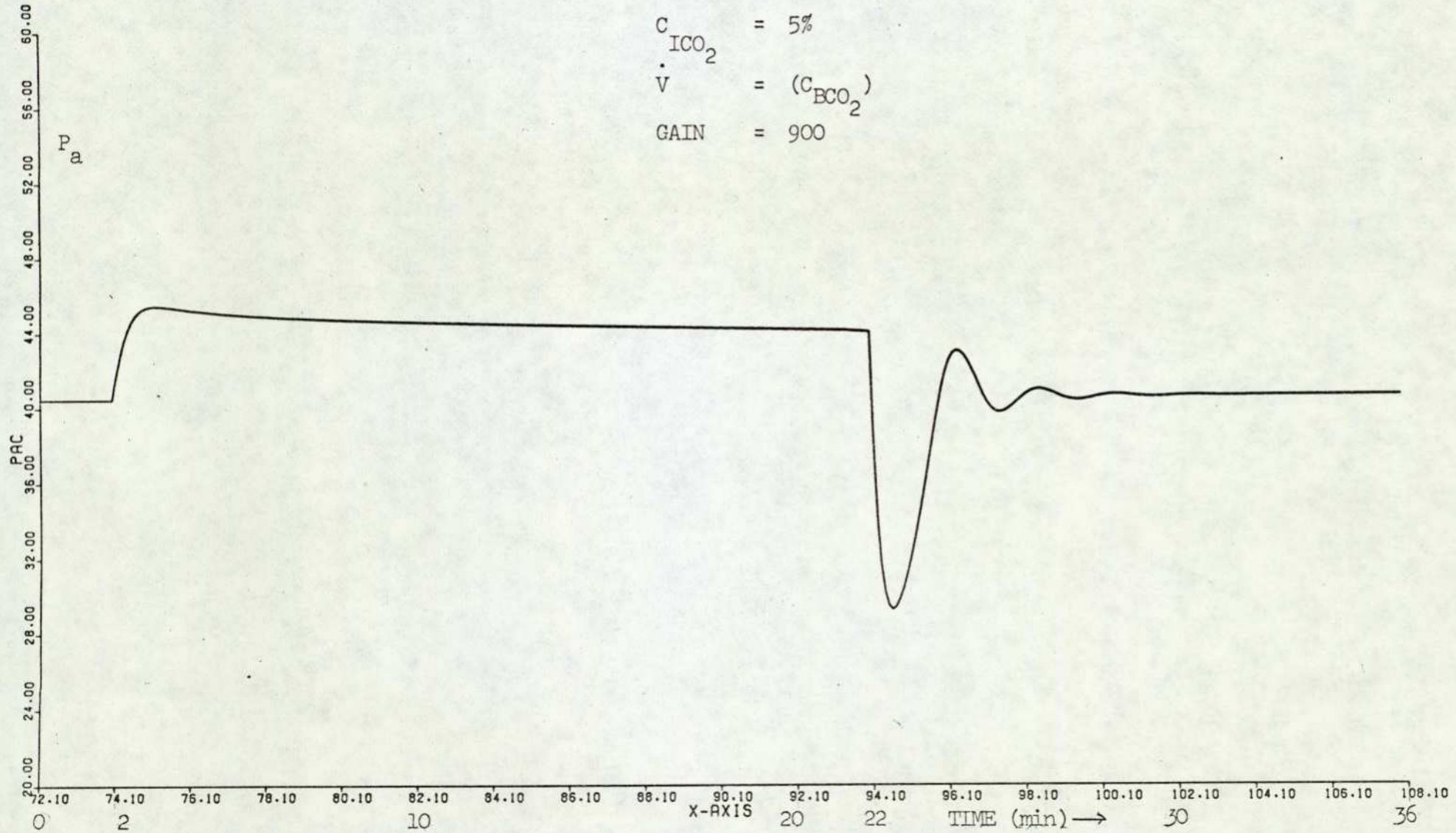

Graph 7.1.6.

C_{ICO_2} = 7%

$\dot{V}$ = f (C_{BCO_2})

GAIN = 900

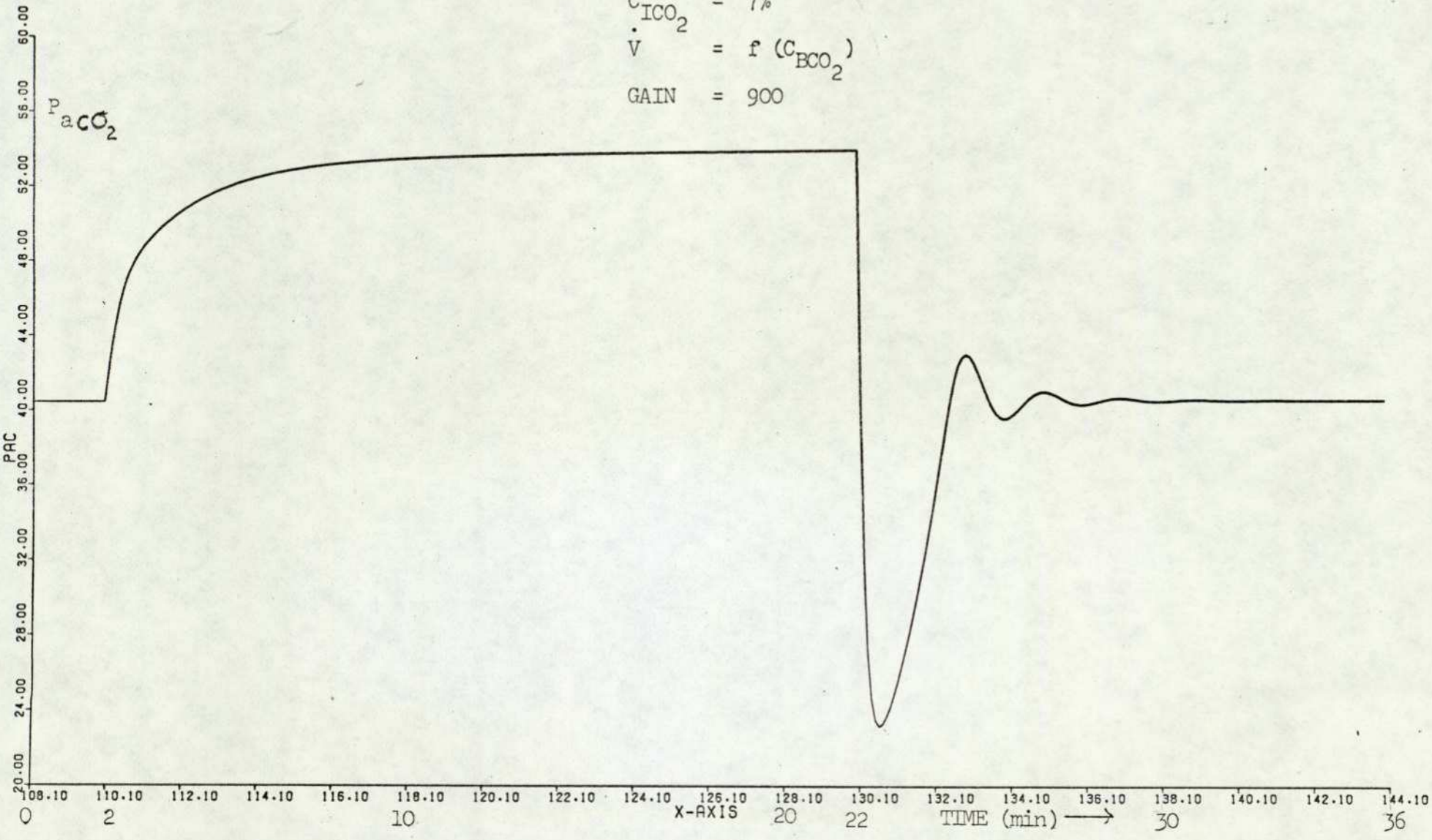

Graph 7.2.1.

3% CO_2

$\dot{V}$ f (C_{BCO_2})

GAIN = 500

* Experimental points

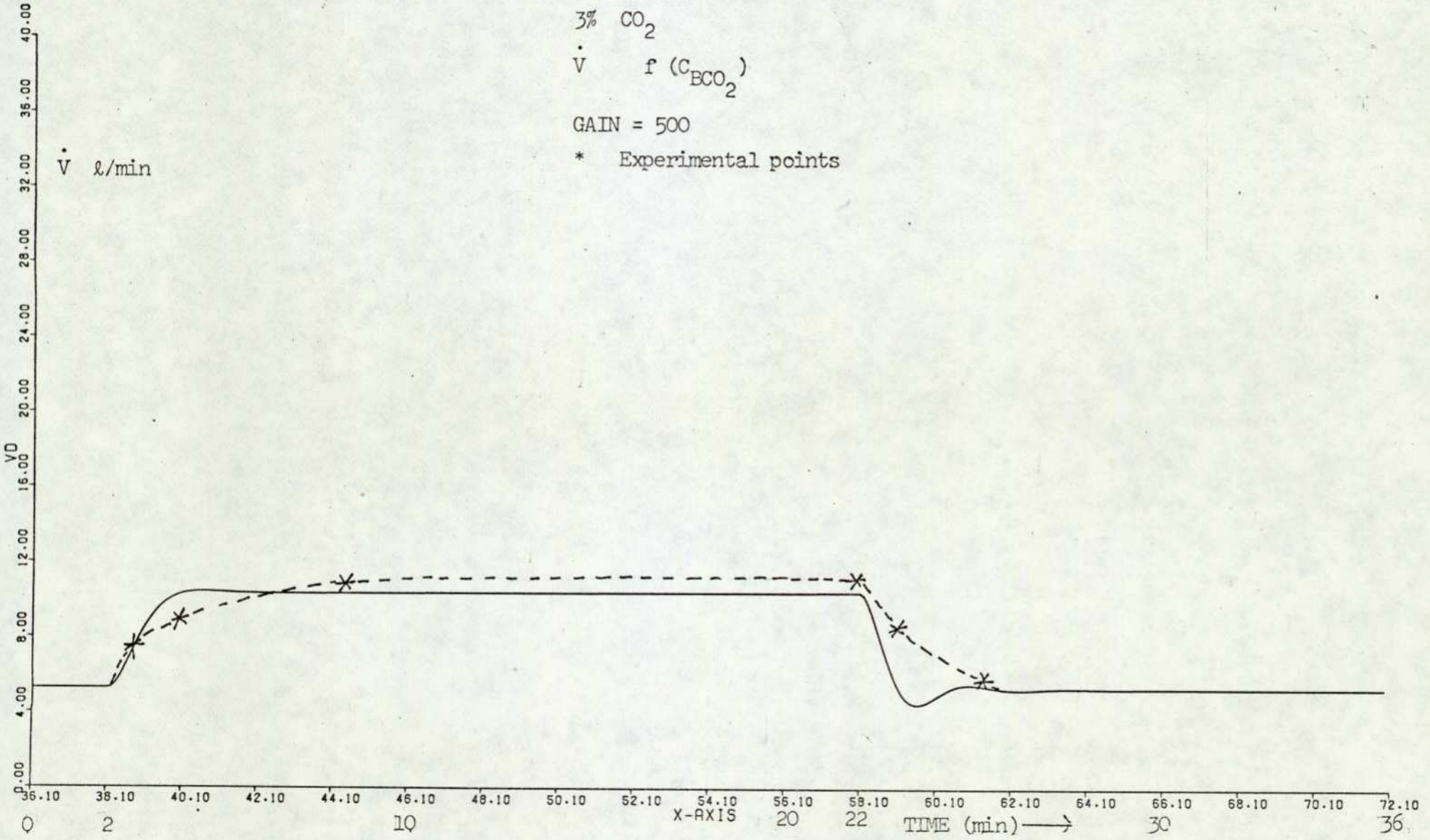

Graph 7.2.2.

5% CO_2

$\dot{V}$ f (C_{BCO_2})

GAIN = 550

* Experimental Points

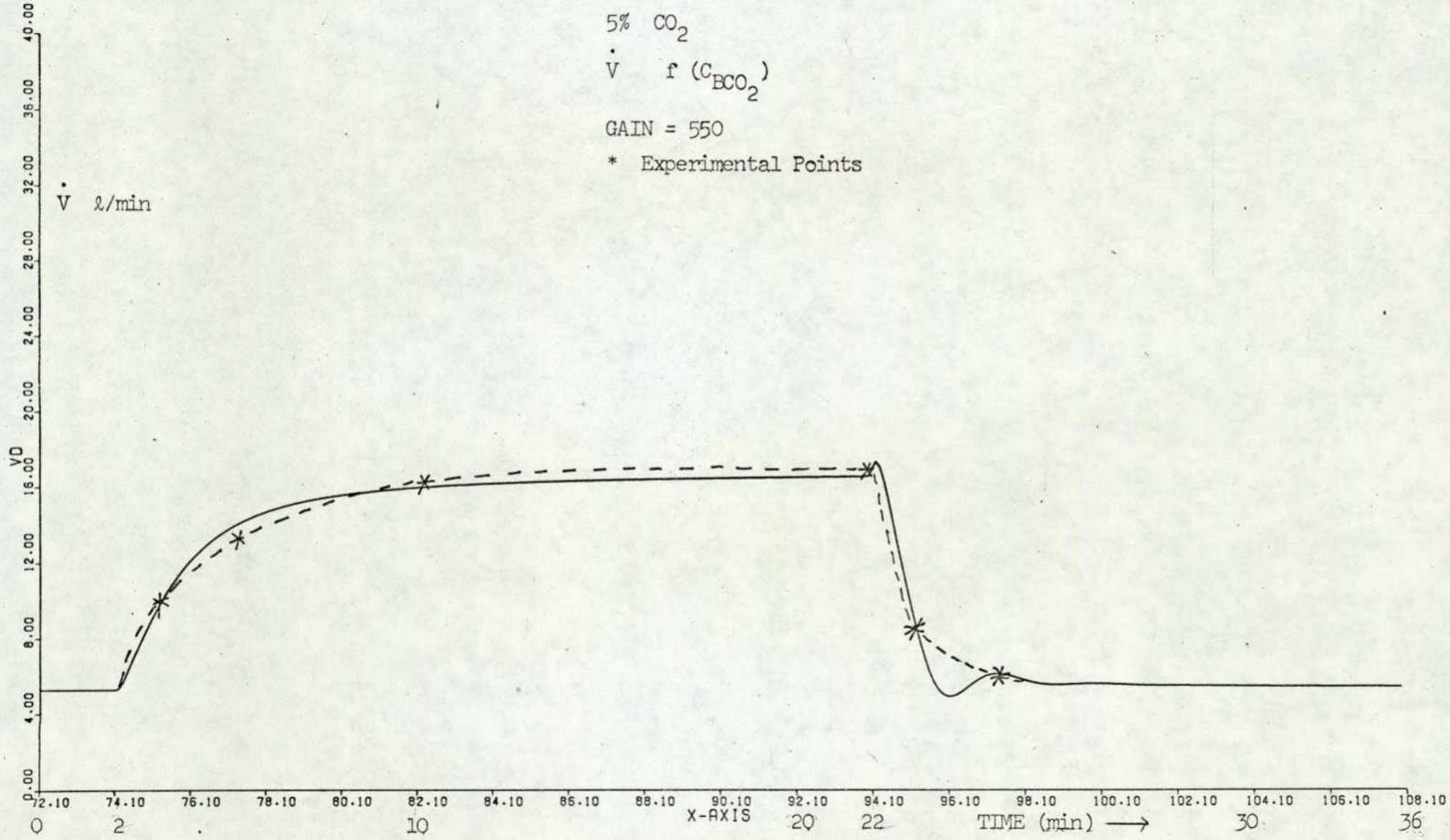

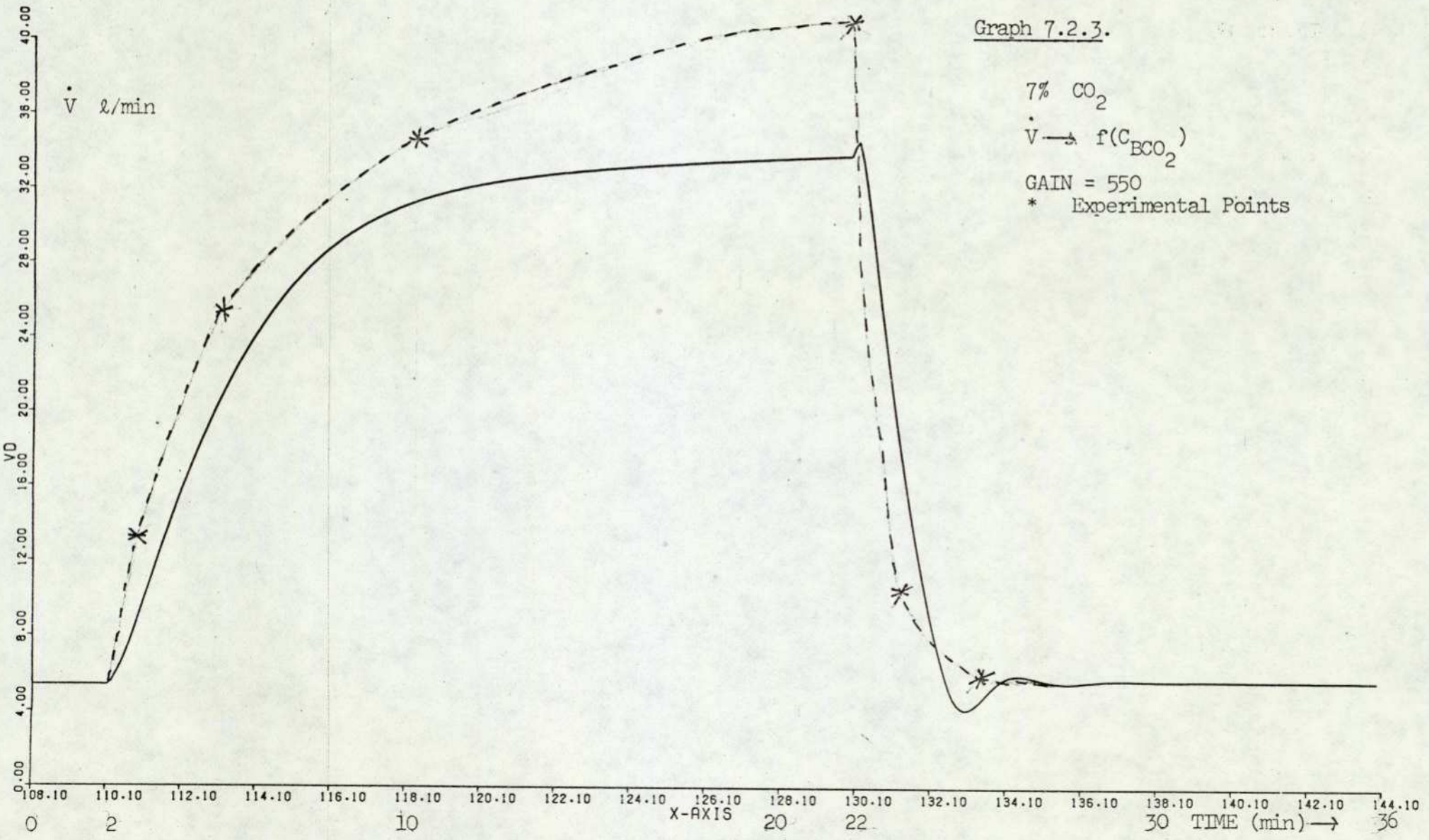

Graph 7.2.3.

7% CO_2

$\dot{V} \longrightarrow f(C_{BCO_2})$

GAIN = 550

* Experimental Points

Graph 7.3.1:

CO_2 = 1%

$\dot{V} \longrightarrow f(C_{BCO_2})$

Gain = 550

Delay 24 secs.

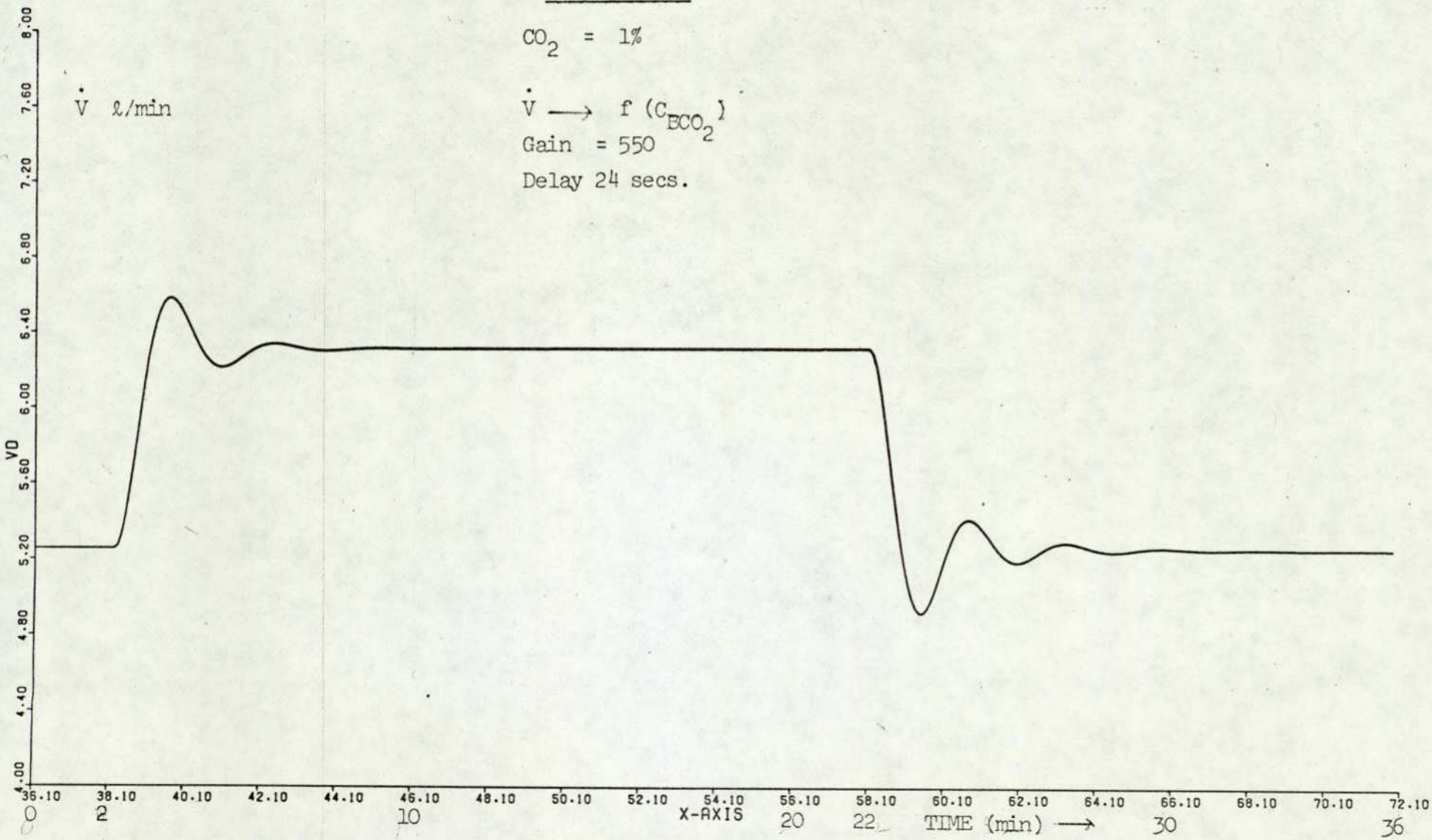

Graph 7.3.2.

CO_2 = 1%

$\dot{V} = f(C_{BCO_2})$

Gain 550

Delay 36 secs.

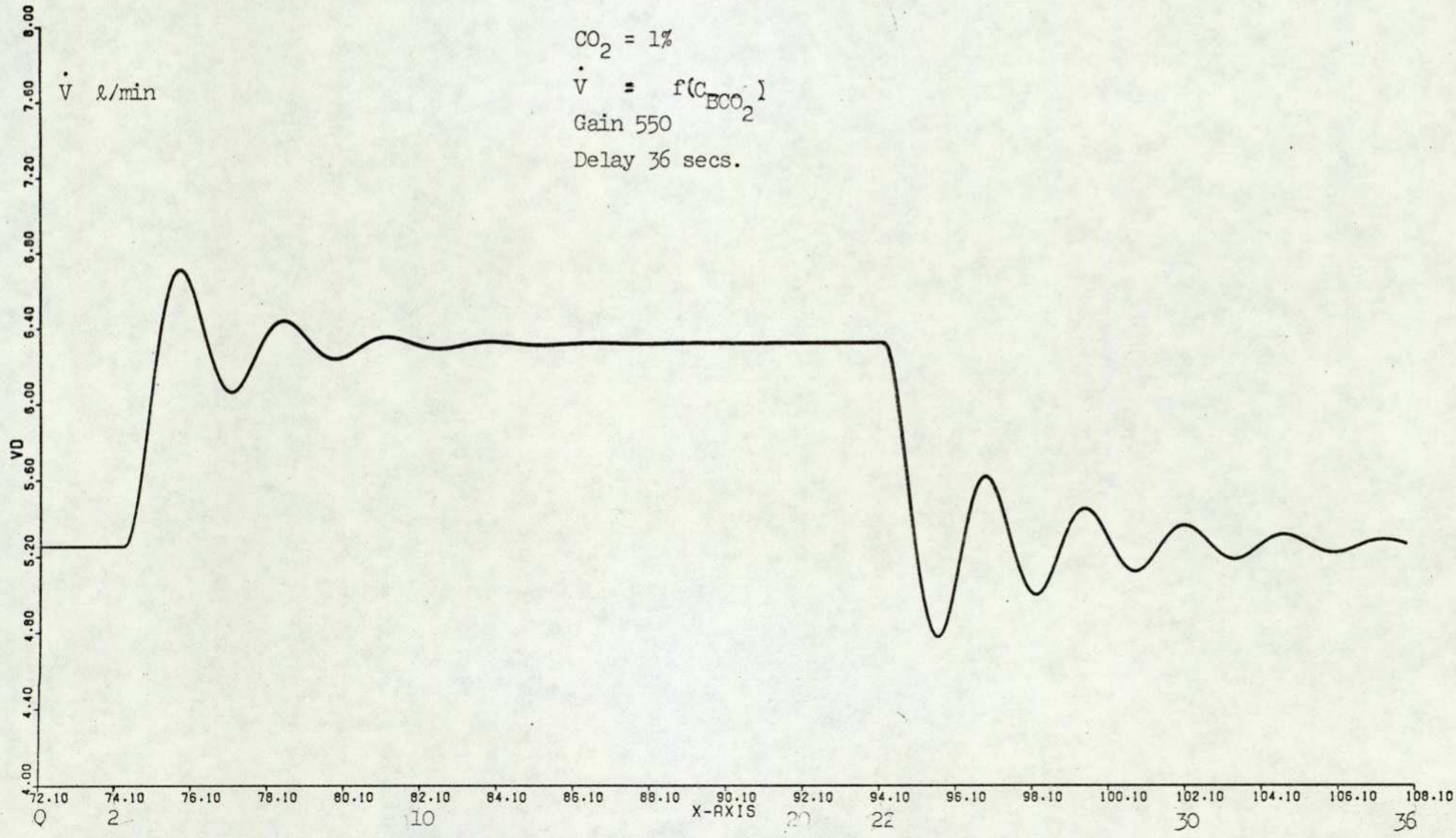

Graph 7.3.3.

CO_2 1%

$\dot{V} \longrightarrow f(C_{BCO_2})$

Gain 550

Delay 48 secs.

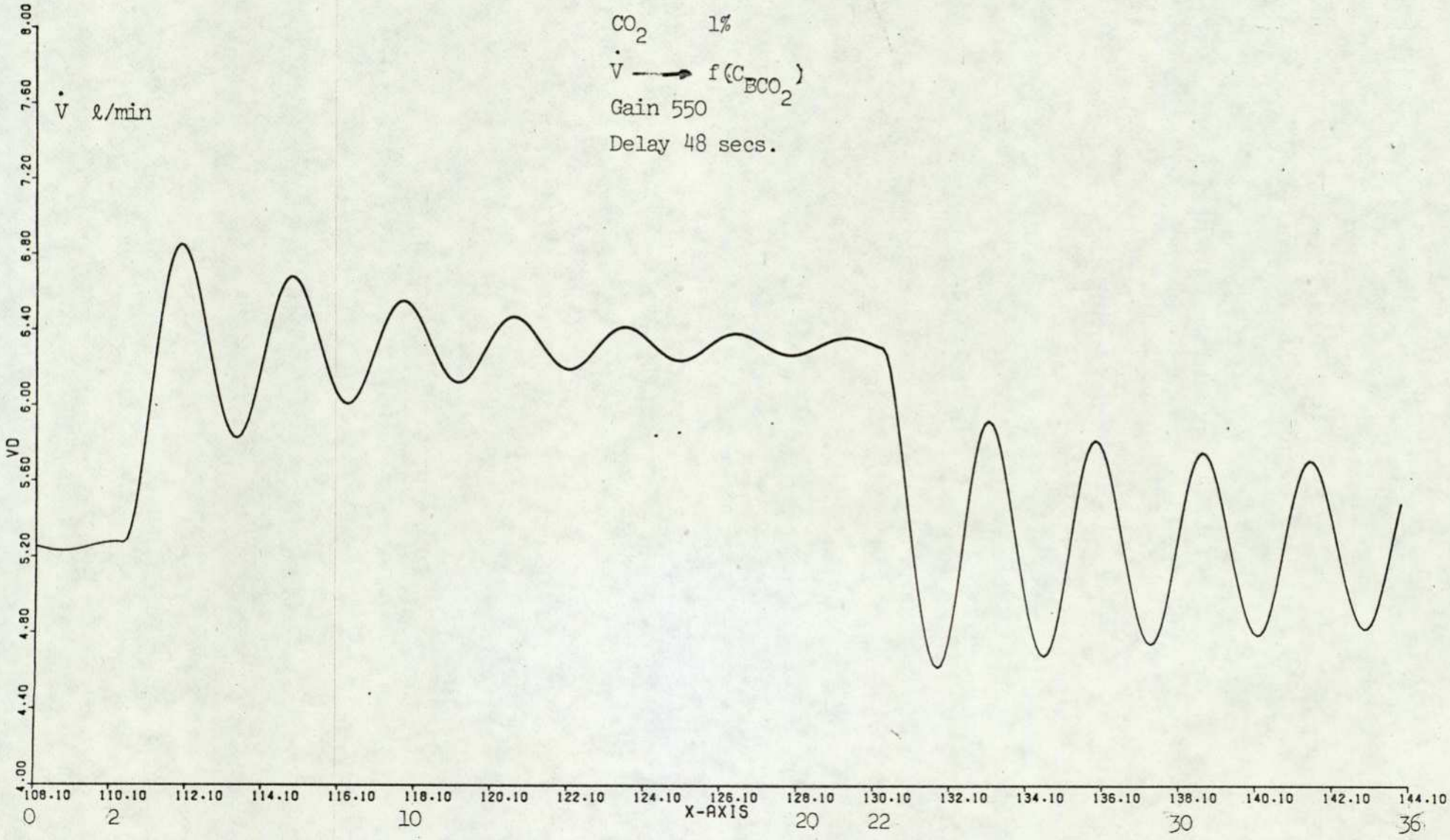

Graph 7.4.2.

1% CO_2 for 22 min.

$\dot{V} \longrightarrow f(C_{BCO_2})$

Gain→550

Delay 36 sec.

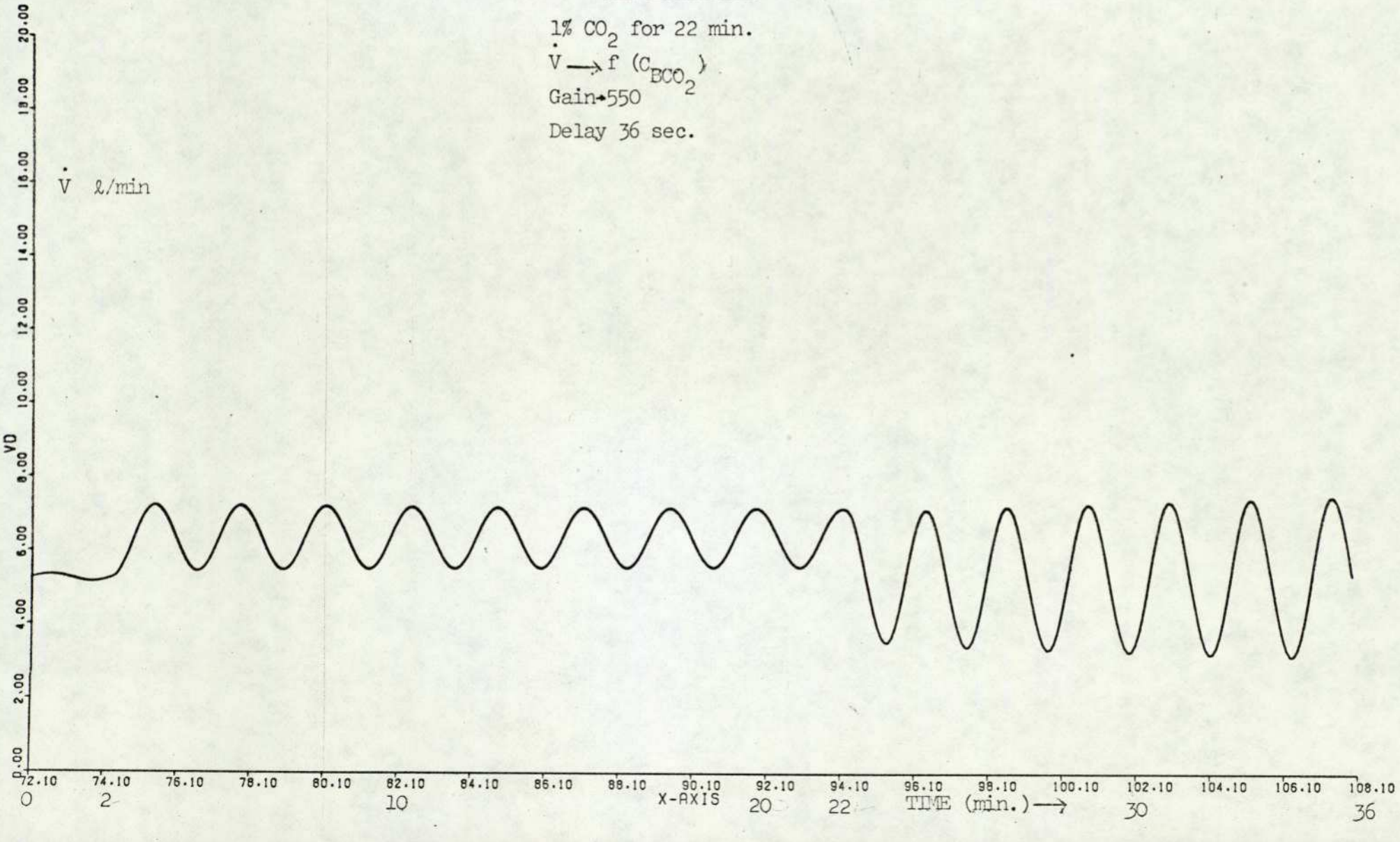

Graph 7.4.1.

1% CO_2 for 22 minutes

$\dot{V} \longrightarrow f(C_{BCO_2})$

GAIN 550

DEIAY 24 sec.

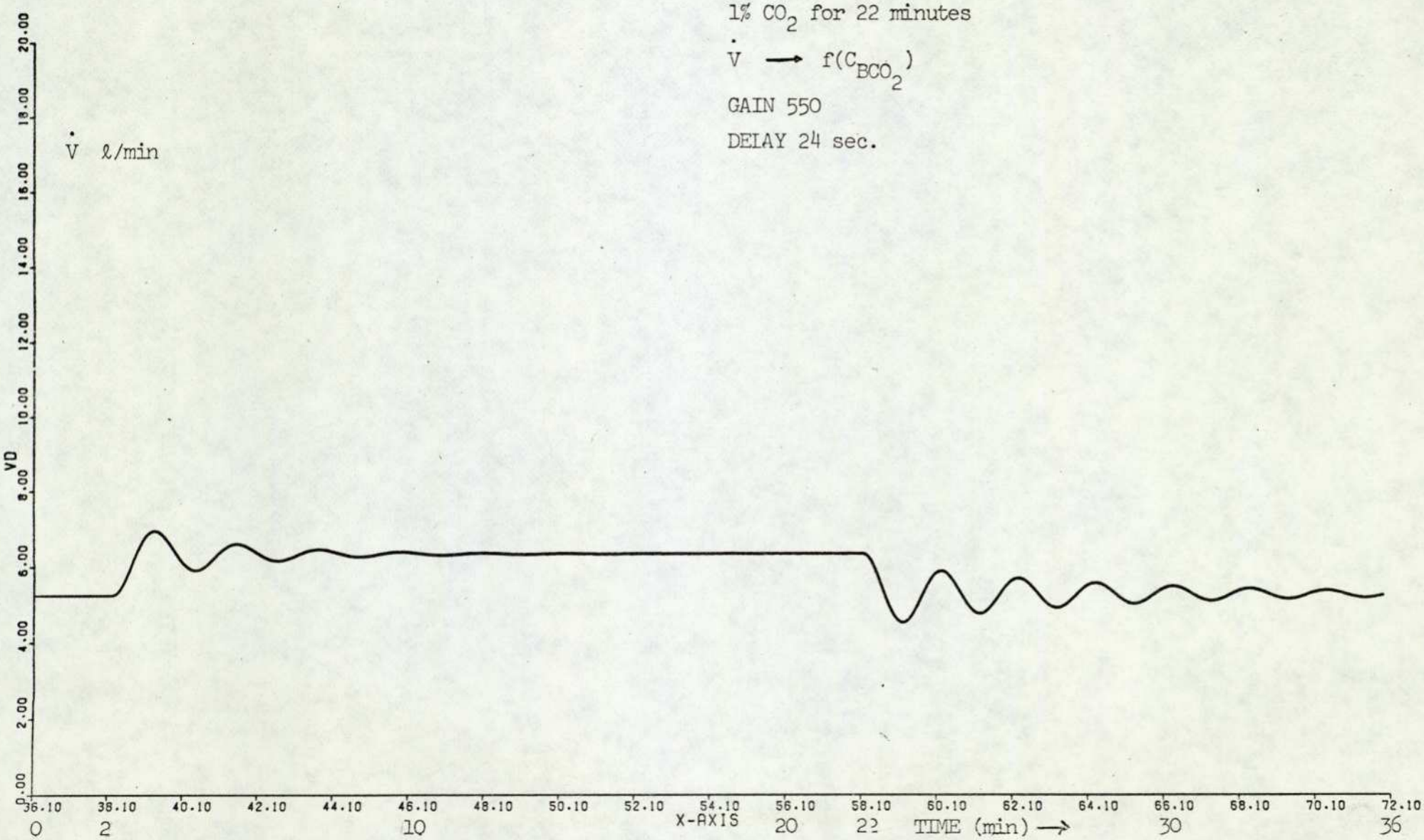

Graph 7.4.3.

1% CO_2 for 22 min.

$\dot{V} \rightarrow f(C_{BCO_2})$

GAIN 550

DELAY 48 sec.

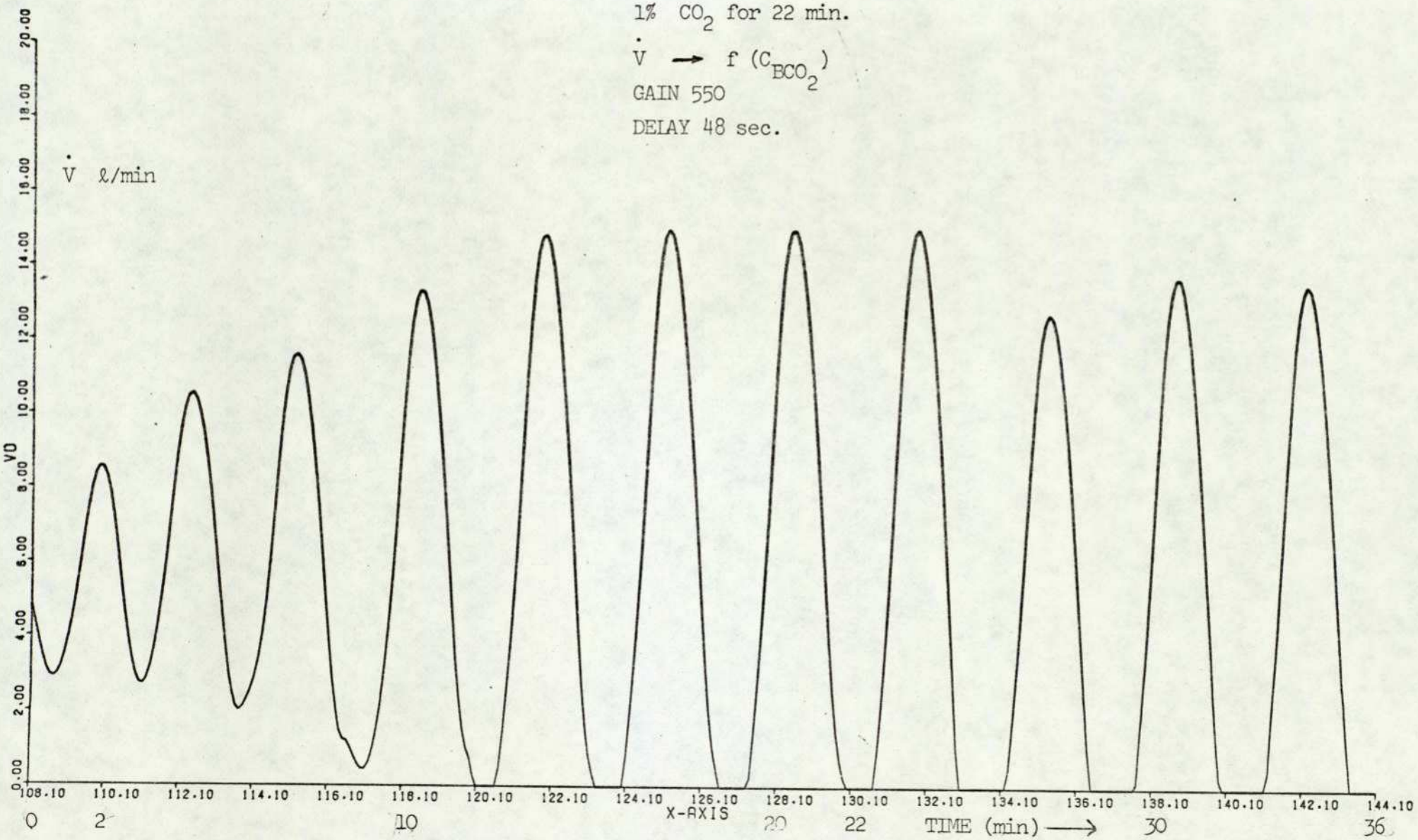

Graph 7.5.1.

9% O_2

$\dot{V} \rightarrow f(C_{BCO_2})$

GAIN 550

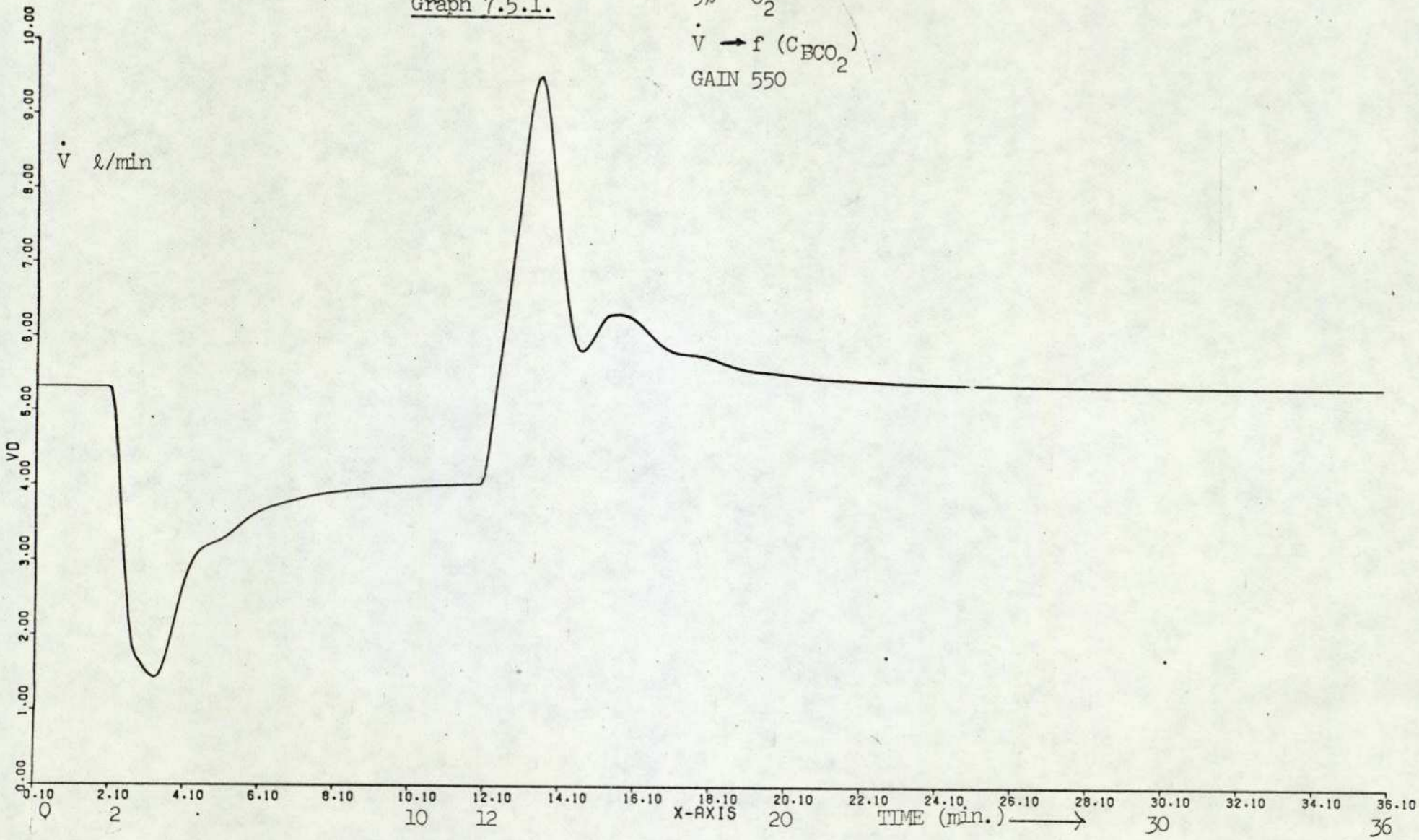

Graph 7.6.1.

$\dot{V} \rightarrow f(P_{aCO_2}$ and $P_{aO_2})$

Longob rdo Equation

3% CO_2 input

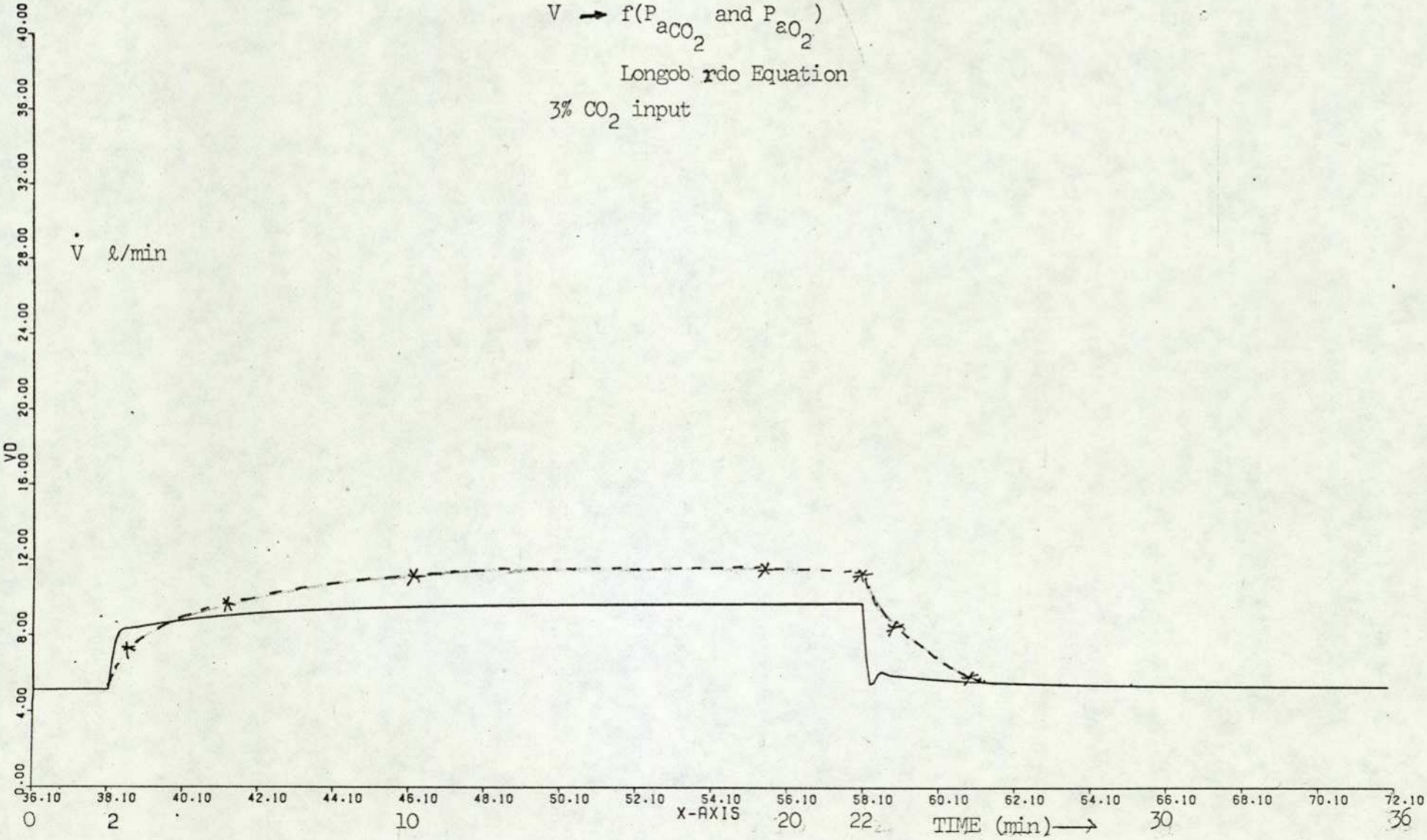

Graph 7.6.2.

$\dot{V} \rightarrow f\ (P_{a\,CO_2}$ and $P_{a\,O_2})$

Longob rdo Equation

5% CO_2 input

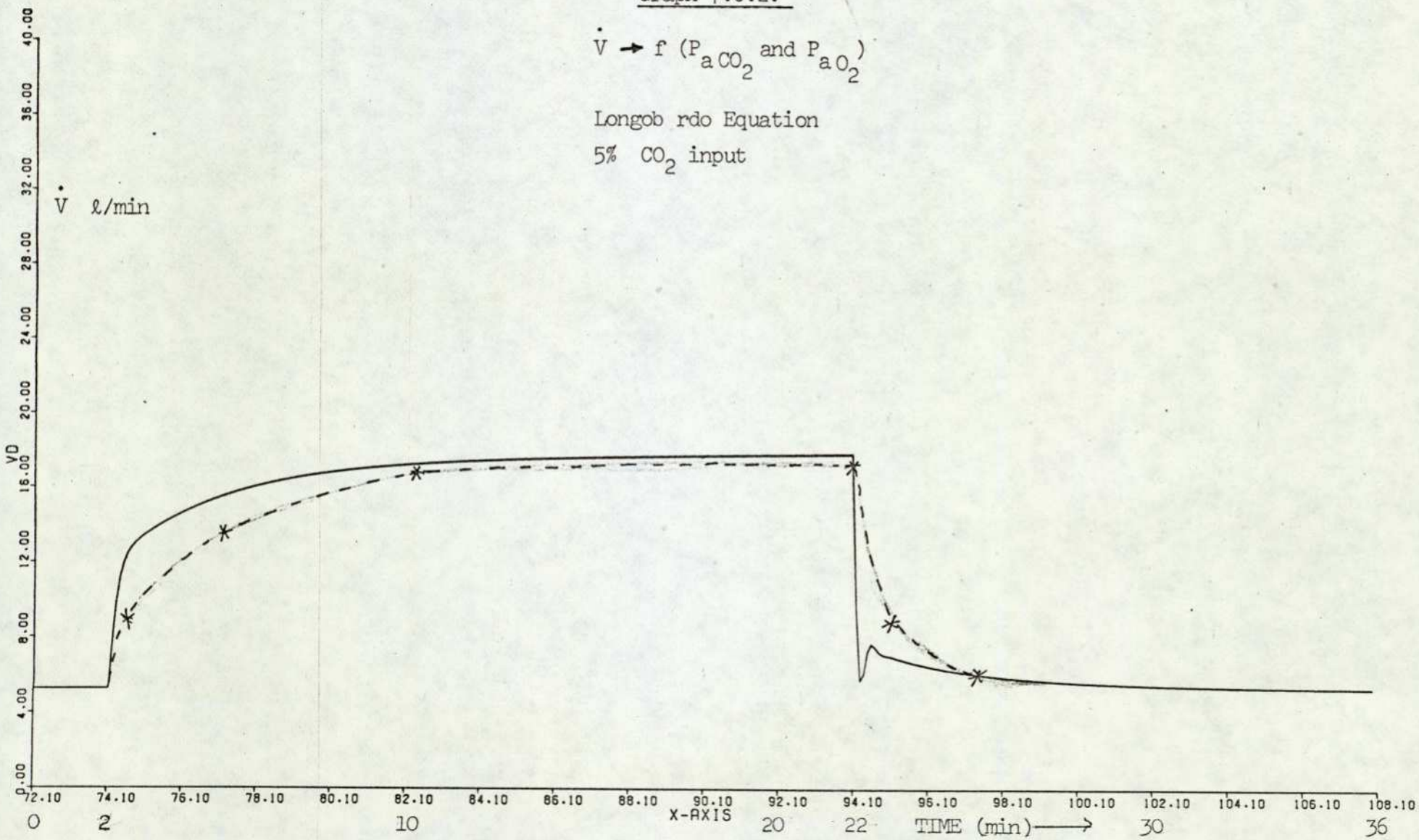

Graph 7.6.3.

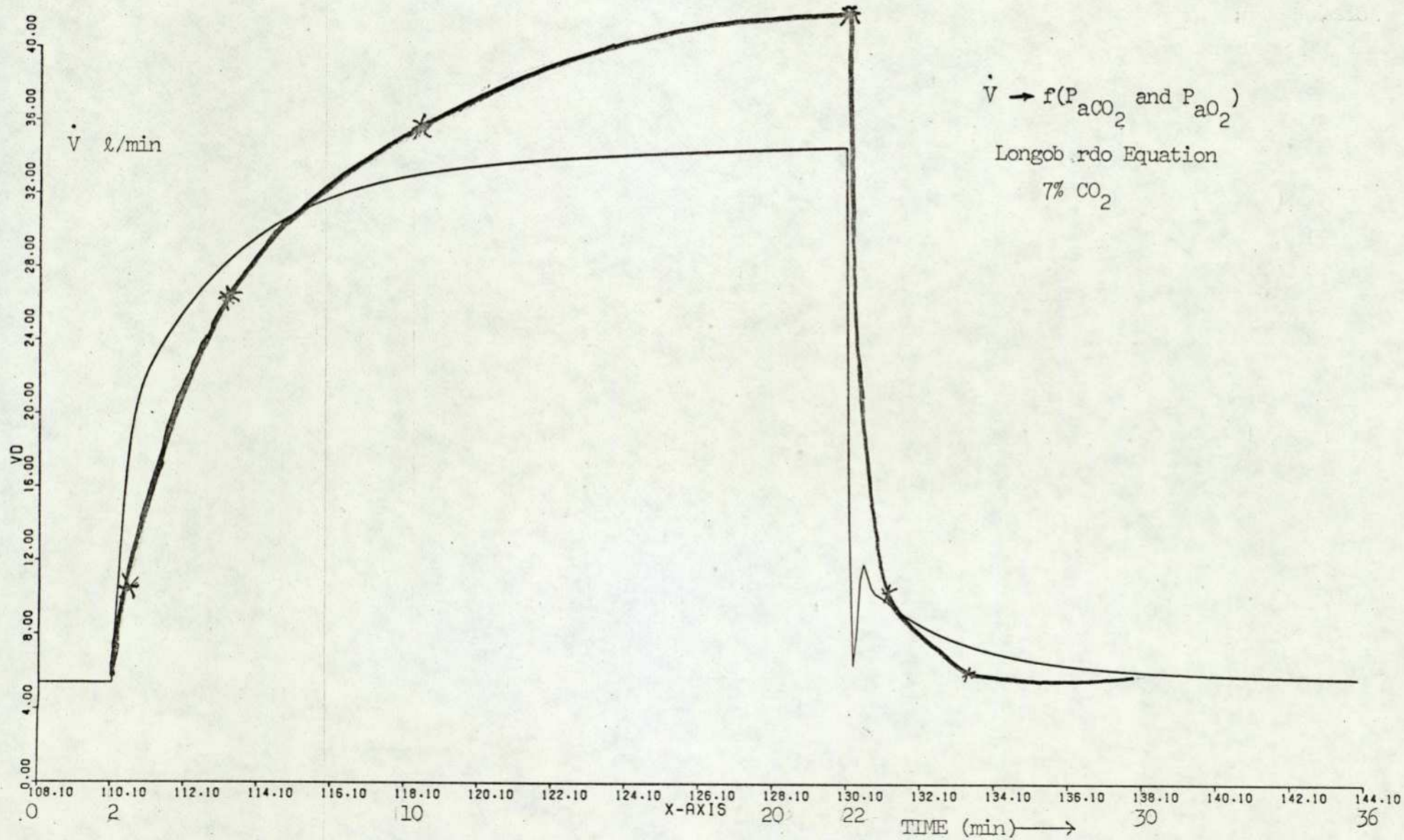
$\dot{V}$ ℓ/min
$\dot{V} \rightarrow f(P_{aCO_2}$ and $P_{aO_2})$
Longob rdo Equation
7% CO_2
VO
0.00
4.00
8.00
12.00
16.00
20.00
24.00
28.00
32.00
36.00
40.00
108.10
110.10
112.10
114.10
116.10
118.10
120.10
122.10
124.10
126.10
128.10
130.10
132.10
134.10
136.10
138.10
140.10
142.10
144.10
0
2
10
X-AXIS
20
22
30
36
TIME (min)

Graph 7.7.1.

Longobardo Equation

$\dot{V}_{O_2}$ $f(P_{aCO_2}$ and $P_{aO_2})$

9%

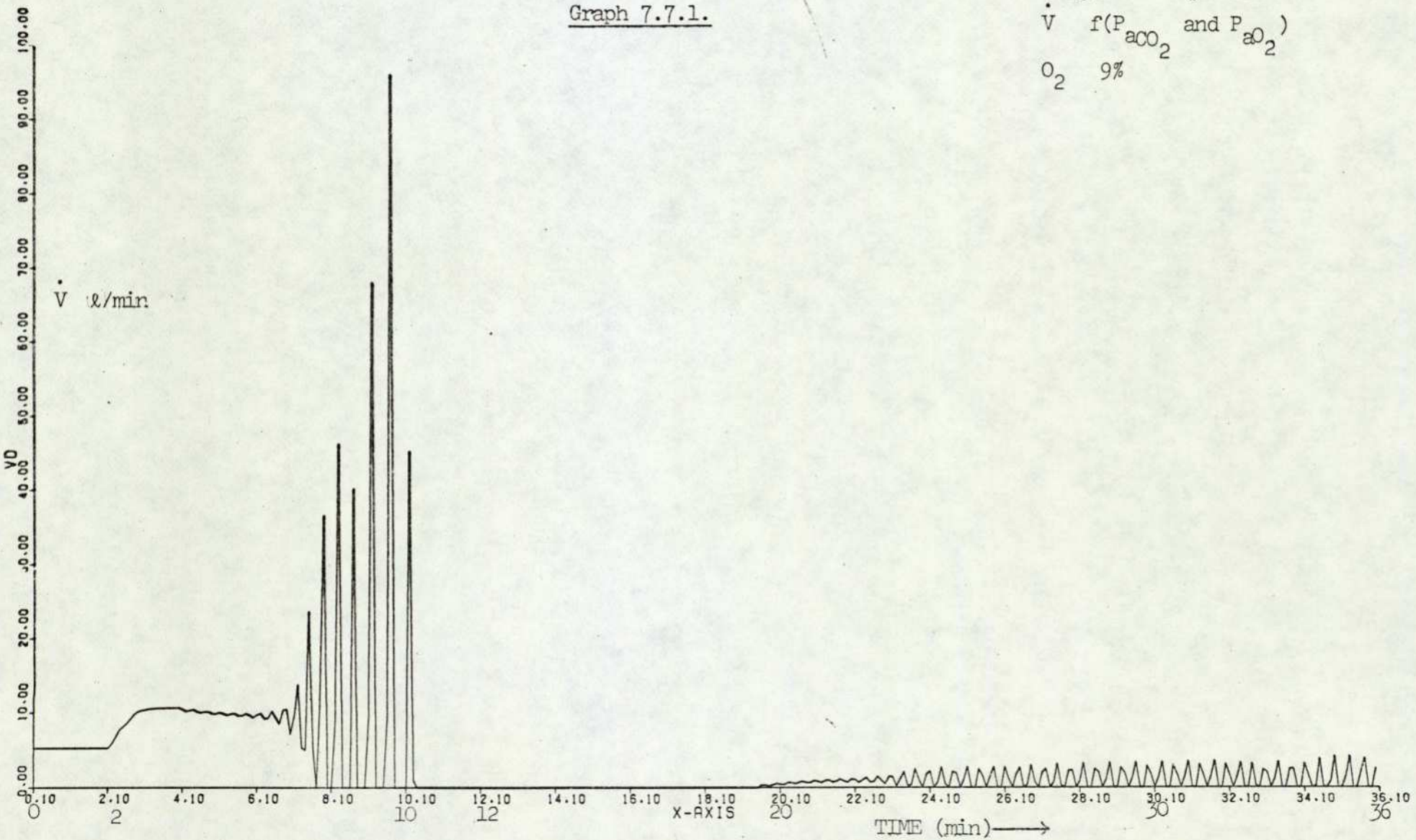

Graph 7.8.1.

Milhorn Controller

3% CO_2

* Experimental points

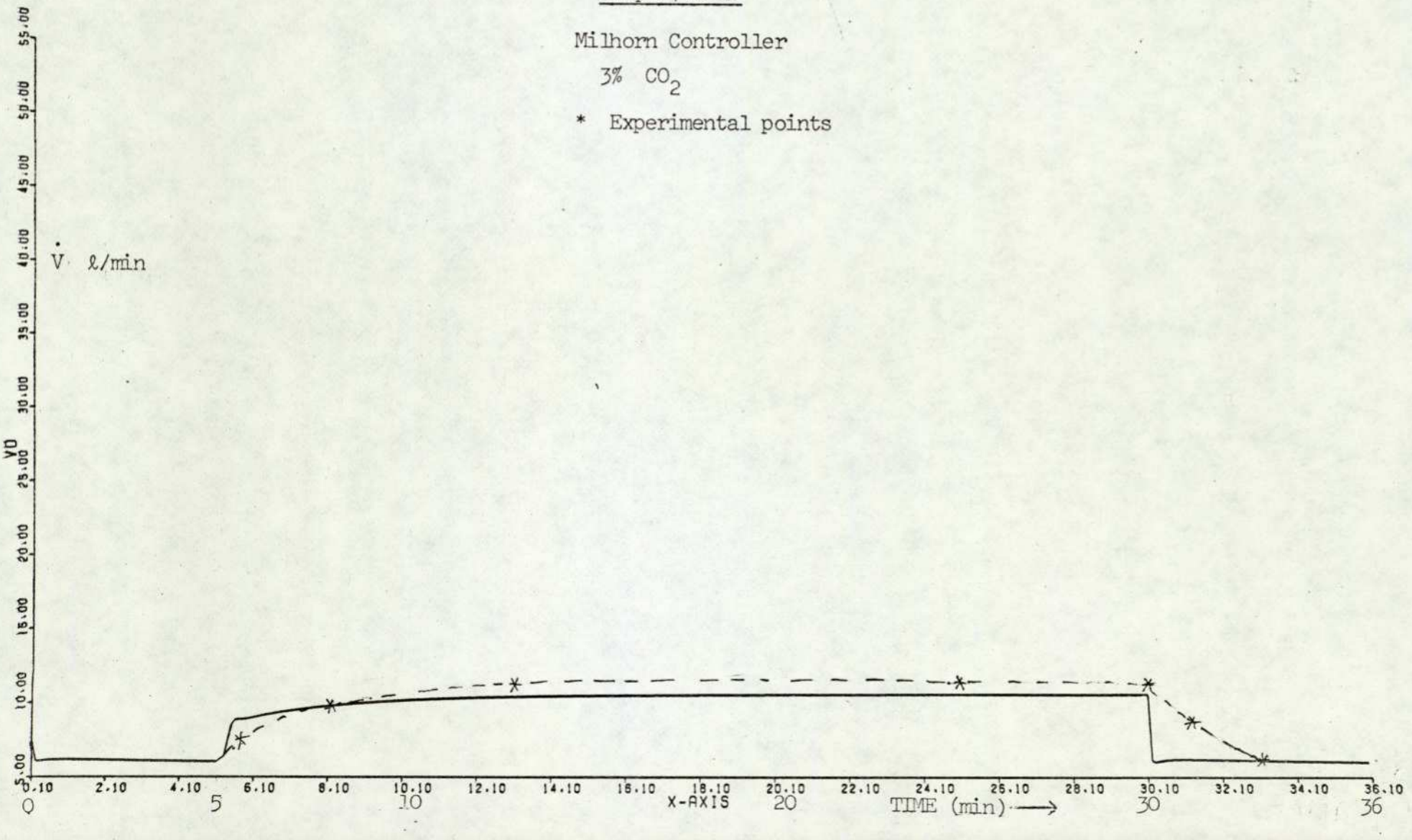

Graph 7.8.2.

Milhorn Controller
5% CO_2

* Experimental points

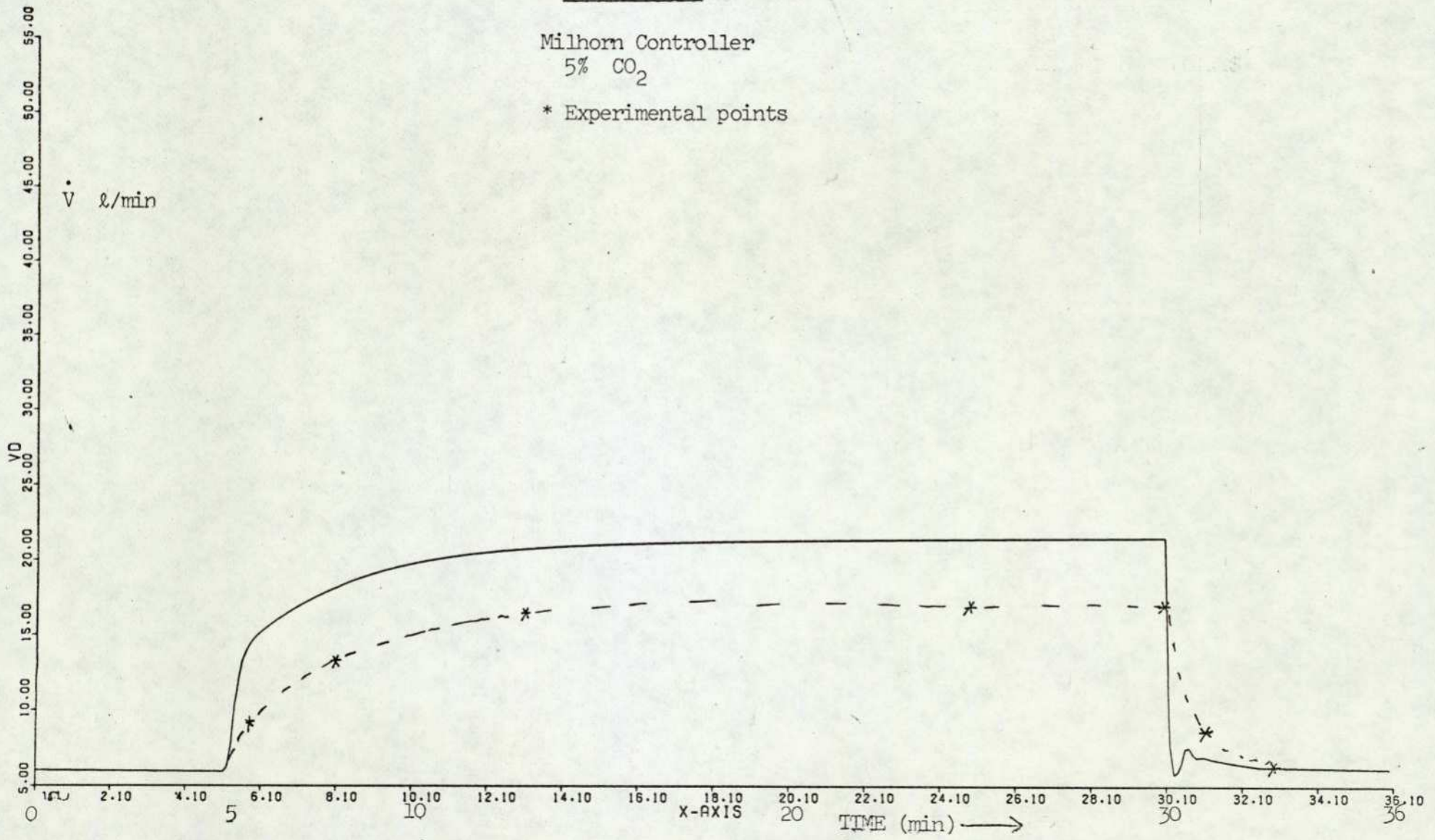

Graph 7.8.3.

Milhorn Controller

7% CO_2

* Experimental points

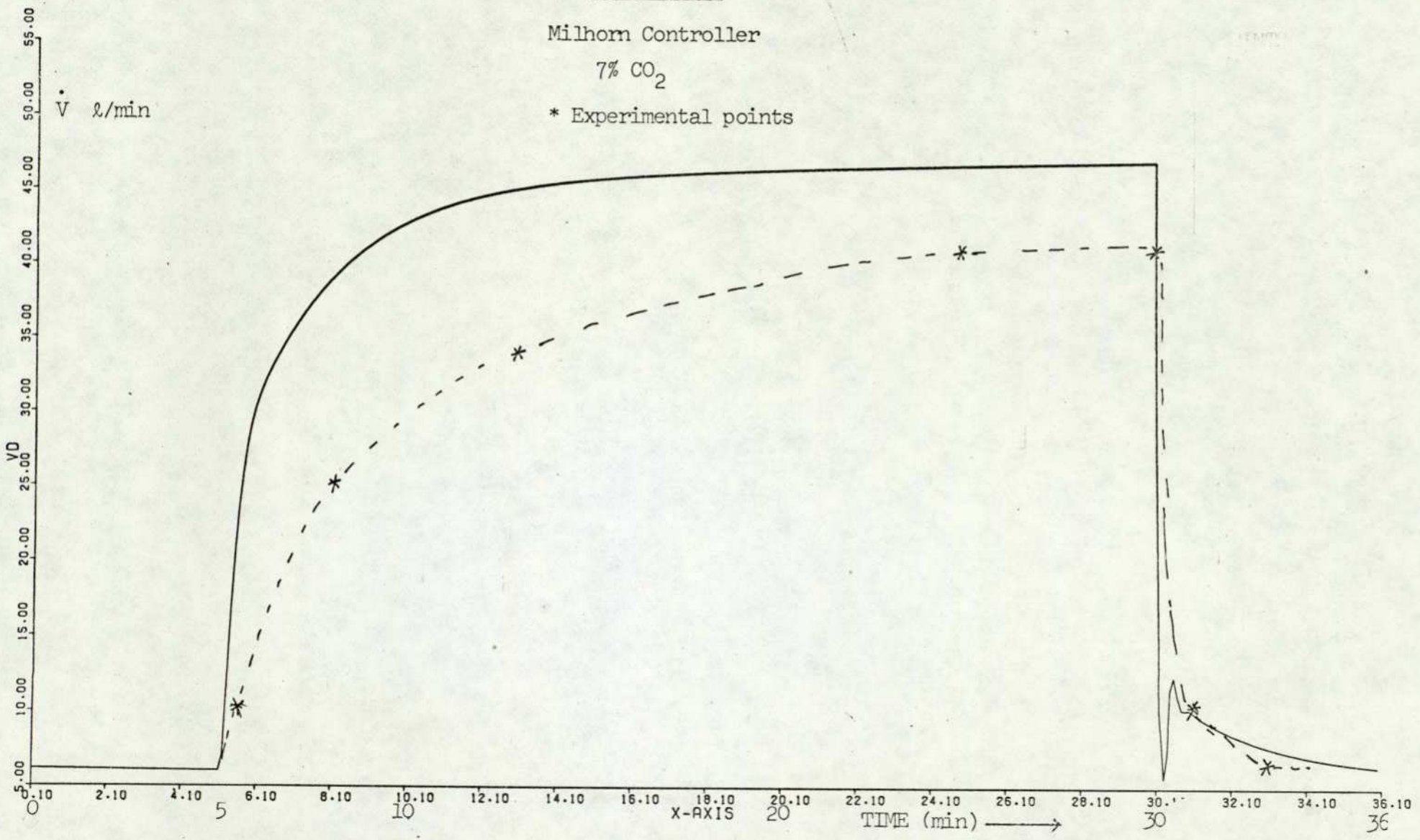

Graph 7.9.1.

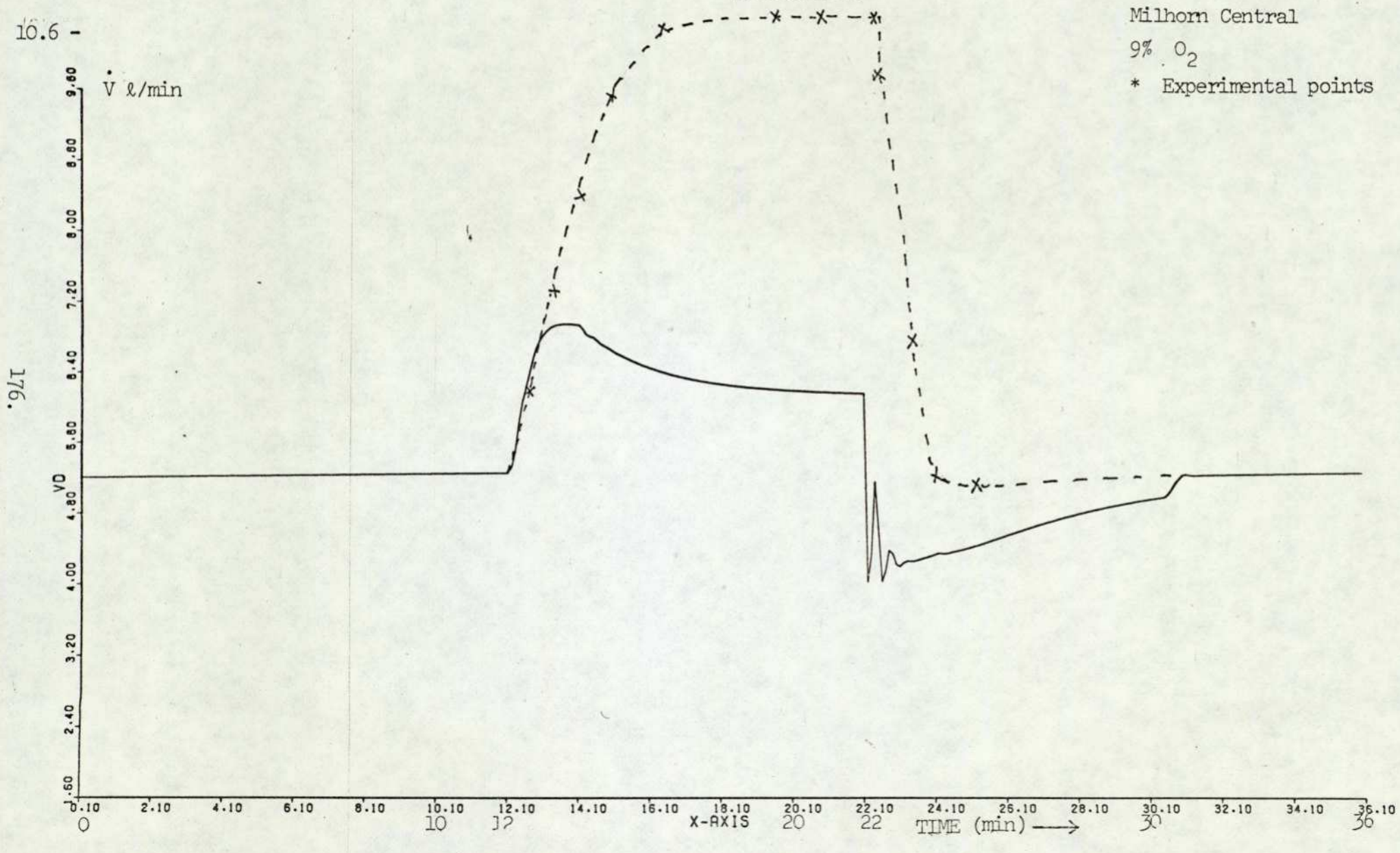
10.6
V̇ ℓ/min
Milhorn Central
9% O_2
* Experimental points
VD
9.60
8.80
8.00
7.20
6.40
5.60
4.80
4.00
3.20
2.40
1.60
0.10
2.10
4.10
6.10
8.10
10.10
12.10
14.10
16.10
18.10
20.10
22.10
24.10
26.10
28.10
30.10
32.10
34.10
36.10
0
10
12
X-AXIS
20
22
TIME (min) ⟶
30
36

Graph 7.10.1.

New Equation

$\dot{V} = f(P_{aCO_2}$ and $P_{aO_2})$

7% CO_2 inhalation

* Experimental points

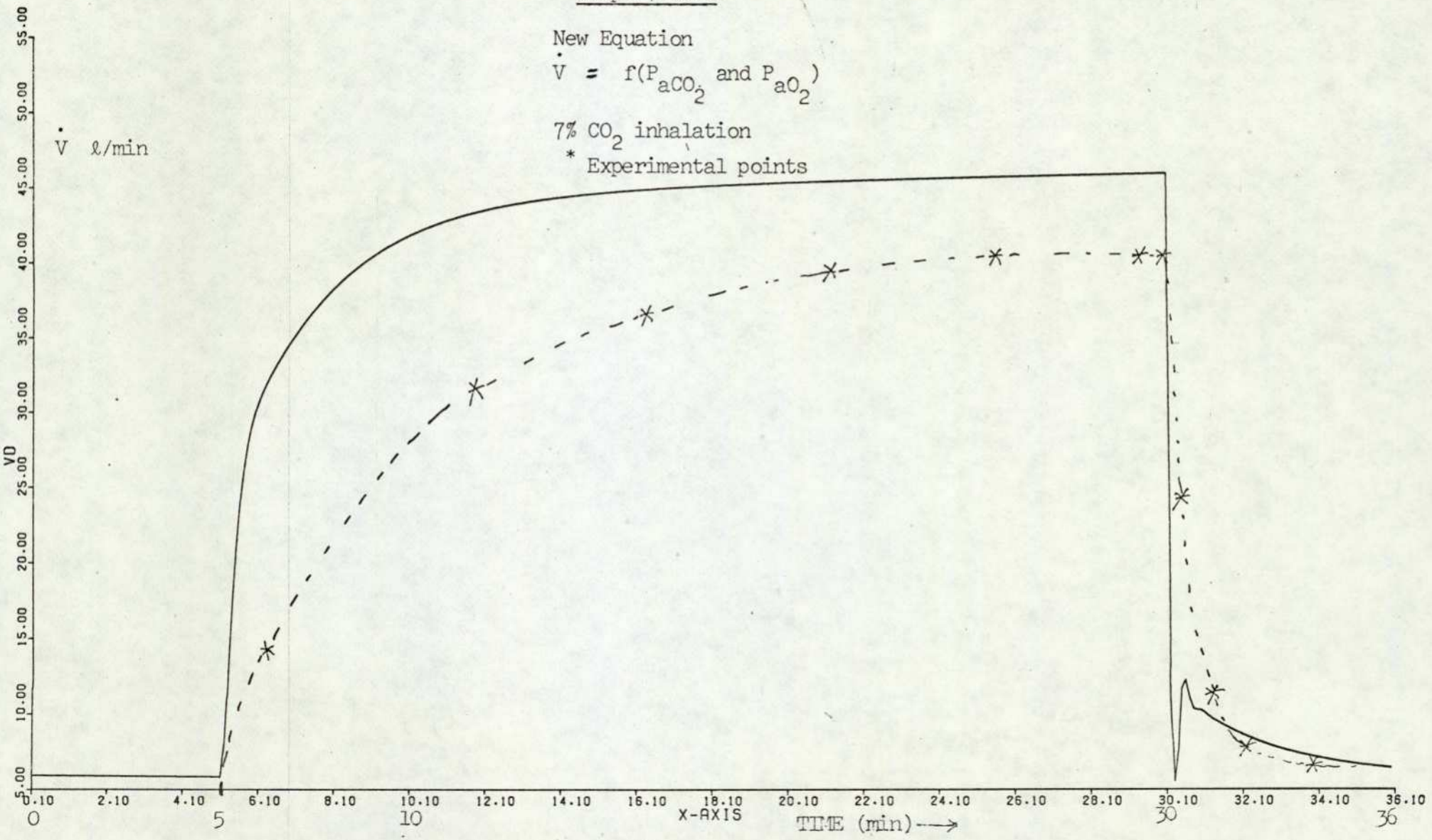

Graph 7.11.1.

New Equation 7.31

Delay 48 secs.

$\dot{V} = f(P_{aCO_2}$ and $P_{aO_2})$

1% CO input

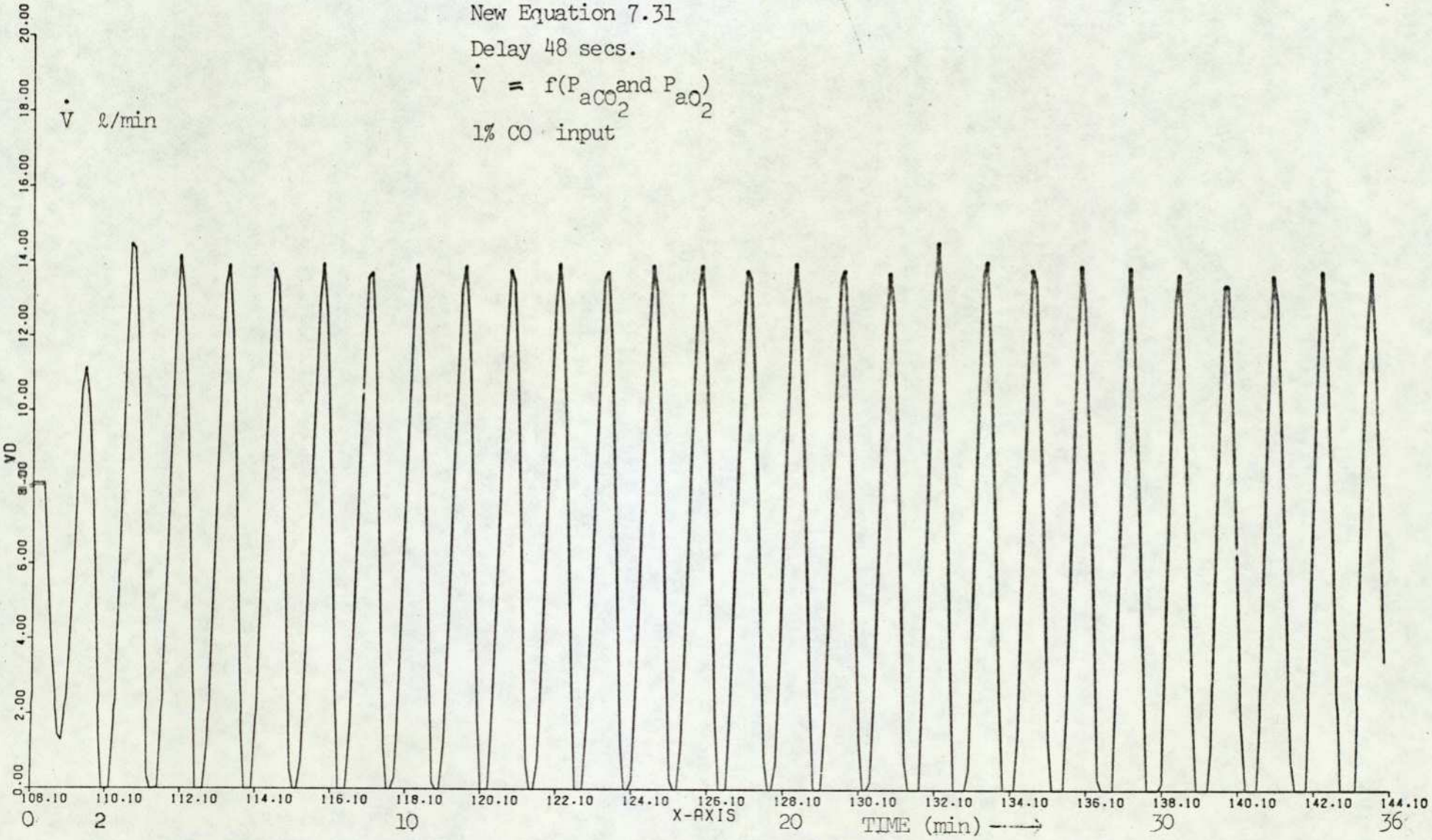

GRAPH 7.12.1 (Isocapnic Hypoxia 9% O_2)

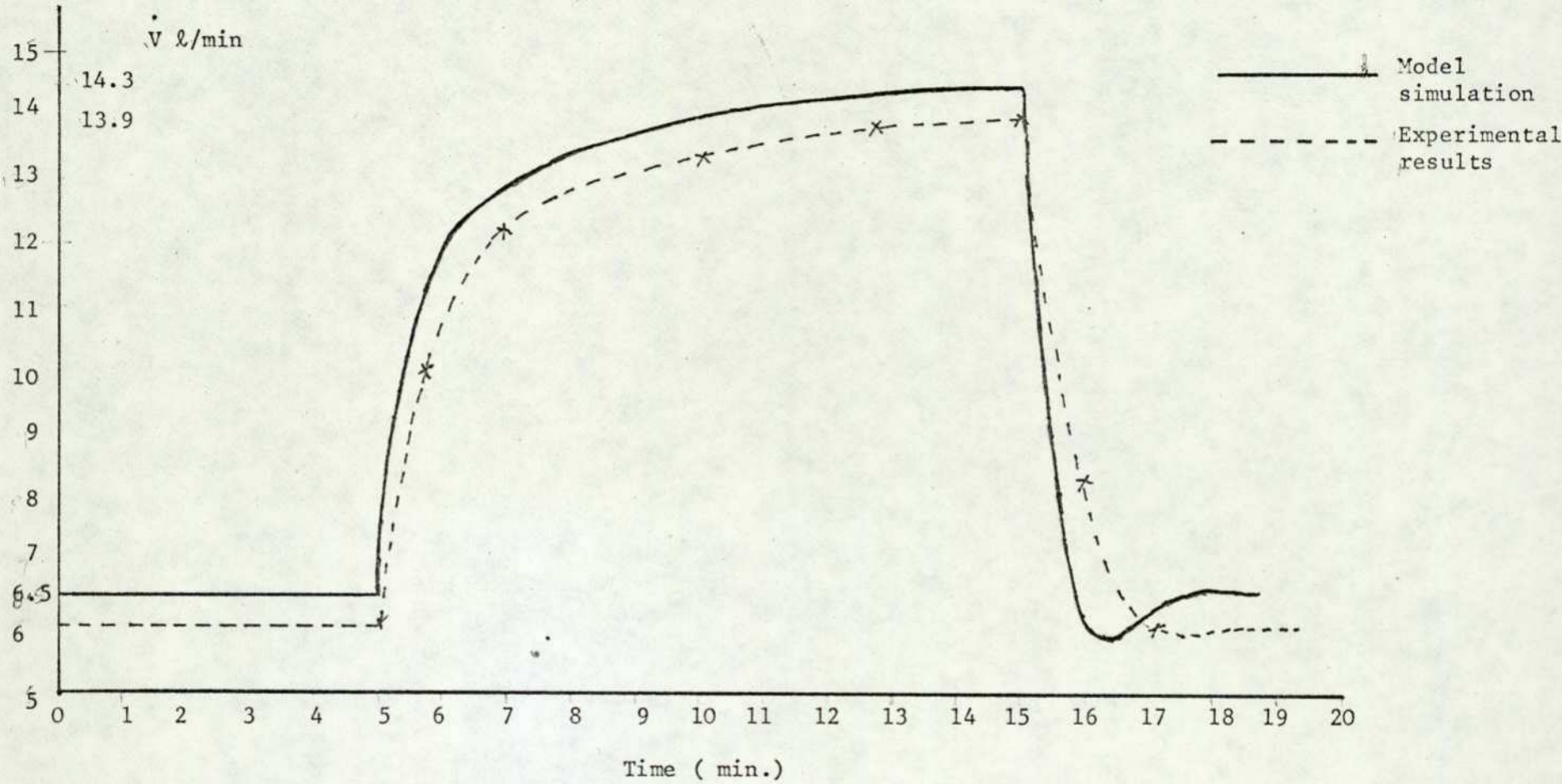

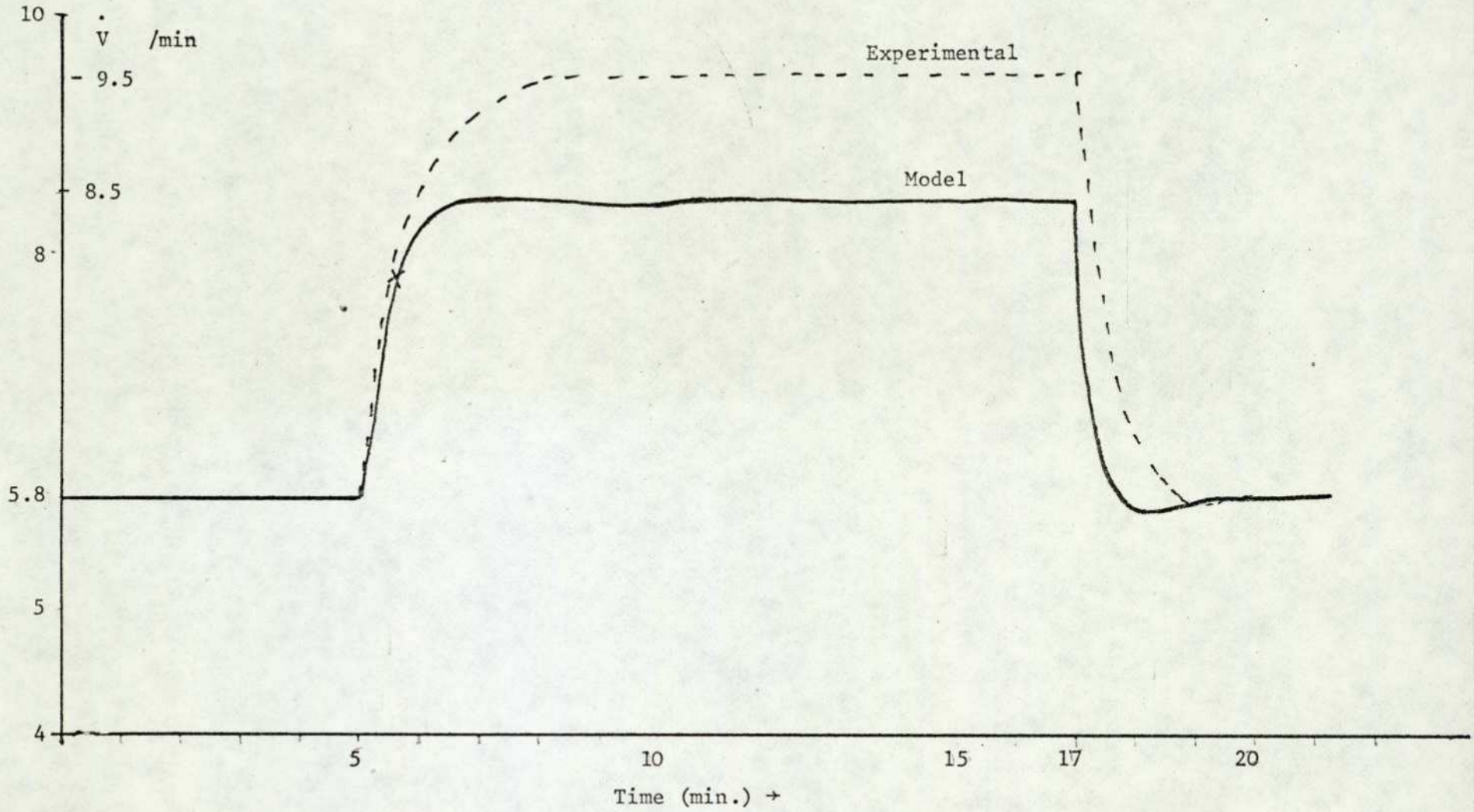

GRAPH 7.12.2. (Hypocapnic Hypoxia - 9% O_2)

CHAPTER 8

LUNG GAS EXCHANGE MODEL (ACTUAL VENTILATION)

So far only a unidirectional flow of air into the lungs has been considered and ventilation has been defined as the quantity of fresh air entering the lung per unit time. The assumption made so far that the lung volume is fixed is also not correct as can be seen from figures 8.1 and 8.2.

In reality the lung volume varies periodically with inspiration and expiration. The peak to peak variation is known as the tidal volume (V_{TV}) and for simplicity this can be represented by a sinusoidal waveform. The positive half represents the change in volume during inspiration, that is when fresh air is going into the lung. The negative half represents expiration.

During inspiration and expiration the alveoli are connected through the dead space to the outer atmosphere. The dead space is assumed to be of fixed volume (fig. 8.2). With this assumption the total change in lung volume is still equal to the tidal volume, but during inspiration the lung receives first the gases in the dead space which have the chemical composition of the alveolar gas at the end of previous expiration, then fresh air. The fresh air taken into the alveoli is thus the tidal volume minus the dead space volume. If instantaneous mixing of gases in the dead space is assumed, equations can be formulated connecting the dead space to the atmosphere and the lung to the dead space.

8.1 FORMULATION OF EQUATIONS:

1. Lung Volume and Actual Ventilation:

Consider that the process of inspiration starts from a volume of V_o (fig. 8.3a). Then the instantaneous lung volume is given by:

$$V = V_o + \frac{V_{TV}}{2} (1 - \cos 2\pi ft). \quad \ldots\ldots 8.1$$

where f is the frequency of breathing.

Differentiating equation 8.1 to yield rate of change of lung volume ($\dot{V}$)

$$\dot{V} = 2\pi f. \frac{V_{TV}}{2} . \sin 2\pi ft \quad \ldots\ldots 8.2$$

as shown in figure 8.3b. The positive half of this curve represents inspiration and the negative half represents expiration.

The total gas flow to the lung, however, is due not only to ventilation but also to the exchange of CO_2 and O_2 across the alveolar membranes, oxygen being taken up by the arterial blood and carbon dioxide being released from venous blood (fig.8.4). This gas exchange between alveoli and blood is a continuous process, occuring during both inspiration and expiration. The rate of exchange is assumed to be proportional to the partial pressure (or concentration) of gases. It also depends upon the rate of blood flow. Using Fick's equations:

$$D_{CO_2} = \dot{q} (C_{vCO_2} - C_{aCO_2}) \quad \ldots\ldots 8.3$$

$$D_{O_2} = \dot{q} (C_{aO_2} - C_{vO_2}) \quad \ldots\ldots 8.4$$

where D_{CO_2} and D_{O_2} are the quantities of carbon dioxide and oxygen being exchanged per unit time.

Therefore actual ventilation is

$$\dot{V}_{AC} = 2\pi f \frac{V_{TV}}{2}. \sin 2\pi ft + (D_{O_2} - D_{CO_2}). K \quad \ldots\ldots 8.5$$

where the factor K is introduced to account for the difference between S.T.P. and B.T.P.S. units since alveolar gas exchange occurs within the body

Using the gas law:

$$\frac{P_O V_O}{T_o} = \frac{P_B V_B}{T_B} \quad \ldots\ldots 8.6$$

where the suffix o represents standard atmosphere and B represents body,

$$\frac{V_B}{V_o} = \frac{P_o T_B}{P_B . T_o} = K \qquad \ldots\ldots 8.7$$

Assuming P_o = 760 mm Hg

T_B = 310°K (body temperature of 37°C)

T_o = 273°K

P_B = 713 (body dry gas pressure)

$$\therefore \quad K = \frac{760 * 210}{273 * 713}$$

$$= \frac{863}{713} \qquad \ldots\ldots 8.8$$

Substituting this value of K in equation 8.5

$$\dot{V}_{AC} = 2\pi f . \frac{V_{TV}}{2} . \sin 2\pi f.t + \frac{863}{713} (D_{O_2} - D_{CO_2}) \qquad \ldots\ldots 8.9$$

Note that D_{O_2} is added to the actual ventilation, for if oxygen was not lost to arterial blood, the actual ventilation would have been higher by that quantity. Similarly D_{CO_2} is subtracted since it came from the body rather than from ventilation. The body's oxygen consumption is higher than the CO_2 production so that the net effect of these terms is to add a positive D.C. bias to the sine waves. This conforms well to the physiological evidence that inspiratory flow is greater than that during expiration. The ratio of expiratory to inspiratory flows or total body CO_2 production to O_2 consumption is termed the respiratory quotient (R.Q.)

The equation 8.9 describes the actual ventilation which is positive during inspiration and negative during expiration.

ii. Gas Exchange Equations: ($\dot{V}_{AC}$ + ve)

(a) Inspiration:

Dead Space

$$\frac{d}{dt} \cdot F_{DCO_2} = \dot{V}_{AC} (F_{oCO_2} - F_{DCO_2})/V_D \quad \ldots\ldots 8.10$$

$$\frac{d}{dt} \cdot F_{DO_2} = \dot{V}_{AC} (F_{oO_2} - F_{DO_2})/V_D \quad \ldots\ldots 8.11$$

where F_o equals the gas fraction in air and F_D equals the gas fraction in the dead space.

During inspiration atmospheric gases enter the dead space whilst those already there pass into the alveoli.

Alveoli

Defining V_{ACO_2} and V_{AO_2} as the quantities of CO_2 and O_2 in the alveolar compartment respectively,

$$\frac{d}{dt} V_{ACO_2} = \dot{V}_{AC} \cdot F_{DCO_2} + \frac{863}{713} \cdot D_{CO_2} \quad \ldots\ldots 8.12$$

$$\frac{d}{dt} V_{AO_2} = \dot{V}_{AC} F_{DO_2} + \frac{863}{713} \cdot D_{O_2} \quad \ldots\ldots 8.13$$

Gases are entering the alveoli from the dead space; CO_2 is entering from the venous blood whilst oxygen is going out with arterial blood.

(b) Expiration: ($\dot{V}_{AC}$ ve).

Dead Space

Defining F_A as the alveolar gas fraction

$$\frac{d}{dt} \cdot F_{DCO_2} = \dot{V}_{AC} (F_{DCO_2} - F_{ACO_2})/V_D \quad \ldots\ldots 8.14$$

$$\frac{d}{dt} \cdot F_{DO_2} = \dot{V}_{AC} F_{DO_2} - F_{AO_2})/V_D \quad \ldots\ldots 8.15$$

$\dot{V}_{AC}$ is negative, therefore to maintain the sign convention outgoing gases are negative and those incoming are positive. $\dot{V}_{AC}F_D$ is a negative quantity representing gas exiting to the atmosphere and $\dot{V}_{AC}$ $(-F_A)$ is a positive quantity representing gas entering from the alveoli.

Alveoli

$$\frac{d}{dt} \cdot V_{ACO_2} = \dot{V}_{AC} \cdot F_{ACO_2} + D_{CO_2} \quad \ldots\ldots 8.16$$

$$\frac{d}{dt} \cdot V_{AO_2} = \dot{V}_{AC} \cdot F_{AO_2} - D_{O_2} \quad \ldots\ldots 8.17$$

During expiration both CO_2 and O_2 are being exhaled to the dead space whereas CO_2 is entering the alveoli from the venous blood, and O_2 is leaving the alveoli with arterial blood continuously.

At any instant, during inspiration and expiration the alveolar fraction of gas is equal to the quantity of gas in the alveoli at that instant divided by the instantaneous volume of the alveoli.

From equation 8.1 the alveolar volume V_A is given by

$$V_A = V_o + \frac{V_{TV}}{2} (1 - \cos 2\pi ft) \quad \ldots\ldots 8.18$$

$$\therefore F_{ACO_2} = V_{ACO_2} / V_A \quad \ldots\ldots 8.19$$

$$\text{and } F_{AO_2} = V_{AO_2} / V_A \quad \ldots\ldots 8.20$$

The partial pressure of dry gas is given by the fraction multiplied by 713.0. Defining P_A as the alveolar gas partial pressure:

$$P_{ACO_2} = 713.0 * F_{ACO_2} \quad \ldots\ldots 8.21$$

$$\text{and } P_{AO_2} = 713.0 * F_{AO_2} \quad \ldots\ldots 8.22$$

At this stage a normal resting man is being considered, for whom it is safe to assume that body tissue CO_2 production and oxygen consumption are constant

From Longobardo et al (1966)

$$D_{CO_2} = 0.228 \text{ ℓ/min} \quad \ldots\ldots 8.23$$

and $$D_{O_2} = 0.28 \text{ ℓ/min} \quad \ldots\ldots 8.24$$

giving rise to an R.Q. of 0.89 which is physiologically acceptable for resting man.

The frequency of breathing is assumed to be a linear function of ventilation of the form

$$f = K_1 + K_2 . \dot{V} \quad \ldots\ldots 8.25$$

where $K_1 = 8.7$)
) Grodins et al (1963)
and $K_2 = 0.267$)

8.2 RESULTS AND DISCUSSIONS:

As no body tissue dynamics is involved in this model, the above equations were tested only for fixed resting ventilations, and no feedback was involved.

Graph 8.1 shows the time variation of P_{ACO_2} during the process of inspiration and expiration. As expected P_{ACO_2} is varying with tidal volume, not only due to the process of gas exchange but also due to the change in lung volume. But tidal volume is rather high at 0.67ℓ. This may well be due to a low breathing frequency of 10.5 cycles per minute. To compensate for that, equation 8.25 was modified using the data of Reynold et al (1971) to

$$f = 10.7 + 0.267 \dot{V} \quad \ldots\ldots 8.26$$

Using equation 8.26 for the frequency of breathing, the time variation of alveolar P_{AO_2} is as shown in graph 8.2. It can be seen that tidal volume has decreased to 0.55ℓ with increased frequency of breathing - 12.5 breaths per minute. Also peak to peak variation, which was rather high in the previous case (3.8 mm Hg, graph 8.1), has been reduced to approximately 3 mm Hg which is physiologically acceptable. (S.J.G. Semple - private communication).

At this stage the model is not tested further for various blood flow rates, or some other change of parameters because there is no feedback loop, i.e., there is no ventilatory response from the model due to the body tissues being absent from the model. It will be of greater advantage to put together the lung gas exchange model and the body tissue and circulation model (Model 3 chapter 7) where feedback of ventilation can be provided either from arterial chemoreceptors sensitive to changes in gas composition in the arterial blood, or from central chemoreceptors sensitive to changes in the brain tissue gas concentrations.

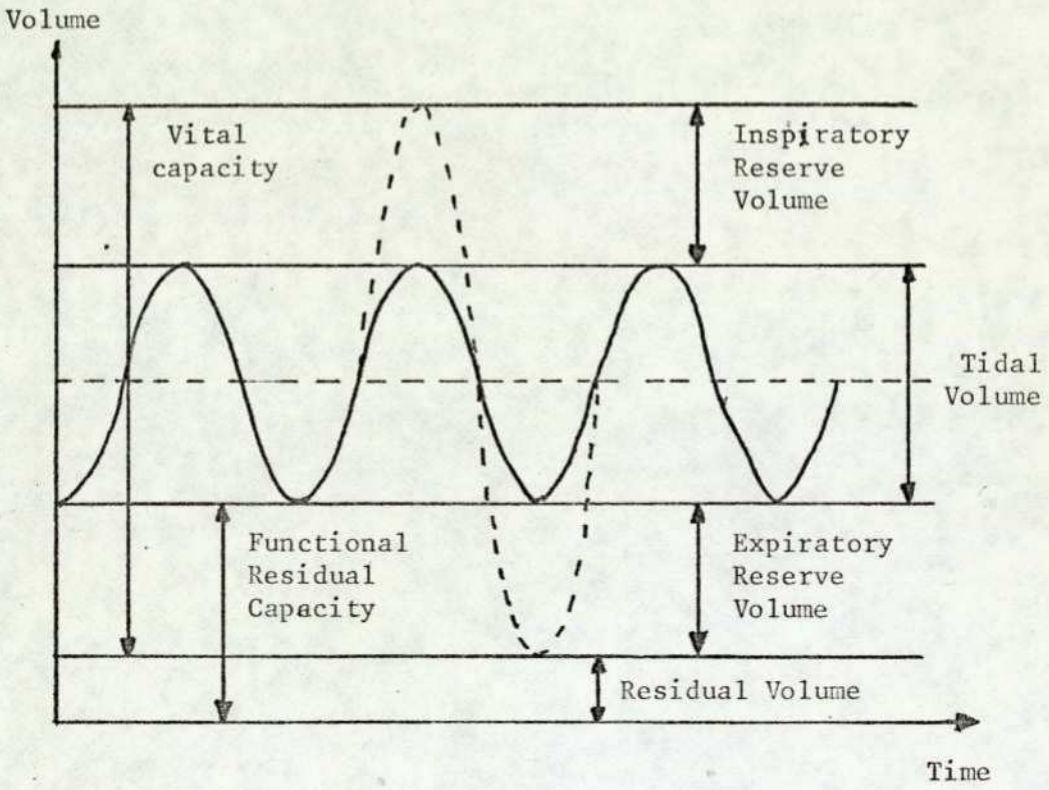
Volume
Vital capacity
Inspiratory Reserve Volume
Tidal Volume
Functional Residual Capacity
Expiratory Reserve Volume
Residual Volume
Time

Figure 8.1

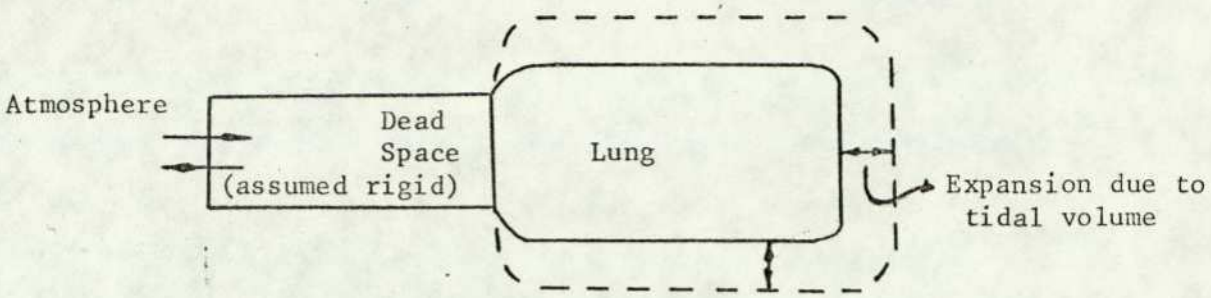

FIGURE 8.2

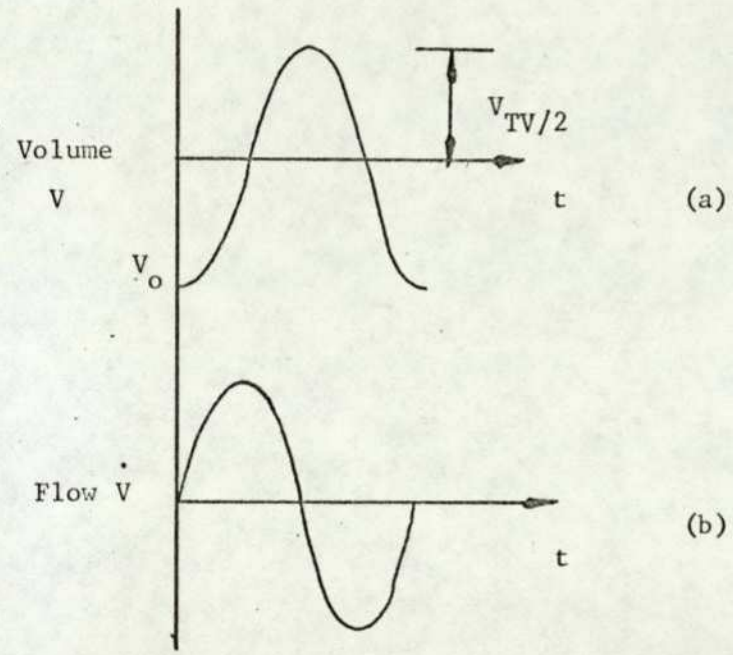

FIGURE 8.3

V_o is variable with tidal volume

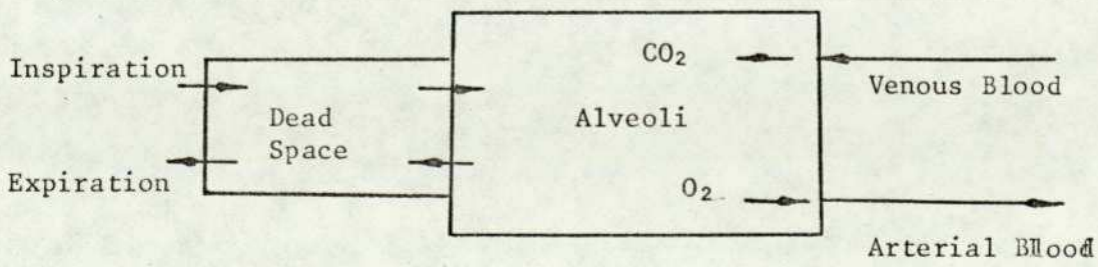

FIGURE 8.4

GRAPH 8.1

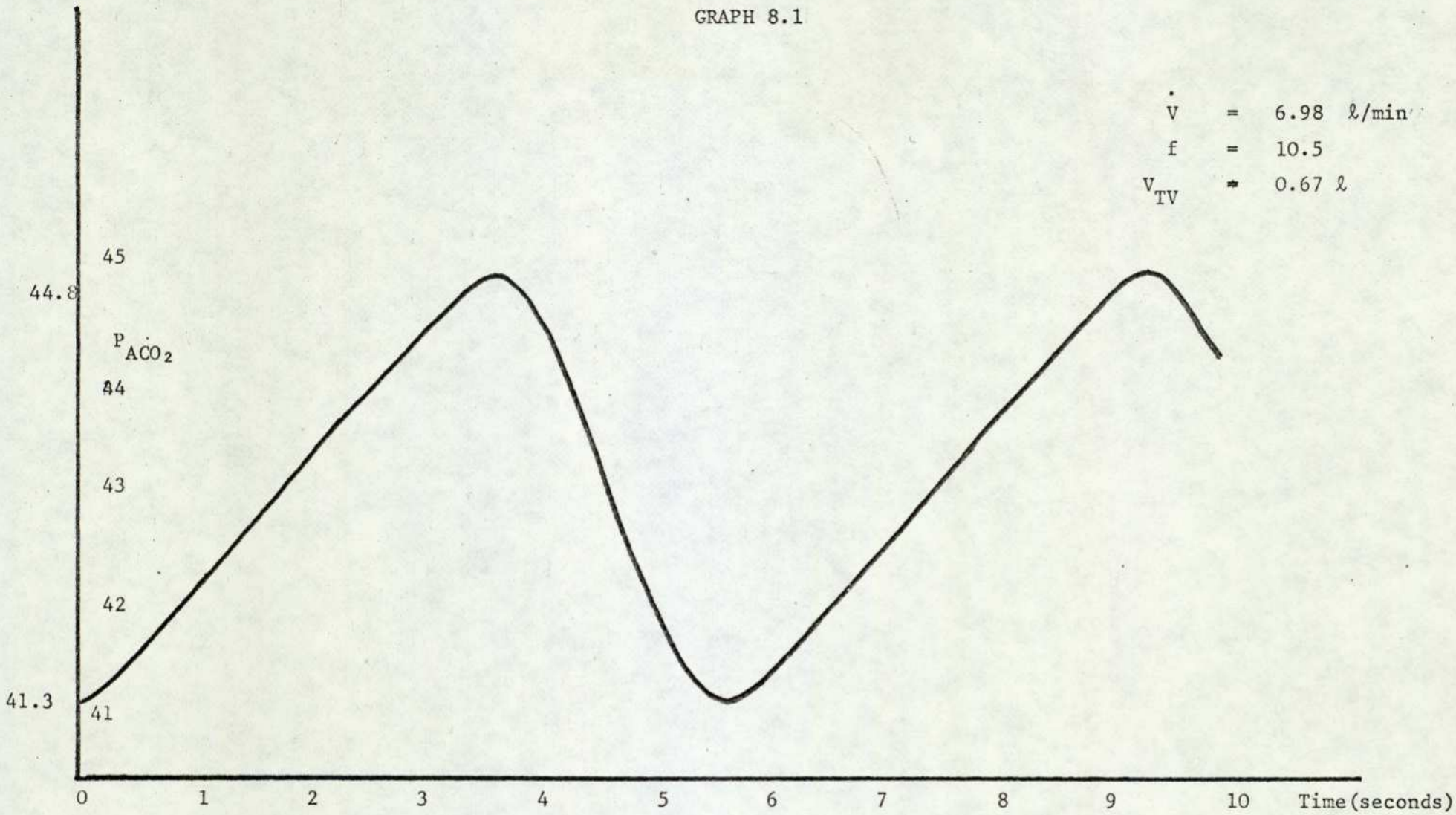
$\dot{V}$ = 6.98 ℓ/min
f = 10.5
V_{TV} = 0.67 ℓ
45
44.8
P_{ACO_2}
44
43
42
41.3
41
0
1
2
3
4
5
6
7
8
9
10
Time (seconds)

GRAPH 8.2

$\dot{V}$ = 6.9 ℓ/min

f = 12.5

V_{TV} = 0.55ℓ

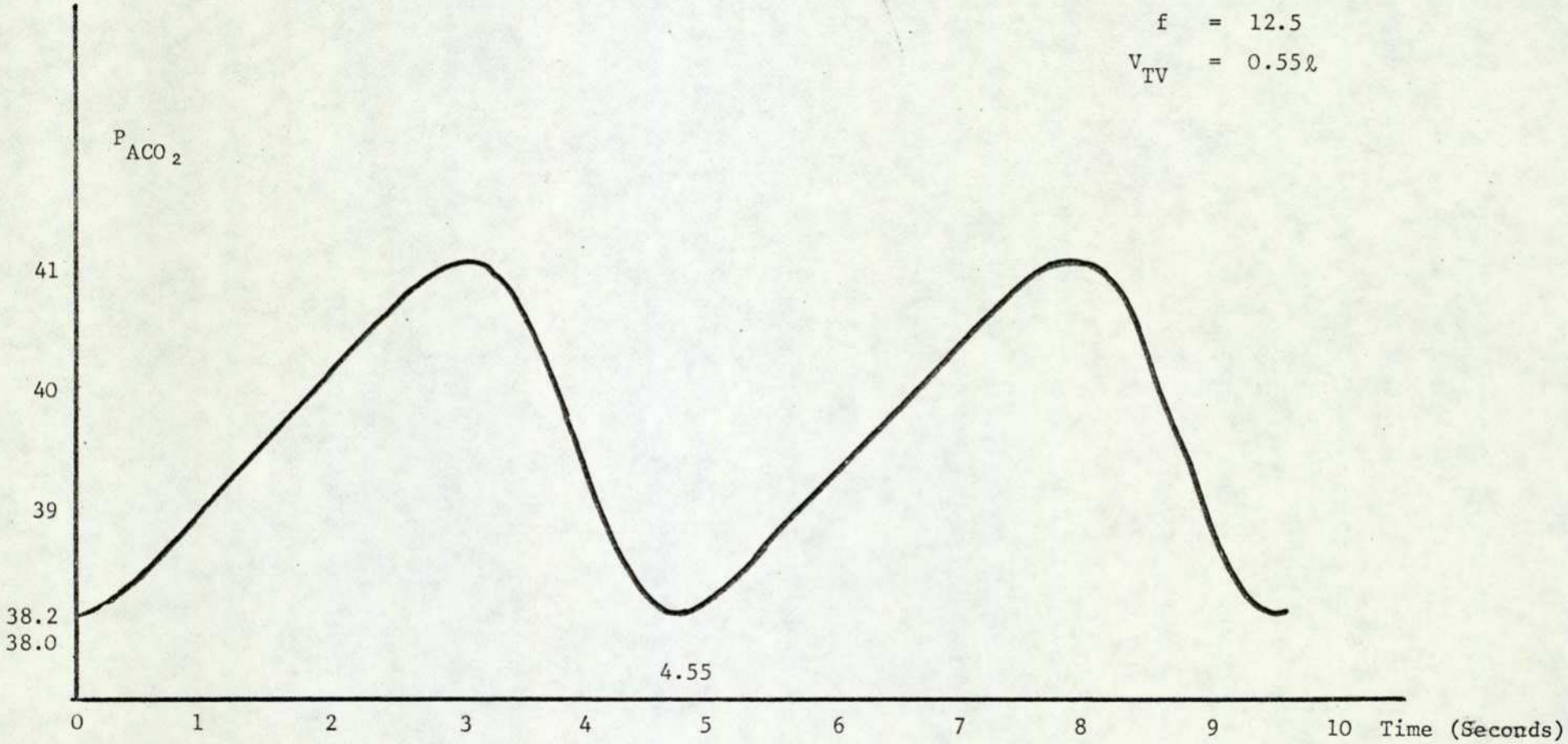

CHAPTER 9

COMPLETE MODEL (INCORPORATING BREATHING)

The lung gas exchange model developed in chapter 8 is now extended to a breathing model. In the lung gas exchange model, relationships were developed to connect the alveoli compartment to air through the dead space, whereas in chapter 7 a four compartment model was developed to connect the lung (alveoli) to the body tissue compartments through the flow of blood, which carries oxygen destined for tissue compartments on the arterial side and the metabolic carbon dioxide on the venous side. This phenomenon of gas flows, to and from the tissues was represented by D_{CO_2} and D_{O_2} in the lung gas exchange model and these quantities were assumed to be fixed. In practice these quantities are highly variable and depend upon gas partial pressures (or concentrations)in venous and arterial blood and in the alveoli. They also are dependent upon the rate of cardiac output which again is a variable quantity and is a function of arterial P_{CO_2} and P_{O_2} (chapter 7). Further, up to model III, the CO_2 dissociation curve has been considered to be linear and fixed. This certainly is contrary to experimental evidence as shown in figure 9.1. Not only is the dissociation curve non-linear, but it is also a function of the partial pressure of oxygen. (This is known as Bohr's effect in physiology). Thus new equations for the CO_2 dissociation curve are developed which take into account any changes due to varying arterial oxygen by curve fitting to experimental data (Grodins et al,1967; Horgan and Lange, 1965).

In model III equations 7.1 and 7.6 were used to obtain the arterial concentrations of carbon dioxide and oxygen respectively, where the arterial blood compartment was directly linked to the atmosphere through the lung model and through linearised CO_2 and O_2 dissocation curves. As from the development of the lung gas exchange model, however, P_{ACO_2} and P_{AO_2} are calculated from equations 8.21 and 8.22 (chapter 8) respectively. C_{aCO_2} and C_{aO_2} can now be calculated directly from P_{ACO_2} and P_{AO_2} using the more accurate CO_2 dissociation curve.

The present complex model which exhibits breathing has been developed through step by step complexification of the simpler model from chapter 5 onwards. It is timely that the assumptions and features of the present model be stated explicitly.

ASSUMPTIONS:

1. The partial pressures of oxygen and of carbon dioxide in the alveoli, are equal to the corresponding partial pressures of these gases in arterial blood at all times, (Grodins et al, 1967):

$$P_{ACO_2} = P_{aCO_2} \text{ and } P_{AO_2} = P_{aO_2}$$

2. The volume of the dead space compartment is fixed at all times and does not change with the cyclic changes in lung volume due to inspiration and expiration.

3. The respiratory frequency, i.e. the number of breaths per unit time is a linear function of the total ventilation (Grodins and James, 1963) giving:

$$f = K_1 + K_2 * \dot{V}$$

Figure 9.2 shows the experimental results of Milhorn and Brown (1973) and mean calculated for use in this model.

4. The tidal volume is a direct function of total ventilation and frequency of breathing such that:

$$V_{TV} = \dot{V}/f \text{ at all times}$$

5. The CO_2 dissociation curve is same for arterial and venous blood and all the tissue compartments.

6. Instant mixing of gas takes place in the dead space compartment during inspiration as well as expiration.

7. The lung as well as all the tissues are perfect gas exchangers and in the lungs the ratio of ventilation to perfusion is unity, i.e., all the cardiac output passes through the gases in the lungs and is perfused by them.

8. The partial pressures of gases in the tissue compartment are equal to the partial pressures of corresponding gases in the venous blood, that is to say

$$P_{vT} = P_T \quad \text{at all times.}$$

9. The volumes of the passages through which the blood flows are constant on the arterial as well as the venous side at all times.

FEATURES OF THE MODEL:

1. Dissociation curves of carbon dioxide are developed through curve fitting to the experimental data and the effect of changes in partial pressure oxygen is taken into account.

2. Ventilation is a cyclic process of alternative inspiration and expiration and the lung volume under-goes changes accordingly. At any instant in time, however, the partial pressure in the alveolar compartment is given by the volumetric fraction of the gas in the alveoli divided by the alveolar volume.

3. Due to changes in alveolar partial pressures with the cyclic process of respiration, the arterial blood concentrations of gases are no longer fixed, instead C_{aCO_2} and C_{aO_2} are oscillating with the respiratory cycle. These oscillations of gas concentration in arterial blood are of prime importance because during inspiration of carbon dioxide gas mixtures these oscillations get smaller although the mean rises, whereas during exercise the mean arterial values may remain unchanged but the peak to peak oscillations increase.

4. The output of the chemoreceptors is a function of the total ventilation. The latter is slightly larger than the actual ventilation, due to the pressure of the dead space.

5. The cardiac output as well as cerebral blood flow rates are functions of partial pressures of oxygen and carbon dioxide in the arterial blood. (Grodins et al, 1967).

6. The circulation delays are variable, depending upon the blood flow rates to various compartments and are different for the same tissues on the arterial and venous sides. (Grodins et al, 1967).

7. For the sake of simplicity the process of respiration is assumed to be sinusoidal with a slight positive constant offset due to alveolar-blood gas exchange which is a continuous process.

8. The functional residual capacity is not fixed but changes with the size of the tidal volume. The residual volume is constant and the size of the tidal volume is limited to vital capacity (Figure 9.3).

9. Under normal resting conditions the ratio of blood flow to muscle tissues and the blood flow to other tissues is fixed, but during exercise the blood flow to muscle tissues greatly increases and so does the cardiac output.

Thus this model represents the real system more closely than any of the previous models. All the relevant compartments (dead space, alveoli, arterial blood, venous blood, brain tissues, muscle tissues) are represented in the model including the instantaneous variations in model variables due to respiratory cycle. This will enable the model to be tested for a wider range of experiments, including the effects of hypoxia (i.e. less than normal oxygen breathing) as well as exercise conditions (higher metabolic CO_2 production rate of muscle tissues) in addition to CO_2 breathing, hyperventilation and asphyxia (zero breathing).

9.1 FORMULATION OF EQUATIONS:

(i) Lung and Alveoli

$$f = K_1 + K_2 \dot{V} \qquad \ldots\ldots 9.1$$

$$V_{TV} = \dot{V}/f \qquad \ldots\ldots 9.2$$

$$V_r = (V_r)_o + \tfrac{1}{2}(V_{TV})_o - \frac{V_{TV}}{2} \qquad \ldots\ldots 9.3$$

where $(V_r)_o$ is the functional residual capacity and $(V_{TV})_o$ is the tidal volume at normal resting conditions.

Equation 9.3 describes the change in functional residual capacity with the changes in tidal volume (Figure 9.2). Thus the alveolar volume at any instant is given by:

$$V_A = V_o + \frac{V_{TV}}{2} (1 - \cos 2\pi ft) \quad \ldots\ldots 9.4$$

and rate of change of alveolar volume:

$$\dot{V}_A = 2\pi f . \frac{V_{TV}}{2} \sin 2\pi ft . \quad \ldots\ldots 9.5$$

Thus using feature no.2

$$F_{ACO_2} = V_{ACO_2} / V_A \quad \ldots\ldots 9.6$$

$$F_{AO_2} = V_{AO_2} / V_A \quad \ldots\ldots 9.7$$

and

$$P_{ACO_2} = 713.0 \; F_{ACO_2} \quad \text{(Dry Gas)} \quad \ldots\ldots 9.8$$

$$P_{AO_2} = 713. \; F_{AO_2} \quad \text{(Dry Gas)} \quad \ldots\ldots 9.9$$

(ii) Gas Dissociation Curves:

Grodins et al (1967) developed a CO_2 dissociation curve using experimental data as follows

$$C_{aCO_2} = 0.375 (0.2 - C_{aO_2}) + 0.547 + 0.6732 * 10^{-3} P_{aCO_2} - 0.62 \log_{10} \frac{C_{aCO_2} - 0.6732 * 10^{-3} . P_{aCO_2}}{0.01 P_{aCO_2} - 0.14} \quad \ldots\ldots 9.10$$

Since C_{aCO_2} appears on both sides of the equality sign in equation 9.10, this has to be solved as an implicit function of C_{aCO_2}. Figure 9.1 shows the dissociation curve for C_{aCO_2} for varying P_{O_2}.

A three piece linearised approximation for the oxygen dissociation curve has been retained (Produced by Longobardo et al,1966). That is

$$C_{aO_2} = K_3 P_{aO_2} + K_4 \qquad \ldots\ldots 9.11$$

where K_3 and K_4 take on 3 different values for various groups of values of C_{aO_2} as follows (Longobardo et al,1966).

$C_{aO_2} < 0.155$: $K_3 = 0.00388$, $K_4 = 0.0$

$0.155 \leq C_{aO_2} \leq 0.187$: $K_3 = 0.00107$, $K_4 = 0.1123$

$C_{aO_2} > 0.187$: $K_3 = 0.0001625$, $K_4 = 0.1756$

In equations 9.10 and 9.11 it is assumed that alveolar gas and arterial blood partial pressures of oxygen and carbon dioxide are equal at all times, i.e.:

$$P_{ACO_2} = P_{aCO_2} \text{ and } P_{AO_2} = P_{aO_2}$$

Thus C_{aCO_2} and C_{aO_2} are directly calculated from the alveolar partial pressures of corresponding gas and using equations 9.10 and 9.11 respectively.

(iii) Circulation System

Cardiac Flow Control

$$\dot{q} = \dot{q}_N + \Delta\dot{q}_{CO_2} + \Delta\dot{q}_{O_2} \qquad \ldots\ldots 9.12$$

where $\dot{q}_N$ is 5.6 litre/min.

$$\Delta\dot{q}_{CO_2} = 0.3\,(P_{aCO_2} - 40.0) \text{ for } 40.0 < P_{aCO_2} < 60.0$$

$$= 0.0 \text{ for all other } P_{aCO_2} \qquad \ldots\ldots 9.13$$

$$\Delta \dot{q}_{O_2} = 9.6551 - 0.2885\, P_{aO_2} + 2.9241 * 10^{-3} (P_{aO_2})^2$$
$$-1.033 * 10^{-6} (P_{aO_2})^4 \text{ for } P_{aO_2} < 104.0 \quad \ldots\ldots 9.14$$
$$= 0.0 \text{ for } P_{aO_2} > 104.0$$

Cerebral Blood Flow Control

$$\dot{q}_B = \dot{q}_{BN} + \Delta \dot{q}_{BCO_2} + \dot{q}_{BO_2} \quad \ldots\ldots 9.15$$

where $\dot{q}_{BN} = 0.748$ ℓ/min.

$$\Delta \dot{q}_{BO_2} = 2.785 - 0.1323\, P_{aO_2} + 2.6033 * 10^{-3} (P_{aO_2})^2$$
$$-2.324\, 10^{-5} (P_{ao_2})^3 + 7.6553 * 10^{-8} (P_{aO_2})^4 \quad \ldots\ldots 9.16$$
$$\text{for } P_{aO_2} < 104.0$$
$$= 0.0 \quad \text{for } P_{aO_2} > 104.0$$

$$\dot{q}_{BCO_2} = 2.323 * 10^{-2} - 3.1073 * 10^{-2} P_{aCO_2} + 8.0163 * 10^{-3} (P_{aCO_2})^2$$
$$\text{for } P_{aCO_2} < 38.0 \quad \ldots\ldots 9.17$$
$$= 0.0 \text{ for } 38.0 < P_{aCO_2} < 44.0$$
$$= 15.58 + 0.7607\, P_{aCO_2} - 1.2947 * 10^{-2} (P_{aCO_2})^2$$
$$+ 9.3981 * 10^{-5} (P_{aCO_2})^3 - 2{,}1748 * 10^{-7} (P_{aCO_2})^4$$
$$\text{for } P_{aCO_2} > 44.0$$

The above equations 9.11 to 9.17 were developed after Grodins et al, (1967).

Calculation of Time delays: (Fig. 9.4)

The variable time delays are calculated assuming the volume through which the blood flows to be constant and the time delays are inversely proportional to flow rate through the fixed volume.

The volumes of various flow passages are taken from Grodins et al, (1967).

Thus the governing equation for the calculation of time delay is:

$$\tau = \frac{\text{Volume}}{\text{Flow Rate}}$$

at any instant, assuming the volume to be fixed

$$\tau_{LB} = \frac{1.062}{\dot{q}} + \frac{0.015}{\dot{q}_B} \qquad \ldots\ldots 9.18$$

$$\tau_{L-OT} = \frac{1.062}{\dot{q}} + \frac{0.3675}{\dot{q}_{OT}} \qquad \ldots\ldots 9.19$$

$$\tau_{L-m} = \frac{1.062}{\dot{q}} + \frac{0.3675}{\dot{q}_m} \qquad \ldots\ldots 9.20$$

$$\tau_{B-L} = \frac{0.06}{\dot{q}_B} + \frac{0.188}{\dot{q}} \qquad \ldots\ldots 9.21$$

$$\tau_{OT-L} = \frac{1.457}{\dot{q}_{OT}} + \frac{0.188}{\dot{q}} \qquad \ldots\ldots 9.22$$

$$\tau_{m-L} = \frac{1.457}{\dot{q}_m} + \frac{0.188}{\dot{q}} \qquad \ldots\ldots 9.23$$

Tissue Compartmental Equations:

$$\dot{q}_m = 0.16\,(\dot{q} - \dot{q}_B) \qquad \ldots\ldots 9.24$$

$$\dot{q}_{OT} = \dot{q} - (\dot{q}_B + \dot{q}_m) \qquad \ldots\ldots 9.25$$

$$\frac{d}{dt} C_{BCO_2} = (\dot{M}_{BCO_2} + \dot{q}_B\,(C_{aCO_2}(\tau_{LB}) - C_{BCO_2}))/g_B \qquad \ldots\ldots 9.26$$

$$\frac{d}{dt} C_{mCO_2} = (\dot{M}_{mCO_2} + \dot{q}_m\,(C_{aCO_2}(\tau_{Lm}) - C_{mCO_2}))/g_m \qquad \ldots\ldots 9.27$$

$$\frac{d}{dt} C_{OTCO_2} = (\dot{M}_{OTCO_2} + \dot{q}_{OT}(C_{aCO_2}(\tau_{LOT}) - C_{OTCO_2}))/g_{OT} \qquad \ldots\ldots 9.28$$

$$\frac{d}{dt} C_{BO_2} = (-\dot{U}_{BO_2} + \dot{q}_B\,(C_{aO_2}\,(\tau_{LB}) - C_{BO_2}))/g_B \qquad \ldots\ldots 9.29$$

$$\frac{d}{dt} C_{mO_2} = (-\dot{U}_{mO_2} + \dot{q}_m (C_{aO_2} (\tau_{Lm}) - C_{mO_2}))/g_B \quad \ldots\ldots 9.30$$

$$\frac{d}{dt} C_{OTO_2} = (-\dot{U}_{OTO_2} + \dot{q}_{OT} (C_{aO_2} (\tau_{LOT}) - C_{OTO_2}))/g_{OT} \quad \ldots\ldots 9.31$$

$$C_{vCO_2} = \frac{\dot{q}_B C_{BCO_2} (\tau_{BL}) + \dot{q}_m C_{mCO_2} (\tau_{mL}) + \dot{q}_{OT} C_{OTCO_2} (\tau_{OT-L})}{\dot{q}} \quad \ldots\ldots 9.32$$

$$D_{O_2} = \dot{q} (C_{aO_2} - C_{vO_2}) \quad \ldots\ldots 9.33$$

$$D_{CO_2} = \dot{q} (C_{vCO_2} - C_{aCO_2}) \quad \ldots\ldots 9.34$$

$$\dot{V}_{AC} = 2 \pi f \frac{V_{TV}}{2} \sin 2 \pi ft + D_{O_2} - D_{CO_2} \quad \ldots\ldots 9.35$$

$\dot{V}_{AC}$ is positive i.e. during inspiration

$$\dot{F}_{DCO_2} = \dot{V}_{AC} (F_{oCO_2} - F_{DCO_2})/V_D \quad \ldots\ldots 9.36$$

$$\dot{F}_{DO_2} = \dot{V}_{AC} (F_{oO_2} - F_{DO_2})/V_D \quad \ldots\ldots 9.37$$

$$\dot{V}_{ACO_2} = \dot{V}_{AC} F_{DCO_2} + D_{CO_2} * \frac{863}{713} \quad \ldots\ldots 9.38$$

$$\dot{V}_{AO_2} = V_{AC} F_{DO_2} - D_{O_2} * \frac{863}{713} \quad \ldots\ldots 9.39$$

$\dot{V}_{AC}$ is negative i.e. during expiration

$$\dot{F}_{DCO_2} = \dot{V}_{AC} (F_{DCO_2} - F_{ACO_2})/V_D \quad \ldots\ldots 9.40$$

$$\dot{F}_{DO_2} = \dot{V}_{AC} (F_{DO_2} - F_{AO_2})/V_D \quad \ldots\ldots 9.41$$

$$\dot{V}_{ACO_2} = \dot{V}_{AC} F_{ACO_2} + D_{CO_2} \quad \ldots\ldots 9.42$$

$$\dot{V}_{AO_2} = \dot{V}_{AC} F_{AO_2} - D_{O_2} \quad \ldots\ldots 9.43$$

The model is shown in Fig. 9.5.

The equations 9.1 to 9.43 are simulated on a CDC computer using FORTRAN.

9.2 RESULTS AND DISCUSSIONS

Most of the test results on this model are very similar to those of model III (chapter 7) except for the oscillations of arterial CO_2 and O_2 concentrations with the breathing cycle i.e. the instantaneous values of the respiratory system variables were achieved rather than their mean. However, there were some unique features of this complex model which are discussed here. The three disturbances applied to this model are as follows:

i. CO_2 input with various controller equations.

ii. Hypoxic input with the arterial controller equation.

iii. Exercise conditions developed by increased muscle tissue CO_2 production rate with various conditions of cardiac output.

i. CO_2 INPUT AND EXERCISE

Graph numbers 9.1A and 9.1B show the variation of actual breathing pattern (VDAC) with time for the step input of 5% CO_2 in the breathing air with brain tissue CO_2 controller equation. The step is applied at time equals 5 min. and removed at time equals 15 minutes. One very interesting feature apparent from these results is the sudden depression in the ventilation at the onset of the step input before the ventilation starts to rise again. Similarly at the removal of step there is an increase in the ventilation rate before the ventilation starts decreasing. This means that as soon as CO_2 is inhaled through the mouth, the concentration of CO_2 in the brain tissue is reduced. Similarly as soon as the CO_2 step is removed, the CO_2 concentration of brain tissue CO_2 is increased. Although

there is a lack of dynamic experimental data for such small intervals of time, the physiological view is that this is highly improbable in real life situation (Dr. K.B. Saunders-personal communication

Considering that it is unlikely to happen in real systems, the equations describing the system were re-examined. It is apparent that the CO_2 concentration in the brain tissue is highly dependent upon the blood flow rate into the brain tissue compartment (equation 9.26). But cardiac output and the blood flow rate to the brain is function of C_{aO_2} and C_{aCO_2}. Thus as soon as the CO_2 is inhaled both the quantities; cardiac output and blood flow rate to brain alter instantaneously as there is practically no time lag involved in the flow of CO_2 from mouth to the alveoli and from there to arterial blood. This immediately changes the CO_2 concentration in the blood flowing through the brain thus changing the concentration of CO_2 in the brain tissue compartment, which in turn instantaneously has a marked effect upon ventilation as exhibited in the graphs number 9.1A and 9.1B. Also as there is a time lag involved from the alveoli to the brain tissue the actual effect of increased CO_2 administration is delayed by a few seconds, (depending upon the variable time delays) which is about 30 seconds. To test this hypothesis an equivalent time delay, i.e. from alveoli to brain, was introduced in the change of blood flow rates to the brain tissue compartment after any change is sensed in the concentrations of CO_2 and O_2 in the arterial blood.

The model was again tested for the same input as before and the results are shown in graphs number 9.1C, 9.1D and 9.1E. It can be seen that the sudden depression and elevation of ventilation due to

the on-set and off-set of the step of 5% CO_2 is no longer present. Thus one can conclude that although there is physiological evidence to show that cardiac output and blood flow rates are affected by the change in arterial blood gas composition, there is a need for further experimentation to test the time lags involved in these changes.

The model was further tested for the effect of CO_2 input at the mouth on the arterial partial pressure of carbon dioxide (P_{aCO_2}). Graphs number 9.2A, 9.2B, 9.2C and 9.2D show the effect of 7% CO_2 input on P_{aCO_2}. The step change in CO_2 concentration in the breathing mixture was introduced at 5 min. and was removed at 25 min. It can be seen from graph 9.2A that the oscillations of P_{aCO_2} with breathing cycle are not present during the rise time of P_{aco_2} but after the transient is over, the mean level of P_{aCO_2} has risen to a higher new level but the peak to peak oscillation is reduced from about 3mm Hg to under 1mm Hg. This confirms in part the hypothesis introduced by Yamamoto et al (1963) which states that if CO_2 is administered through the mouth with the breathing mixture, the arterial partial pressure of CO_2 increases to a new higher mean level but the peak to peak oscillations are reduced, whereas if the CO_2 is increased from the tissue side, i.e. increased tissue CO_2 production (as in exercise) then little or no change occurs in the mean level of P_{aCO_2} (after the transients) but the size of oscillations with the breathing cycle. (i.e. the peak to peak oscillations) increase.

To test the second part of the above hypothesis under various conditions, the model was subjected to a sudden change in muscle tissue CO_2 production rates. For the sake of simplicity and also due to lack of experimental data available linear relationships were assumed for the first test. As in exercise the muscle tissue CO_2 production increases, so does the muscle tissue oxygen consumption and also the cardiac output increases. In the first instant the muscle tissue CO_2 production was doubled, along with doubled oxygen consumption and cardiac output. Graphs number 9.3A, 9.3B and 9.3C show the time variation of arterial carbon dioxide concentration. The CO_2 production of muscle tissue was doubled at time equals 5 min. and restored to normal at time equals 25 min., with corresponding changes in oxygen consumption rate of muscle tissue and cardiac output. It is apparent that the above hypothesis of Yamamoto is well substantiated. After the onset transients have died, which lasted for about 1.5 minutes, the mean C_{aCO_2} level is restored although the size of the oscillations is slightly increased. When the initial conditions are suddenly restored at time equals 25 min. the transients last for about 1.3 minutes. The graphs number 9.3E, 9.3F and 9.3G show the corresponding changes in the variation of ventilation with time. The interesting feature of the ventilatory response to exercise as apparent from these graphs, is that the durations of transients for on and off conditions are similar, as opposed to the ventilatory response to CO_2 inhalation where the on-transients are longer in time than off-transients.

To test the model further for exercise conditions, another test run was made where the metabolic output of muscle tissue and the oxygen consumption was increased to 4 times the normal but the cardiac output was changed only to the amount so as to meet the increased demand of the muscle tissue compartment, which was assumed to increase four times. The results of this test are shown in graphs number 9.4A through to 9.4G for the time response of arterial CO_2 concentration, and graph numbers 9.5A through to 9.5D for ventilatory time response.

Again it can be seen that the hypothesis of Yamamoto et al (1963) is well substantiated. Again for C_{aCO_2} the time duration of the on-transient is about 4.3 minutes whereas for the off-transient it is about 2 minutes. Similarly the on-transient for the ventilatory response is about 5 minutes whereas the off-transient lasts about 1.5 minutes. This pattern is similar to CO_2 inhalation ventilatory response which showed that the ventilatory on-transient time responses lasted longer for increased CO_2 inputs, with little change in the time duration of the off-transients.

Although at this stage the model fits well qualitatively with the medical evidence and physiological hypotheses (Yamamoto et al, 1963) some further dynamic data from real system tests are needed to compare the results of the model.

ii. HYPOXIC AND CO_2 INPUT ARTERIAL CONTROL

As discussed earlier (chapter 7) the brain tissue CO_2 controller was of no use to test hypoxic conditions because the oxygen levels are not represented in the controller equation.

Thus to test for oxygen variation in breathing mixtures arterial controllers had to be used. The problem in the use of the arterial controller was the breath to breath variation of arterial gas composition . As these quantities are now varying sinusoidally with the inhalation and expiration, the output of the controller equation will also be varying in similar fashion. To overcome this difficulty a second order filter was designed to remove any fluctuations in the P_{aCO_2} and P_{aO_2} before these quantities were fed into the controlling system.

The model was tested for 9% oxygen in the breathing mixture and results are shown in the graph number 9.6A through to 9.6D. Although the off-transients are qualitatively similar to experimental evidence (Milhorn and Brown,1973), the on-transients seem to be different. The response seems to be similar to a second order system response as opposed to first order as indicated by experimental evidence. This may well be due to the second order filter used in the controlling system to smooth out the breath to breath oscillations of P_{aCO_2} and P_{aO_2}. On the other hand this may be due to the oxygen being in the denominator of the controller equation thus producing second order effects.

To test the above discrepancy between the model response shape and the experimental results, this model was tested for CO_2 input (5%) with the same controlling system incorporating a second order filter. The results are shown in graph numbers 9.7A through to 9.7D. It can be seen that both on and off transients are similar in shape to the experimental evidence. Thus the inclusion of a second order filter does not seem to have any effect upon the shape of the response.

However as there is physiological evidence that the respiratory control includes some dynamic terms as well as tissue CO_2 and arterial P_{aO_2} control, it is not possible at this stage to go any further into the development of the model equations on the basis of currently available physiological data. Further as has been shown in the previous chapters, neither the tissue CO_2 controller nor the arterial controller is capable of simulating all the test results on the real system. The final controlling system must be a mixture of the two types of controls. As there is no physiological evidence and data available for developing a hypothesis and its testing on the model as regards to type and mode of controlling system, one can hypothesise by considering the results developed and discussed in this and previous chapters. A controller equation may be developed which includes both controlling actions, i.e. brain tissue CO_2 control as well as arterial C_{aCO_2} and C_{aO_2} control. Not only will the parameters of such an equation be difficult to estimate, but the structure of the controlling system will also have to be estimated.

The problems of identification and parameter estimation are briefly discussed in the next chapter and a composite controller equation is developed.

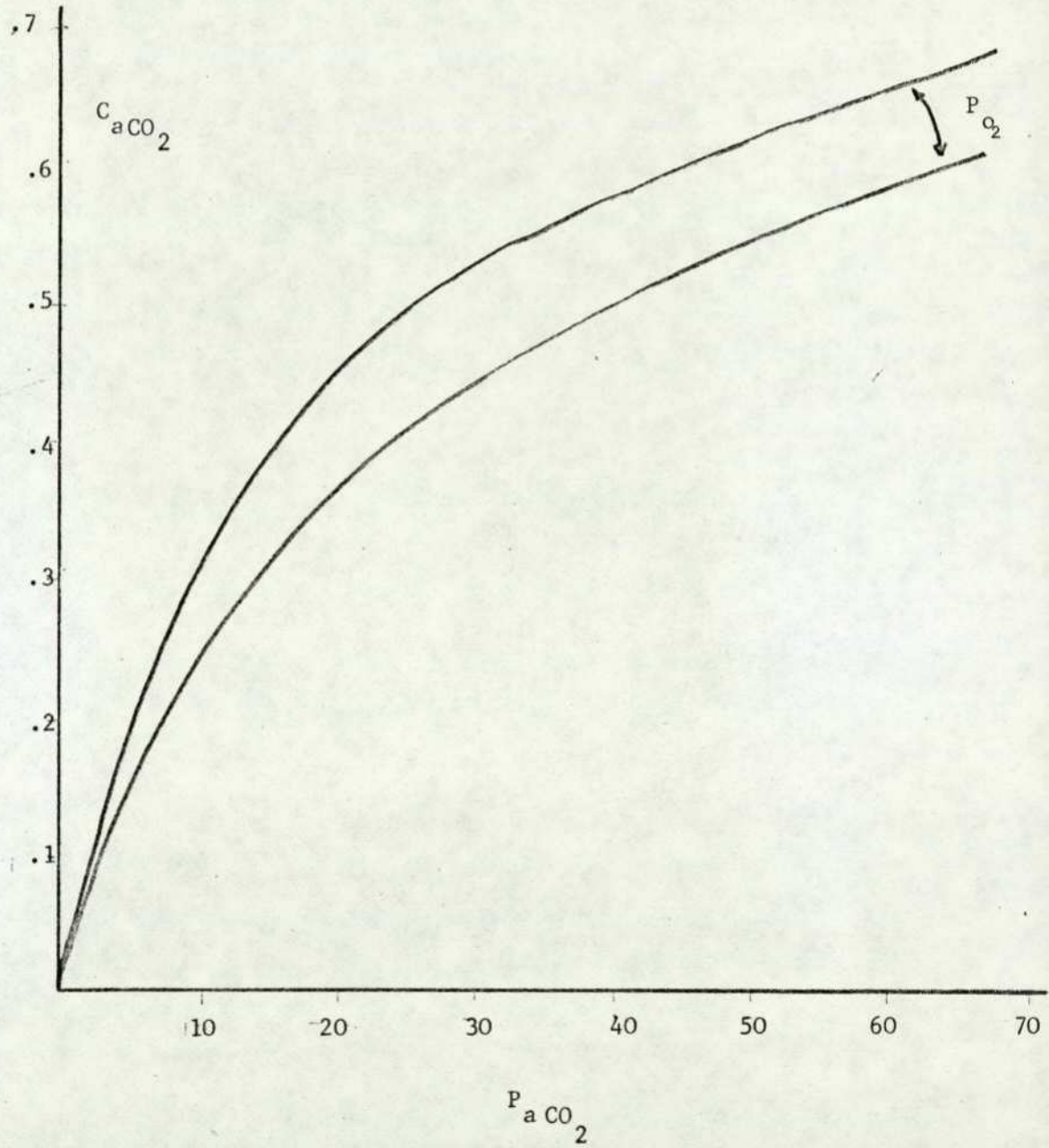

FIGURE 9.1

FIGURE 9.2

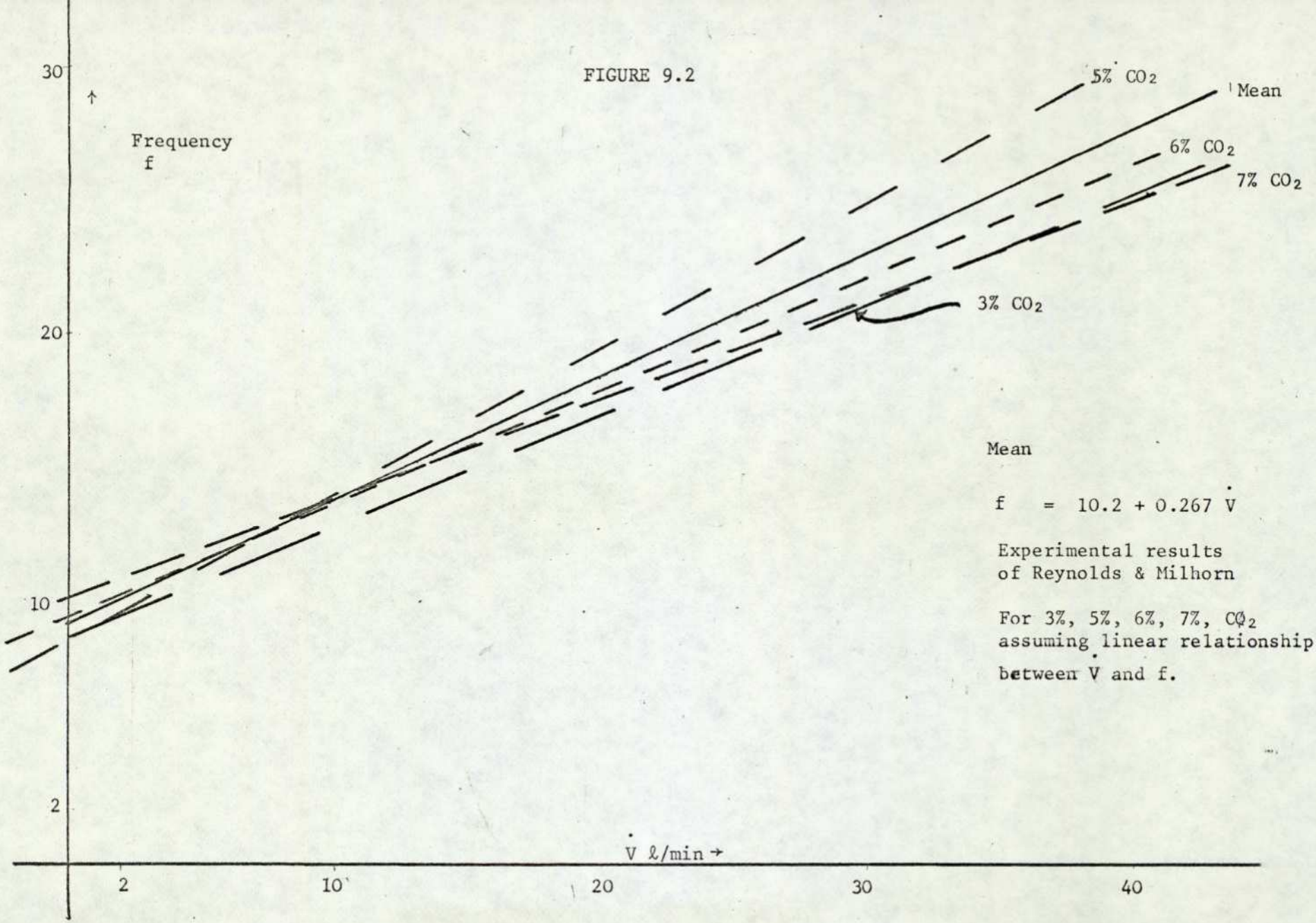
30
Frequency
f
20
10
2
5% CO_2
Mean
6% CO_2
7% CO_2
3% CO_2
Mean
$f = 10.2 + 0.267 \dot{V}$
Experimental results
of Reynolds & Milhorn
For 3%, 5%, 6%, 7%, $C\dot{Q}_2$
assuming linear relationship
between $\dot{V}$ and f.
$\dot{V}$ ℓ/min →
2
10
20
30
40

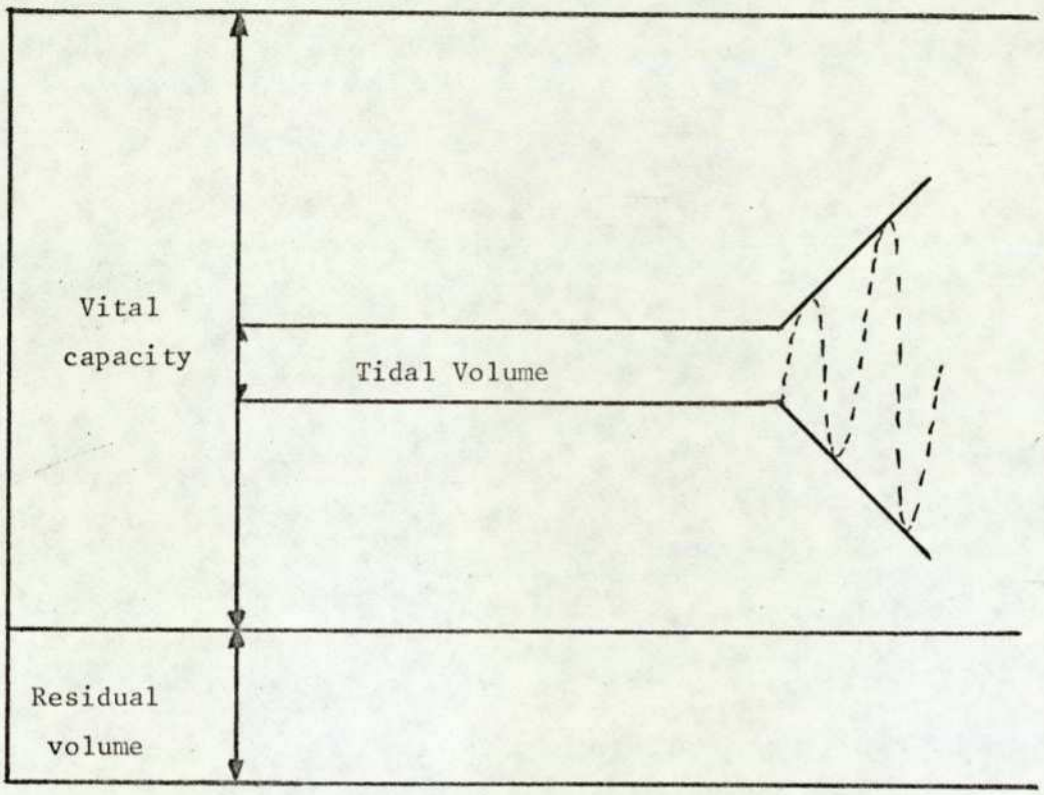

FIGURE 9.3

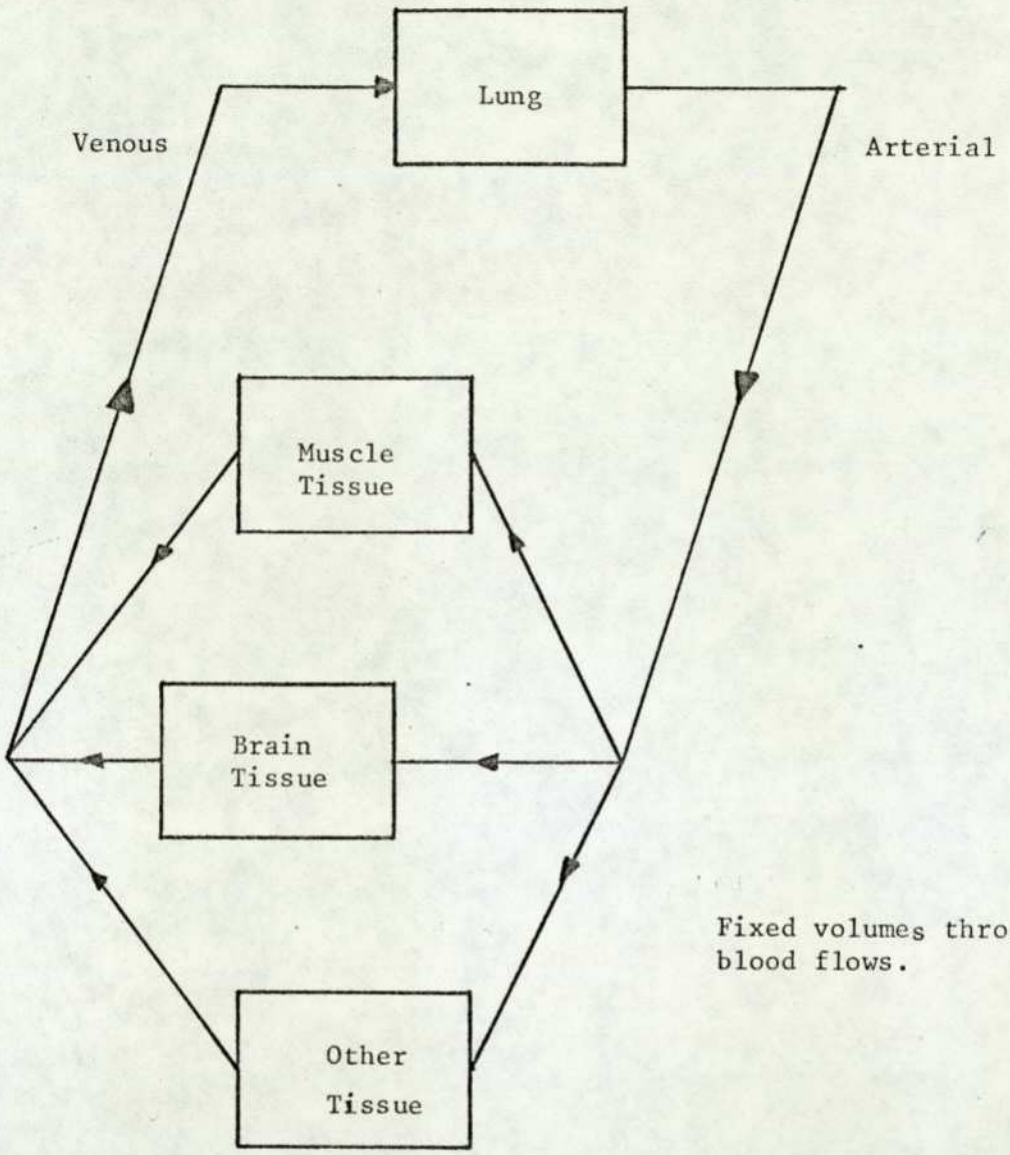
Lung
Venous
Arterial
Muscle Tissue
Brain Tissue
Other Tissue
Fixed volumes through which blood flows.

FIGURE 9.4

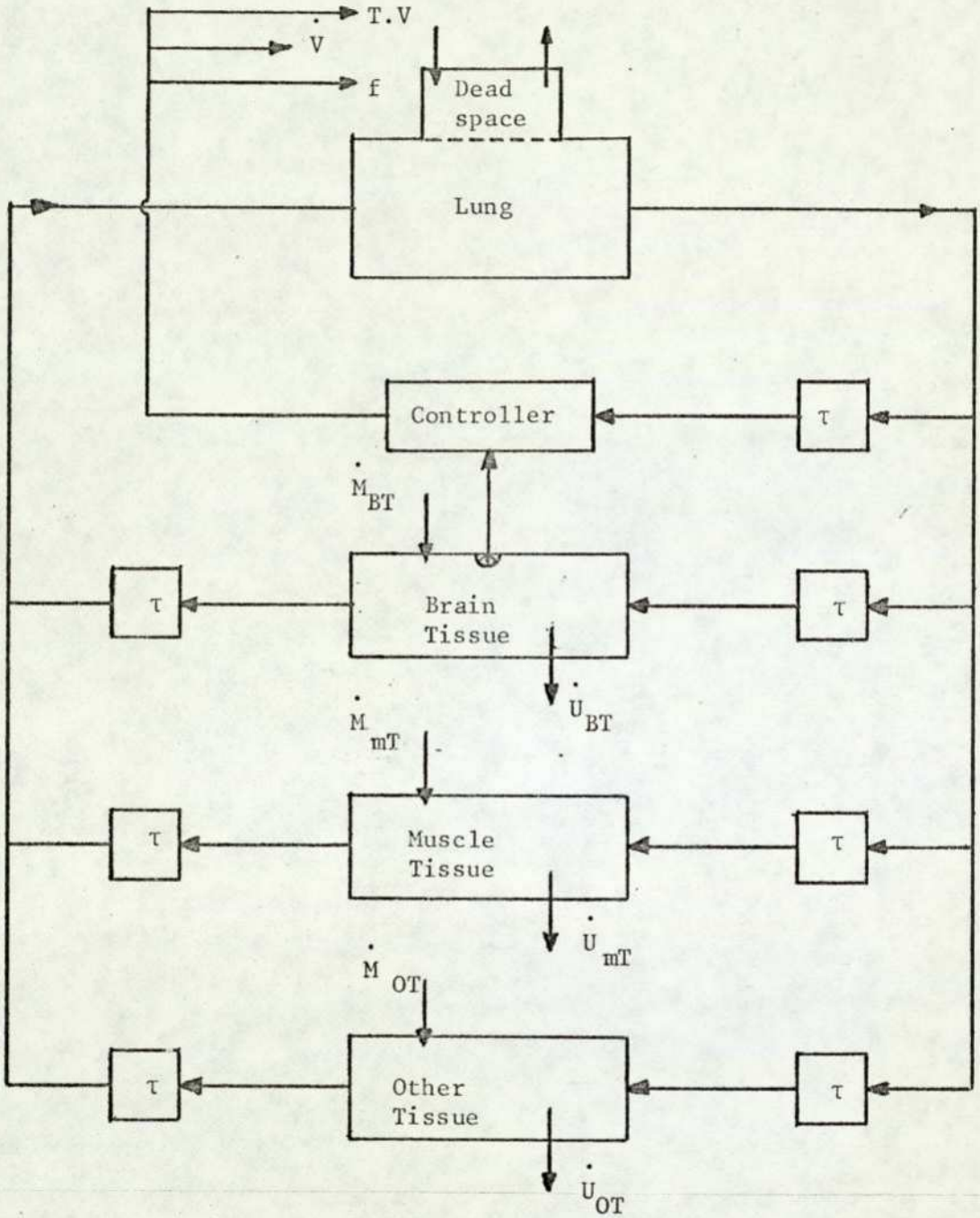
T.V
V
f
Dead space
Lung
Controller
τ
$\dot{M}_{BT}$
τ
Brain Tissue
τ
$\dot{U}_{BT}$
$\dot{M}_{mT}$
τ
Muscle Tissue
τ
$\dot{U}_{mT}$
$\dot{M}_{OT}$
τ
Other Tissue
τ
$\dot{U}_{OT}$

FIGURE 9.5

Graph 9.1A

5% CO_2

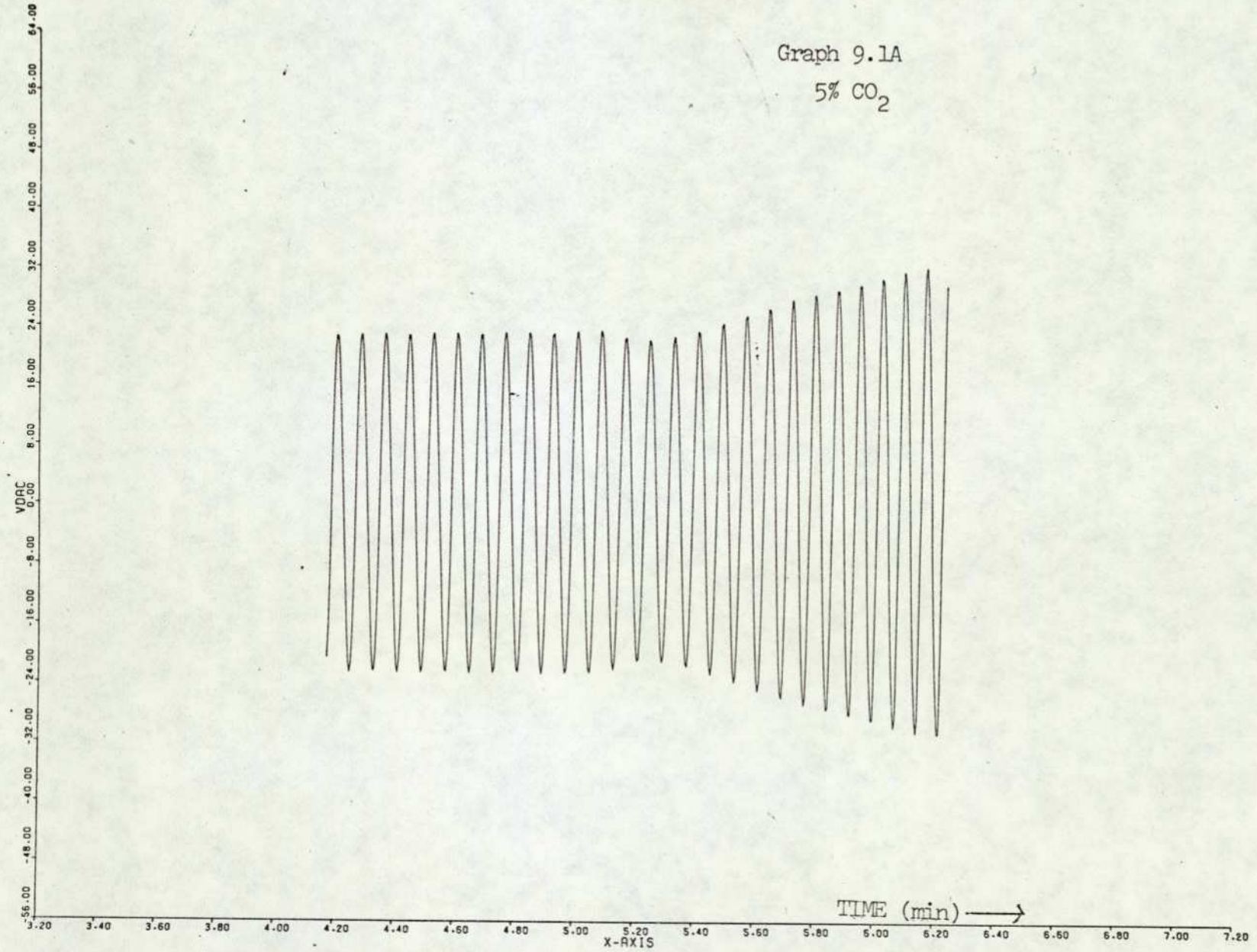

Graph 9.1B

5% CO_2

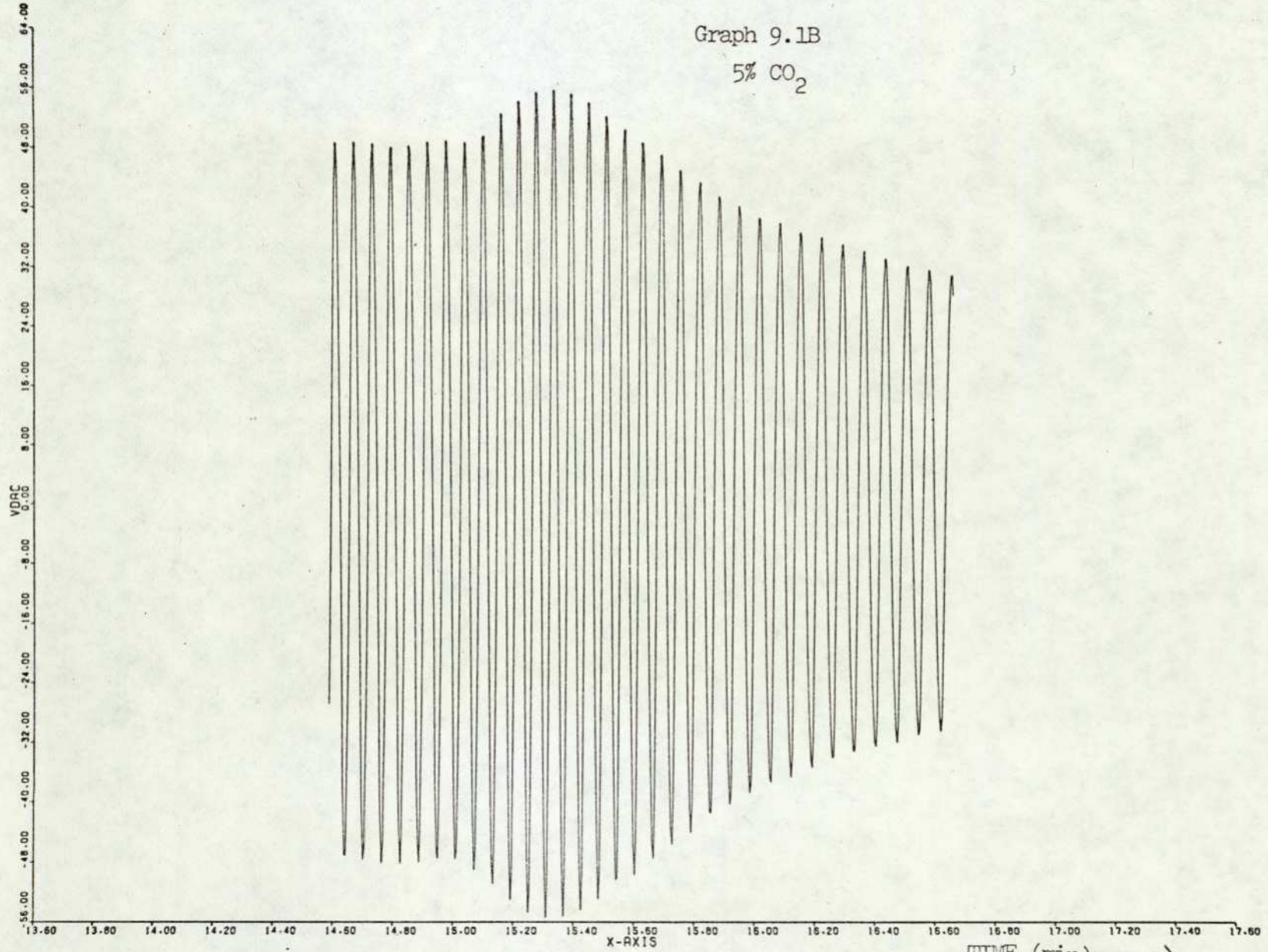

Graph 9.1 C

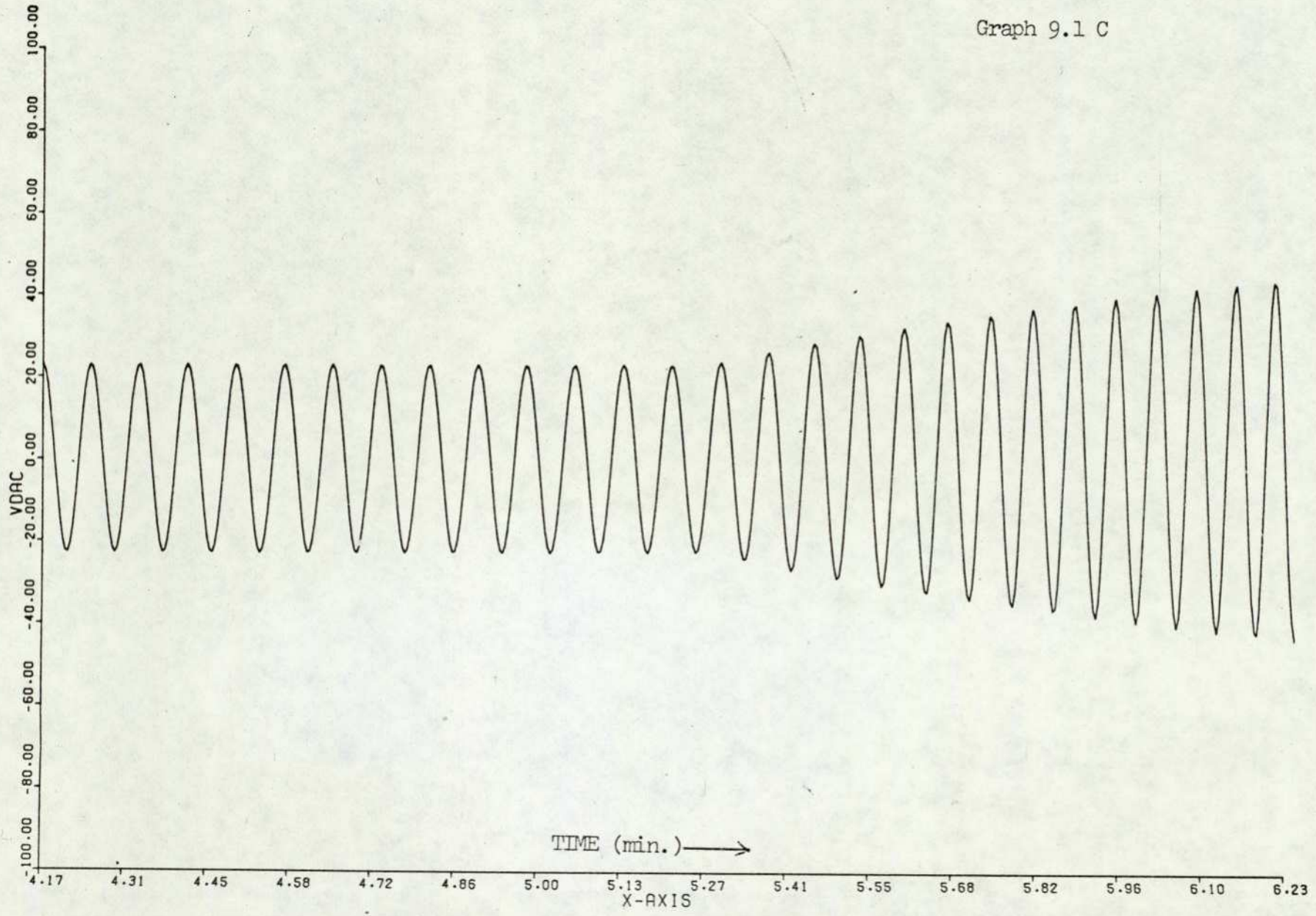
VDAC
100.00
80.00
60.00
40.00
20.00
0.00
-20.00
-40.00
-60.00
-80.00
-100.00
TIME (min.)
4.17
4.31
4.45
4.58
4.72
4.86
5.00
5.13
5.27
5.41
5.55
5.68
5.82
5.96
6.10
6.23
X-AXIS

Graph 9.1 D

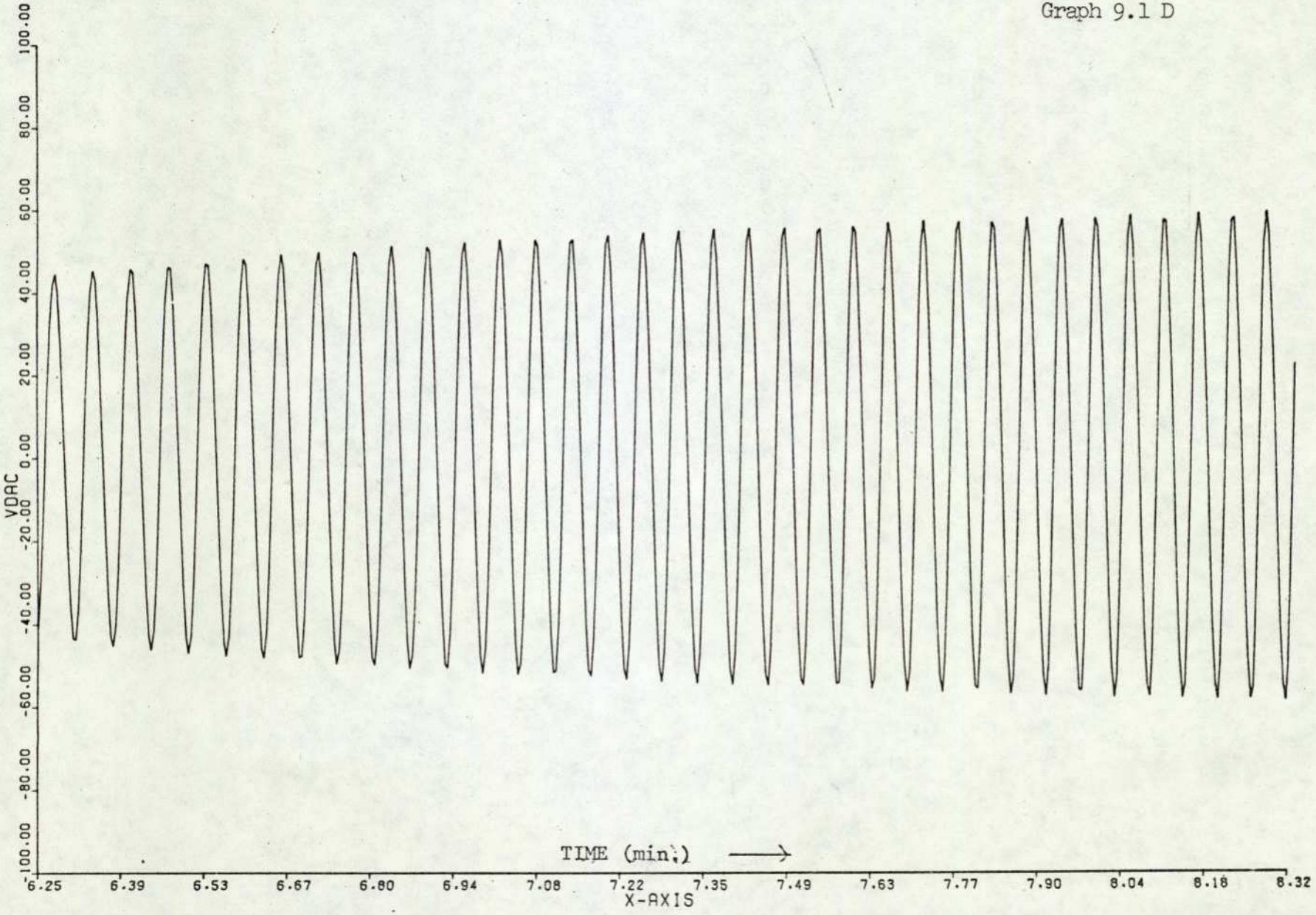
100.00
80.00
60.00
40.00
20.00
0.00
-20.00
-40.00
-60.00
-80.00
-100.00
VDAC
TIME (min.) ⟶
6.25
6.39
6.53
6.67
6.80
6.94
7.08
7.22
7.35
7.49
7.63
7.77
7.90
8.04
8.18
8.32
X-AXIS

Graph 9.1E

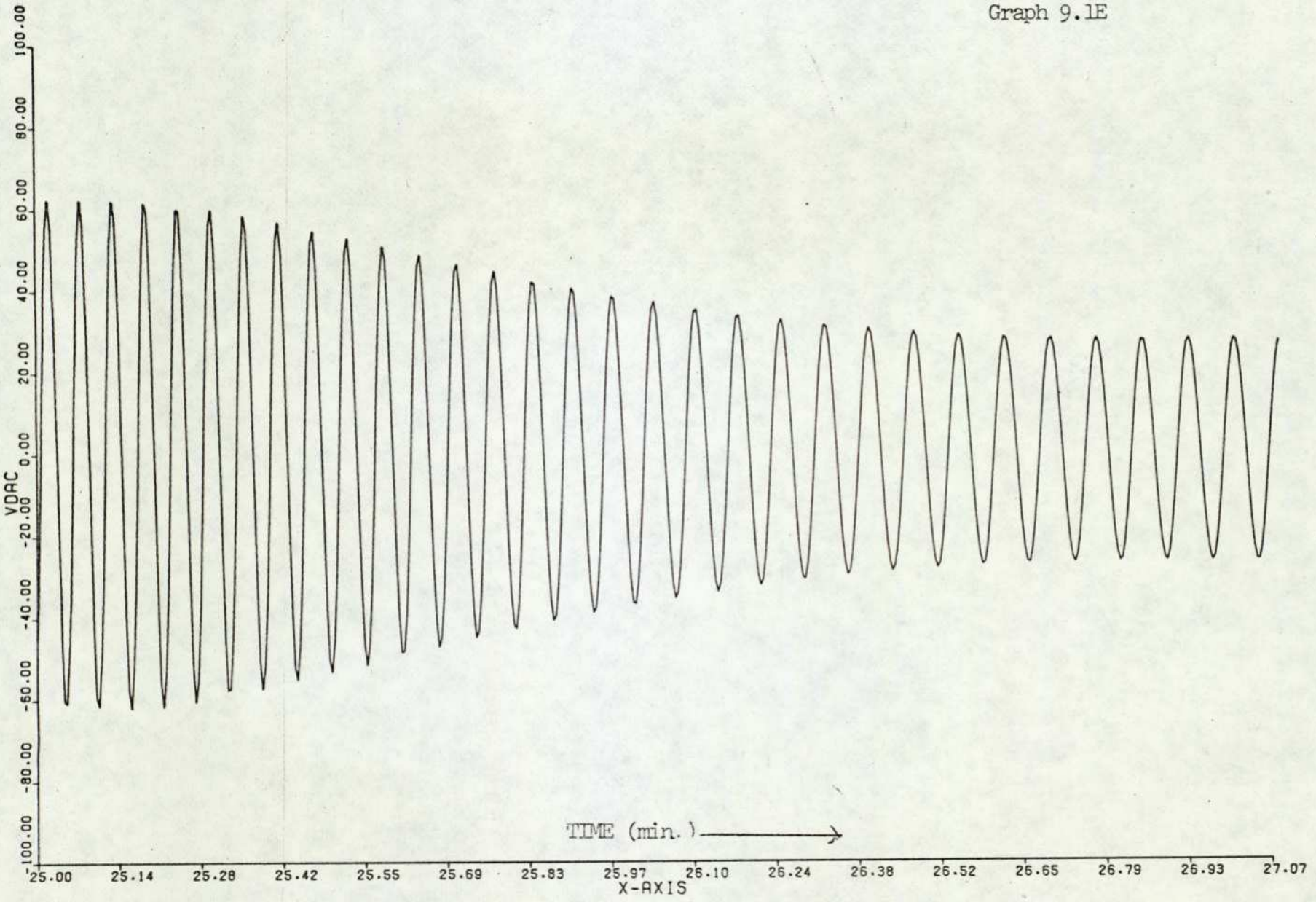
100.00
80.00
60.00
40.00
20.00
0.00
-20.00
-40.00
-60.00
-80.00
-100.00
VDAC
TIME (min.)
25.00
25.14
25.28
25.42
25.55
25.69
25.83
25.97
26.10
26.24
26.38
26.52
26.65
26.79
26.93
27.07
X-AXIS

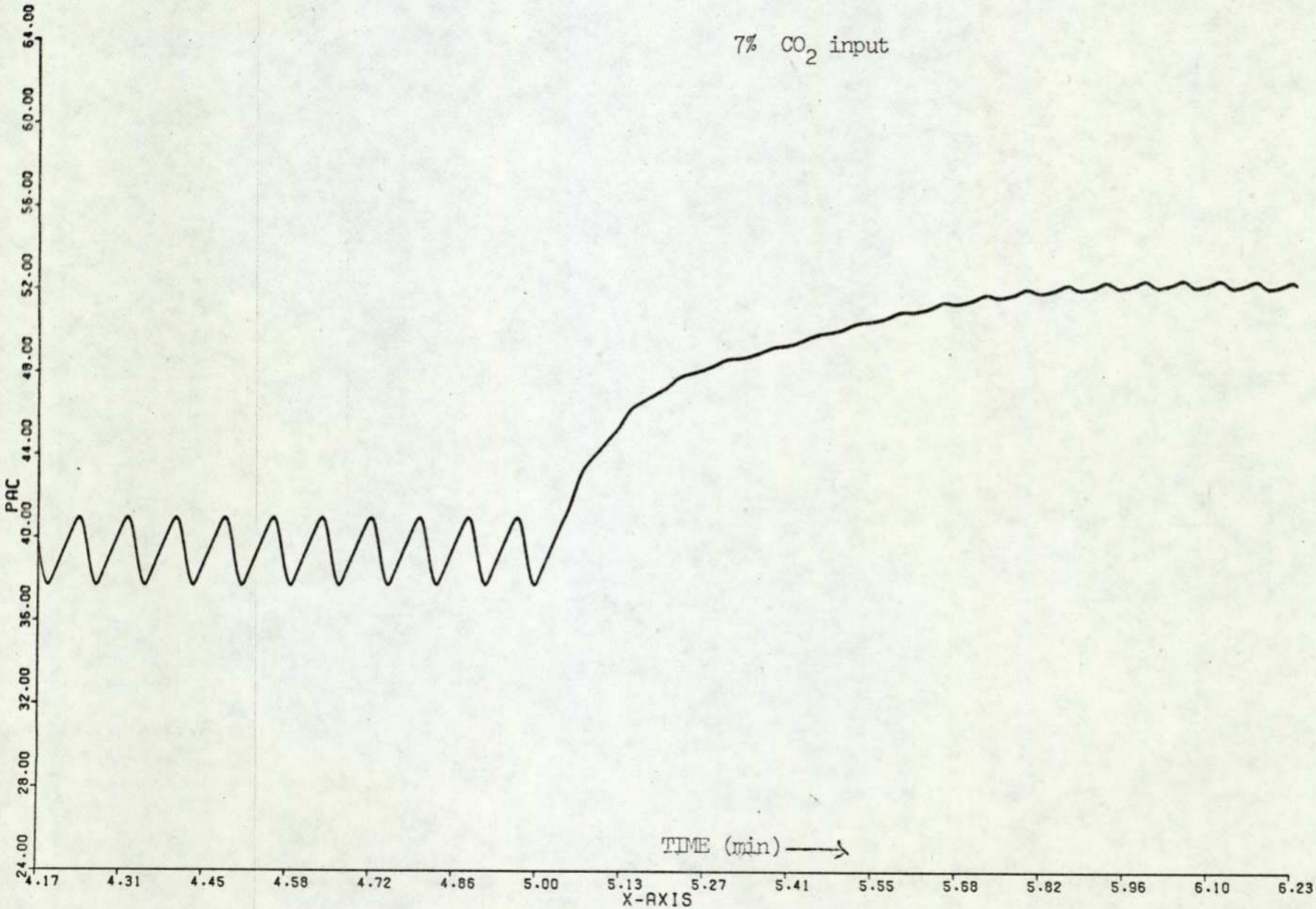
7% CO_2 input
PAC
64.00
60.00
56.00
52.00
48.00
44.00
40.00
36.00
32.00
28.00
24.00
TIME (min) ⟶
4.17
4.31
4.45
4.58
4.72
4.86
5.00
5.13
5.27
5.41
5.55
5.68
5.82
5.96
6.10
6.23
X-AXIS

Graph 9.2A

7% CO_2 input

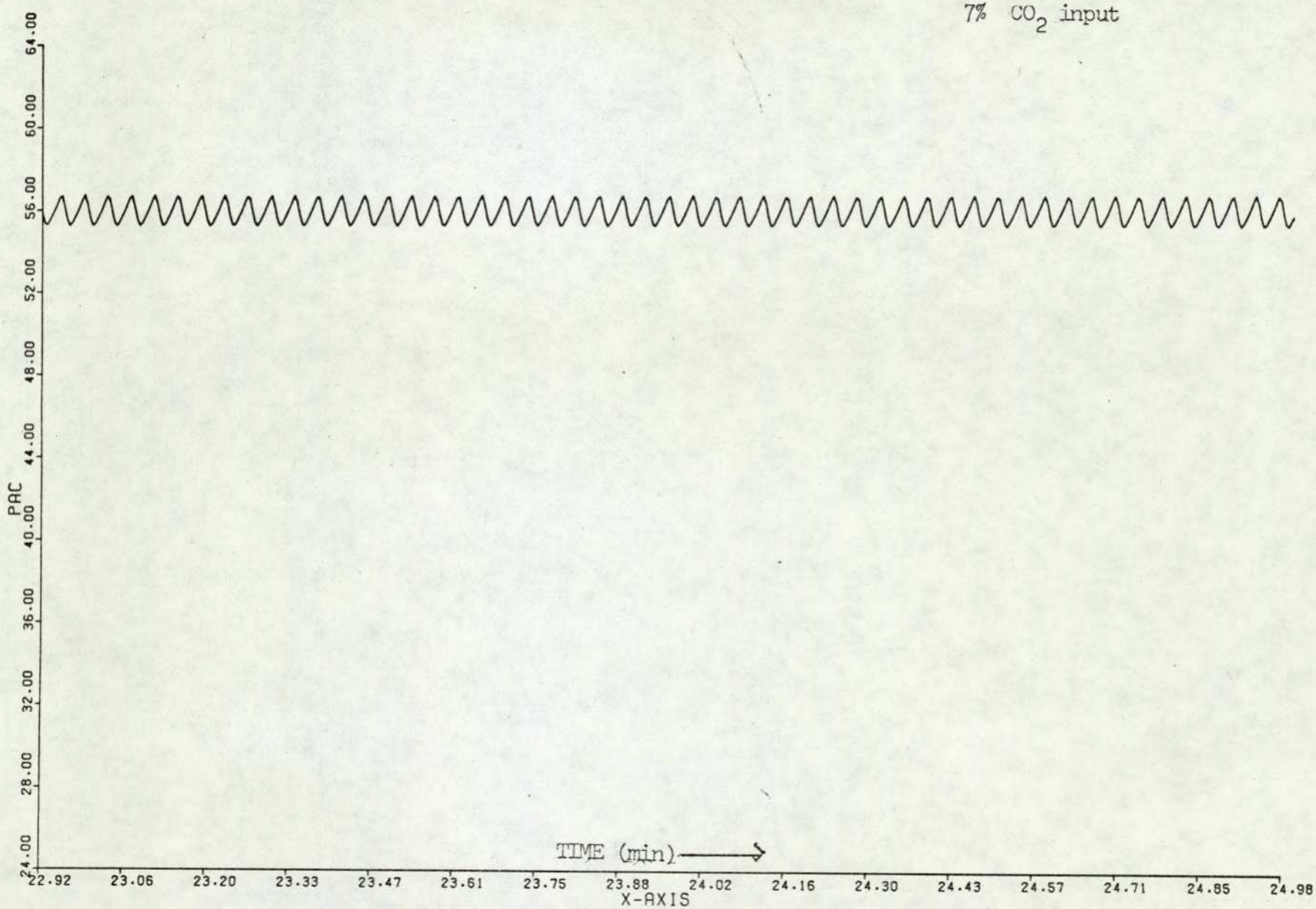

Graph 9.2.B

7% CO_2 input

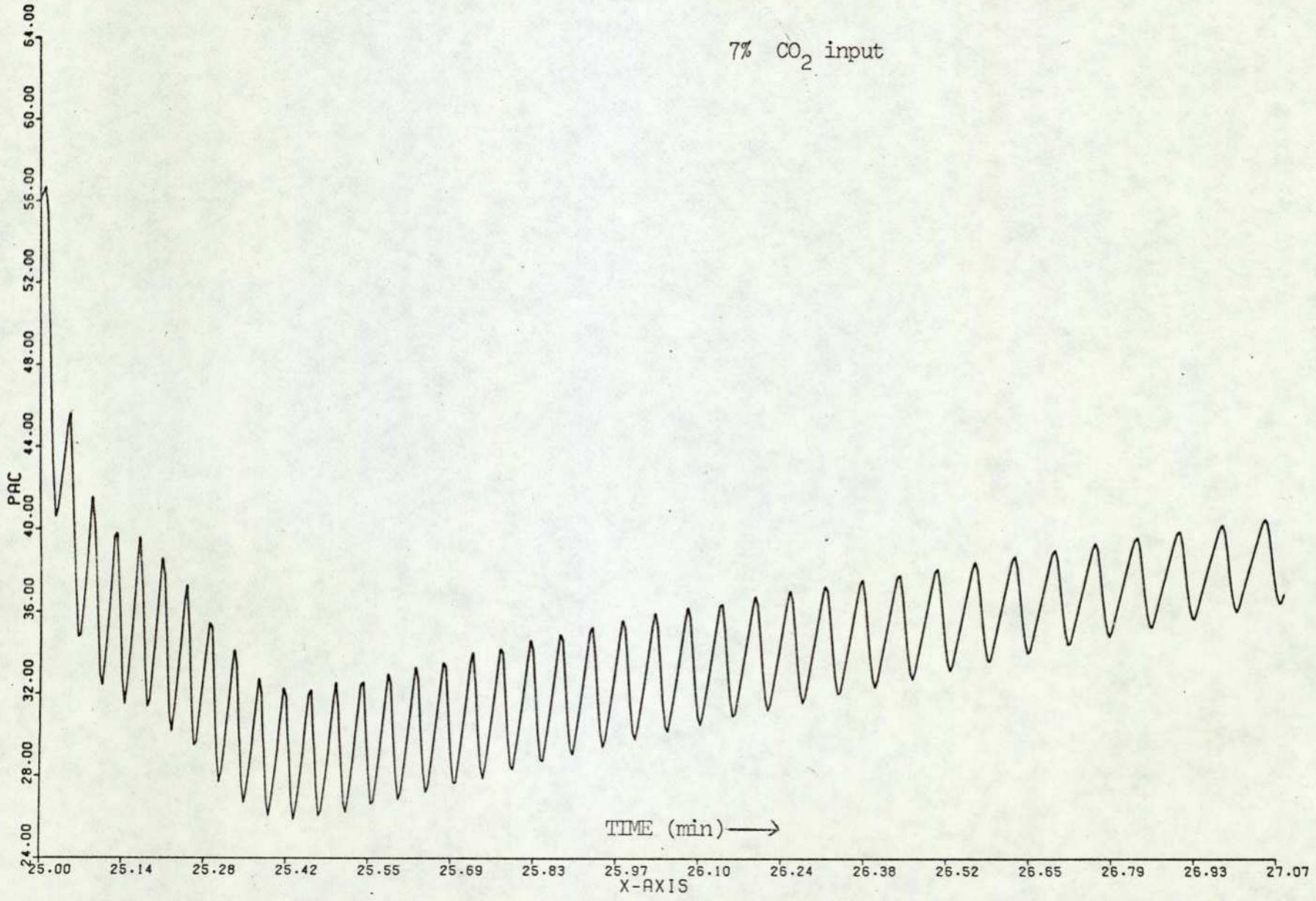

Graph 6.20

7% CO_2 input

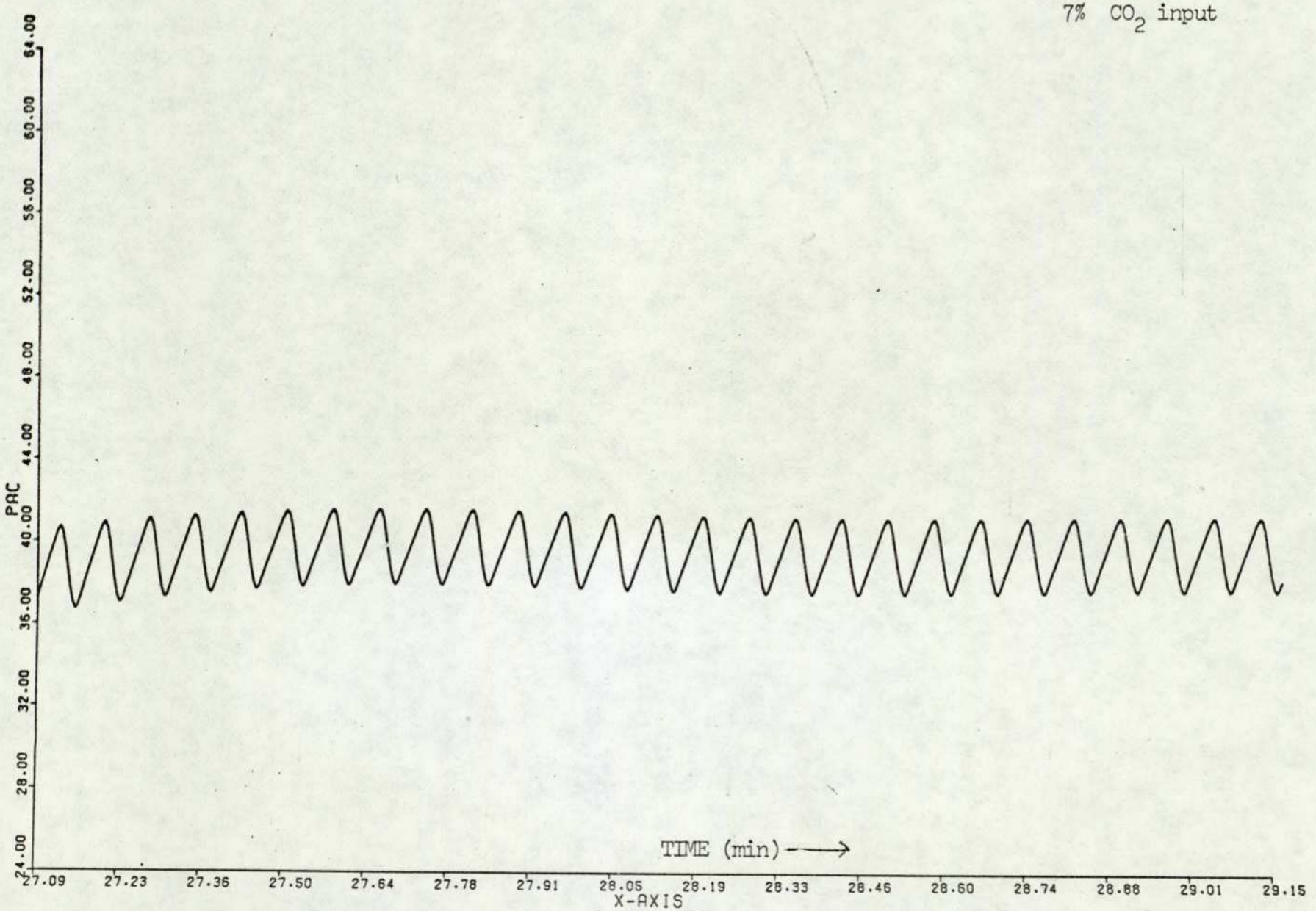

Graph 9.2D

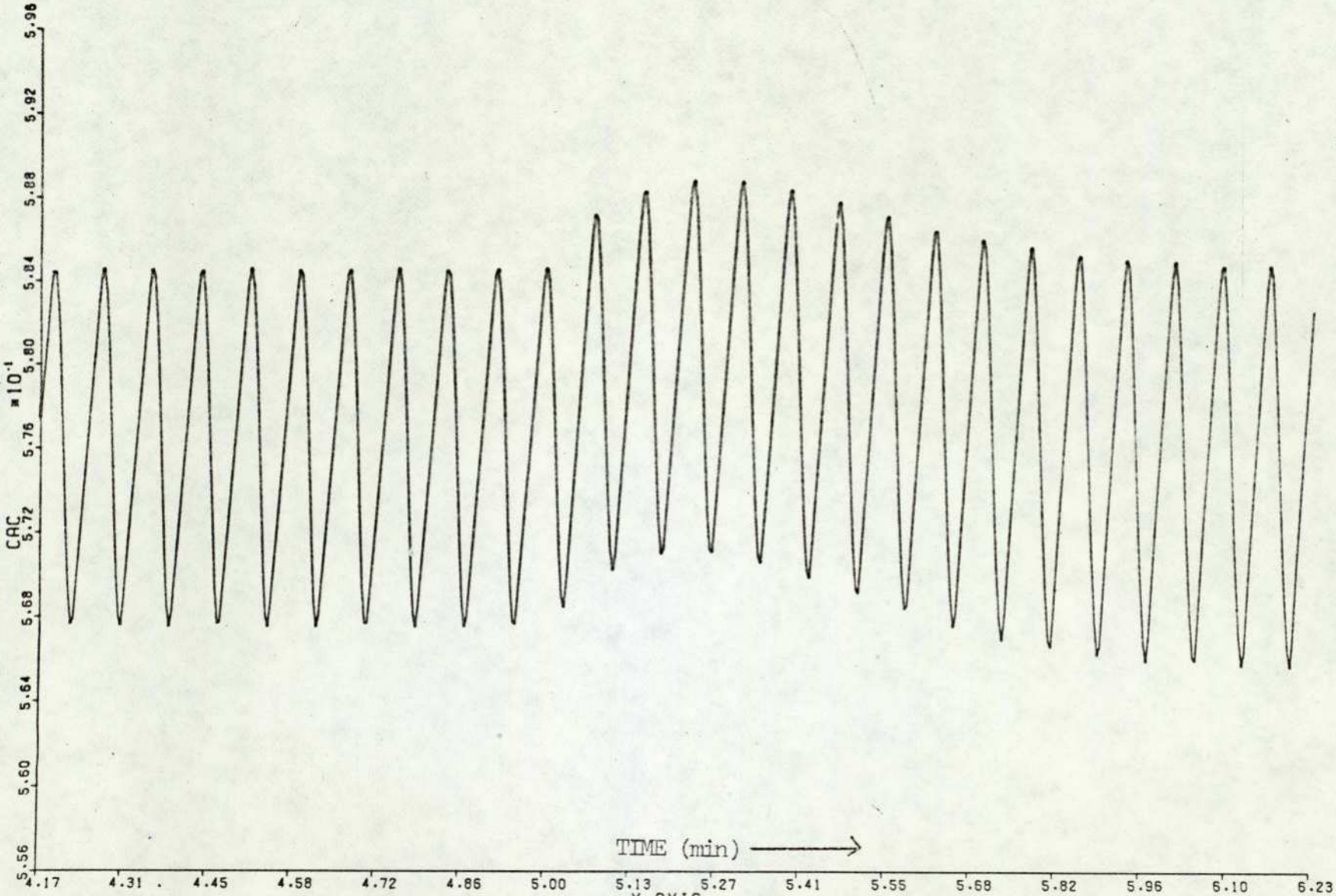
CAC
$\times 10^{-1}$
5.96
5.92
5.88
5.84
5.80
5.76
5.72
5.68
5.64
5.60
5.56
TIME (min) ⟶
4.17
4.31
4.45
4.58
4.72
4.86
5.00
5.13
5.27
5.41
5.55
5.68
5.82
5.96
6.10
6.23
X-AXIS

Graph 9.3A

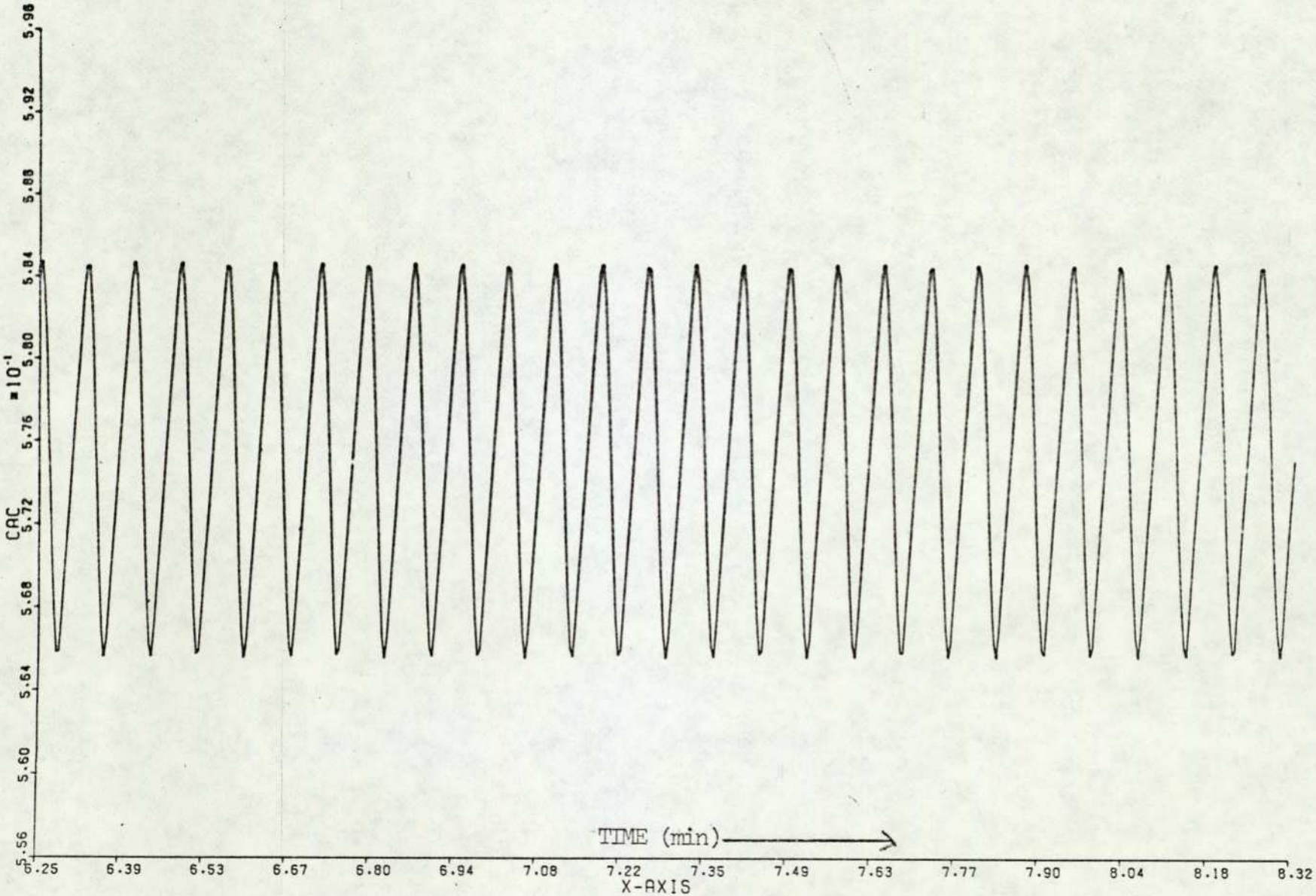
CAC
x10⁻¹
5.96
5.92
5.88
5.84
5.80
5.76
5.72
5.68
5.64
5.60
5.56
TIME (min)
6.25
6.39
6.53
6.67
6.80
6.94
7.08
7.22
7.35
7.49
7.63
7.77
7.90
8.04
8.18
8.32
X-AXIS

Graph 9.3B

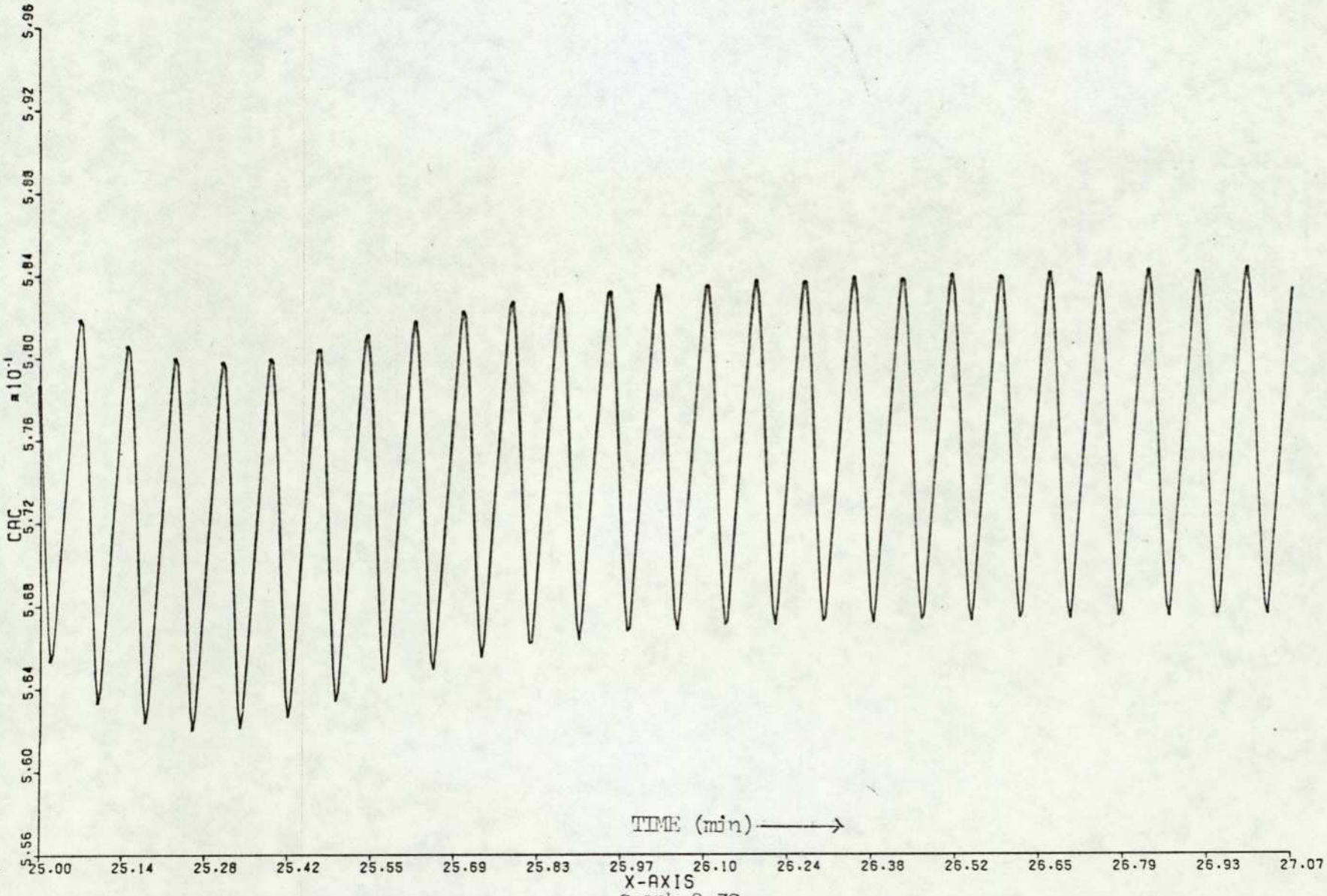
CAC
x10⁻¹
5.96
5.92
5.88
5.84
5.80
5.76
5.72
5.68
5.64
5.60
5.56
TIME (min) ⟶
25.00
25.14
25.28
25.42
25.55
25.69
25.83
25.97
26.10
26.24
26.38
26.52
26.65
26.79
26.93
27.07
X-AXIS

Graph 9.3C

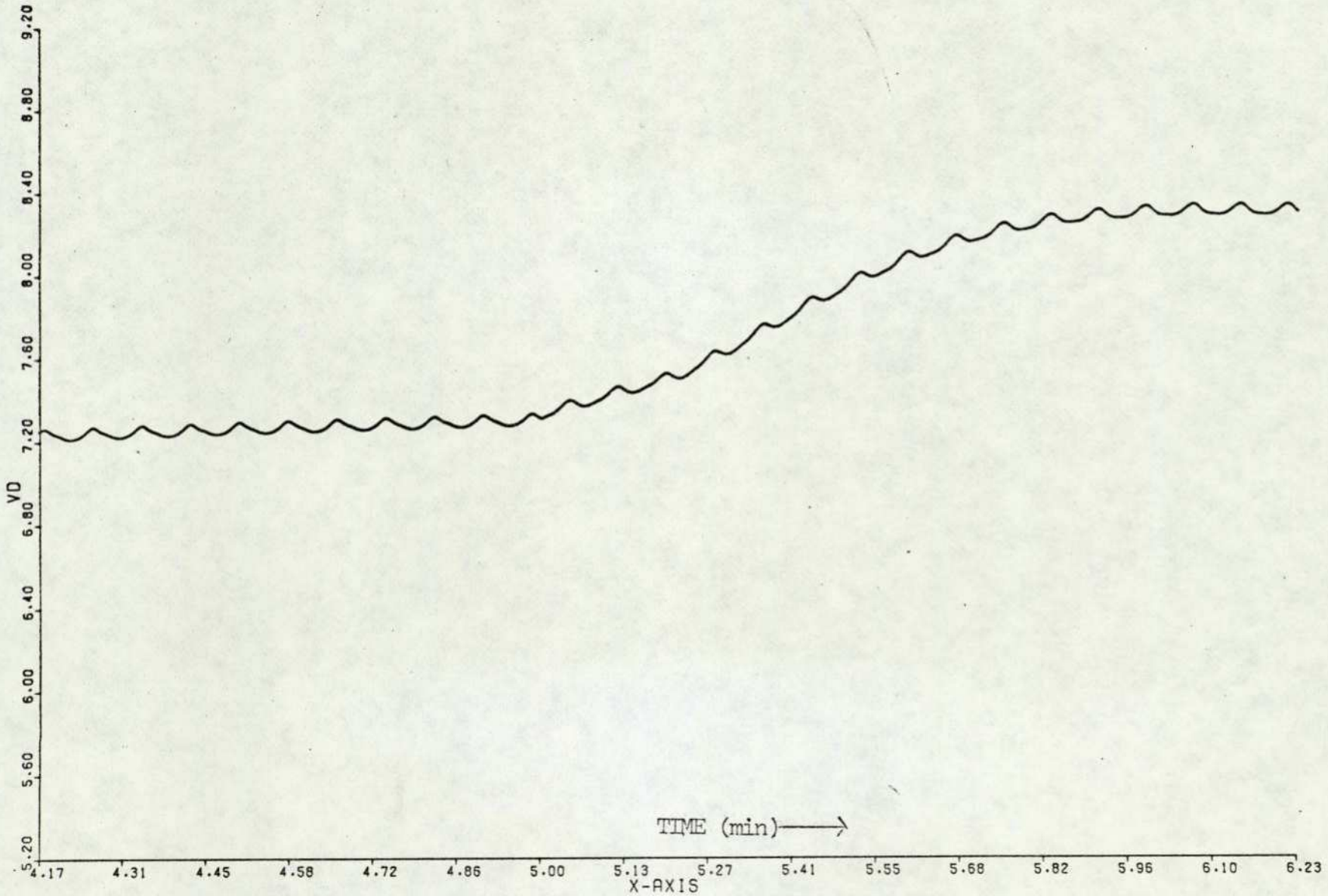
VD
9.20
8.80
8.40
8.00
7.60
7.20
6.80
6.40
6.00
5.60
5.20
TIME (min)
4.17
4.31
4.45
4.58
4.72
4.86
5.00
5.13
5.27
5.41
5.55
5.68
5.82
5.96
6.10
6.23
X-AXIS

Graph 9.3E

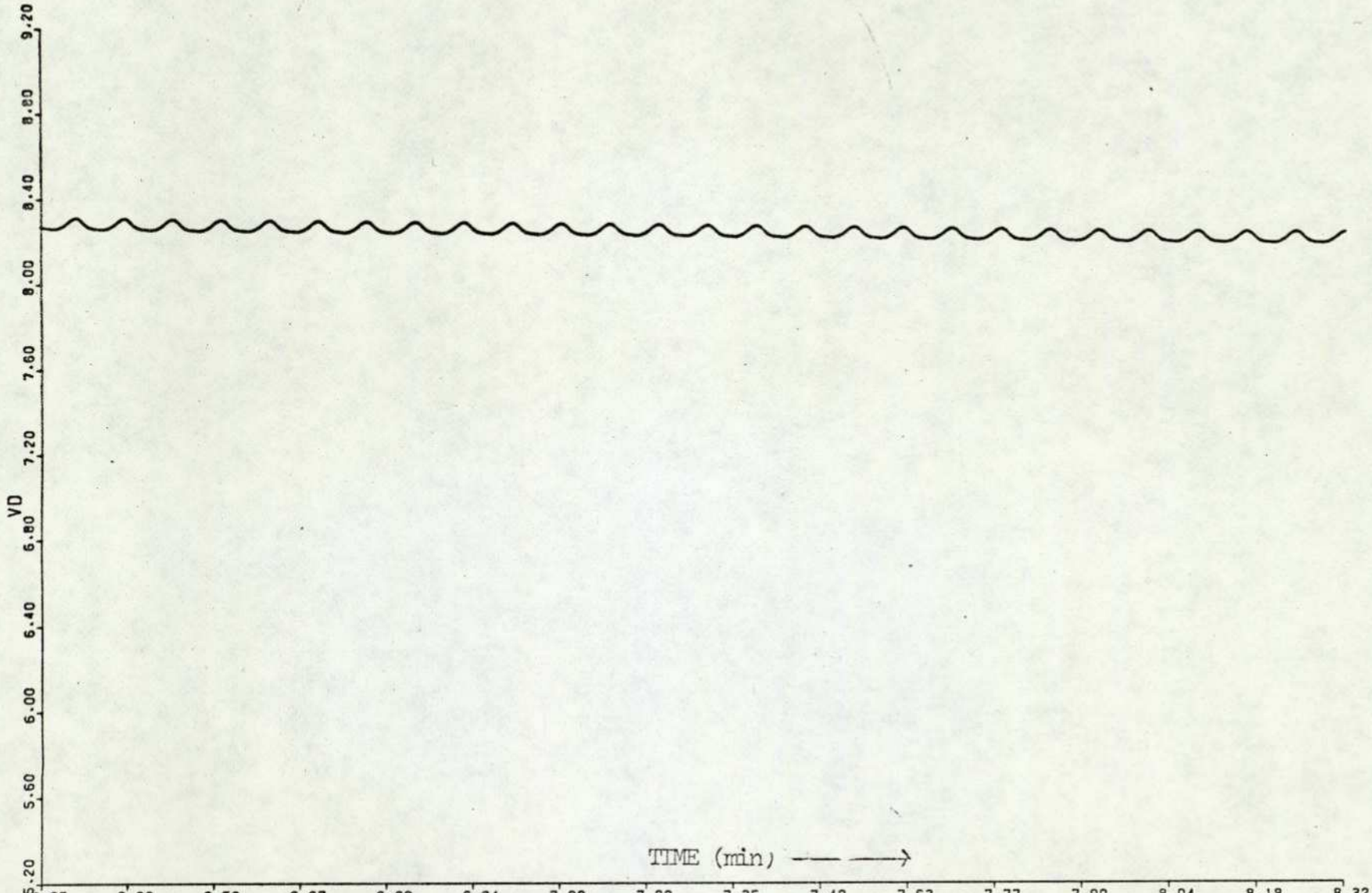
VD
9.20
8.80
8.40
8.00
7.60
7.20
6.80
6.40
6.00
5.60
5.20
TIME (min) ——→
6.25
6.39
6.53
6.67
6.80
6.94
7.08
7.22
7.35
7.49
7.63
7.77
7.90
8.04
8.18
8.32
X-AXIS

Graph 9.3F

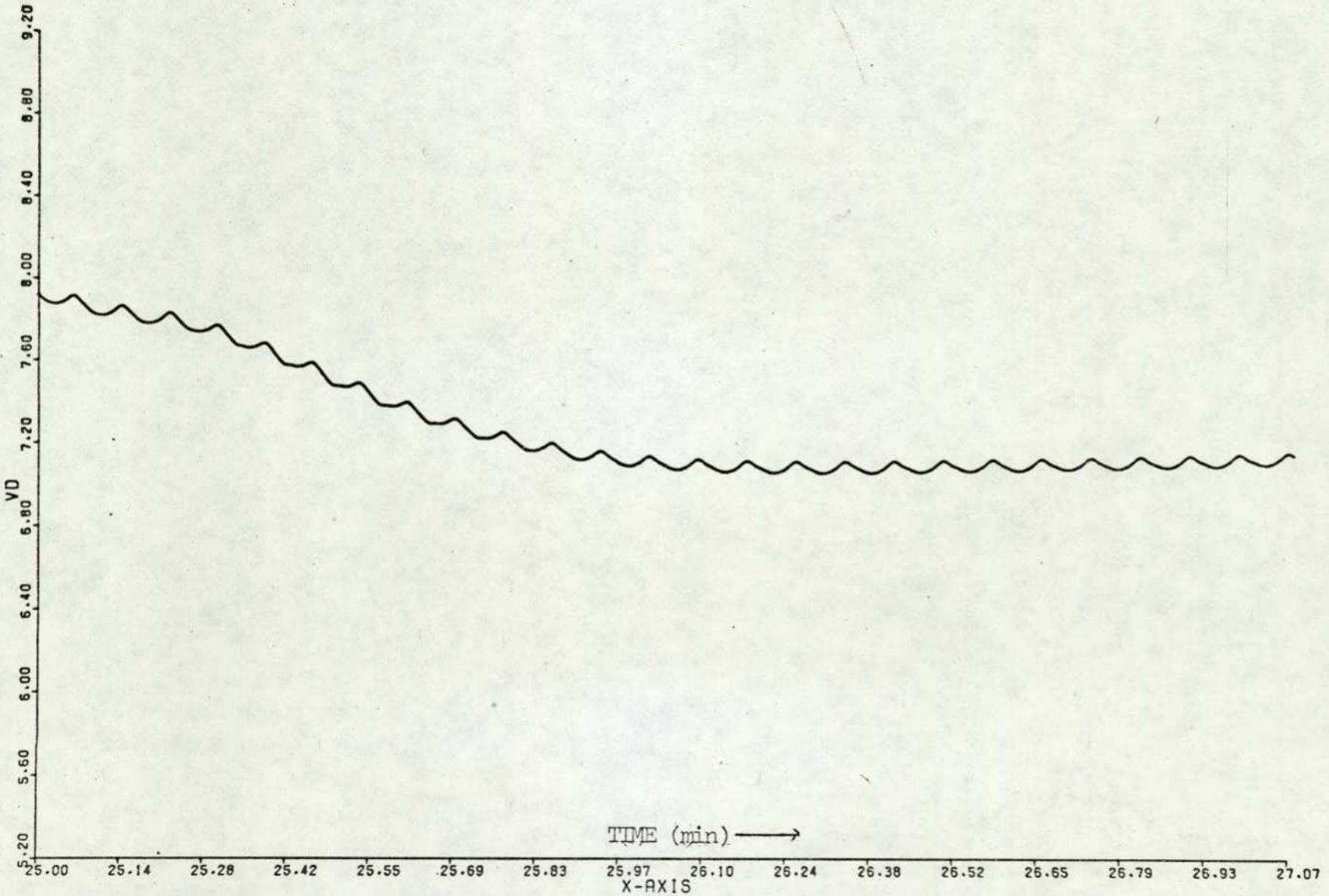
9.20
8.80
8.40
8.00
7.60
7.20
6.80
6.40
6.00
5.60
5.20
VD
TIME (min) ⟶
25.00
25.14
25.28
25.42
25.55
25.69
25.83
25.97
26.10
26.24
26.38
26.52
26.65
26.79
26.93
27.07
X-AXIS

Graph 9.3 G

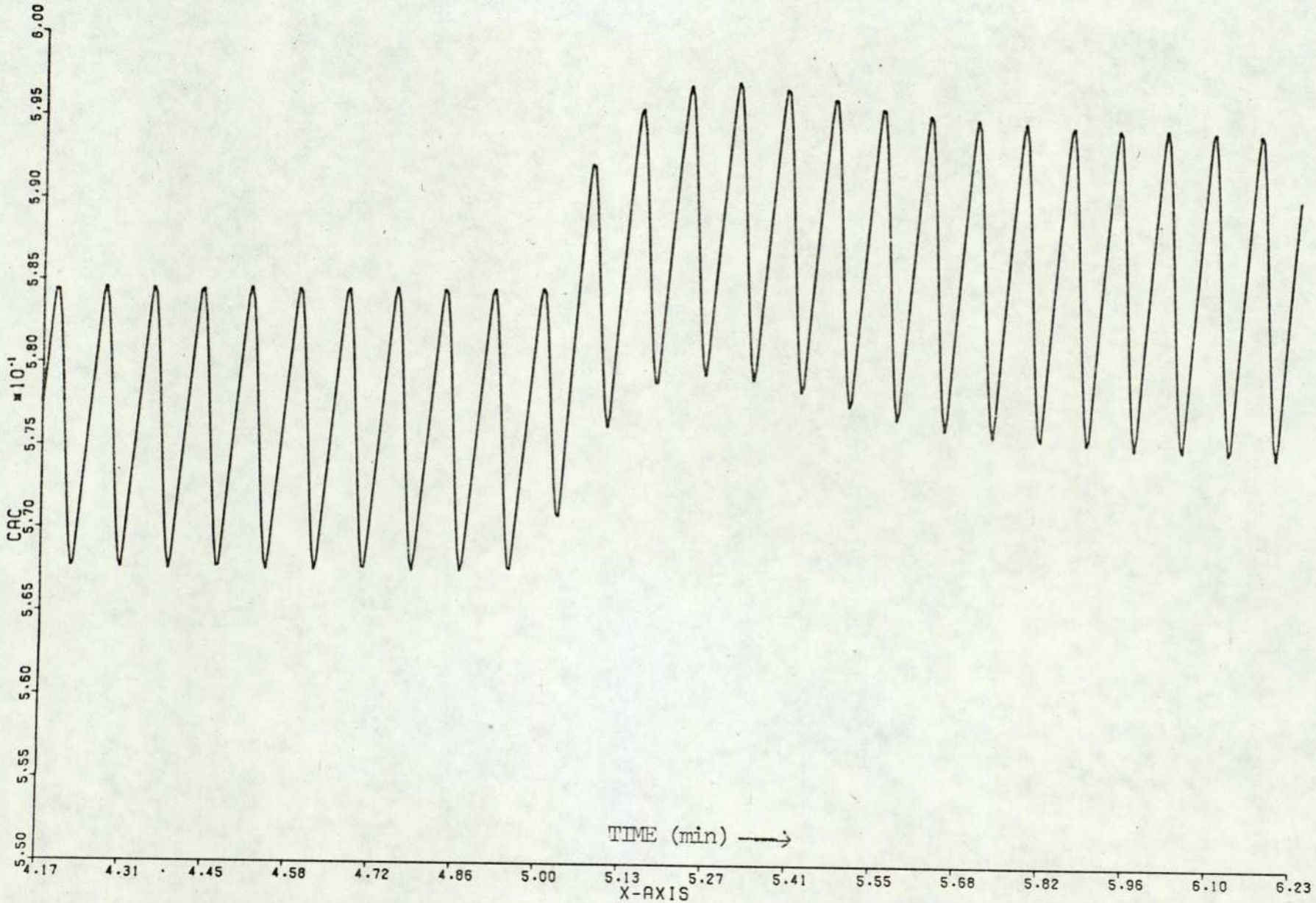
CAC
$\times 10^{-1}$
5.50
5.55
5.60
5.65
5.70
5.75
5.80
5.85
5.90
5.95
6.00
TIME (min) ⟶
4.17
4.31
4.45
4.58
4.72
4.86
5.00
5.13
5.27
5.41
5.55
5.68
5.82
5.96
6.10
6.23
X-AXIS

Graph 9.4A

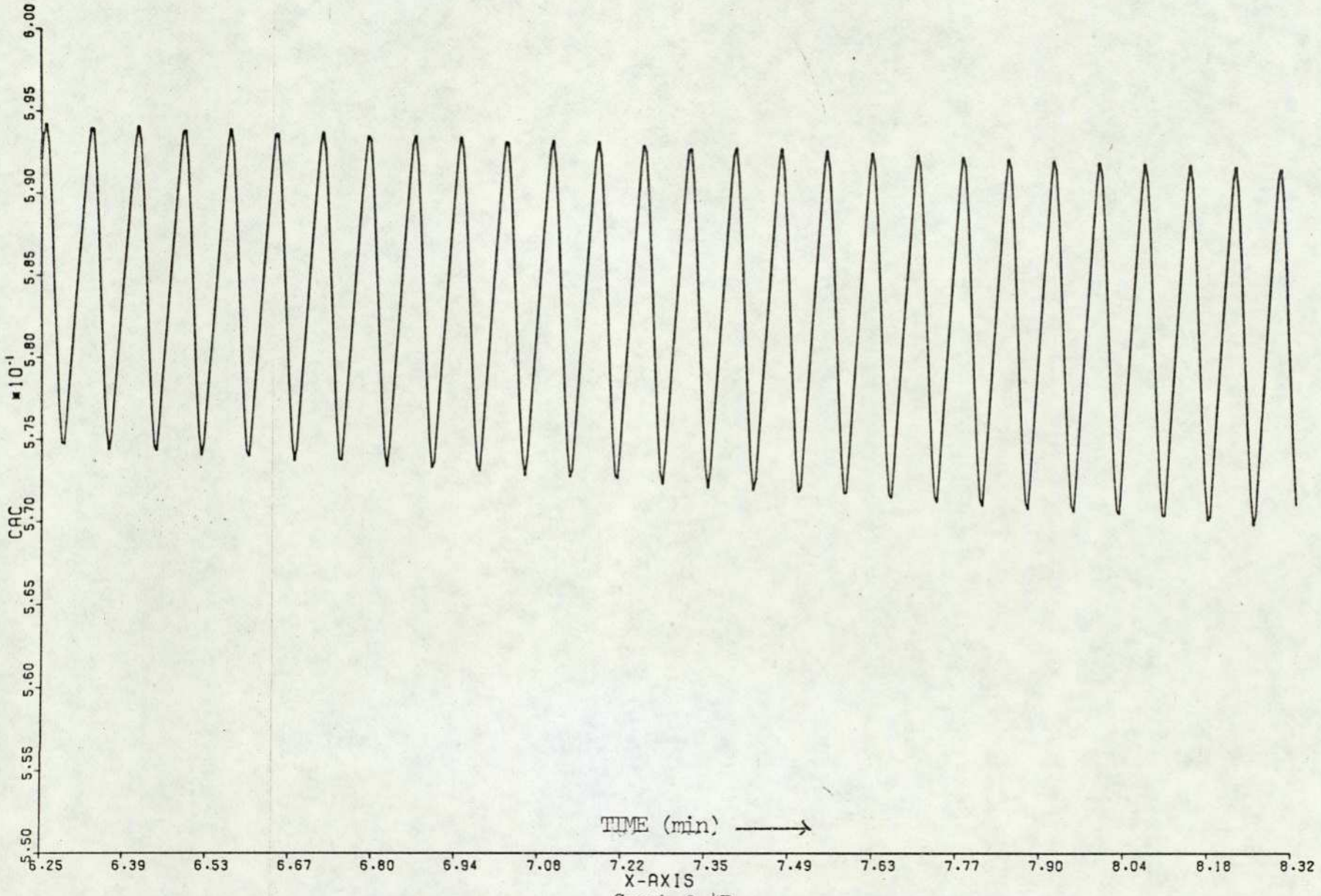
CAC
×10⁻¹
6.00
5.95
5.90
5.85
5.80
5.75
5.70
5.65
5.60
5.55
5.50
6.25
6.39
6.53
6.67
6.80
6.94
7.08
7.22
7.35
7.49
7.63
7.77
7.90
8.04
8.18
8.32
TIME (min) ⟶
X-AXIS

Graph 9.4B

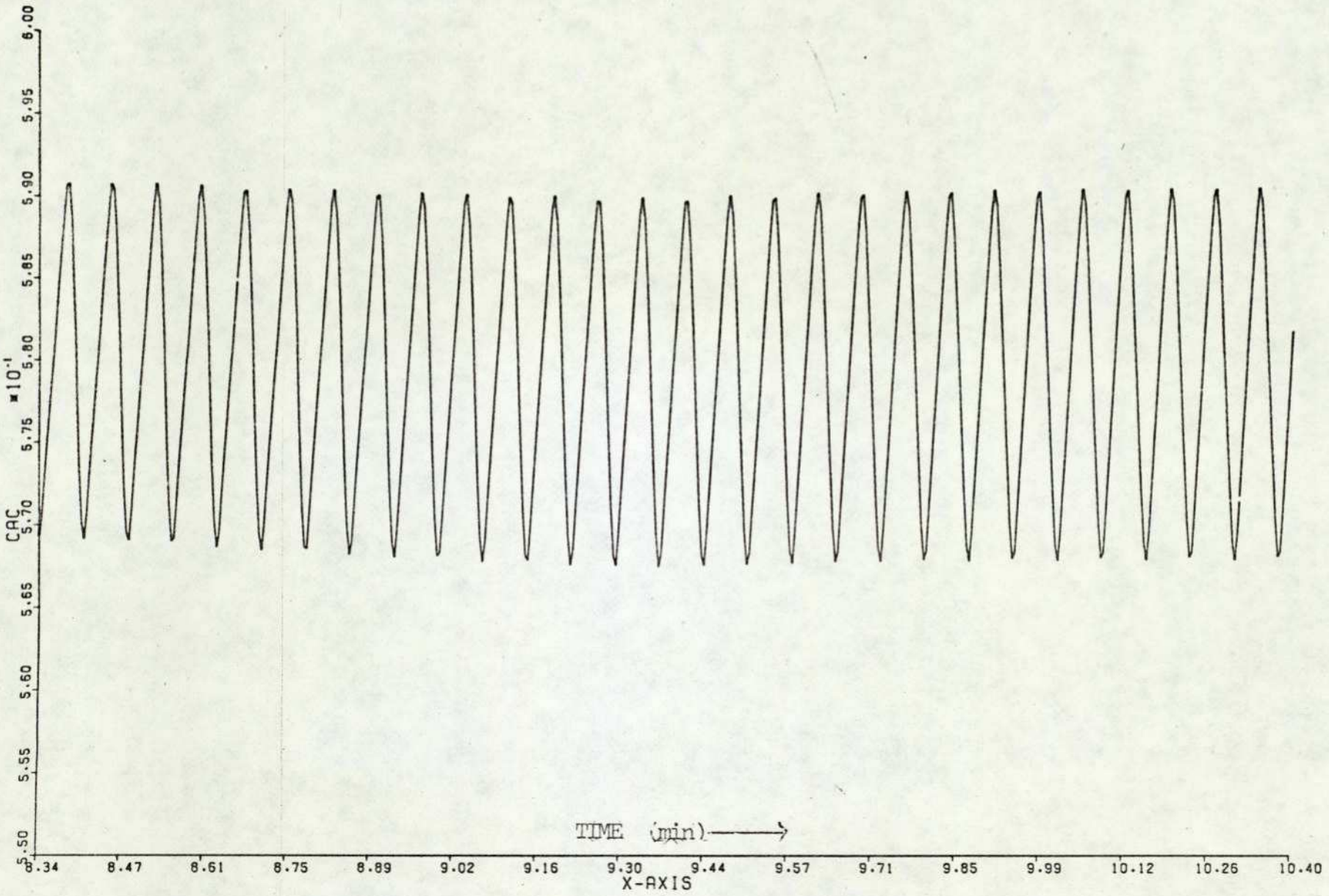
CAC
*10⁻¹
6.00
5.95
5.90
5.85
5.80
5.75
5.70
5.65
5.60
5.55
5.50
TIME (min)
8.34
8.47
8.61
8.75
8.89
9.02
9.16
9.30
9.44
9.57
9.71
9.85
9.99
10.12
10.26
10.40
X-AXIS

Graph 9.4C

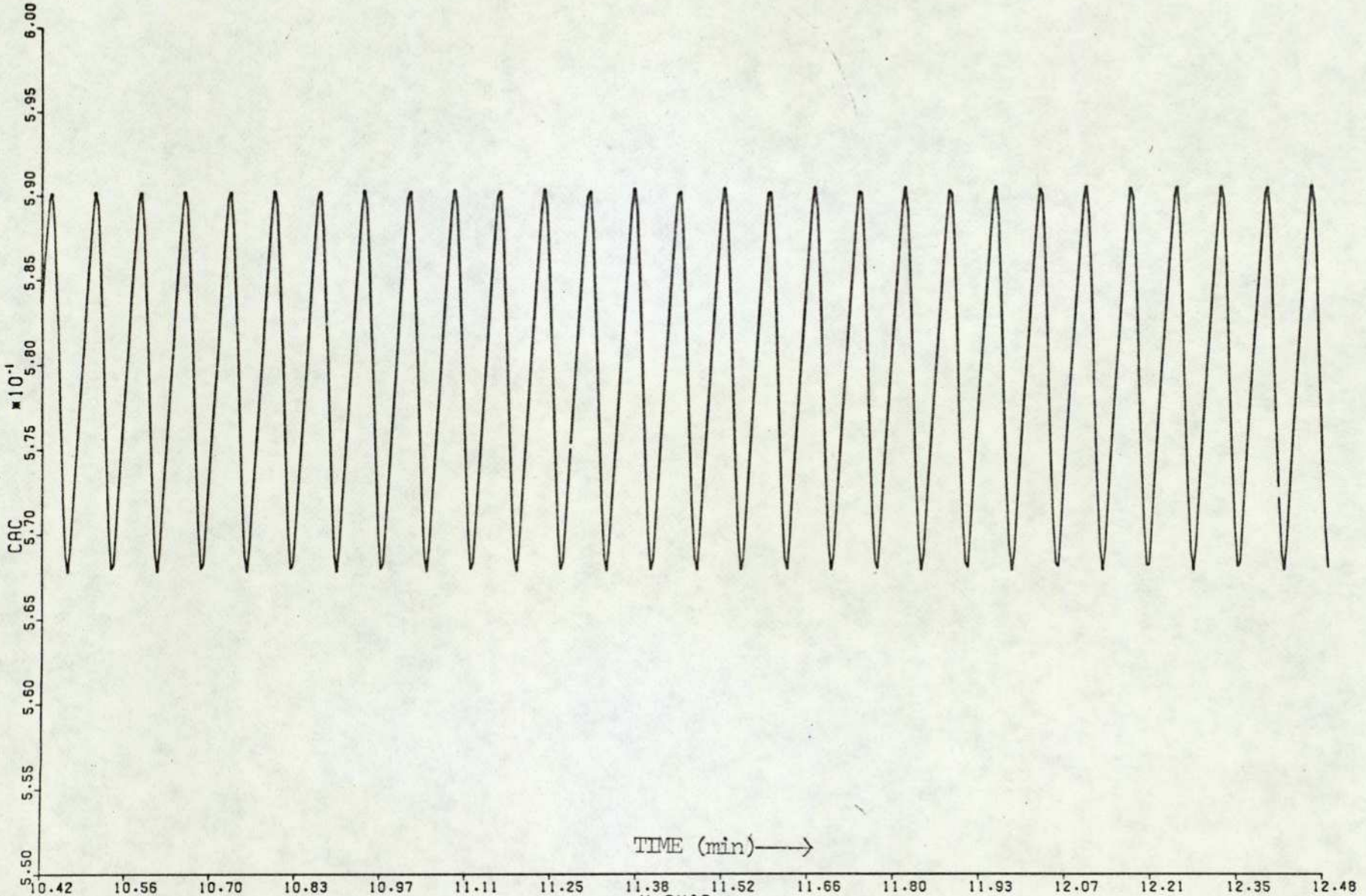
CAC
*10⁻¹
6.00
5.95
5.90
5.85
5.80
5.75
5.70
5.65
5.60
5.55
5.50
TIME (min)——→
10.42
10.56
10.70
10.83
10.97
11.11
11.25
11.38
11.52
11.66
11.80
11.93
12.07
12.21
12.35
12.48
X-AXIS

Graph 9.4D

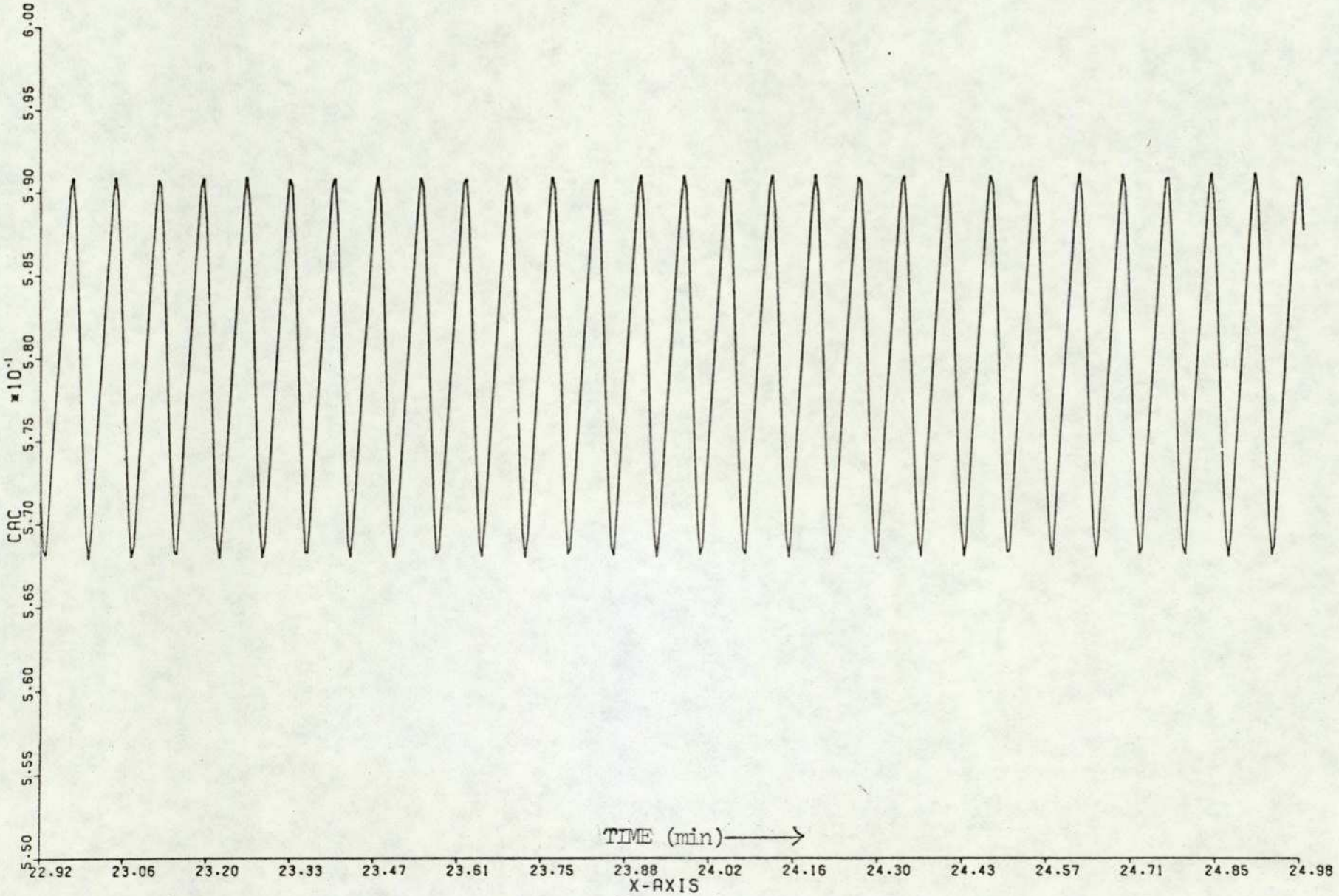
CAC
×10⁻¹
6.00
5.95
5.90
5.85
5.80
5.75
5.70
5.65
5.60
5.55
5.50
TIME (min)⟶
22.92
23.06
23.20
23.33
23.47
23.61
23.75
23.88
24.02
24.16
24.30
24.43
24.57
24.71
24.85
24.98
X-AXIS

Graph 9.4E

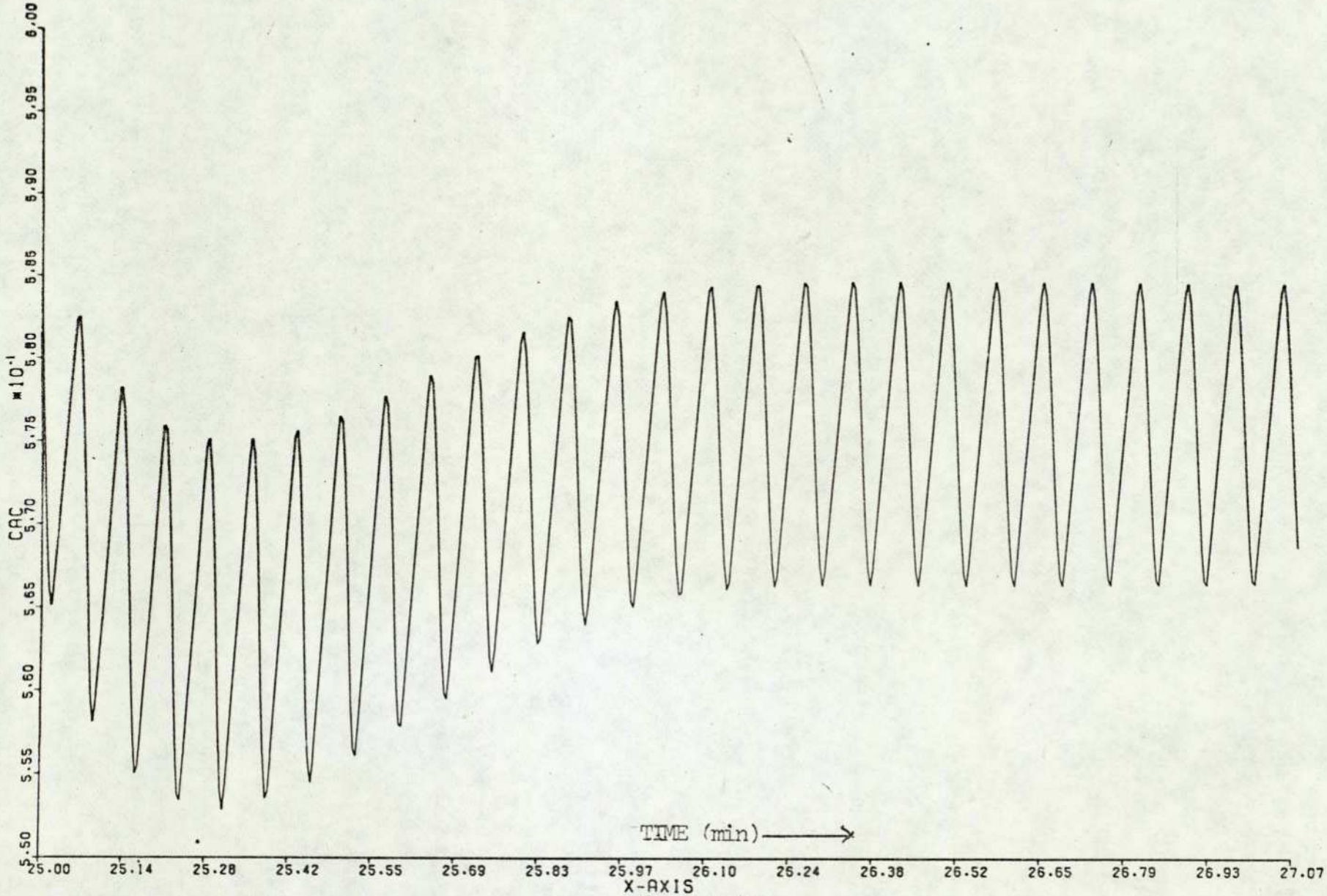
CAC
x10⁻¹
6.00
5.95
5.90
5.85
5.80
5.75
5.70
5.65
5.60
5.55
5.50
TIME (min)
25.00
25.14
25.28
25.42
25.55
25.69
25.83
25.97
26.10
26.24
26.38
26.52
26.65
26.79
26.93
27.07
X-AXIS

Graph 9.4F

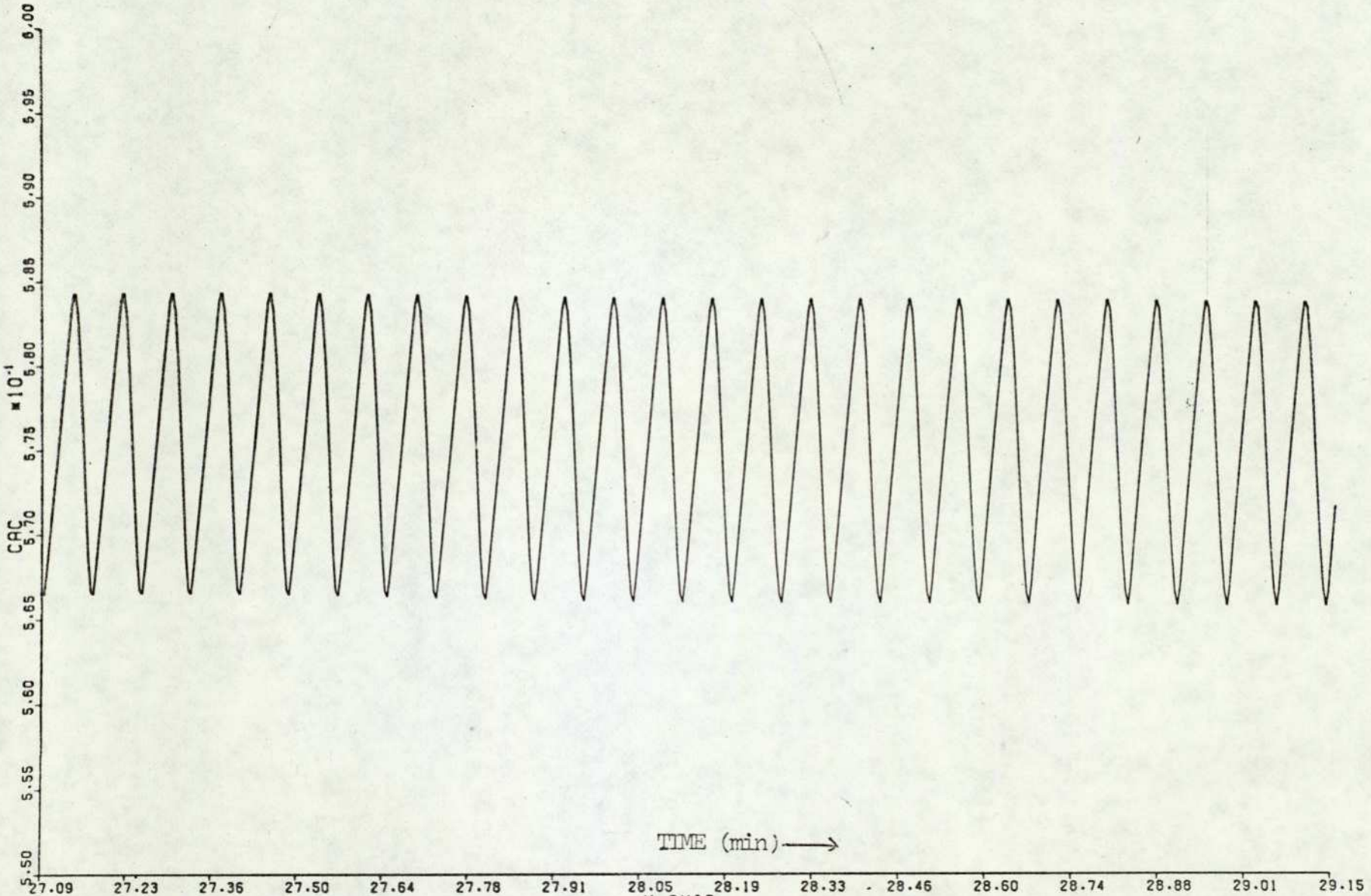
CAC
x10⁻¹
5.50
5.55
5.60
5.65
5.70
5.75
5.80
5.85
5.90
5.95
6.00
TIME (min)⟶
27.09
27.23
27.36
27.50
27.64
27.78
27.91
28.05
28.19
28.33
28.46
28.60
28.74
28.88
29.01
29.15
X-AXIS

Graph 9.4G

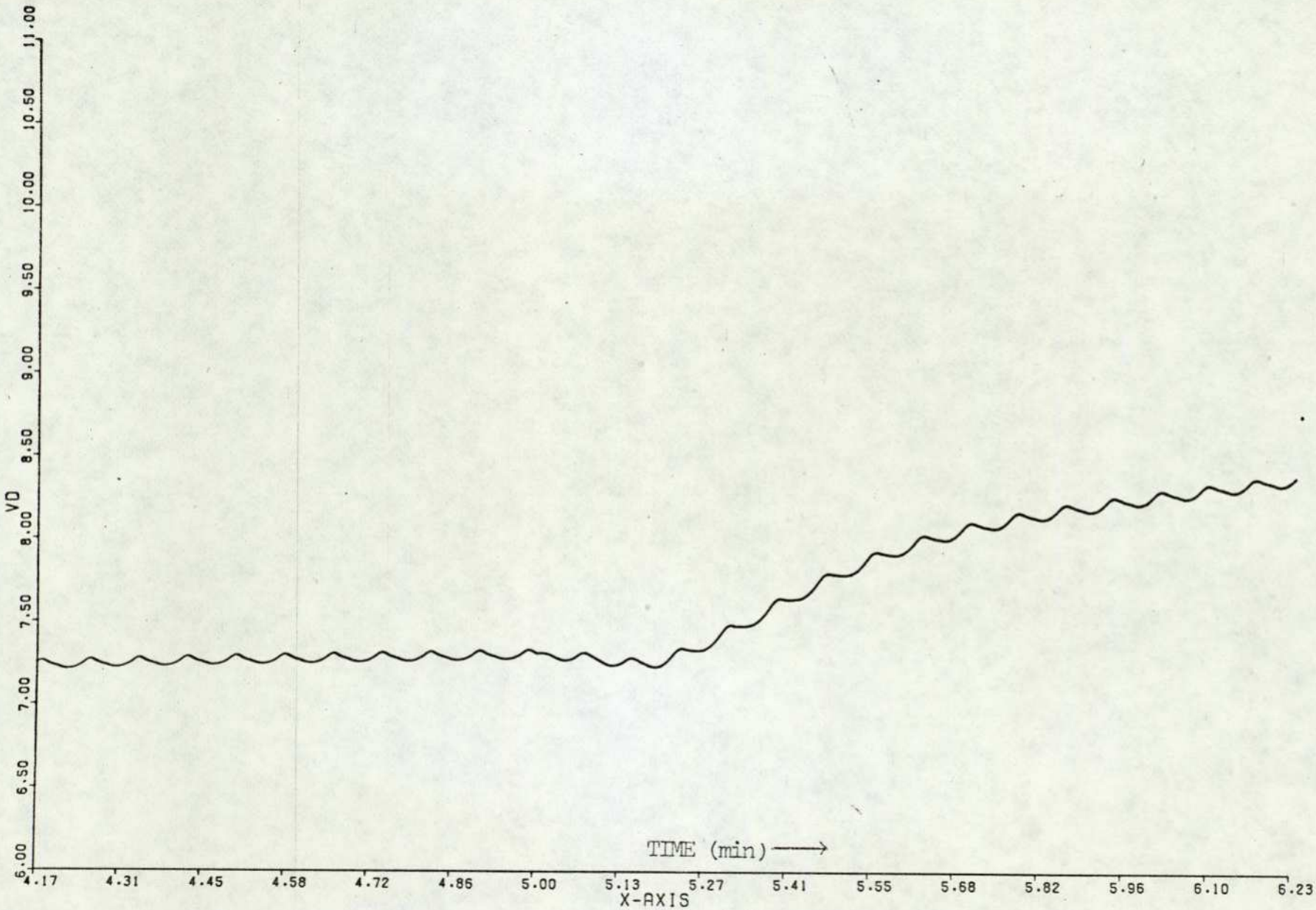
VD
11.00
10.50
10.00
9.50
9.00
8.50
8.00
7.50
7.00
6.50
6.00
TIME (min) ⟶
4.17
4.31
4.45
4.58
4.72
4.86
5.00
5.13
5.27
5.41
5.55
5.68
5.82
5.96
6.10
6.23
X-AXIS

Graph 9.5A

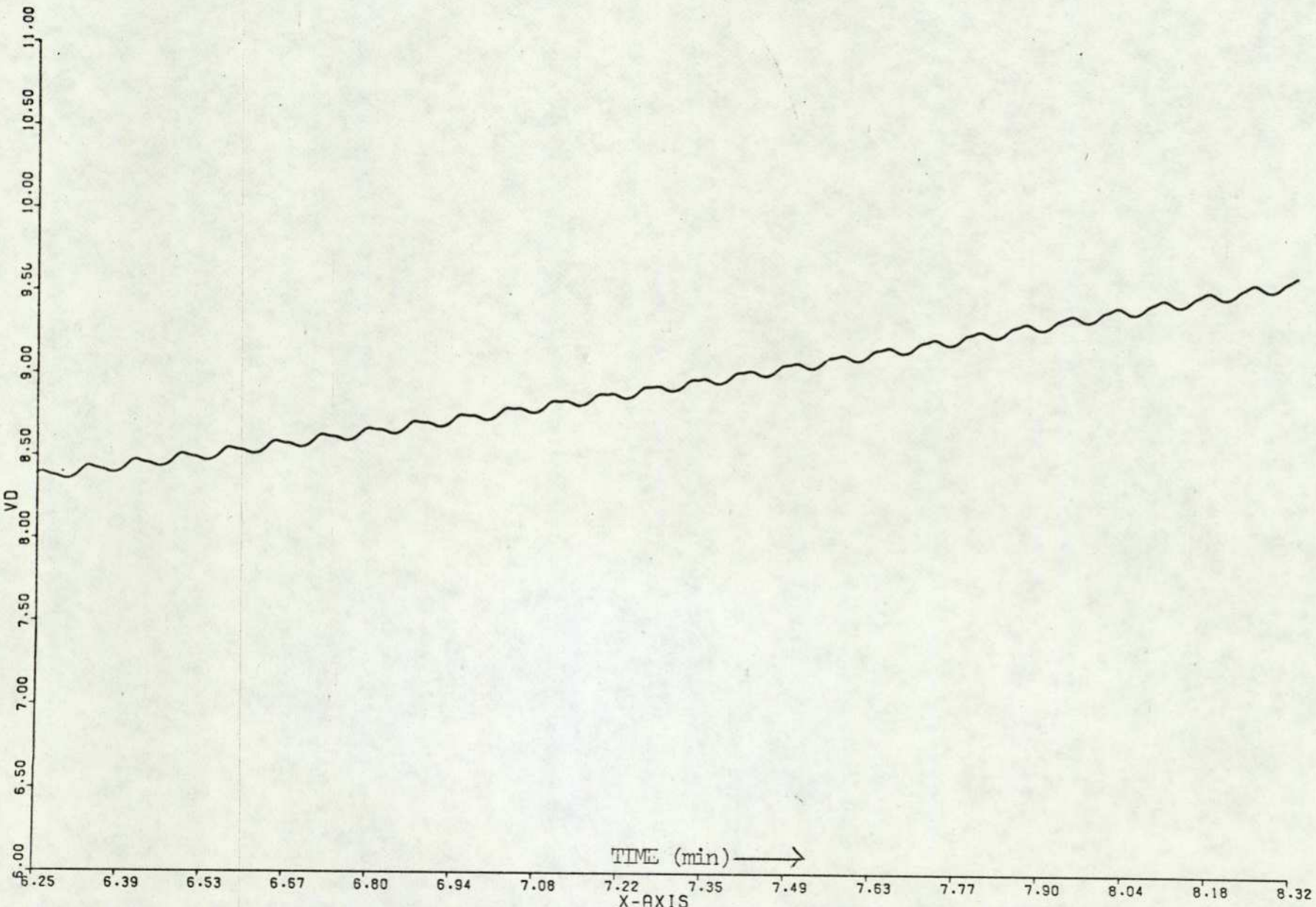
VD
11.00
10.50
10.00
9.50
9.00
8.50
8.00
7.50
7.00
6.50
6.00
TIME (min)
6.25
6.39
6.53
6.67
6.80
6.94
7.08
7.22
7.35
7.49
7.63
7.77
7.90
8.04
8.18
8.32
X-AXIS
Graph 9.5B

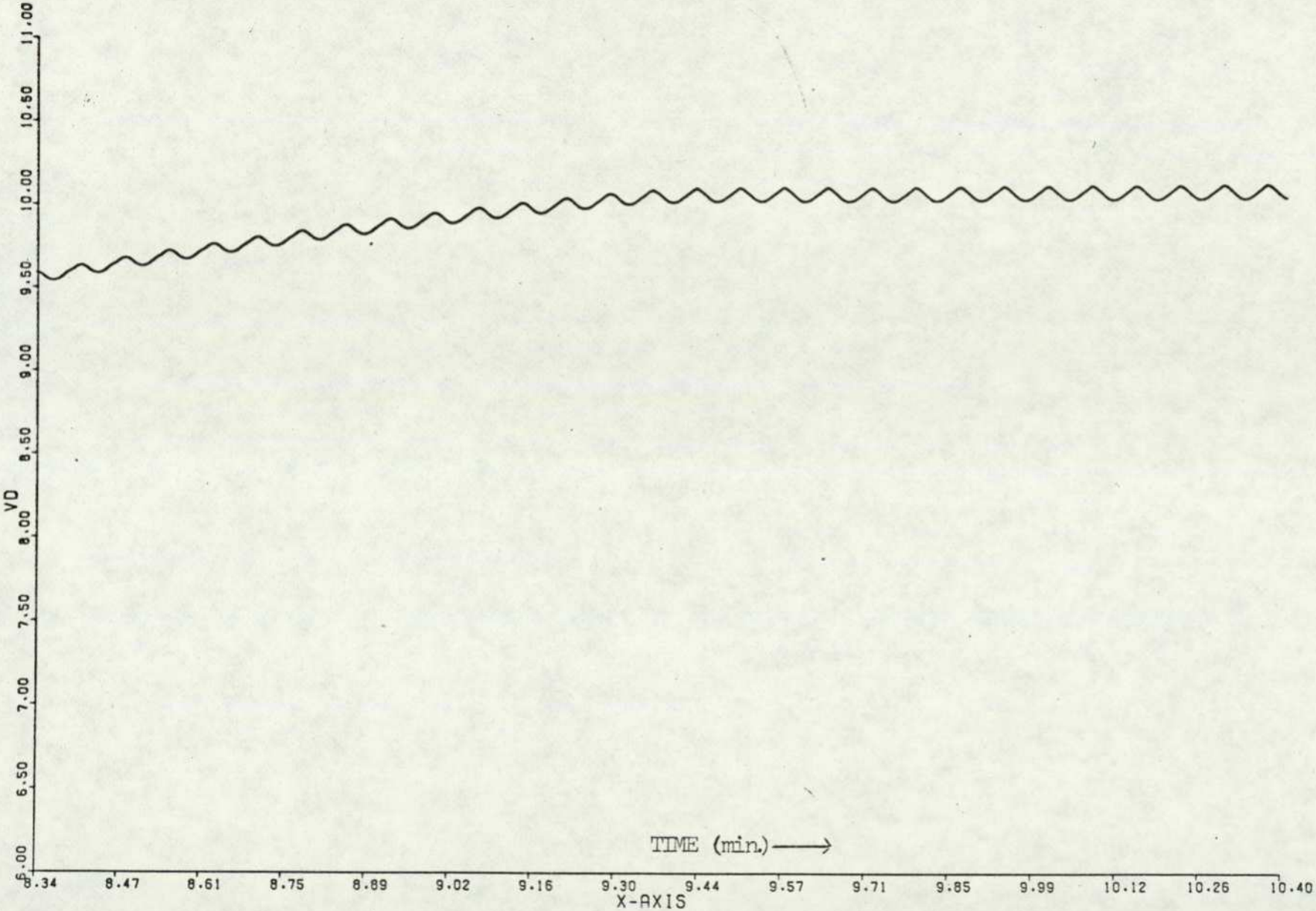
VD
11.00
10.50
10.00
9.50
9.00
8.50
8.00
7.50
7.00
6.50
6.00
TIME (min.) ⟶
8.34
8.47
8.61
8.75
8.89
9.02
9.16
9.30
9.44
9.57
9.71
9.85
9.99
10.12
10.26
10.40
X-AXIS

Graph 9.5C

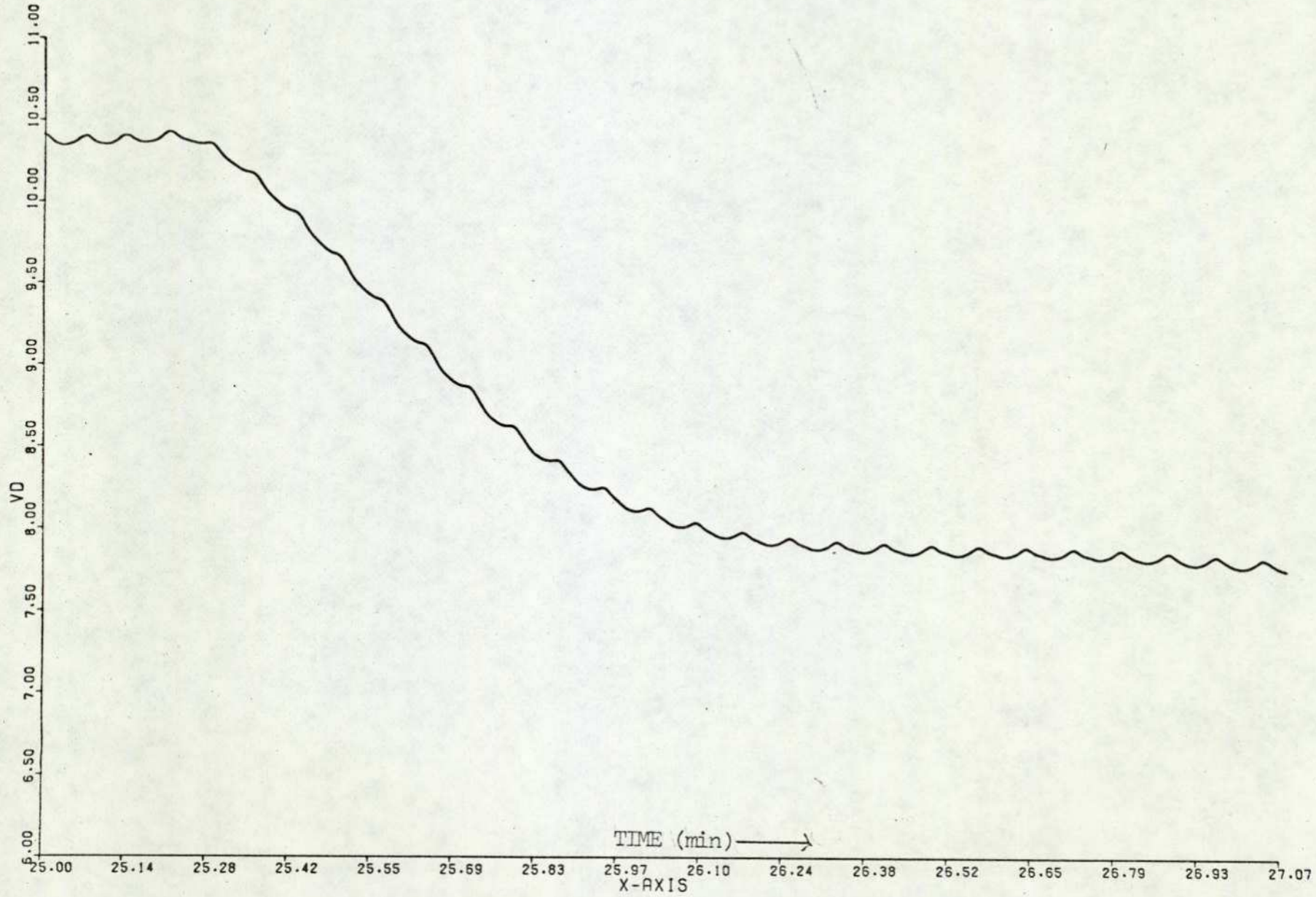
VD
11.00
10.50
10.00
9.50
9.00
8.50
8.00
7.50
7.00
6.50
6.00
25.00
25.14
25.28
25.42
25.55
25.69
25.83
25.97
26.10
26.24
26.38
26.52
26.65
26.79
26.93
27.07
TIME (min)
X-AXIS

Graph 9.5D

VD
6.30
7.30
8.30
9.30
10.30
11.30
12.30
13.30
14.30
15.30
16.30
4.17
4.31
4.45
4.58
4.72
4.86
5.00
5.13
5.27
5.41
5.55
5.68
5.82
5.96
6.10
6.23
TIME (min)
X-AXIS

Graph 9.6A

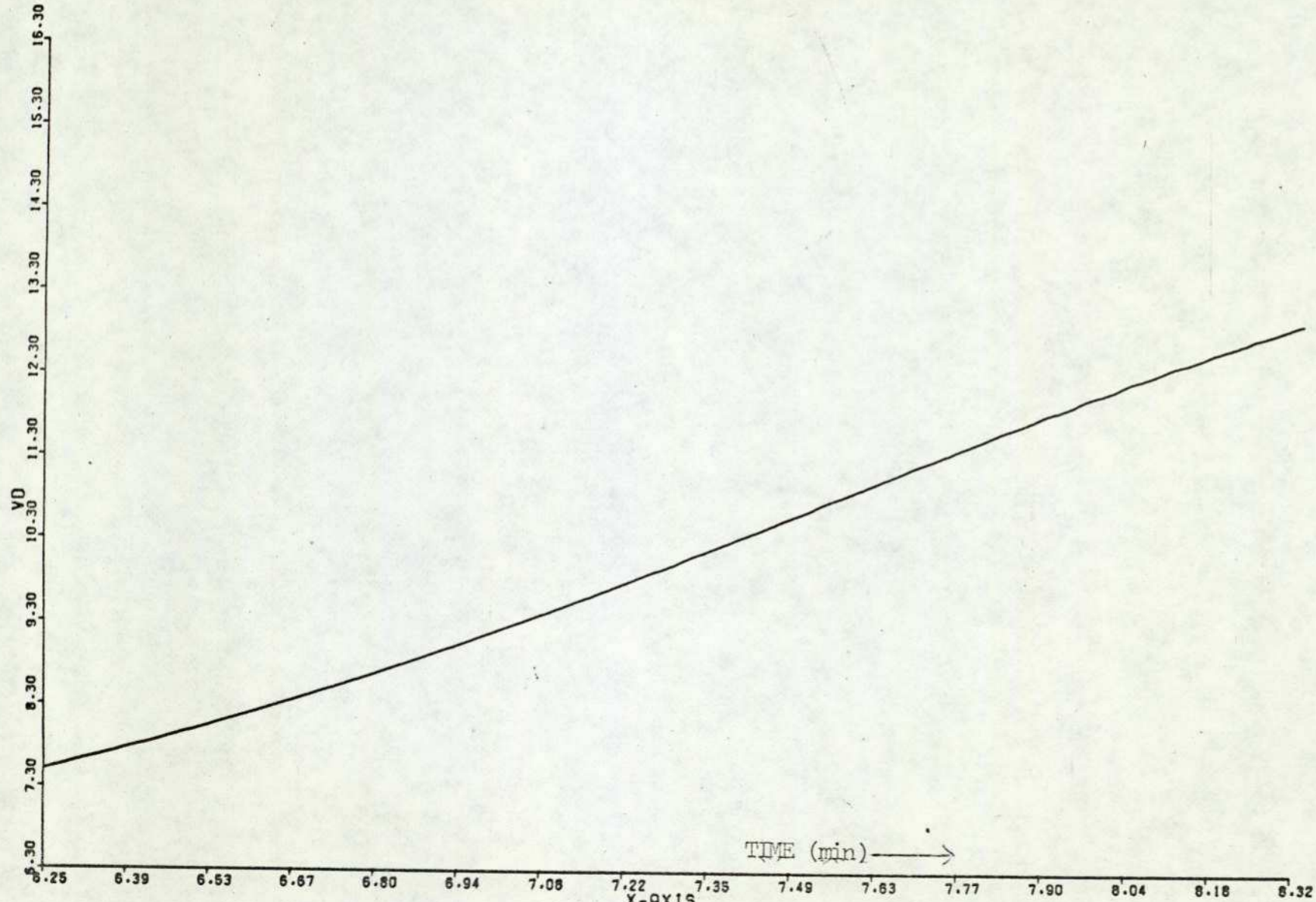
YD
5.30
7.30
8.30
9.30
10.30
11.30
12.30
13.30
14.30
15.30
16.30
6.25
6.39
6.53
6.67
6.80
6.94
7.08
7.22
7.35
7.49
7.63
7.77
7.90
8.04
8.18
8.32
X-AXIS
TIME (min)

Graph 9.6B

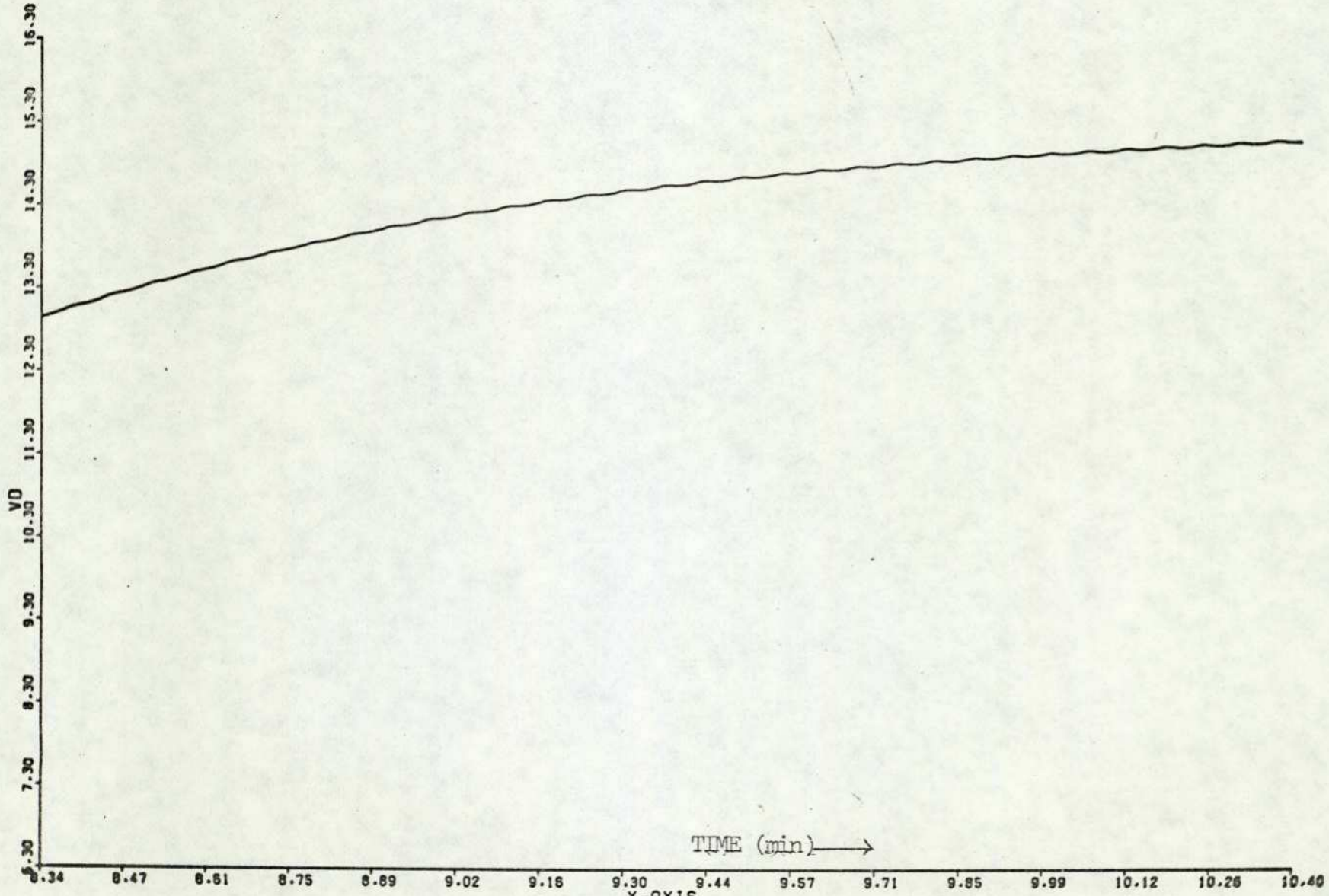
VO
16.30
15.30
14.30
13.30
12.30
11.30
10.30
9.30
8.30
7.30
6.30
8.34
8.47
8.61
8.75
8.89
9.02
9.16
9.30
9.44
9.57
9.71
9.85
9.99
10.12
10.26
10.40
TIME (min)
X-AXIS

Graph 9.6C

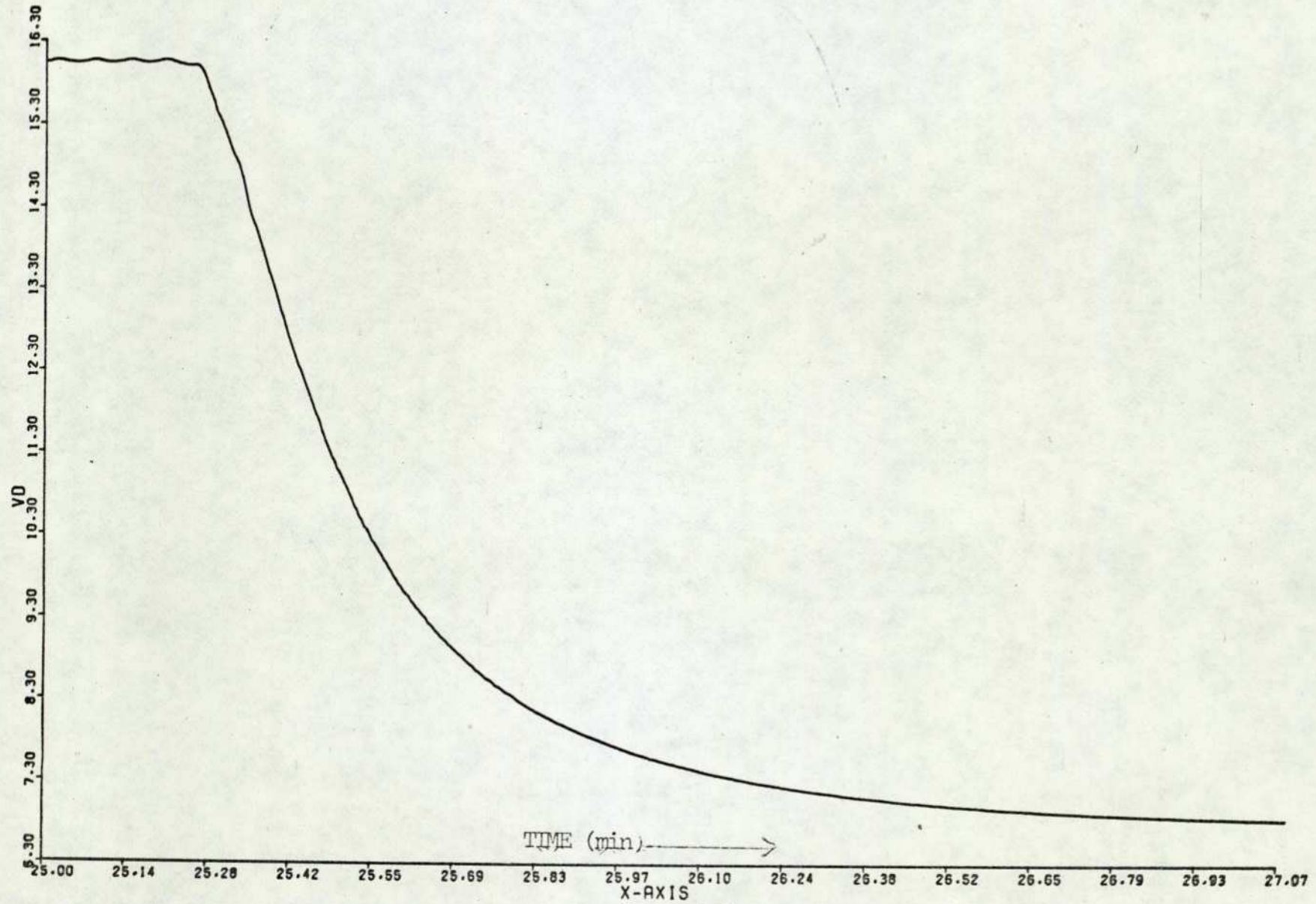
VD
16.30
15.30
14.30
13.30
12.30
11.30
10.30
9.30
8.30
7.30
6.30
TIME (min)
25.00
25.14
25.28
25.42
25.55
25.69
25.83
25.97
26.10
26.24
26.38
26.52
26.65
26.79
26.93
27.07
X-AXIS

Graph 9.6D

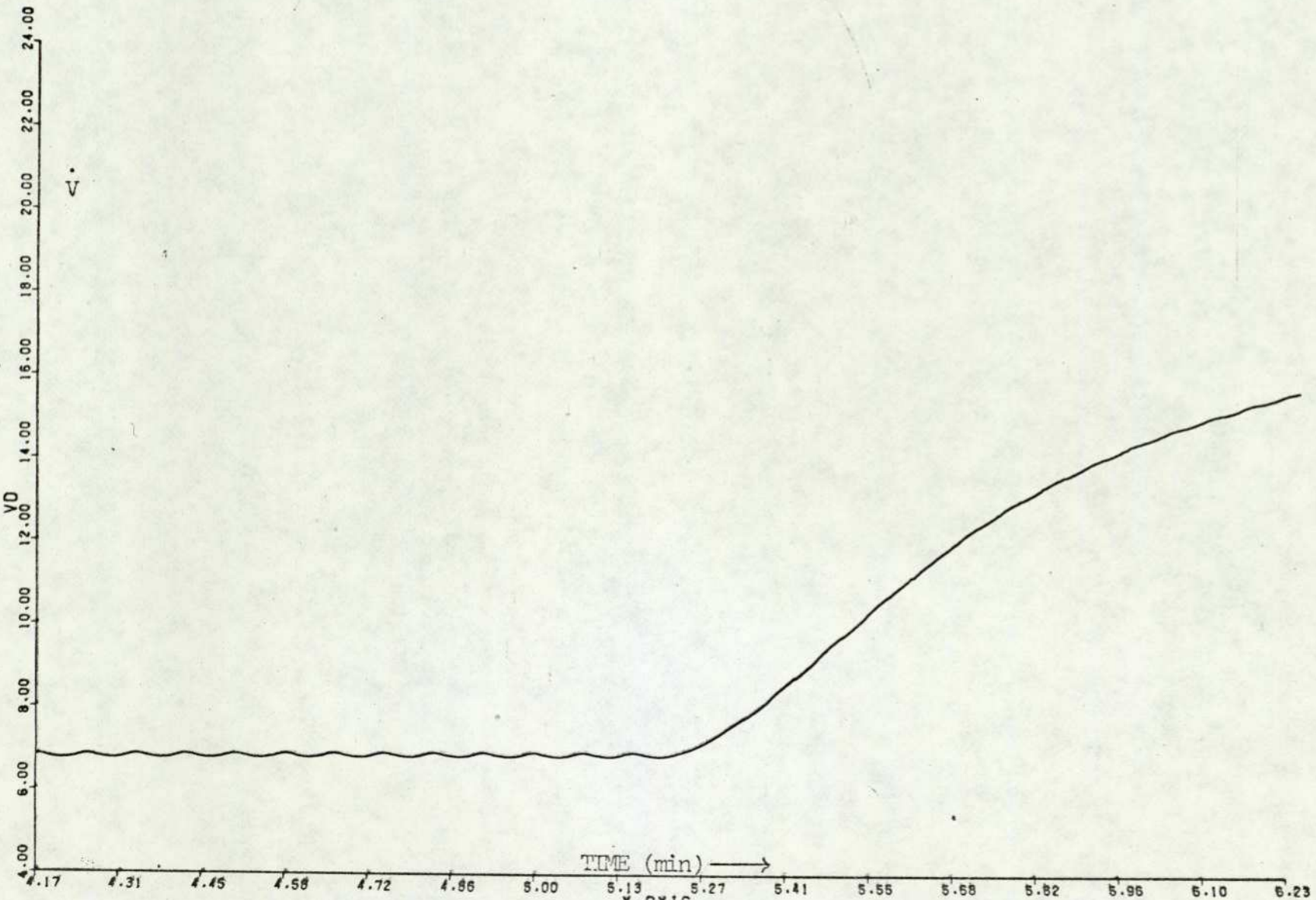
V
VO
24.00
22.00
20.00
18.00
16.00
14.00
12.00
10.00
8.00
6.00
4.00
TIME (min) ⟶
4.17
4.31
4.45
4.58
4.72
4.86
5.00
5.13
5.27
5.41
5.55
5.68
5.82
5.96
6.10
6.23
X-AXIS

Graph 9.7A

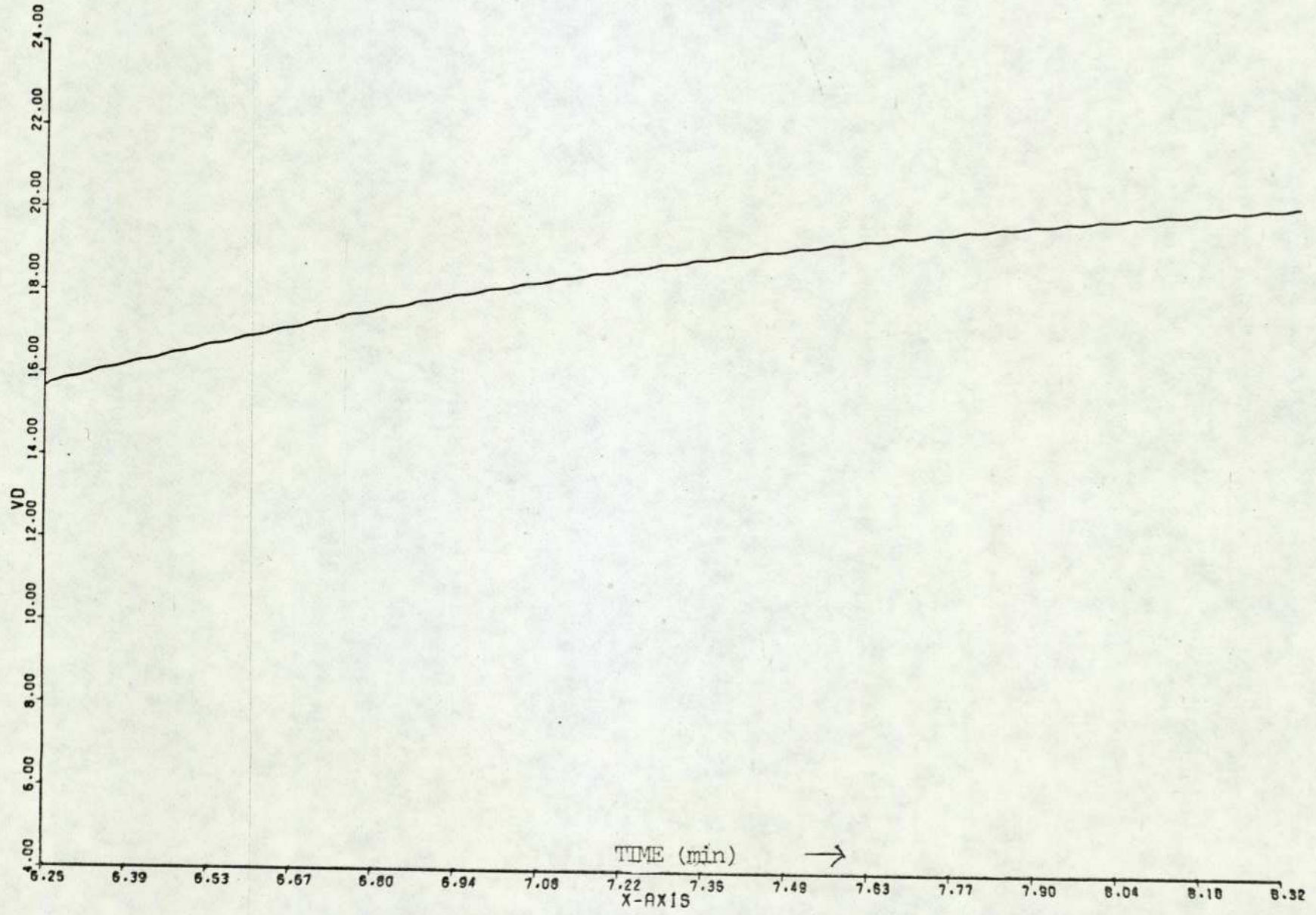
VD
24.00
22.00
20.00
18.00
16.00
14.00
12.00
10.00
8.00
6.00
4.00
6.25
6.39
6.53
6.67
6.80
6.94
7.08
7.22
7.35
7.49
7.63
7.77
7.90
8.04
8.18
8.32
TIME (min) →
X-AXIS

Graph 9.7B

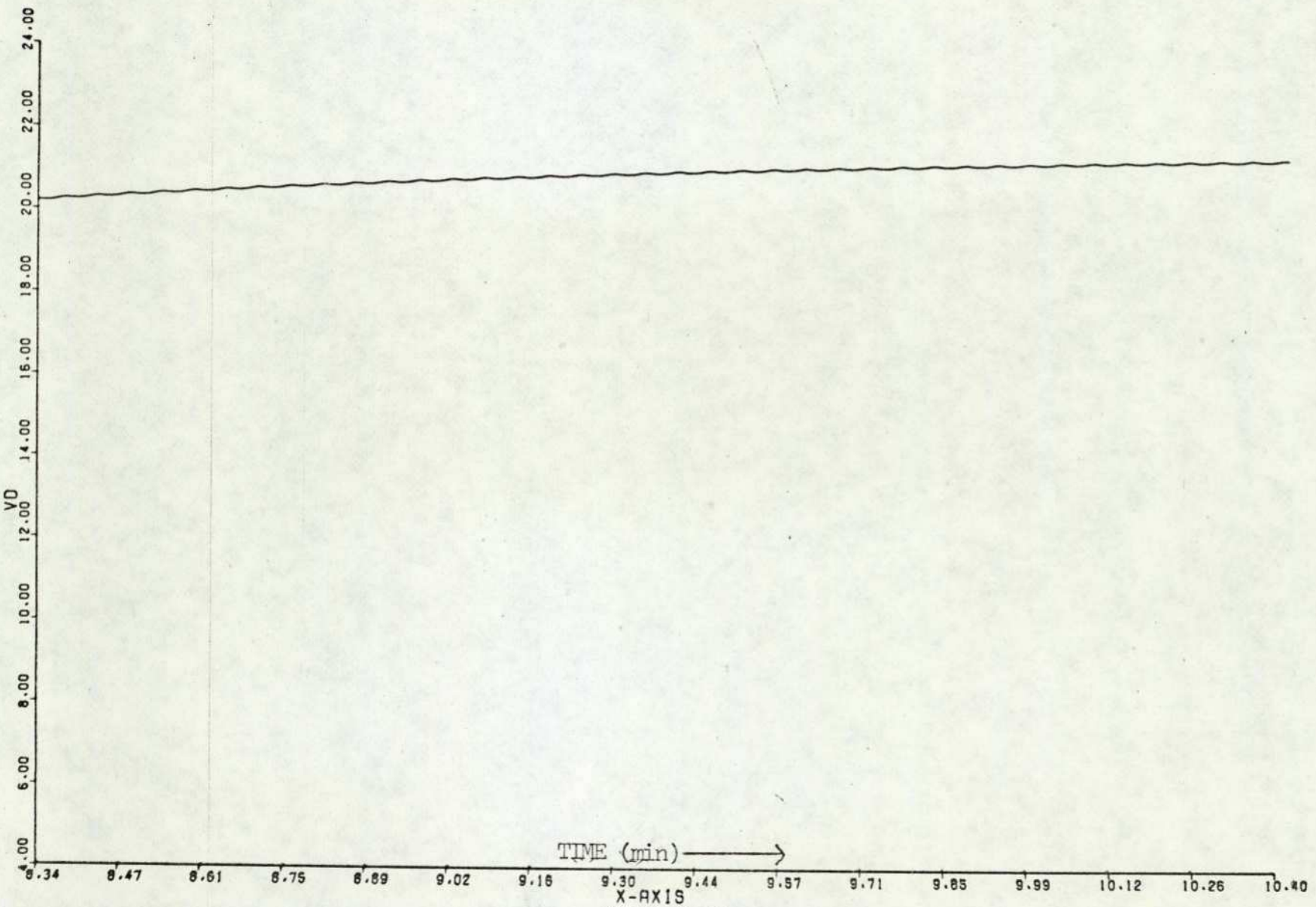
VD
24.00
22.00
20.00
18.00
16.00
14.00
12.00
10.00
8.00
6.00
4.00
TIME (min)
X-AXIS
8.34
8.47
8.61
8.75
8.89
9.02
9.16
9.30
9.44
9.57
9.71
9.85
9.99
10.12
10.26
10.40

Graph 9.7C

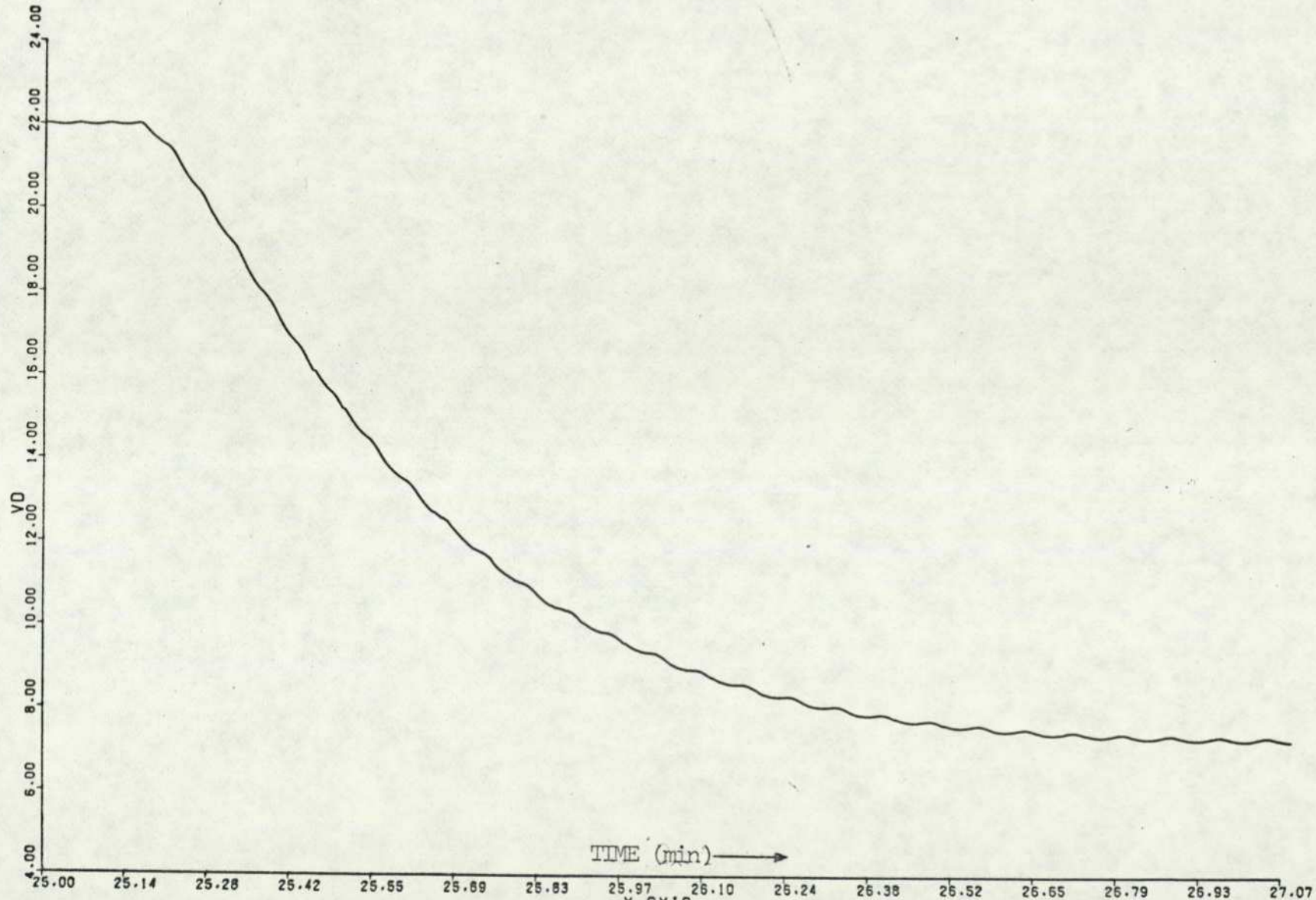
VD
24.00
22.00
20.00
18.00
16.00
14.00
12.00
10.00
8.00
6.00
4.00
TIME (min)
25.00
25.14
25.28
25.42
25.55
25.69
25.83
25.97
26.10
26.24
26.38
26.52
26.65
26.79
26.93
27.07
X-AXIS

Graph 9.7D

CHAPTER 10

MODEL VALIDATION

Model validation is concerned with the capability of the model to reproduce the real system responses for a given set of inputs or disturbances. The two features essential for any model validation process are structural identification and parameter estimation. This is true whether the model is to define some input-output causal relationships through curve fitting or the model is to mirror the real system as far as possible i.e. an isomorphic model. When one of the main objectives of the modelling exercise is to study the behaviour of the system (as in this case) and if a priori knowledge is not available for some parts of the system, then one tries to incorporate structures to which parameters are assigned which are more likely to describe the behaviour of the system.

The problems of validity of the model of the respiratory system are predominantly structural, particularly the structure of the respiratory controller. Another problem encountered in the validation is the non-uniqueness of the model. If a mathematical model can successfully simulate a single experiment, then the model may be considered to be one of large numbers of models which may be able to do the same thing. But if the model can simulate two essentially different experiments, the number in the set of models which can do the same thing decreases considerably. The larger the number of experiments which can be simulated, the smaller the number of alternative model structures.

There is no satisfactory technique of structural identification of models apart from testing each compartment of the system separately which is not feasible in the case of the respiratory system. Thus one can only postulate a structure, to which parameters may be assigned with the view of satisfying all the available data. On the other hand the development of the model itself uses a considerable amount of available experimental data, thus limiting the extent of validity of the model to that data. One important feature that can be used for the purpose of validation is that the model has to simulate the real system response in dynamic as well as steady state, i.e. the model has to reproduce similar time constants during transients.

The mathematical model of the respiratory system developed in the previous chapters was developed in stages due to non-uniqueness of the models leading to a complex model. At each stage the complexity of the model was increased along with the number of experiments simulated. The data used for the validation at each stage were CO_2 breathing, hyperventilation, asphyxia and hypoxia, and the parameter sensitivity was tested for circulation delay times and controller gains. This stage by stage validation of the model in chapters 5 to 9 highlighted the uncertainty of the structure of the controlling system. It was found that no single structure could reproduce all the responses of the real system for the same inputs or disturbances. This leads to formulation of new structures. Also as seen in chapter 5 the tissue CO_2 controller reproduced comparable responses for CO_2 inhalation of 3%, 5% and 7% but still there was some variance in the model response with the percentage

CO_2 inhaled. Thus a further test of the structure of the data may be that for different values of CO_2 inhaled the parameters fitted to that structure should not have to be changed, but if parameters change with the change in this level of disturbance then that particular structure is not correct and a new structure has to be hypothesised.Thus a large part of validation is the validation and testing of the alternative structures. There are many mathematical techniques available for identification and parameter estimation but few of them, if any, are applicable to non-linear, multivariable, complex systems. Åström and Eykhoff (1971) have published an excellent survey of the various techniques available for System-Identification but in their own words for non-linear systems, "The techniques currently used simply convert the identification problem to an approximation problem by postulating a structure. The few non-parametric techniques available are computationally extremely time consuming". Thus more of the conventional techniques of identification and parameter estimation may be conveniently used for the validation purposes of such a complex process as the respiratory system whose mathematical model is developed in chapter 9.

Considering the above problems,two separate techniques are used to study and evaluate the structure and parameters of the controlling system. One of them is functional minimisation through the use of an error function which is similar to, but far more adaptable than least squares method and the other is the use of pattern recognition techniques in response 'features' of model simulation compared to similar 'features' produced by the real system.

As discussed above there are two sites for the chemoreceptors in the body which sense the chemical composition of gases around them and produce signals to alter the ventilation rate. The first are the central chemoreceptors considered to be in the brain tissue compartment and the second are the arterial chemoreceptors responsive to arterial P_{CO_2} and P_{O_2}. From the discussions in previous chapters it is clear that the central chemoreceptors are primarily responsive to carbon dioxide changes whereas the arterial chemoreceptors are responsive to oxygen changes. But as there is interdependence of the two gases involved it is possible that a controlling system incorporating both the chemoreceptors may result in removing the discrepancies between the model and the real system responses to CO_2 inhalation.

10.1 Functional minimisation technique:

The method for identifying parameters of the controlling system of the mathematical model is shown in the figure 10.1.

The computer program used was developed by J. Letia (1974). The system output response was taken from Reynolds and Milhorn (1972) and was digitised at intervals of 1 minute (1 second computer time) over a total response time of 32 minutes. Spline interpolation is employed to determine the system output response between the one minute intervals.

The model output response is obtained by digital simulation using various controller equation formulations.

Error Index:

An integral squared error criterion is used defined as

$$J = \int_0^{32} \tfrac{1}{2} (\dot{V} - \dot{V}_E)^2 \, dt \qquad \ldots\ldots 10.1$$

where $\dot{V}$ is the output of the biological controller such that

$$\dot{V} = f (C_{TCO_2}) \qquad \ldots\ldots 10.2$$

$$\dot{V} = f (C_{TCO_2}, \frac{d}{dt} C_{TCO_2}) \qquad \ldots\ldots 10.3$$

$$\dot{V} = f (C_{BTCO_2}, P_{aCO_2}, P_{aO_2}) \qquad \ldots\ldots 10.4$$

and $\dot{V}_E$ is the corresponding output from the real biological system. The equations 10.2 and 10.4 describe the controlling system consisting of brain tissue CO_2 control and arterial CO_2 and O_2 plus brain tissue CO_2 control and equation 10.3 includes the rate of change of C_{TCO_2}.

Optimisation Algorithm

The optimisation algorithm used to determine the parameters $K_1, K_2 \ldots, K_6$ to minimise the error index J is based on direct linear searches using the iterative scheme

$$\underline{K}_{i+1} = \underline{K}_i + \alpha_i \underline{\delta}_i \qquad \ldots\ldots 10.4$$

where $\underline{K}_i$ is the vector of parameter at iteration i and α_i is chosen to minimise J along a search direction $\underline{\delta}_i$. A quaderatic interpolation formula is employed to estimate the optimum of α_i and successive search directions are computed using the Powell-Zurgwill direct search procedure. An adaptive scheme is used for determining the initial step along a search direction and also for the accuracy parameter employed for convergence of the quadratic interpolation.

10.1.1 Results and Discussions:

A TISSUE CO_2 control:

Figures 10.1.1, 10.1.2 and 10.1.3 show the results of model simulation compared with experimental evidence of ventilation (Reynolds and Milhorn 1973) for 3%, 5% and 7% CO_2 inhalation with proportional and proportional plus derivative control. As expected from earlier discussions of tissue CO_2 control (chapter 5) the value of the controller gain differed for each percentage of CO_2 inhaled. The various values of K in the equation:

$$\dot{V} = 6.0 + K (C_{TCO_2} - C_{TCO_2}(o)) \quad \ldots\ldots 10.5$$

found by using optimisation techniques are as follows:

K = 1292 for 3% CO_2 inhalation

K = 971 for 5% CO_2 inhalation

K = 1002 for 7% CO_2 inhalation

Not only the values of gain differ in each case but the dynamic response is faster in the cast of 3% CO_2 and slower in; the case of 7% CO_2 as compared to the experimental evidence. To improve upon the dynamic response of the model a dynamic controller of the form in equation 10.3 was postulated. That is to say

$$\dot{V} = 6.0 + K_1 (C_{TCO_2} - C_{TCO_2}(o)) + K_2 \frac{d}{dt} C_{TCO_2} \quad \ldots\ldots 10.6$$

The simulation results for this controller strategy are shown in dotted lines in figures 10.1.1, 10.1.2 and 10.1.3 for 3%, 5% and 7% CO_2 inhalation respectively. In the case of 3% CO_2 there was no difference in the model response but for 5%

and 7% CO_2 there is a marked improvement in the model responses which correspond very closely to the experimental curves.

The following table shows the values of K_1 and K_2 for equation 10.6 for various percentages of CO_2 inhalations .

% CO_2 inhalation	K_1	K_2
3	1249	96.2
5	968	315.3
7	995	906.9

Thus it can be seen that although the inclusion of derivative control in the model improves the performance of the model there is no unique set of values of either K_1 or K_2 which can be used for all percentages of CO_2 inhalation. This confirms the belief that although the central chemoreceptors are responsive mainly to CO_2 concentration, they alone are not responsible for the changes in time course of ventilation induced through the inhalation of CO_2 in breathing gas mixtures. As previously discussed in chapter 6 the arterial chemoreceptors are not capable of simulating the real system response on their own, hence it is reasonable to hypothesise a controlling system which includes both the controller actions, i.e., central chemoreceptors control responsive to brain tissue CO_2 concentration changes and arterial chemoreceptor control responsive to changes in arterial concentrations of oxygen as well as carbon dioxide.

B Complex Controller:

In view of the above discussion a complex controller equation was hypothesised of the form:

$$\dot{V} = 6.0 + K_1 (C_{BTCO_2} - C_{BTCO_2}(o)) + K_2 (C_{aCO_2} - K_3)(1 + \frac{K_4}{C_{aO_2} - K_5}) \quad \ldots\ldots 10.7$$

It can be seen that equation 10.7 represents a mixture of the two controller strategies independently tested in the previous chapters. The form of the equation is so chosen as to be able to represent the two control actions together but each controller in part still retaining the same form as used in chapters 6 and 7. At this stage it must be noted that equation 10.7 cannot be used for simulating any changes in ventilation rate due to changes in oxygen concentration in the gas mixture inhaled because the value of K_3 will be set as near to the normal value of C_{aCO_2} as possible because of the presence of 6.0 (normal ventilation rate in litre per minute) on the right hand side of equation. Still this equation (10.7) can be used to study the model response to CO_2 mixtures in breathing air.

The following values of the constants K_1 to K_5 were found

$K_1 = 250.3$
$K_2 = 18.05$
$K_3 = 0.524$
$K_4 = 0.0652$
$K_5 = 0.179$

It can be seen that the value of $K_3 = 0.524$ is very nearly equal to the normal value of C_{aCO_2} of 0.533. The simulation results are shown in graph 10.1.4 in comparison to the experimental evidence for 5% and 7% CO_2 inhalation.

Although the results produced by the controller equation 10.7 are very similar to the experimental results, there is still some disparity in the dynamic regions. The simulated results

are slower than the experimental results for both cases, i.e. 5% and 7% CO_2 inhalation. This is particularly evident for the off transient of 5% CO_2. This may be due to the fact that the role of the arterial controller is considerably dimished due to the inclusion of 6.0 in the right hand side of equation 10.7. (As discussed in earlier chapters the arterial controller has a faster time response for CO_2 inhalation). To study the above hypothesis equation 10.7 was remodelled in the form

$$\dot{V} = K_1 (C_{BICO_2} - C_{BICO_2}(o)) + K_2 ((C_{aCO_2} - K_3)(1 + \frac{K_4}{C_{aO_2} - K_5})) \quad \ldots\ldots 10.8$$

The omission of 6.0 from the equation 10.7 put a constraint on the values of K_2, K_3, K_4 and K_5 such that these constants have to satisfy normal conditions of ventilation as well as the time course of ventilation due to inhalation of CO_2 gas mixtures. The following values of the constants were found using the optimisation routine:

$K_1 = 255.2$; $K_2 = 23.9$; $K_3 = 0.41$

$K_4 = .244$; $K_5 = .179$

The results of the model simulation with this controller are shown in graph 10.1.5. It can be seen that the model response of time course of ventilation follows very closely to the experi- results and the values of constants do not change with percentage of CO_2 inhaled.

Although using the above optimisation technique a complex controller of the form in equation 10.7 is formulated, it is

yet to be seen if any dynamic terms are to be included in the controller equation and if so what are the variables which should be included in the controller. A dynamic controller as in equation 10.5 hypothesised and tested, showed that the dynamic results are improved but still the parameter values changed with change in per cent CO_2 inhaled. Further experimental work is needed to provide further stimulus to hypothesising new controller strategies.

10.2 Parameter Estimation Through Feature Selection:

In this technique only certain features of the whole time response of ventilation are used which characterise a particular response, instead of using the whole time response. This technique may be particularly useful in identification of highly complex, non linear and multivariable systems.

The occurence of certain features in a system response to a test stimulus provide useful indicators as to system structure. For example at the trivial level, the presence of oscillations in a step response of a linear system indicates that the system is of at least second order. The oscillatory feature yields this information, there being no need to perform a detailed analysis of the complete time course of the response. Particularly in the case of complex models, it is such features rather than overall time courses of response which are of prime importance in parameter estimation.

If a model is such that the parameters do have a direct physiological meaning, then changes in the parameters must lead to the appropriate changes in the features of the model response.

It is the reproduction of such features, for example overshoot and frequency of oscillation, which are important in this model validation rather than necessarily minimising a loss function. This indicates that pattern recognition techniques can be applied with benefit to system identification and parameter estimation of biological processes so that response features are obtained corresponding to the specific physiological classification.

The technique requires a model which yields appropriate responses under an adequate variety of test conditions. Each distinct test condition corresponds to a pattern class, where the class numbers are those responses which are appropriate for that condition. In practice the criterion of appropriateness is the liklihood that a human subject would yield such a response in the same circumstances.

Clearly each class is likely to contain an infinite number of different responses, but certain features are common to all, allowing their class membership to be determined. Within the pattern recognition frame work a feature is simply any measurable characteristic of a response. In one sense, a feature is defined by a set of instructions, which may be simple or complex, which associate a real number with each response. The recognition problem is that of determining the class membership of the response from the set of feature values.

With this representation, each response corresponds to a single point in an N - dimensional space in which each co-ordinate is associated with a single feature. The entire space includes all

possible combination of feature values and therefore of all possible responses and can be regarded as the universe in which the pattern recognition system operates. The entire feature space must be pre-classified, being divided into disjoint regions, each being assigned to an appropriate class. This partition amounts to a decision rule specifying those combinations of feature values which are appropriate to the responses from each class and voting their location in the space. This requires a 'training set' comprising a representative collection of responses, of known classification, for each class. Effectively a system is designed to reproduce these classifications and to yield appropriate classifications of new 'unseen' responses. Many techniques are available for partitioning an N-dimensional feature space on the basis of a training set (Duda & Hart, 1973). The concept is illustrated in figure 10.2 for a two dimensional feature space.

Concerning the feature selection process, in many cases it is possible to define a large number of features, all of which may be expected to contribute to class separation. Computer programmes can then be used to search through this candidate set in an attempt to find a few good features. Clearly the training set can be used to judge the worth of any feature combination, based on resulting mis-classification.

For this study a simple recognition strategy is employed. For each class (test condition) a set of weights is desired, one for each feature used - w_{ij}, $j = 0, 1, 2 \ldots N$; $i = 1, 2, \ldots L$, classes and N features. These weight values are determined from the training set. A response to be classified yields N

feature values X_j ; $j = 1, 2, \ldots N$. A weighted sum is formed for each class:

$$W_i = \sum_{j=1}^{N} w_{ij} X + w_{io}, \quad i = 1, 2, \ldots L. \qquad \ldots\ldots 10.9$$

and the response is assigned to that class yielding the smallest value of W_i. Details of the feature space programme are given in a research memorandum by W.J. Hill (1972).

For the training set 16 waveforms were used from the data of Reynolds & Milhorn (1973), for each of the test conditions which correspond to step inputs of 3%, 5%, 6% and 7% carbon dioxide in breathing gas mixtures. Each waveform was sampled at 1 minute interval providing 36 sample values from each dynamic response. The training set was correctly classified by the feature space computer programme using leave-one-out evaluation. Three features were sufficient for this operation, namely sample values 4, 29 and 35 from each waveform.

Thus in this example L = 4 and N = 3 and the weighted sums generated by the program are:

$$W_1 = -0.07 X_4 + 0.04 X_{29} - 0.47 X_{35} + 3.53 \qquad \ldots\ldots 10.10A$$

$$W_2 = 0.09 X_4 - 0.39 X_{29} + 0.71 X_{35} - 2.45 \qquad \ldots\ldots 10.10B$$

$$W_3 = -0.19 X_4 + 0.5 X_{29} + 0.48 X_{35} - 4.23 \qquad \ldots\ldots 10.10C$$

$$W_4 = 0.18 X_4 - 0.15 X_{29} - 0.72 X_{35} + 3.13 \qquad \ldots\ldots 10.10D$$

where W_1, W_2, W_3, W_4 correspond to the four test conditions (classes of 7, 6, 5 and 3% carbon dioxide input respectively).

10.2.1. Results and Discussions

The recognition strategy, developed from the training set of experimental test responses to 7, 6, 5 and 3% carbon dioxide step inputs, is now used to test the model responses corresponding to carbon dioxide step inputs of 7, 5, and 3%.

A Tissue Control: As discussed in chapter 5 the two important parameters of the model are the gain K in the controller equation and the circulation delay time τ. The equation is of the form

$$\dot{V} = K.(C_{TCO_2} - C_{TCO_2}(o)) + 6.0 \quad \ldots\ldots 10.11$$

Estimates are now sought for the parameters K and τ. If physiologically plausible values of these parameters are adopted, the model responses should be correctly classified assuming the controller equation 10.11 to be applicable for the control of ventilation. As the parameter estimates are varied in a systematic manner so the response pattern classification changes. Results corresponding to K = 500 with variation of τ are shown in table 1.

τ(s)	Test Input	W_1(7%)	W_2(6%)	W_3(5%)	W_4(3%)
0	3%	0.79	- 0.15	- 0.84	0.26
	5%	0.19	0.40	1.27	0.81
	7%	0.67	- 0.03	- 1.83	0.60
12	3%	0.61	0.23	- 0.13	-0.42
	5%	0.16	0.70	- 0.98	0.20
	7%	-0.03	0.78	- 1.56	0.94
24	3%	0.42	0.02	0.28	-0.70
	5%	0.34	0.06	0.30	-0.59
	7%	0.30	- 0.75	1.10	-0.67

Table 1 Tissue Control:

With τ = 12 seconds, a parameter value within the physiologically plausible range, the responses corresponding to 3 and 5% carbon-dioxide inputs are correctly classified. Reducing τ to 0 seconds, results in a misclassification of the 3% response whilst with τ set to

24 seconds, the 5% response is incorrectly classified. Thus for 3 and 5% test inputs τ = 12 is an acceptable parameter estimate whilst 0 and 24 are not. In this way the physiologically acceptable range of the parameter τ can be defined, the estimates resulting from the pattern recognition technique lying within the physiological range. A similar procedure can be adopted for the controller gain K.

Whilst the tissue controller structure leads to successful parameter estimation for 3 and 5% CO_2 inputs, extension to 7% input reveals incorrect classification over the parameter values examined. Hence whilst the tissue control model structure provides an acceptable description of 3 and 5% data, the inadequacy of this structural hypothesis is revealed by applying the pattern recognition technique to the 7% data.

B Arterial Control: In a similar manner the arterial controller strategy is tested, leading to the results shown in table 2, where the controller equation is of the form

$$\dot{V} = K_1 (P_{aCO_2} - K_2) \left(1 + \frac{K_3}{P_{aO_2} - K_4}\right) \quad \ldots\ldots \quad 10.12$$

where K_1 may be considered to be the gain of the controller equation. The development of such an equation and the values of parameters K_1 to K_4 are discussed in chapter 6.

With a controller gain K_1 = 2.2 (Milhorn and Brown, 1971), τ = 16 and 20 seconds, give a correct classification of 3 and 5% data whereas 12 and 24 seconds give incorrect classifications.

Hence the acceptable range of estimates for this parameter can be defined as it can for controller gain K_1. As with the tissue control, inadequacy of the arterial controller structure hypothesis is revealed from the pattern recognition results for the 7% response.

τ(s)	Test Input	W_1(7%)	W_2(6%)	W_3(5%)	W_4(3%)
12	3	0.5	0.05	- 0.45	-0.03
	5	- 0.04	0.71	- 1.75	1.22
	7	- 1.22	1.99	- 4.30	3.83
20	3	0.23	0.31	- 0.10	-0.42
	5	- 0.21	0.92	- 1.18	0.62
	7	- 1.29	1.78	- 3.02	2.82
24	3	0.08	0.50	- 0.29	-0.2
	5	- 0.55	1.97	- 2.99	1.74
	7	- 1.17	3.10	- 4.51	2.82

Table 2 Arterial Control

C Combined Controller Structure: Since both of the controller structure hypotheses have been shown to be inadequate, a new controller equation is developed incorporating both tissue and arterial control. Using the feature space identification techniques, controller gain and circulatory delay parameters can be estimated for this new structure. The results for variation of τ for a chosen controller gain are shown in table 3. The controller equation is:

$$\dot{V} = 6.0 + 250.3\,(C_{BTCO_2} - C_{BTCO_2}(o)) + 18.05\left[(C_{aCO_2} - 0.524) + \frac{0.625}{C_{aO_2} - 0.179}\right]$$

τ(s)	Test Input	W_1(7%)	W_2(6%)	W_3(5%)	W_4(3%)
0	3	0.42	0.03	0.28	-0.73
	5	0.34	-0.06	0.30	-0.59
	7	0.30	-0.75	1.12	-0.67
12	3	0.30	0.26	-0.07	-0.43
	5	0.02	0.43	-0.27	-0.08
	7	-1.10	0.45	0.99	-0.15
16	3	0.23	0.36	0.07	-0.59
	5	-0.92	0.92	-0.57	0.25
	7	-0.35	1.91	-0.35	0.98
24	3	0.23	0.35	-0.08	-0.42
	5	-0.06	0.91	-1.35	0.62
	7	-0.30	0.49	-0.58	0.64

Table 3. Combined Controller

From table 3 it is clear that a range of values can be estimated for τ satisfying not only the 3 and 5% CO_2 input responses but also the corresponding to a 7% input of carbon dioxide. The limit of the range of τ values which are physiologically acceptable are clearly revealed since estimates of 0 or 24 seconds result in misclassification of the model responses. Both, model structure and parameter estimates for that structure have been developed, therefore, capable of reproducing the features found in the dynamic physiological responses to all three inputs.

The application of pattern recognition techniques to the system and model responses can also be used to study the sensitivity of the parameters of system or model, as changes in parameter values bring about changes in the response patterns.

These two techniques, discussed in sections 10.1 and 10.2 can be used for the identification and parameter estimation of complex systems. The technique of pattern recognition is particularly useful in the study of complex systems e.g. biological, social, economic etc., where there is considerable variation in parameter values of subjects or sybsystems and also the features of the responses are of greater importance rather than the actual values.

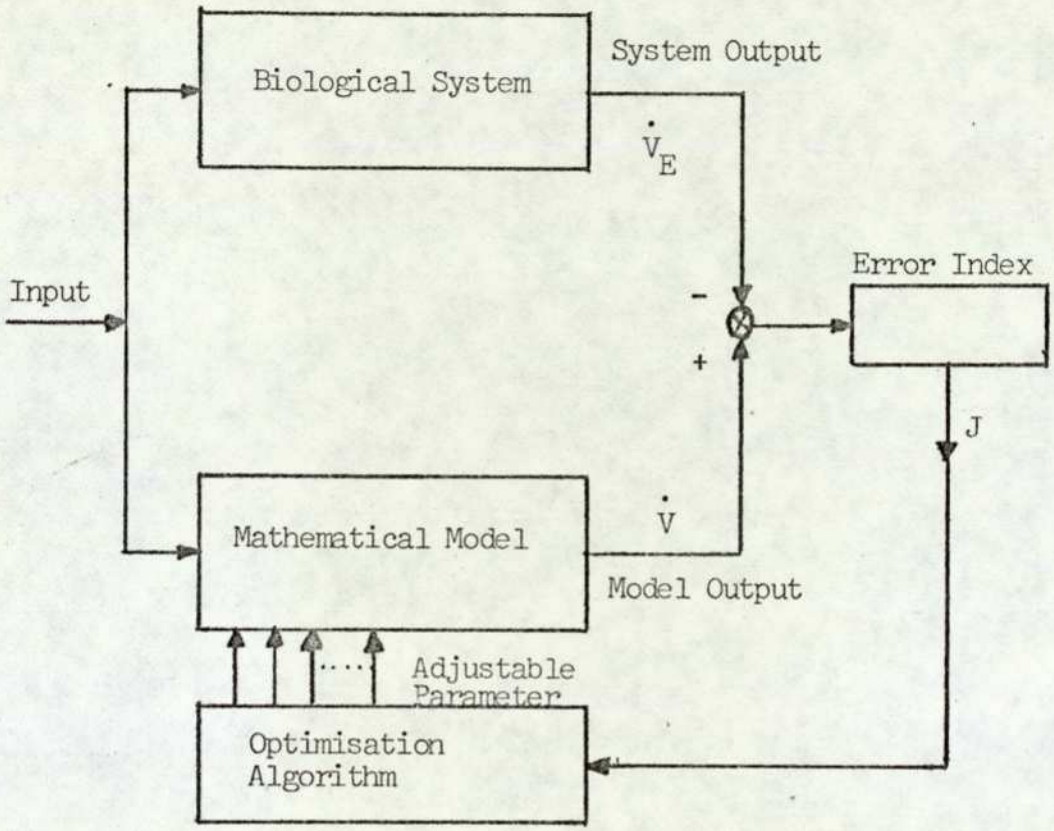
Biological System
System Output
$\dot{V}_E$
Input
Error Index
-
+
J
Mathematical Model
$\dot{V}$
Model Output
Adjustable Parameter
Optimisation Algorithm

Figure 10.1

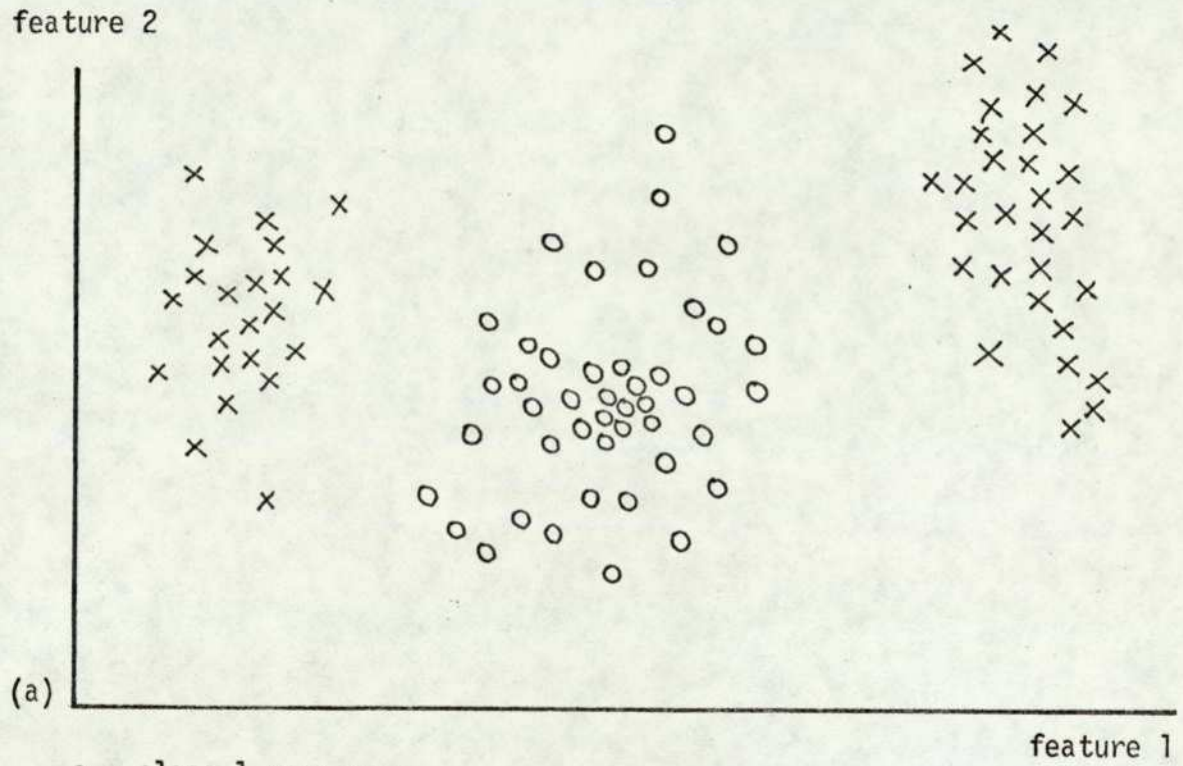

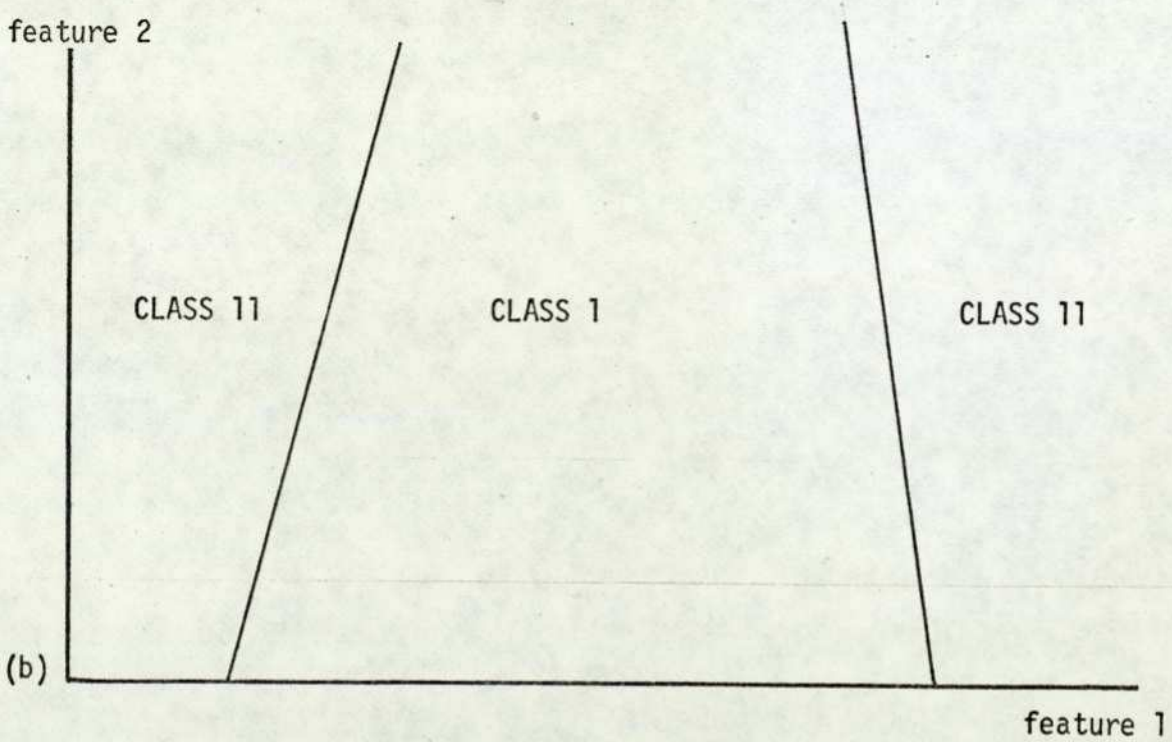

Figure 10.2 (a) TRAINING SET IN A TWO-DIMENSIONAL FEATURE SPACE

(b) A LIKELY PARTITION (DECISION RULE) CORRESPONDING TO THE ABOVE TRAINING SET

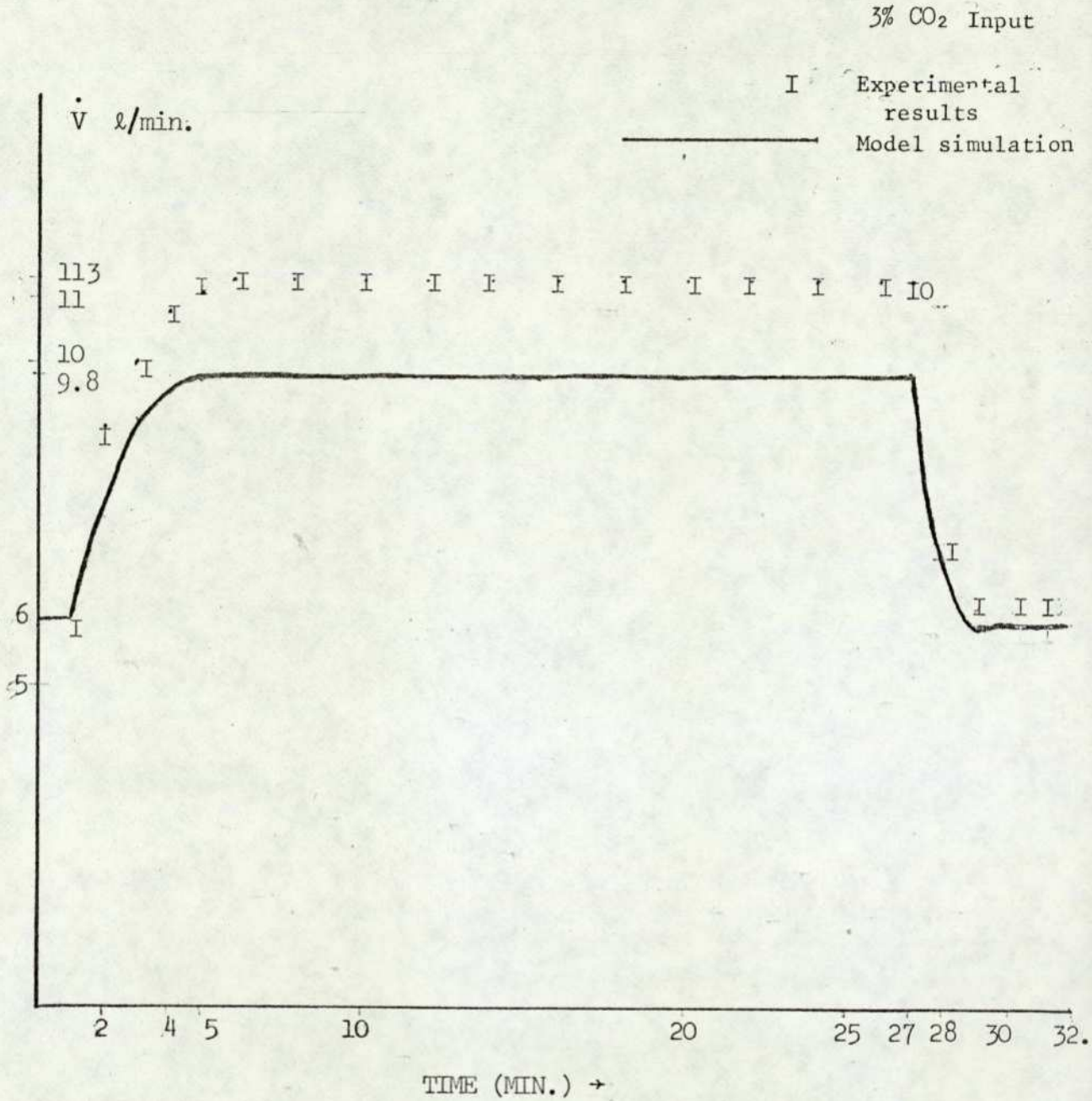
3% CO_2 Input
I Experimental results
Model simulation
$\dot{V}$ ℓ/min.
113
11
10
9.8
6
5
2
4
5
10
20
25
27
28
30
32.
TIME (MIN.) →

GRAPH 10.1.1.

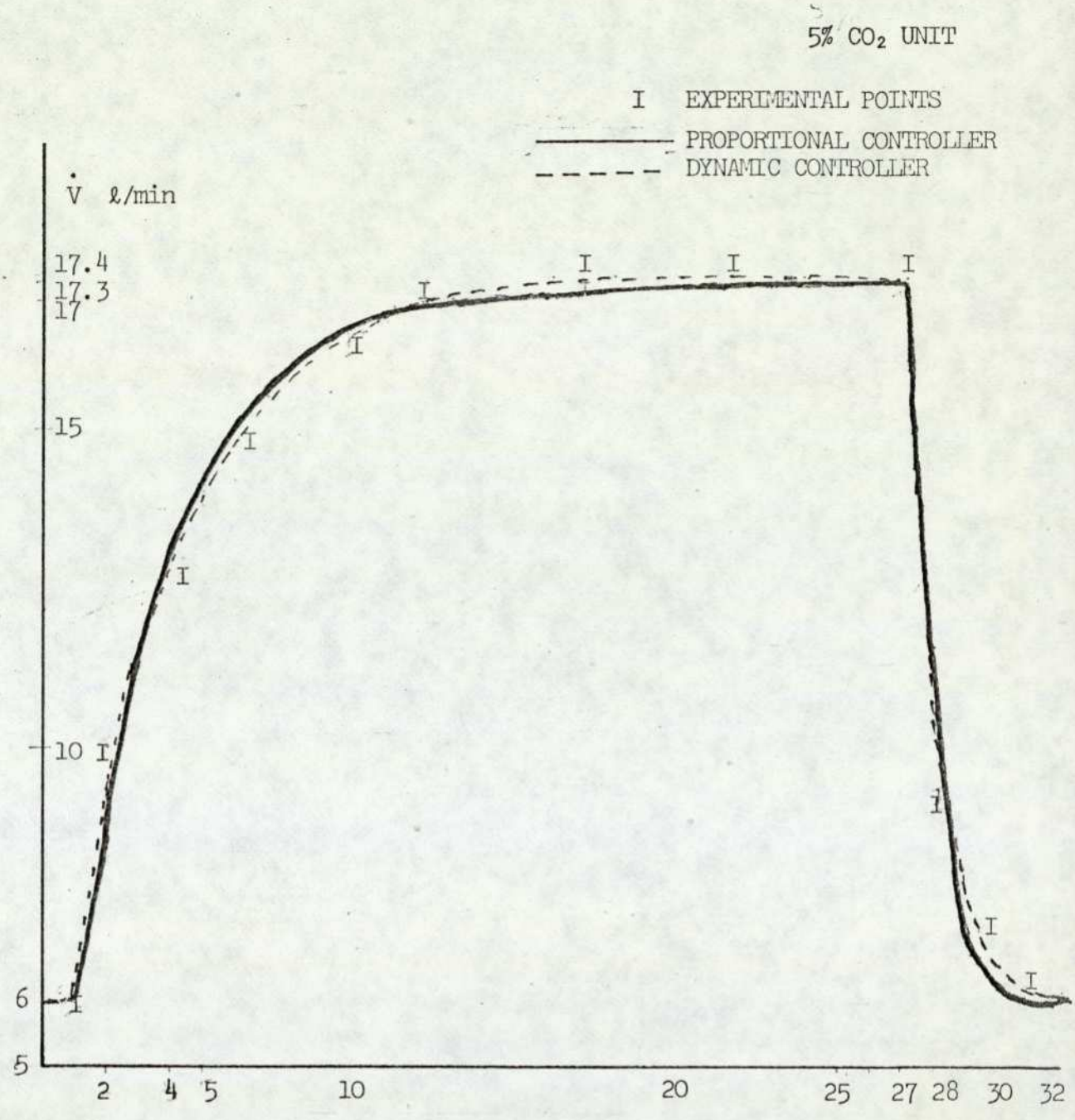
5% CO_2 UNIT
I EXPERIMENTAL POINTS
PROPORTIONAL CONTROLLER
DYNAMIC CONTROLLER
$\dot{V}$ ℓ/min
17.4
17.3
17
15
10
6
5
2
4
5
10
20
25
27
28
30
32
TIME (MIN.)

GRAPH 10.112.

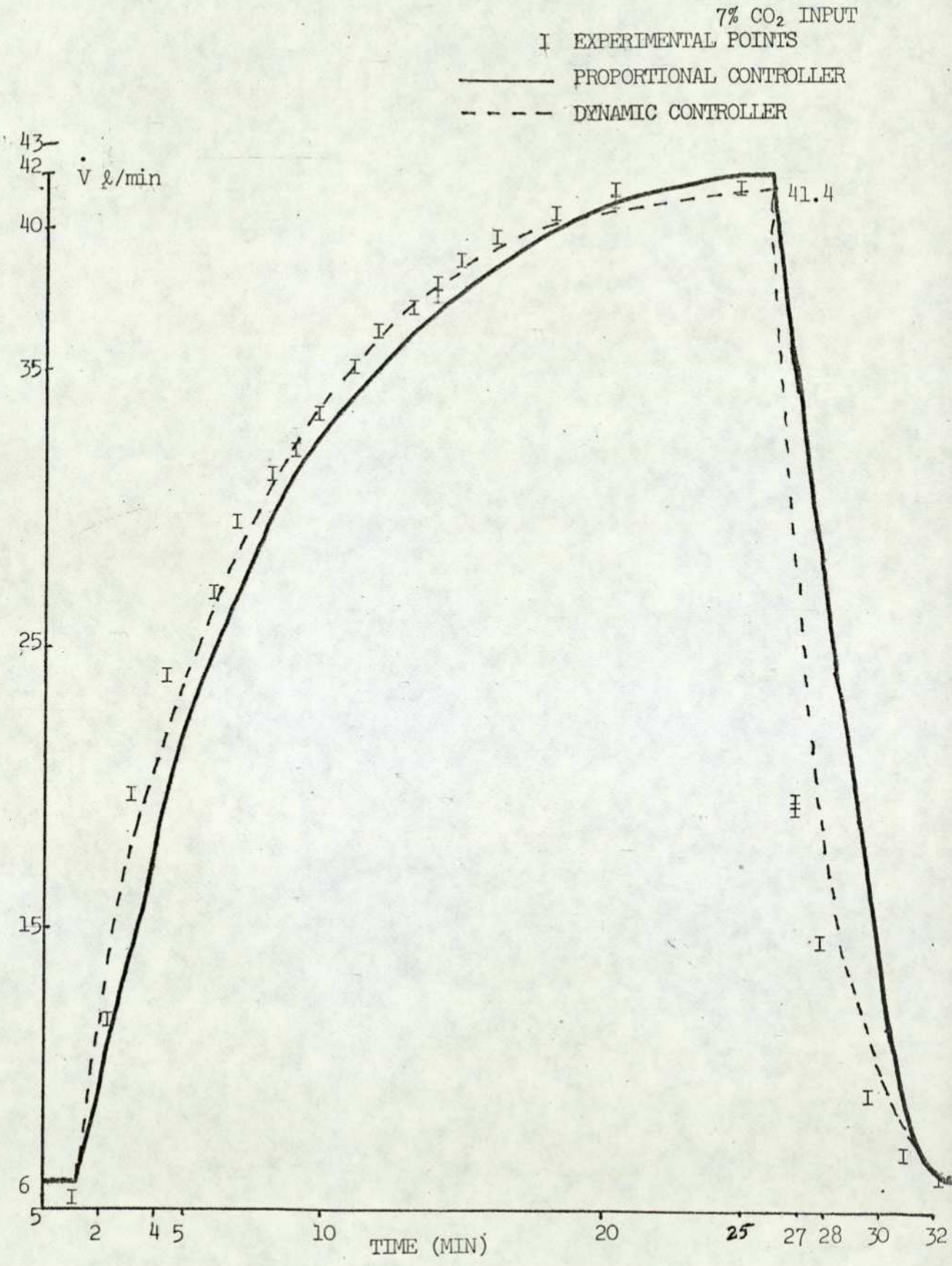
7% CO_2 INPUT
I EXPERIMENTAL POINTS
PROPORTIONAL CONTROLLER
DYNAMIC CONTROLLER
$\dot{V}$ ℓ/min
43
42
40
35
25
15
6
5
41.4
2
4
5
10
20
25
27
28
30
32
TIME (MIN)

GRAPH 10.1.3.

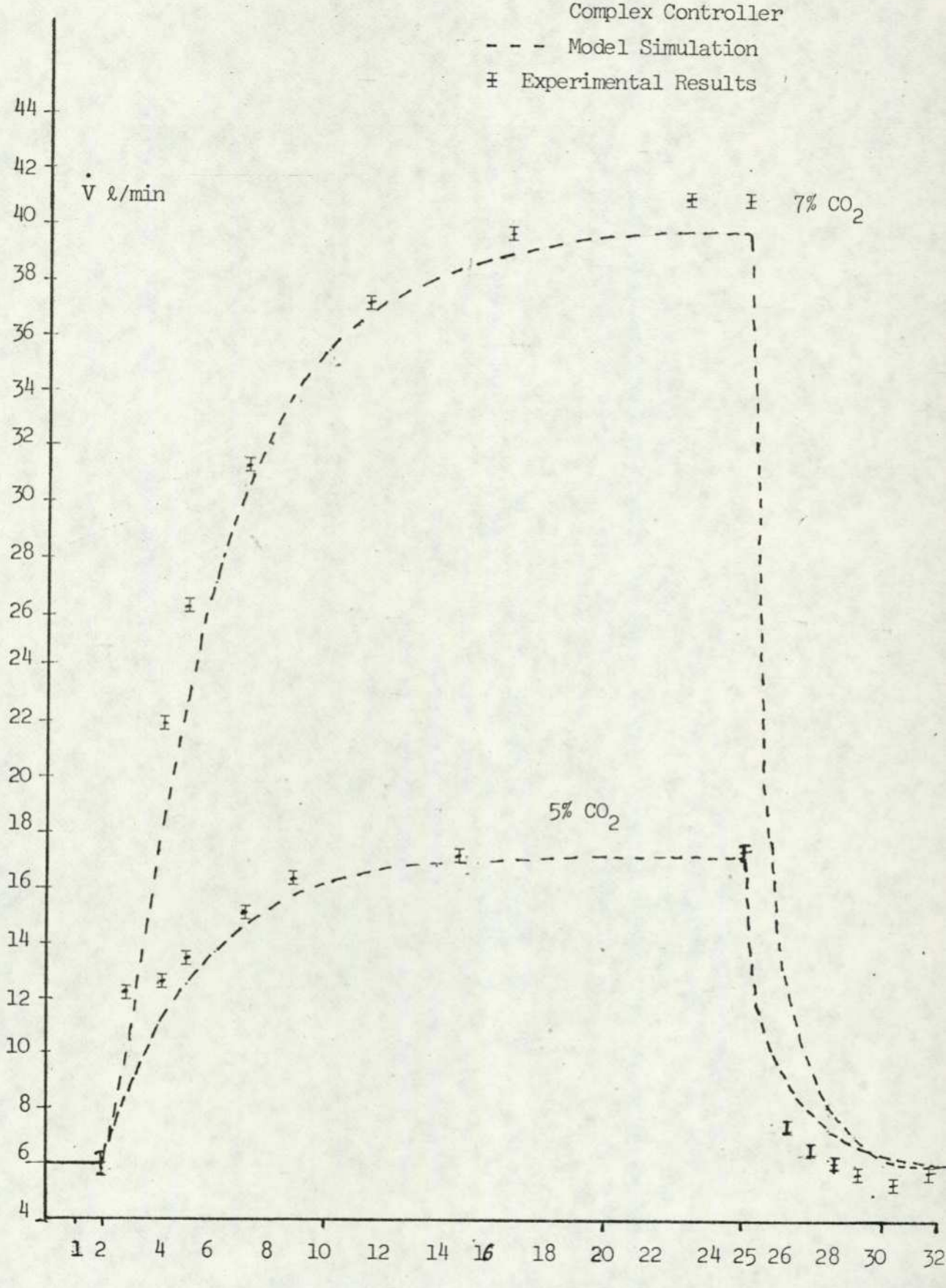

Figure 10.1.4 Time (min).

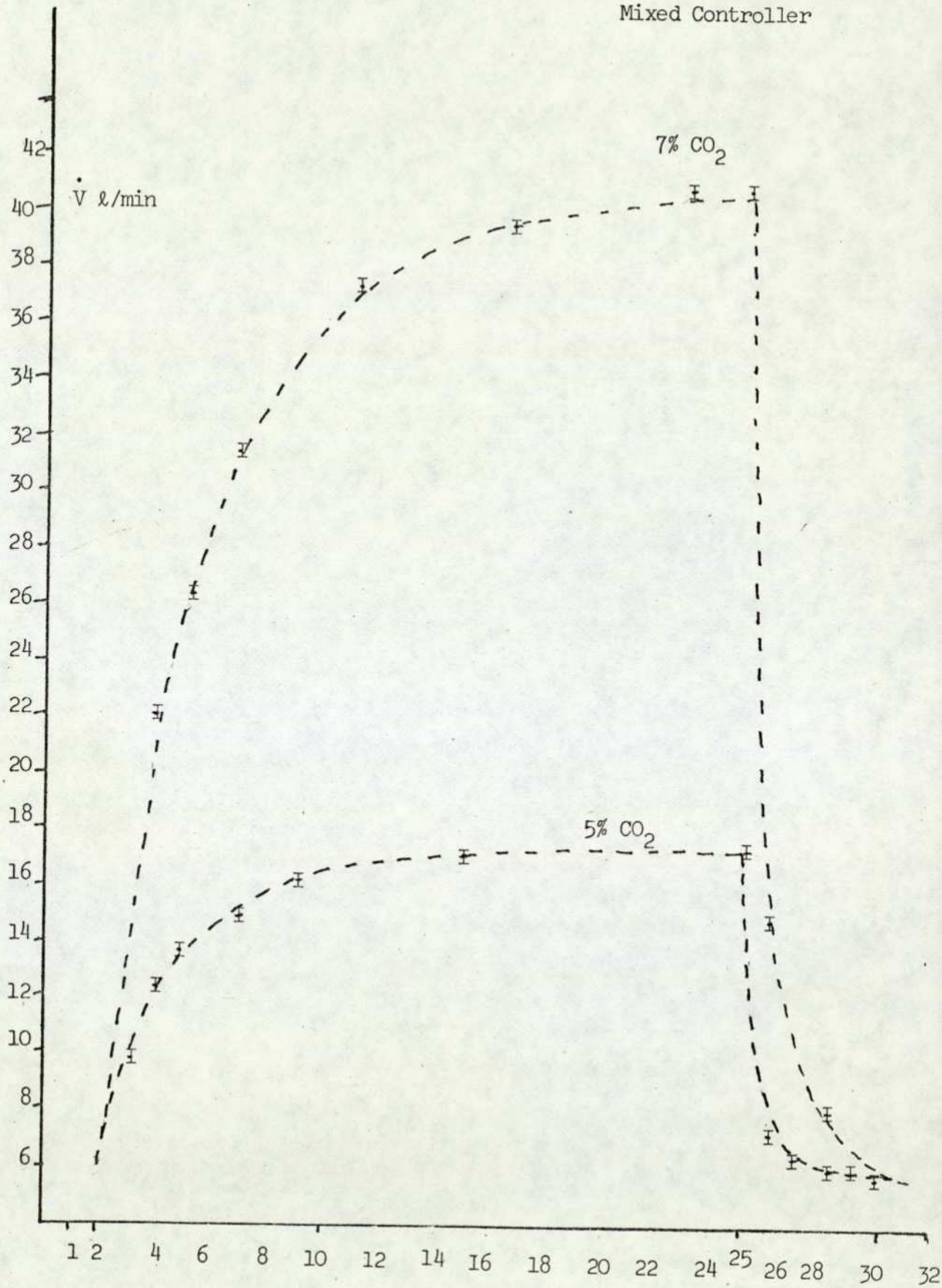

Figure 10.1.5 Time (min).

CHAPTER 11

CONCLUSIONS

In the present study the respiratory model has been made much more realistic approximating more closely towards isomorphism by a systematic process of model extension and model testing. At each stage of development the model was tested for variety of conditions i.e. CO_2 breathing, circulation delay time variations, controller gain sensitivity and the phenomenon of Cheyne-Stokes breathing. This process of development led to a complete model (chapter 9) which exhibits breathing and incorporates local blood flow controls.

Unlike many of the models published to date (chapter 4) this comprehensive model has variable lung volume which undergoes changes with the respiratory cycle and also includes variable time delays in blood transport to and from various tissue compartments. Thus the model simulates the breath to breath oscillations of arterial blood gas compositions. This makes the model far more adaptable to various test conditions. Unlike previously published models, this comprehensive model is developed through the use of some real tests which included CO_2 breathing, oxygen breathing, hyperventilation etc. The following show the clinical and experimental tests which have been simulated on the model:

1. Increased CO_2 in inspired air.
2. Decreased O_2 in inspired air.
3. Cheyne-Stokes breathing induced due to

i) Hyperventilation

ii) Apnoea.

iii) Increased circulation delay times (congestive heart failure).

iv) Increased controller gain (neurological disorders).

v) Minimisation of Cheyne-Stokes breathing due to CO_2 and O_2 inhalation.

vi) Exercise conditions (increased metabolic CO_2 output of muscle tissues).

vii) Capability of breath to breath analysis of arterial gas concentrations.

Apart from the above the inadequacy of each controller used in previously published models is shown, i.e. that tissue CO_2 control may successfully simulate CO_2 breathing but cannot simulate the phenomenon of Cheyne-Stokes breathing and vice versa. In addition none of the controller equation devised so far were able to simulate the breathing of air mixtures with less than normal oxygen concentrations. This lead to the development of new controller strategies which were a mixture of two types of controller equations.

In chapter 10, in the study of identification and parameter estimation of the model two new techniques were developed and employed which showed the tissue CO_2 control above cannot simulate even the CO_2 breathing for various percentages of CO_2 gas mixtures inspired. The same was true for arterial controller. Thus using these techniques, namely functional minimisation and pattern recognition techniques through the measurement of features of responses, a new controller equation is developed which not only simulates the various percentages of CO_2 gas mixtures in breathing air in steady state but also in transients as well.

The pattern recognition technique developed for the parameter estimation of the model can be used for any system but is particularly useful in the study of biological systems. Due to variation in the parameter values of individual subjects, the features of the response are of greater importance for the purposes of identification rather than the actual values.

The comprehensive model developed with its new controller equation is adaptable to any set of experimental situations in physiology. The future work may include some further experimental work to define the controller structure whose parameters may be fitted through the use of the two techniques discussed in chapter 10. If required, further physiological tests, e.g. acid base balance, the effect of lung volume dead space variations, changes in heart blood flow rates etc. may successfully be simulated by the model with minor modifications and compared with the experimental results from the patients.

Appendix 1

References

1. Adolph, E.F., Nance, F.D. and Schiling, M.S. (1928).
"The carbon dioxide capacity of the human body and progressive effects of CO_2 upon breathing". American Journal of Physiology Vol.87 pages 532-541.

2. Astrom, K.J. and Eykhoff, P. (1971).
"Systems Identification - A Survey". Automatica Vol.7, No.2. pages 123-162.

3. Bali, H.N. (1971).
"Development of Mathematical Model of the Respiratory System". M.Sc. Thesis, The City University, London.

4. Bali, H.N., McLeod, E.S. and Carson, E.R. (1972).
"Mathematical Model of the Respiratory System". Research memorandum DSA/HNB-ESMcL-ERC/13. The City University, London.

5. Bali, H.N. and Carson, E.R. (1974).
"Towards a Breathing Model of the Respiratory System". Research memorandum DSA/HNB-ERC/65. The City University, London.

6. Cunningham, D.J.C. and Lloyd, B.B. (Ed.) (1963).
"The Regulation of Human Respiration". Philadelphia - Davis.

7. Defares, J.G., Derksen, H.E. and Duyff, J.W. (1960).
"Cerebral Blood Flow in Regulation of Respiration". Acta. Physiol. Pharmacol. Neerlandica, No.9. pages 327-360.

8. Dejours, P. (1959).
"Control of respiration in muscular exercise", in 'Handbook of Physiology', Section 3, Respiration Vol.1. Washington D.C. Am. Physio Soc. 1964. pages 631-648.

9. Dittmer, D.S. and Grebe, R.M. (editors) (1958),"Handbook of Respiration" Philadelphia: Saunders.

10. Douglas, C.G. and Haldane, J.S. (1909).
"The Causes of Periodia or Cheyne-Stokes Breathing". J. Physiol (London) Vol. 38: pages 401-419.

11. Duda and Hart (1973).
"Pattern Classification and Semi Analysis". John Wiley.

12. Farhi, L.E. and Rahn, H. (1955).
"Gas stores of body and the unsteady state". J. Appl. Physiol. Vol.7. pages 472-484.

13. Farhi, L.E. and Rahn, H. (1960)

"Dynamics of changes in carbon dioxide stores". Anaesthesiology, Vol.2, pages 604-614.

14. Gray, J.S. (1950)

"Pulmonary ventilation and its physiological regulation". Charles C. Thomas, Pub., Springfield, Ill.

15. Green, J.H. (1972)

"An introduction to Human Physiology" Oxford University Press.

16. Grodins, F.S., Gray, J.S., Schroeder, K.R., Norins, A.L. and Jones, R.W. (1954).

"Respiratory responses to CO_2 inhalation. A theoretical study of a non-linear biological regulator". J. Appl. Physiol. Vol.7, pages 283-308.

17. Grodins, F.S. and James G. (1963)

"Mathematical models of respiratory regulation". Ann. N.Y. Acad. Sci. Vol. 109, pages 852-868.

18. Grodins, F.S., Buell, J. and Bart, A.J. (1967).

"Mathematical analysis and digital simulation of the respiratory control system". J. Appl. Physiol, Vol.22, No.2., pages 260-276.

19. Guyton, A.C., Crowell, J.W. and Moore, J.W. (1956).

"Basic oscillatory mechanism of Cheyne-Stokes breathing". Am. J. Physiol, Vol. 187, pages 395-398.

20. Haldane, J.S. and Priestley, J.G. (1905).

"The regulation of the lung ventilation". J. Physiol, Vol.32, pages 225-266.

21. Hill, W.J. (1972) Research Memorandum, DSA/WJH/32. The City University, London.

22. Horgan, J.D. and Lange, R.L. (1962 - 1)

"Simulation of the chemical and circulatory factors in the dynamic analysis of the human respiratory control system". Digest 15th annual conference, Engineering in Medicine and Biology, page 53.

23. Horgan, J.D. and Lange, R.L. (1962-2)

"Analog computer studies of periodic breathing". I.R.E. Trans. on Biomedical Electronics, BME-9. pages 221-228.

24. Horgan, J.D. and Lange, R.L. (1963).

"Digital Computer Simulation of the Human Respiratory System" I.E.E.E. International Convention record, pages 149-157.

25. Horgan, J.D. and Lange, R.L. (1964).

"A model of the respiratory control system which includes the effect of cerebospinal fluid and brain tissue". Proc. 17th Ann. conference on Engineering in Med. and Biol., Cleveland, Ohio, page 10.

26. Kety, S.S. and Schmidt, C.F. (1948).

"The effect of altered arterial tensions of carbon dioxide and oxygen on cerebral blood flow and cerebral oxygen consumption of normal young men". J. Clin. Invest. Vol. 27, pages 484-492.

27. Letia, J. (1974).

"Piecewise Constant Solutions in Modelling and Control of Non-linear Systems". Ph.D. Thesis. The City University, London.

28. Lloyd, B.B. and Cunningham, D.J.C. (1963).

"A quantitative approach to the regulation of human respiration", in 'The Regulation of Human Respiration', F.A. Davis Co. Philadelphia.

29. Lamburtson, C.J., Wollman, H., Gelfaud, R. (1961).

"The dynamics of change in respiration and arterial blood and C.S.F. acid-base parameters during administration and withdrawal of CO_2". Federation Proc. 20, page 430.

30. Longobardo G.S., Cherniack, W.S. (1965).

"The dynamics of carbon dioxide store changes". Clin. Res. Vol.13, page 423.

31. Longobardo, G.S., Cherniack, W.S., Fishman, W.S. (1966).

"Cheyne-Stokes breathing produced by a model of the human respiratory system". J. Appl. Physiology Vol.21, pages 1839-1946.

32. Longobardo, G.S., Cherniack, W.S., Lenine, O.R., Mellins, R., and Fishan, A.P. (1966).

"Periodic Breathing in Dogs". J. Appl. Physiol - Vol 21, pages 1847-54

33. Milhorn, H.T. and Guyton,A.C., (1965).

"An analog comutor analysis of Cheyne-Stokes breathing". J. of Appl. Physiol. Vol 20, pages 328-333.

34. Milhorn, H.T., Benton, R., Rose, R. and Guyton, A.C. (1965).

"A mathematical model of the human respiratory control system". Comput. Biophys. J. Vol 5, pages 27-46.

35. Milhorn, H.T., Brown, D.R. (1971).

"Steady state simulation of the human respiratory system". Comput. Biomed. Res. Vol 3, pages 604-619.

36. Milhorn, H.T., Reynolds, W.J. and Holloman, G.H. (1972).

"Digital simulation of the Ventilatory Response to CO_2 inhalation and CSF perfusion". Computors and Biomed. Res. Vol 5, pages 301-314.

37. Mitchel, R.A., Loeschke, H.H., Marsion, W.H., Severinghas, J.W.(1963).

"Respiratory responses mediated through superficial chemosensitive areas on the medulla". J. App. Physiol. Vol 18, page 523.

38. Neilson, M. and Smith, H. (1951).

"Studies on the regulation of respiration in acute hypoxia". Acta Physiol, Scand. Vol 24, pages 293-313.

39. Reynolds, W.J., Milhorn, H.T. and Hollman, J.R. (1972).

"Transient ventilatory response to graded hypercapnia in man". J. Appl. Physiol. Vol 33. No.1. pages 47-54.

40. Reynolds, W.J., Milhorn, H.T. (1973).

"Transient Ventilatory Response to Hypoxia with and without controlled Alveolar P_{CO_2} J. Appl. Physiol, Vol.35, No.2, pages 187-196

41. Weil, J.V., Byrne-Quinn, E., Sodal, I.E. (1970).

"Hypoxic ventilatory drive in normal man". J. Clin. Invest. Vol 49, pages 1061-1072.

42. Yamamoto, W.S. and Edwards, M.W. (1960).

"Homeostasis of carbon dioxide during intravenous infusion of carbon dioxide". J. Appl. Physiol. Vol 15. pages 807-818.

43. Yamamoto, W.S. and Raub, W.F. (1967).

"Models of the regulation of external respiration in mammals. Problem and promises". Computers and Biomed. Res. Vol 1. pages 65-104.

Appendix II

Nomenclature

C	-	concentration	p	-	partial pressure
D	-	diffusion coefficient	P_B	-	barometric pressure
f	-	function	$\dot{q}$	-	actual blood flow rate
f	-	respiratory frequency	$\dot{Q}$	-	instantaneous blood flow rate
F	-	gas fraction	t	-	time
g,V	-	volume	τ	-	time delay
g_r	-	functional residual capacity	$\dot{U}$	-	metabolic utilisation rate
k,K	-	constants	$\dot{V}$	-	ventilation
$\dot{M}$	-	metabolic production rate	V_{AX}	-	volumetric fraction of gas X in alveoli

Subscripts

A	-	alveolar	N	-	normal value
a	-	arterial	o	-	air
AC	-	actual	O_2	-	oxygen
B	-	brain	OT	-	other tissue
CO_2	-	carbon dioxide	r	-	residual capacity
D	-	dead space	T	-	tissue
I	-	inspired gas	TV	-	tidal volume
L	-	lung	v	-	venous
m	-	muscle			

Appendix III

Glossary of Physiological Terms

Alveolus - Minute air-filled sac in vertibrate lung, thin walled and surrounded by blood vessels. There are large numbers of alveoli in each lung and it is through their surfaces that the respiratory exchange of CO_2 and oxygen occur.

Apnoea - Strictly maintained expiration, but used to describe any breath holding.

Cerebral Blood Flow - Blood flow through the brain.

Chemoreceptor - Receptor which detects and differentiates substances according to their chemical structure, by contact with their molecules.

Dead Space - Only the first 250 ml. of the tidal volume reaches the alveoli. The last 150 ml. is still in the air passage and is exhaled as unchanged room air. This is known as dead space.

Hyperventilation - Increase in rate or depth of breathing.

Hypoxia - Situation in which there is insufficient oxygen (in limiting case zero oxygen).

Proprioceptors - Receptor which detects position and movement, usually not exhibiting sensory adaptation.

Pulmonary Ventilation - equals respiratory rate x tidal volume. Alveolar ventilation equals respiratory rate x (tidal volume - dead space).

Tidal Volume - the lungs after a normal quiet expiration still contain 3 litres of air in erect position. At the next inspiration the volume of the thorax is increased by 400 ml. The lungs increase in volume to 3.4 litres and 400 ml. enter the air passage. This is termed as the tidal volume.

Appendix IV

Fortran Program Structure:

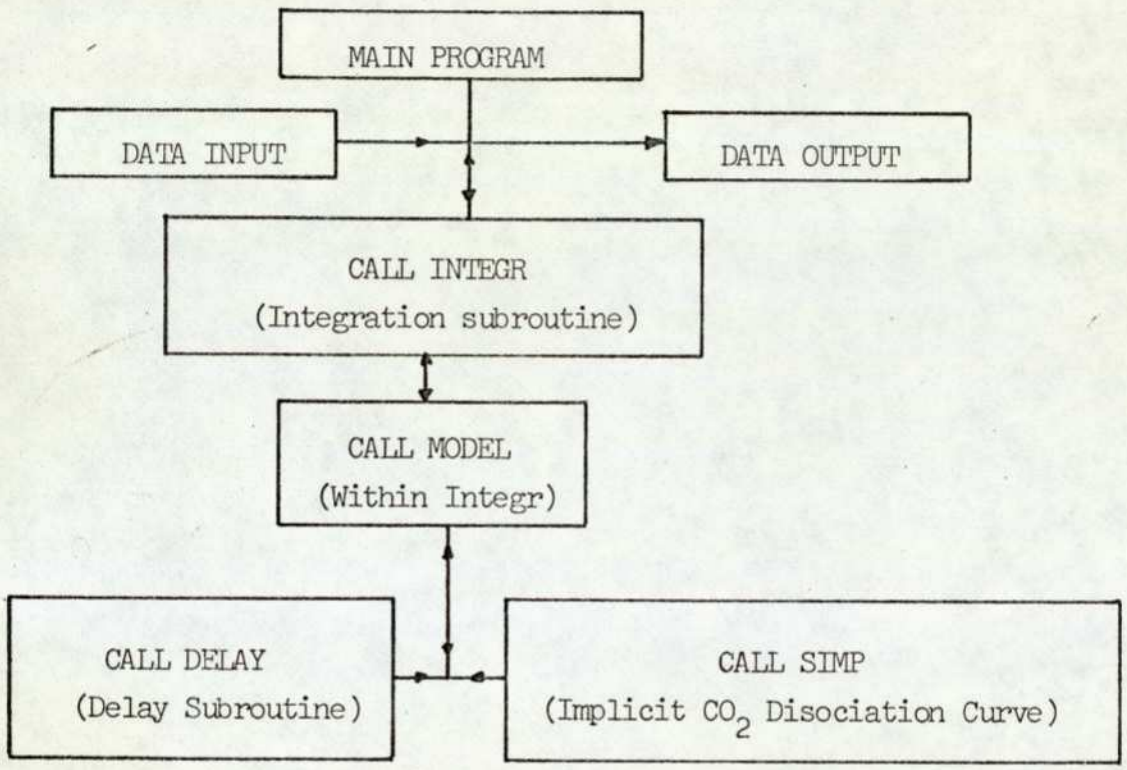

Delay and disociation curve subroutines called within the Model subroutines.

The computer programmes for the complete model when simulated on the CDC 7600 computer, required:

Store: 17500 units

simulation time: 500 seconds for 30 minutes of real time on the model.

MIMIC SOURCE-LANGUAGE PROGRAM

```
          CON(VA,VT,VR,QDOT,MT,MR)
          PAR(AMPCI)
DTMIN     0.0001
DT        0.1
CI        FSW(T-20.,0.,AMPCI,AMPCI)
VADOT     4.71*CRVD-253.
CRVD      TDL(CRV,0.25,500.)
ENA       ((CI-CCAPA)*VADOT-(CSMLA-CVD)*QRDOT)/VA
CVD       TDL(CV,0.5,500.)
CCAPA     INT(ENA,5.17)
ENB       (MT+(CSMLAD-CV)*QRDOT)/VT
CT        INT(ENB,52.4)
ENC       (MR+(CSMLAD-CRV)*QRDOT)/VR
CSMLAD    TDL(CSMLA,0.25,500.)
CR        INT(ENC,54.7)
CSMLA     31.2+3.23*CCAPA
CV        1.685*CT-36.
CRV       2.74*CR-95.3
END       0.46*CSMLA-17.
ENE       END*END+23.
QRDOT     FSW(CSMLA-47.8,47.8,47.8,ENE)
          FIN(T,45.)
          OUT(T,CI,CCAPA,VADOT,CSMLAD)
          OUT( ,CCAPAD,CVD,CT,CRVD,CR)
          OUT
          END
```

MIMIC SOURCE-LANGUAGE PROGRAM

```
MODEL 2  OXYGEN AND CO2
         CON(X1,X2,X3)
         PAR(X4)
DTMIN    0.001
DT       0.1
Z        FSW(CAO-0.155,X1,X1,Z1)
Z1       FSW(CAO-0.187,X2,X3,X3)
D        FSW(CAO-0.155,0.,0.,D1)
D1       FSW(CAO-0.187,0.1123,0.1756,0.1756)
CVC      (0.395*CMC+4.705*COTC)/5.6
K2       2.5+1711.2*Z
K3       CAC-0.4455
K4       CAO-D-32.44*Z
YI1      (25.953*(CVCD-CAC)-VD*(CAC-0.244))/13.623
YI2      (0.038+0.895*(CACD-CMC))/29.14
YI3      (0.19+4.705*(CACD-COTC))/12.
YI4      (5.6*(CVOD-CAO)*713.*Z+Z*VD*150.-VD*(CAO-D))/K2
YI5      (5.6*(CAOD-CVO)-0.28)/3.6
COTC     INT(YI3,0.543)
CMC      INT(YI2,0.543)
CAC      INT(YI1,0.503)
CAO      INT(YI4,0.192)
CVO      INT(YI5,0.142)
VDA      (1.81*K3+(23.53*K3*Z)/K4)/0.0065-15.
DELAY    CSP(CAC,CAO,CVC,CVO,VDA)
         RSP(CACD,CAOD,CVCD,CVOD,VD1)
DELAY    BSP(CAC,CAO,CVC,CVO,VDA)
CACD     TDL(CAC,0.2,150.0)
CAOD     TDL(CAO,0.2,150.0)
CVCD     TDL(CVC,0.2,150.0)
CVOD     TDL(CVO,0.2,150.0)
VD1      TDL(VDA,0.1,150.0)
DELAY    ESP(CACD,CAOD,CVCD,CVOD,VD1)
VD3      FSW(VD1-0.,0.,0.,VD1)
VD       FSW(T-X4,30.,30.,VD3)
         FIN(T,30.0)
         OUT(T,CVC,CVO,CAO,CAC,VD)
         OUT(,CVCD,CVOD,CAOD,CACD,VDA)
         OUT
         END
```

```
*LUNG EXCHANGE MODEL      SINUSOIDAL
                  CON(K1)
                  PAR(CCCO)
         DTMIN    0.0001
         DT       2./140.
         RAD      88.
         VTV      400.0
         VD       RAD*VTV*SIN(RAD*T)/2.0+310.*(DCO+DO+DN)/273.0
         VDI      FSW(VD,0.0,0.0,VD)
         VDE      FSW(VD,VD,0.0,0.0)
         IFDCO    INT(VDI*(0.0-IFDCO)/175.0,0.0526)
         IFDO     INT(VDI*(0.217-IFDO)/175.0,0.1514)
         IFDN     INT(VDI*(0.783-IFDN)/175.0,0.7959)
         EFDCO    INT(VDE*(EFDCO-EFACO)/175.0,0.0)
         EFDO     INT(VDE*(EFDO-EFAO)/175.0,0.217)
         EFDN     INT(VDE*(EFDN-EFAN)/175.0,0.783)
         IQTCO    INT(VDI*(IFDCO)+310.0*DCO/273.0,0.0526*2600.0)
         IQTO     INT(VDI*IFDO-310.0*DO/273.0,0.1514*2600.0)
         IQTN     INT(VDI*IFDN-310.0*DN/273.0,0.7959*2600.0)
         EQTCO    INT(VDE*EFACO+310.0*DCO/273.0,-0.0526*3000.)
         EQTO     INT(VDE*EFAO-310.0*DO/273.0,-0.1514*3000.0)
         EQTN     INT(VDE*EFAN-310.0*DN/273.0,-0.7959*3000.0)
         VA       INT(RAD*VTV*SIN(RAD*T)/2.0,2600.0)
         EFACO    EQTCO/VA
         EFAO     EQTO/VA
         EFAN     EQTN/VA
         PAN      IQTN*713.0/VA
         PAO      -EQTO*713.0/VA
         PACO     -EQTCO*713.0/VA
         DCO      5600.0*(CVCO-CCCO)
         DO       5600.0*(CCO-CVO)
         DN       5600.0*(CCN-CVN)
         CACO     INT(5600.0*(CCCO-CACO)/50.0,0.501)
         CAO      INT(5600.0*(CCO-CAO)/50.0,0.192)
         CAN      INT(5600.0*(CCN-CAN)/50.0,0.0)
         CVCO     INT((5600.0*(CACO-CVCO)+200.0)/21000.0,0.551)
         CVO      INT((5600.0*(CAO-CVO)-250.0)/5000.0,0.142)
         CVN      INT(5600.0*(CAN-CVN)/42000.0,0.0)
         CCN      K1*PAN
*DISSOCIATION CURVE DOR CO2
         BHCO     24.4
         S        12.0
         Z        (44.3*CCCO-0.03*PACO)/(0.03*PACO)
         ZZ       LOG(Z)
         ZX       ZZ/2.3026
         PH       6.1+ZX
         Y        0.3*(0.2-CCO)*44.5+0.03*PACO
         RHS      0.0222*(BHCO+S*(7.4-PH)+Y)
         HCO      0.0222*(44.3*CCCO-0.03*PACO)
         CCCO     IMP(CCCO,RHS)
         R        -0.04*PAO
         RR       EXP(R)
         RRR      1.0-RR
         RRRR     SR1(RRR)
         CCO      0.2*RRRR
                  OUT(T,CAO,CACO,PAO,PACO,VD)
                  OUT(DCO,DO,CCO,CCCO,CVO,CVCO)
                  OUT(,EQTO,EQTCO,IQTCO,IQTO)
                  OUT(,IFDO,IFDCO,EFDO,EFDCO,VA)
                  OUT(..PH.HCO)
                  PLO(T,PAO,CAO)
                  PLO(T,PACO,CACO)
                  PLO(T,VD)
                  FIN(T,5.0)
                  END
```

```
1*        PROGRAM RESP(INPUT,OUTPUT,TAPE1=INPUT,TAPE2=OUTPUT)
                                        ********************************
     C    FIRST COMPLETE RESP. SYSTEM
 2*        COMMON/DE/X(50),DX(50),N,T,DT,DTMIN
 3*        COMMON/PM/VDAC,CAC,CVC,PAO,PAC,CAO
 4*        COMMON/QM/QDH,QDBT,QDMT,QDOT,D10,D3,D4,D5
 5*        COMMON/VM/CACBD,CACND,CAOBD,CAOND,CBCD,COTCD,CMCD
 6*        COMMON/CN/VD,PH
 7*        COMMON/OX/CVO,CBOD,CMCD,COTOD
 8*        COMMON/OF/F
 9*        READ(1,500)N
     C     N IS THE NO. OF D.E. IN THE MODEL TOTAL IS 10
10*  500   FORMAT(I2)
11*        DT = 1.0/240.0
12*        TMAX = 30.0
13*        TMIN = 0.0
14*        DTMIN = 0.00001
15*        T = TMIN
16*        READ(1,501)(X(I),I=1,N)
     C X1 IS FDCO,X2 IS FDO , X3 IS QTCO, X4 IS QTO, X5 IS CBC, X6 IS CMC,X7
     C      X8 IS CBO,X9 IS CMO, AND X10 IS COTO
17*  501   FORMAT(10F7.4)
18*        WRITE(2,550)T,X(1),X(2),X(3),X(4),X(5),X(6),X(7),X(8),X(9),X(10)
19*  550   FORMAT(1H0,4HT = ,1PE13.6,4X,5HFDCO ,1PE11.5,4X,5HODO  ,1PE11.5,
           14X,5HQTCO ,1PE11.5,4X,5HQTO  ,1PE11.5,4X,5HCBC  ,1PE11.5/21X,5HCMC
           1  ,1PE11.5,4X,5HCOTC ,1PE11.5,4X,5HCVO  ,1PE11.5/21X,5HCMO  ,1PE11
           1.5,4X,5HCOTO ,1PE11.5/)
20*        NO=0
21*        DO 552 I =  1, N
22*  552   EREL = 0.0001*X(I)
23*        ERAB = DTMIN
24*  600   CALL INTEGR(EREL,ERAB,NO)
25*        WRITE(2,551) T,VDAC,VD,PAO,PAC,F,PH
26*  551   FORMAT(1H0,2HT ,1PE11.4,2X,5HVDAC ,1PE10.3,2X,3HVD ,1PE9.3,2X,4HPA
           10 ,1PE9.3,2X,4HPAC ,1PE9.3,2X,2HF ,1PE9.3,2X,3HPH ,1PE11.5)
27*        IF(T.LT.TMAX) GO TO 600
28*        STOP
29*        END
```

```
      SUBROUTINE INTEGR(EREL,ERAB,N0)
      REAL K1
      DIMENSION K1(50),XS(50),XZ(50),OLD(50)
      COMMON/DE/X(50),DX(50),N,T,DT,DTMIN
      COMMON/PM/VOAC,CAC,CVC,PAO,PAC,CAO
      COMMON/QM/QDH,QDBT,QDMT,QDOT,D10,D3,D4,D5
      COMMON/VM/CACBD,CACND,CAOBD,CAOND,CBCD,COTCD,CMCD
      COMMON/CN/VD,PH
      COMMON/OX/CVO,CBOD,CMOD,COTOD
      COMMON/OF/F
      DO 60 I=1,N
60    XS(I)=X(I)
      T0=T
      N1=1
      N0=MAX0(1,N0/4)
      H=DT/FLOAT(N0)
5     DO 2 J=1,N0
      CALL MODEL
      DO 10 I=1,N
10    XZ(I)=X(I)
      T=T+0.5*H
      DO 20 I=1,N
      K1(I)=DX(I)
20    X(I)=XZ(I)+0.5*K1(I)*H
      CALL MODEL
      DO 30 I=1,N
      K1(I)=DX(I)*2.0+K1(I)
30    X(I)=XZ(I)+0.5*DX(I)*H
      CALL MODEL
      DO 40 I=1,N
      K1(I)=DX(I)*2.0+K1(I)
40    X(I)=XZ(I)+DX(I)*H
      T=T+0.5*H
      CALL MODEL
      DO 2 I=1,N
      DX(I)=(DX(I)+K1(I))/6.0
2     X(I)=XZ(I)+DX(I)*H
      IF(N1.EQ.1)GO TO 3
      DO 50 I=1,N
50    IF(ABS(OLD(I)-X(I)).GT.(ABS(EREL*X(I))+ERAB))GO TO 3
- VARIABLE OR ARRAY - OLD NOT DEFINED AT THIS POINT
      GO TO 4
3     H=H*0.5
      IF(H.LT.DTMIN)GO TO 6
      DO 70 I=1,N
      OLD(I)=X(I)
70    X(I)=XS(I)
      N1=0
      T=T0
      N0=N0*2
      GO TO 5
      WRITE(2,7)T
      FORMAT(27H CONVERGENCE FAILURE AT T = ,F10.4)
      RETURN
      END
```

```
      SUBROUTINE MODEL
      DIMENSION DV1(100,2),DV2(100,2),DV3(100,2),DV4(100,2)
      DIMENSION DV5(100,2),DV6(100,2),DV7(100,2),DV8(100,2)
      DIMENSION DV9(100,2),DV10(100,2),DV11(100,2),DV12(100,2)
      COMMON/DE/X(50),DX(50),N,T,DT,DTMIN
      COMMON/PM/CAC,CVC,PAC,PAO,CAO,CVO
      COMMON/VM/CACBD,CACOD,CACMD,CAOBD,CAOOD,CAOMD
      COMMON/VN/CBCD,COTCD,CMCD,CBOD,COTOD,CMOD
      COMMON/CN/VD,PIC,TLB,TLOT,TLM,PIO
      COMMON/QM/QDH,QDBT,QDMT,QDOT
      COMMON/TP/TBL,TOTL,TML
      PIO = 150.0
      S = 0.0065
      B = 0.244
      IF(X(2).LT.0.155)Z=0.00388
      IF(X(2).LT.0.155)D = 0.0
      IF(X(2).GE.0.155)Z=0.00107
      IF(X(2).GE.0.155)D=0.1123
      IF(X(2).GT.0.187)Z=0.0001625
      IF(X(2).GT.0.187)D=0.1756
      PAC = (X(1)-B)/S
      PAO = (X(2)-D)/Z
      DQO = 0.0
      IF(PAO.LT.104.0) DQO = 9.6551-0.2885*PAO+0.0029241*PAO*PAO-0.00001
     1033*(PAO**3.0)
     ** FLOATING POINT INTEGER CORRECT - ** INTEGER ASSUMED
      DQC = 0.0
      IF(PAC.GE.40.0) DQC = 0.3*(PAC-40.0)
      IF(PAC.GT.60.0) DQC = 0.0
      QDH = 5.6+DQC+DQO


      DQBO = 0.0
      IF(PAO.LT.104.0) DQBO = 2.785-0.1323*PAO+0.0026033*(PAO**2.0)-
     10.23240E-04*(PAO**3.0)+0.76553E-07*(PAO**4.0)
     ** FLOATING POINT INTEGER CORRECT - ** INTEGER ASSUMED
      IF(PAC.LT.38.0) DQBC = 0.23230E-01-0.031073*PAC+0.80163E-03*PAC*
     1PAC
      IF(PAC.GE.38.0) DQBC = 0.0
      IF(PAC.GT.44.0) DQBC = -15.58+0.7607*PAC-0.012947*PAC*PAC+0.93981E
     1-04*(PAC**3.0)-0.21748E-06*(PAC**4.0)
     ** FLOATING POINT INTEGER CORRECT - ** INTEGER ASSUMED
      QDBT = 0.75+DQBC+DQBO
      QDNB = QDH-QDBT
      QDMT = 0.16*QDNB
      QDOT = QDNB-QDMT
      CALL DELAY(T,TLB,DV1,X(1),CACBD,0.0,Y1)
      DX(3) = (0.068+QDBT*(CACBD-X(3)))/1.4
      CALL DELAY(T,TLOT,DV2,X(1),CACOD,0.0,Y2)
      DX(4) = (0.18+QDOT*(CACOD-X(4)))/9.6
      CALL DELAY(T,TLM,DV3,X(1),CACMD,0.0,Y3)
      DX(5) =(0.049+QDMT*(CACMD-X(5)))/29.14
      CALL DELAY(T,TLB,DV4,X(2),CAOBD,0.0,Y4)
      DX(6) = (-0.068+QDBT*(CAOBD-X(6)))/1.4
      CALL DELAY(T,TLOT,DV5,X(2),CAOOD,0.0,Y5)
      DX(7) = (-0.18+QDOT*(CAOOD-X(7)))/9.6
      CALL DELAY(T,TLM,DV6,X(2),CAOMD,0.0,Y6)
      DX(8) = (-0.049+QDMT*(CAOMD-X(8)))/29.14
      CALL DELAY(T,TBL,DV7,X(3),CBCD,0.0,Y7)
      CALL DELAY(T,TOTL,DV8,X(4),COTCD,0.0,Y8)
      CALL DELAY(T,TML,DV9,X(5),CMCD,0.0,Y9)
      CVC = (QDBT*CBCD+QDOT*COTCD+QDMT*CMCD)/QDH


      CALL DELAY(T,TBL,DV10,X(6),CBOD,0.0,Y10)
      CALL DELAY(T,TOTL,DV11,X(7),COTOD,0.0,Y11)
      CALL DELAY(T,TML,DV12,X(8),CMOD,0.0,Y12)
      CVO = (QDBT*CBOD+QDOT*COTOD+QDMT*CMOD)/QDH
      VD = 1.81*(PAC-31.0)+23.53*(PAC-31.0)/(PAO-32.44)-14.3
      DX(1) = (S*713.0*QDH*(CVC-X(1))-VD*(X(1)-0.244-S*PIC))/13.623
      DX(2) = (Z*713.0*QDH*(CVO-X(2))-VD*(X(2)-D-PIO*Z))/(2.5+1711.2*Z)
      RETURN
      END
```

```
      SUBROUTINE MODEL
      DIMENSION DV1(100,2),DV2(100,2),DV3(100,2),DV4(100,2)
      DIMENSION DV5(100,2),DV6(100,2),DV7(100,2),DV8(100,2)
      DIMENSION DV9(100,2),DV10(100,2),DV11(100,2),DV12(100,2)
      COMMON/DE/X(50),DX(50),N,T,DT,DTMIN
      COMMON/PM/VDAC,CAC,CVC,PAO,PAC,CAO
      COMMON/QM/QDH,QDBT,QDMT,QDOT,D1,D3,D4,D5
      COMMON/VM/CACBD,CACND,CAOBD,CAOND,CBCD,COTCD,CMCD
      COMMON/CN/VD,PH
      COMMON/OX/CVO,CBOD,CMOD,COTOD
      COMMON/OF/F
      DATA I1/0/
      FOO=0.209
      FOCO = 0.0
      IF(T.GE.5.0) FOCO =0.05
      IF(T.GT.15.0) FOCO = 0.0
      GO = 0.175
      VD = 470.6*X(5)-305.0
      IF(T.LT.1.0) VD=0.0
      F = 10.7+0.267*VD
      THETA = 0.0
      IF(I1.EQ.0) GO TO 100
      THETA = (F1-F)*T+THETA1

      THETA = AMOD(THETA,1.0)
     - RESULT - THETA TO LEFT OF = APPEARED TO LEFT OF PREVIOUS =
  100 THETA1 = THETA
      F1 = F
      I1 = 1
      VTV=VD/F
      VO=2.75
      BHCO = 24.4
      S = 12.0
      PI = 3.1416
      VA = VO+VTV*(1.0-COS(2.0*PI*(F*T+THETA)))/2.0
      VDV = 2.0*PI*F*VTV*SIN(2.0*PI*(F*T+THETA))/2.0
      FACO = X(3)/VA
      FAO = X(4)/VA
C  X(3) IS QTCO AND X(4) IS QTO, QUANTITY IN LUNG IN L
      PAC = FACO*713.0
      PAO = FAO*713.0
C  O2 ASSOCIATION CURVE
      R = -0.04*PAO
      RR = EXP(R)
      RRR = ABS(1.0-RR)
      RRRR = RRR**0.8
      CAO = 0.2*RRRR
C  CALL SIMP SUBROUTINE TO DO CAC = F(CAC,CAO,PAC)
      CALL SIMP(PAC,CAO,BHCO,S,CAC)
C  WORK OUT CARDIAC OUTPUT,QDBT,QDMT,QDOT,AND TIME DELAYS
      DQO = 0.0
      IF(PAO.LT.104.0) DQO = 9.6551-0.2885*PAO+0.0029241*PAO*PAO-0.00001
     1033*(PAO**3.0)
     - IS ** FLOATING POINT INTEGER CORRECT - ** INTEGER ASSUMED
      DQC = 0.0
      IF(PAC.GE.40.0) DQC = 0.3*(PAC-40.0)
      IF(PAC.GT.60.0) DQC = 6.0
      DQDC = DQC+DQC
      DQDH = (1.0-EXP(-T/0.1))*DQDC
```

```
      QDH = 5.6+DQDH
      DQBO = 0.0
      IF(PAO.LT.104.0) DQBO = 2.785-0.1323*PAO+0.0026033*(PAO**2.0)-
     10.23240E-04*(PAO**3.0)+0.76553E-07*(PAO**4.0)
- IS ** FLOATING POINT INTEGER CORRECT - ** INTEGER ASSUMED
      IF(PAC.LT.38.0) DQBC = 0.23230E-01-0.031073*PAC+0.80163E-03*PAC*
     1PAC
      IF(PAC.GE.38.0) DQBC = 0.0
      IF(PAC.GT.44.0) DQBC = -15.58+0.7607*PAC-0.012947*PAC*PAC+0.93981E
     1-04*(PAC**3.0)-0.21748E-06*(PAC**4.0)
- IS ** FLOATING POINT INTEGER CORRECT - ** INTEGER ASSUMED
      DQB = DQBO+DQBC
      DQDB = (1.0-EXP(-T/0.1))*DQB
      QDBT = 0.750+DQDB
      QDNB = QDH-QDBT
      QDMT = 0.16*QDNB/1.0
- MULTIPLY OR DIVIDE BY 1
      QDOT = QDNB-QDMT
      D10 = 0.06/QDBT+0.188/QDH
      D3 = 1.47/QDNB+0.188/QDH
      D4 = 1.062/QDH+0.735/QDNB
      D5 = 1.062/QDH+0.015/QDBT
      PH=6.1+ALOG10((44.9*CAC-0.03*PAC)/(0.03*PAC))
C  DELAY CAC BY D5 TO GIVE CACBD
 301  CALL DELAY (T,D5,DV1,CAC,CACBD,0.0,Y1)
      DX(5) = (0.068+QDBT*(CACBD-X(5)))/1.4
C  DELAY CAC BY D4 TO GIVE CACND
      CALL DELAY(T,D4,DV2,CAC,CACND,0.0,Y2)
      DX(6) = (0.038+QDMT*(CACND-X(6)))/29.14
C  DELAY CAC BY D4 TO GIVE CACND
      CALL DELAY(T,D4,DV3,CAC,CACND,0.0,Y3)
      DX(7) = (0.14+QDOT*(CACND-X(7)))/9.6
C  DELAY CAO BY D5 TO GIVE CAOBD
      CALL DELAY(T,D5,DV4,CAO,CAOBD,0.0,Y4)
      DX(8) = (-0.068+QDBT*(CAOBD-X(8)))/1.4
C  DELAY CAO BY D4 TO GIVE CAOND
      CALL DELAY(T,D4,DV5,CAO,CAOND,0.0,Y5)
      DX(9) = (-0.049+QDMT*(CAOND-X(9)))/29.14
C  DELAY CAO BY D4 TO GIVE CAOND
      CALL DELAY(T,D4,DV9,CAO,CAOND,0.0,Y9)
      DX(10) = (-0.18+QDOT*(CAOND-X(10)))/9.6
C   DELAY CBO BY D10 TO GIVE CBOD
      CALL DELAY(T,D10,DV10,X(8),CBOD,0.0,Y10)
C   DELAY CMO BY D3 TO GIVE CMOD
      CALL DELAY(T,D3,DV11,X(9),CMOD,0.0,Y11)
C   DELAY COTO BY D3 TO GIVE COTOD
      CALL DELAY(T,D3,DV12,X(10),COTOD,0.0,Y12)
      CVO = (QDBT*CBOD+QDMT*CMOD+QDOT*COTOD)/QDH
C  DELAY CBC BY D10 TO GIVE CBCD (X(5))
      CALL DELAY(T,D10,DV6,X(5),CBCD,0.0,Y6)
C  DELAY COTC BY D3 TO GIVE COTCD(X(7))
      CALL DELAY(T,D3,DV7,X(7),COTCD,0.0,Y7)
C  DELAY CMC BY D3 TO GIVE CMCD (X(6))
      CALL DELAY(T,D3,DV8,X(6),CMCD,0.0,Y8)
      CVC =(QDBT*CBCD+QDOT*COTCD+QDMT*CMCD)/QDH
C  WORK OUT DO AND DCO AND PUT = 0.0 IF -VE
      DO = QDH*(CAO-CVO)*863.0/713.0
      IF(DO.LE.0.0) DO = 0.0
      DCO = QDH*(CVC-CAC)*863.0/713.0
      IF(DCO.LE.0.0) DCO = 0.0
```

```
      DVD = DO-DCO
      IF(DVD.LT.0.0)DVD = 0.0
      VDAC = VDV+DVD
      IF(VDAC.LT.0.0) GO TO 200
      DX(1) = VDAC*(FOCO-X(1))/GD
      DX(2) = VDAC*(FOO-X(2))/GD
      DX(3) = VDAC*(X(1))+DCO
      DX(4)= VDAC*X(2)-DO
      GO TO 201
200   DX(1) = VDAC*(X(1)-FACO)/GD
      DX(2) = VDAC*(X(2)-FAC)/GD
      DX(3) = VDAC*FACO+DCO
      DX(4) = VDAC*FAO-DO
201   RETURN
      END
```

```
      SUBROUTINE SIMP(PAC,CAO,BHCO,S,CAC)
      CAC=0.45
      XA = 0.0006732*PAC
      XB = 0.547+XA+0.375*(0.2-CAO)
 11   XC = -(CAC+0.62*(ALOG10((CAC-XA)/(0.01*PAC))-0.14))
      FCAC = XB+XC
      DFCAC = -(1.0+0.62/((CAC-XA)*2.3026))
      CACN = CAC-FCAC/DFCAC
      ERRR= (CACN-CAC)/CAC
      ERR = ABS(ERRR)
      CAC = CACN
      IF(ERR.GT.0.0001) GO TO 11
      RETURN
      END
```

```
      SUBROUTINE DELAY(X,T,DV,Y,Z,X0,YINT)
      DIMENSION DV(100,2)
      IF(X.GT.X0) GO TO 201
 200  Z=Y
      YINT=Y
      DO 209 N = 1,100
      DV(N,1) = X
      DV(N,2) = Y
 209  CONTINUE
      RETURN
 201  IF((X-DV(100,1)).LT.(T/80.)) GO TO 202
      DO 203 N=1,99
      DV(N,1)=DV(N+1,1)
 203  DV(N,2)=DV(N+1,2)
      DV(100,1)=X
      DV(100,2)=Y
 202  IF((X-T).GT.X0) GO TO 205
      Z=YINT
      RETURN
 205  DO 206 N=1,100
      IF(DV(N,1)-(X-T)) 206,207,208
 206  CONTINUE
 207  Z=DV(N,2)
      RETURN
 208  F0=DV(N-1,2)
      F1=DV(N,2)
      P=((X-T)-DV(N-1,1))/(DV(N,1)-DV(N-1,1))
      Z=F0+P*(F1-F0)
      RETURN
      END
```